SEISMIC MICROZONATION OF IMPHAL CITY AND PROBABILISITC SEISMIC HAZARD ASSESSMENT OF MANIPUR STATE

Submitted for the degree of

DOCTOR OF PHILOSOPHY

by

KUMAR PALLAV



Department of Civil Engineering

Indian Institute of Technology Guwahati

Guwahati – 781 039, India

August 2010

Department of Civil Engineering
Indian Institute of Technology Guwahati

Certificate

This is to certify that the thesis entitled ***'Seismic Microzonation of Imphal City and Probabilistic Seismic Hazard Assessment of Manipur State'*** being submitted by ***Mr. Kumar Pallav*** to the Indian Institute of Technology Guwahati for the award of the degree of ***Doctor of Philosophy*** is a record of bonafide research work carried out by him. The thesis work in my opinion has reached the requisite standard for the degree of ***Doctor of Philosophy***.

The results embodied in this thesis have not been submitted to any other University/ Institute for the award of any Degree or Diploma.

Date:

Place: Guwahati

Dr. Konjengbam Darunkumar Singh

Assistant Professor

Indian Institute of Technology Guwahati,
Assam, India-781039

TH-994_06610404

to my dearest parents

Sri Ramesh and Smt Sadhana

&

my beloved wife

Amrita

and charming daughter

Tiya

TH-994_06610404

Contents

Acknowledgments v

Abstract vii

List of Figures x

List of Tables xvi

Nomenclature xviii

Publications based on the work xxvii

1. Introduction 1-7

1.1. General 1

1.2. Thesis organization 4

2. Literature review 8-60

2.1. Introduction 8

2.2. Seismic status of Northeast India and adjoining regions 10

2.2.1. Cachar earthquake (M_w 7.5, 1869) 13

2.2.2. Shillong earthquake (M_w 8.7, 1897) 13

2.2.3. Srimangal earthquake (M_w 7.6, 1918) 14

2.2.4. Dhubri earthquake (M_w 7.1, 1930) 15

2.2.5. Great Assam earthquake (M_w 8.6, 1950) 15

2.2.6. Indo-Burma earthquake (M_w 7.2, 1988) 16

2.3. Strong ground motion 17

2.3.1. Estimation of ground motion 20

2.3.2. Stochastic seismological models 21

2.4. Ground motion attenuation relationship 24

TH-994_06610404

2.4.1. Shallow active region 25

2.4.2. Stable region 26

2.4.3. Subduction zone 27

2.5. Indian standard code (IS:1893, 2002) 29

2.5.1. Seismic zone map during 1962-1970 30

2.5.2. Seismic zone map during 1970-2002 31

2.5.3. Limitations of macro-zoning 32

2.6. Seismic hazard assessment 34

2.6.1. Earthquake data and its completeness 35

2.6.2. Recurrence relation 36

2.6.3. Limitations of deterministic approach 37

2.7. Probabilistic seismic hazard assessment 37

2.8. Deaggregation of seismic hazard 40

2.9. Hazard estimation in NE India 41

2.10. Seismic microzonation 43

2.10.1. Local site effects 45

- Site coefficients 45

2.10.2. Site amplification 47

2.10.3. Equivalent linear wave propagation 48

2.10.4. Liquefaction potential 50

- Liquefaction and its mechanism 50

2.11. Seismic microzonation studies 52

2.12. Conclusions 58

3. Deterministic Seismic Scenario for Imphal city 61-94

3.1. Introduction 61

3.2. About Imphal city 62

3.3. Seismic status of Imphal city 65

3.3.1. Indo-Burmese Ranges 67

3.3.2. Eastern Himalaya 67

TH-994_06610404

3.3.3. Mishmi Thrust 68

3.3.4. Shillong Mikir Massif 69

3.3.5. Naga Disang Thrust 70

3.3.6. Bengal Basin 71

3.3.7. Assam Valley 72

3.4. Damages due to past earthquakes 73

3.5. Earthquake catalogue 74

3.5.1. Regional recurrence 76

3.5.2. Deaggregation 81

3.6. Ground motion simulation 82

3.7. Comparison with the SRR data of 6th August 1988 earthquake 88

3.8. Synthesis of ground motion during the 1869 Cachar earthquake (M_w 7.5) 91

3.9. Synthesis of ground motion for hypothetical earthquake of M_w 8.1 in IBR 92

3.10. Conclusions 93

4. Local site effects on ground motion for Imphal city 95-127

4.1. Introduction 95

4.2. Geography and Geology of Imphal valley 96

4.3. Local soil condition 99

4.4. Soil amplification 101

4.5. Comparison with the SRR data of 6th August 1988 earthquake 102

4.6. Ground motion during the 1869 Cachar earthquake (M_w 7.5) 104

4.7. Ground motion due to hypothetical M_w 8.1 earthquake in the Indo-Burmese Ranges 112

4.8. Determination of site coefficients 115

4.9. Conclusions 125

5. Probabilistic seismic hazard estimation at surface level for Imphal city 128-146

TH-994_06610404

5.1. Introduction 128

5.2. Attenuation relationship 129

5.2.1. EH, SP, MT, BB and AV attenuation 130

5.2.2. IBR subduction zone attenuation 131

5.3. Probabilistic seismic hazard analysis 133

5.4. Seismic hazard curves for Imphal city 134

5.5. Uniform hazard response spectra 136

5.6. Surface level hazard map for Imphal city 137

5.7. Conclusions 145

6. Liquefaction potential status of Imphal city 147-163

6.1. Introduction 147

6.2. Methodology 149

6.2.1. Semi-empirical approach 149

6.2.2. Liquefaction Potential Index 157

6.2.3. Liquefaction Severity Index 158

6.3. Conclusions 162

7. Probabilistic seismic hazard analysis of Manipur state 164-177

7.1. Introduction 164

7.2. Seismic hazard curves 165

7.3. Uniform hazard response spectra 169

7.4. Comparison with other studies 175

7.5. Conclusions 176

8. Conclusions and Suggestions for further research 178-184

8.1. Conclusions 178

8.2. Suggestions for further research 182

References 185-218

Appendix A Terminology 219-232

Appendix B Soil Investigation data 233-257

Appendix C Site coefficients 258-278

TH-994_06610404

Acknowledgements

The following acknowledgments are an account of the indebtedness I feel towards those who have been a guiding light and source of inspiration towards the completion of this thesis.

I express my deepest sense of gratitude and reverence to ***Dr. STG Raghukanth*** and ***Dr. Konjengbam Darunkumar Singh*** for their constant valuable guidance; enthusiastic involvement and kind help throughout my research work. They have been a constant source of motivation and have treated me as a good friend. I will forever remain indebted to them for their untiring effort and help extended to me that went even beyond academics. The extraordinary experience of working with them would be remembered in my life.

I am thankful to *Mr Yendrembam Arunkumar Singh*, IIT Guwahati, *Mr N Subhas*, PWD Manipur, *Mr Yambem Ibotombi*, PWD Manipur for their help in obtaining soil data. *Dr. Soibam Ibotombi* and *Dr. S Manichandra*, Manipur University and *Dr. RK Hemanta Singh* and *Dr. Khuraijam Mohon Singh*, Imphal College are gratefully acknowledged for their helpful discussion. *Mr. Madhu*, *Mr. Tapas* and *Mr Sambhal* for their help in good quality map preparations.

I would like to thank the Department of Civil Engineering for providing the required facilities for my research work. Cooperation extended by the Head of the Department and office staffs (*Alok, Rajib, Juri*, and *Dipak*) deserve special thanks from my side. I would like to express my sincere thanks to all faculty members, who helped me directly or indirectly during my research work.

TH-994_06610404

I would like to express my sincere gratitude for the privilege of having associated with good friends like *Arun da*, *Jonali*, *Nripen*, and *Pathak*. I express my heartfelt thanks *Hariram, Mrinal,* and *Priyananda* for their cooperation.

I will cherish the friendship of *Manas, Sunil, Suraj, Jayoti, Monjit Nilotpal, Pankaj, Narayan da, Prabir da* and *Rajeev* from the very first day in Guwahati. My stay in IIT Guwahati campus, especially in A-type, has been one of the most enriching experiences of my life. Especially having vibrant, cheerful and entertaining company of *Anil and Swati* makes life more enjoyable.

I would always be indebted to my beloved wife *Amrita* and my lovely daughter *Tiya* for their unwavering support and immense affection that has enlivened my research journey.

The episode of acknowledgement would remain incomplete without mentioning the care of my parents, my sisters, my in-laws, my Jijus, *Amit*, all my nephews and nieces who are an inseparable part of my life. I owe my gratitude to all of them.

I would express my deepest gratitude to all my well wishers.

Last but not the least, I express my thanks to ***Lord Vishnu*** and ***Ma Gayatri*** for blessing me and giving the strength to complete this work.

Kumar Pallav

TH-994_06610404

Indian Institute of Technology Guwahati

Department of Civil Engineering

Doctor of Philosophy

Seismic Microzonation of Imphal City and Probabilistic Seismic Hazard Assessment of Manipur State

Abstract

Increase in damages due to earthquakes in the recent past *viz.*, Bhuj (2001), Sumatra (2004), Kashmir earthquakes (2005) etc., has woken up engineers and planners to the possibility of seismic risk in densely populated Indian cities such as Imphal city. Imphal city, the capital of Manipur state, lies in one of the most seismically active regions (i.e. Northeast region of India) of the world and hence it is of paramount importance to understand the existing earthquake hazard of Imphal city on an engineering basis. Thus, the first part of the present research effort is directed towards systematic seismic microzonation studies of Imphal city by using an engineering approach. In this study seismic sources around Imphal city have been identified from Seismotectonic atlas of India (GSI, 2000). By assembling past earthquakes into a catalogue and analyzing the database statistically recurrence relationship has been established for the region. Due to the lack of strong motion data stochastic finite fault model has been used in generating deterministic time histories for three earthquake scenarios *viz.*, 1988 Indo-Burmese (M_w 7.2) earthquakes, 1869 Cachar (M_w 7.5) earthquake in Kopilli fault, and a hypothetical Mw 8.1 event in Indo-Burmese subduction zone. Further using regional parameters e.g. stress drop, pulsing percentage, slip distribution, rupture velocity etc., ten samples of rock level acceleration time histories for

TH-994_06610404

both higher magnitude earthquakes *viz.,* the 1869 Cachar (M_w 7.5) and hypothetical (M_w 8.1) earthquakes have been simulated for Imphal city. Seismic susceptibility of Imphal city with respect to synthetically generated ten samples for both the events is presented in conjunction with nonlinear site response analysis. Site response analysis has been carried out and surface level ground motion has been determined for Imphal city for these two earthquake scenario using soil investigation data of 122 boreholes that have been collected (for the present study) from several construction projects in Imphal city. The results are presented in the form of mean and standard deviation of surface level spectral acceleration at Peak Ground Acceleration (PGA) and natural periods of 0.3 s and 1.0 s.

Further, effect of local soils has been modeled in terms of site coefficients (ratio of surface level response to the rock level response) using synthetically generated 700 earthquake time histories (based on various combinations of magnitude and distance of faults that can affect the Imphal city). These site coefficients are used in surface level probabilistic seismic hazard analysis (PSHA) by incorporating ground motion induced by each of the twenty-seven major faults of potential seven seismic zones (*i.e.,* Indo-Burmese Ranges, Eastern Himalaya, Mishmi Thrust, Shillong Plateau, Naga Disang Thrust, Bengal Basin and Assam Valley) present around Imphal city. PSHA results are presented in the form of surface level PGA and response spectra for return periods of 500 and 2500 years as recommended by IBC (2006).

As most of the sites in Imphal city come under E-type category (and hence susceptible to liquefaction) as per IBC (2006), the present study has been extended for liquefaction potential hazard studies using two indices *i.e.,* Liquefaction Potential Index (LPI) and Liquefaction Severity Index (LSI).

The liquefaction hazard map shows that a large part of Imphal city is vulnerable to liquefaction.

Finally, PSHA is extended for entire Manipur state. Here, annual frequencies of exceedance of ground motion level (expressed in terms of PGA or spectral acceleration) have been evaluated. Based on the PSHA, probabilistic hazard map has been prepared by determining the seismic hazard at 0.05° x 0.05° (~ 5.5 km x 5.5 km) grid size along EW (94°45′E to 92°58′E) and NS (25°42′N to 23°50′N) directions at rock level. In addition, Uniform Hazard Response Spectra (UHRS) have been derived for return periods of 100, 500 and 2500 years for all nine districts headquarters (*viz.*, Senapati, Tamenglong, Churachandpur, Chandel, Imphal East, Imphal West, Ukhrul, Thoubal, Bishnupur) of Manipur state.

The present study is expected to help planners and engineers for site selection and identification of vulnerable areas, design of earthquake resistant structures, and can further assist Manipur State administration in seismic hazard mitigation. In addition, the systematic procedure followed in the present research for probabilistic seismic microzonation at surface level is anticipated for easy adaptation for any city.

TH-994_06610404

List of Figures

Figure 2.1 NE India along with States and its capital

Figure 2.2a Strong motion data for earthquakes in NE India

Figure 2.2b Example strong motion record of 1988 earthquake in Indo-Burmese arc (Station: Hajadisa, India, Source: http://db.cosmos-eq.org/)

Figure 2.3 Seismic zonation map of India (Adapted from IS: 1893: 2002)

Figure 2.4 Response spectra for rock and soil sites for 5 percent damping

Figure 2.5 Steps of a probabilistic seismic hazard analysis a) Identification and Characterization, b) Recurrence relationship, c) Uncertainty Inherent in predictive relationship, and d) Parameter Exceedance value in particular time

Figure 2.6 Kelvin-Voigt solid subjected to horizontal shearing (Kramer, 2008)

Figure 2.7 One dimension system of vertical wave propagation

Figure 3.1 Imphal city with important places, rivers and transportation network (Origin (0 km, 0 km) corresponds to latitude of 24.81^0 & longitude of 93.94^0, at Kangla palace, Source: flashearth.com)

Figure 3.2 An ever developing Imphal city

Figure 3.3a Seismotectonic map of NE India along with epicenters (1866-2007)

Figure 3.3b Fault map along with fault numbers

Figure 3.4 Variation of σ_x versus time interval and magnitude

Figure 3.5 Regional magnitude-frequency relationships

Figure 3.6 Deaggregation of regional hazard in terms of fault recurrence

Figure 3.7 B-type rock site near Chingmeirong in Imphal city

Figure 3.8 Amplification function for soft rock sites

Figure 3.9 Sample slip field on rupture plane for 1988 earthquake

Figure 3.10 Comparison of simulated response spectra with SRR data of 1988 earthquake in Indo-Burmese Ranges

Figure 3.11 Sample slip field on rupture plane (a) 1869 Cachar earthquake (M_w 7.5) and (b) hypothetical earthquake in IBR (M_w 8.1)

Figure 3.12 Synthesis of ground motion due to 1869 Cachar earthquake (M_w 7.5)

Figure 3.13 Synthesis of ground motion due to a hypothetical earthquake (M_w 8.1) in the Indo-Burmese Ranges

Figure 4.1 Imphal city along with boreholes location

Figure 4.2 Soil profile, SPT-N value at a site near Langol hill

Figure 4.3 Surface level response spectra at Imphal city due to 6th August 1988 earthquake (5 % damping)

Figure 4.4 Frequency response functions of soil profiles in Imphal city

Figure 4.5 Surface level ground motion at a borehole (Figure 4.1) in Imphal city

Figure 4.6 Response spectra for one bore hole along with μ and $\mu \pm \sigma$ due to 1869 Cachar earthquake

Figure 4.7a Mean Surface level PGA due to 1869 Cachar earthquake

TH-994_06610404

Figure 4.7b Standard deviation of surface level spectral acceleration at PGA due to 1869 Cachar earthquake

Figure 4.8a Mean Surface level spectral acceleration at 0.3 s (5 % damping) due to 1869 earthquake

Figure 4.8b Standard deviation of surface level spectral acceleration at 0.3 s due to 1869 Cachar earthquake

Figure 4.9a Mean Surface level spectral acceleration at 1.0 s (5 % damping) due to 1869 earthquake

Figure 4.9b Standard deviation of surface level spectral acceleration at 1.0 s due to 1869 Cachar earthquake

Figure 4.10 Mean response spectra for all sites due to 1869 Cachar earthquake (5 % damping)

Figure 4.11a Mean surface level PGA due to hypothetical earthquake (M_w 8.1) in IBR

Figure 4.11b Standard deviation of PGA due to hypothetical earthquake (M_w 8.1) in IBR

Figure 4.12a Mean surface level spectral acceleration at 0.3 s (5% damping) due to hypothetical earthquake (M_w 8.1) in IBR

Figure 4.12b Standard deviation of surface level spectral acceleration at 0.3 s due to hypothetical earthquake (M_w 8.1) in IBR

Figure 4.13a Mean surface level spectral acceleration at 1 s (5% damping) due to hypothetical earthquake (M_w 8.1) in IBR

Figure 4.13b Standard deviation of surface level spectral acceleration at 1 s due to hypothetical earthquake (M_w 8.1) in IBR

Figure 4.14 Mean Response spectra for all sites due to hypothetical earthquake in IBR (M_w 8.1) (5 % damping)

Figure 4.15 Mean PGA distribution

Figure 4.16 Site coefficients for surface level ground motion corresponding to zero period for a typical D-Type soil

Figure 4.17 Site coefficients for surface level ground motion corresponding to zero period for a typical E-Type soil

Figure 4.18a Coefficient a_1 at PGA in Imphal city

Figure 4.18b Coefficient a_2 at PGA in Imphal city

Figure 4.18c Standard deviation at PGA in Imphal city

Figure 4.19 Ground motion at PGA in Imphal city for 0.36g (using site coefficients)

Figure 5.1 Fault rupture model

Figure 5.2 Seismic hazard curve for Imphal at rock level

Figure 5.3 Seismic hazard curve for Imphal city at rock level for eight frequencies

Figure 5.4 Comparison of IS-1893 with Uniform Hazard Response Spectra for 500 and 2500 year return periods at rock level

Figure 5.5a PGA contours with 10% probability of exceedence in 50 years (Return period= ~500 years) over Imphal city.

Figure 5.5b Short period spectral acceleration at 0.3 s with return period of 500 years over Imphal city (5% damping)

Figure 5.5c Long period spectral acceleration at 1.0 s with return period of 500 years over Imphal city (5% damping).

Figure 5.6a PGA contours with 2% probability of exceedence in 50 years (Return period= ~2500 years) over Imphal city.

Figure 5.6b Short period spectral acceleration at 0.3 s with return period of 2500 years over Imphal city (5% damping)

Figure 5.6c Long period spectral acceleration at 1.0 s with return period of 2500 years over Imphal city (5% damping).

TH-994_06610404

Figure 5.7 UHRS at surface level for 500 year return period for all sites in Imphal city (5% damping)

Figure 5.8 UHRS at surface level for 2500 year return period for all sites in Imphal city (5% damping)

Figure 6.1 Imphal city

Figure 6.2 Soil profiles at two locations 1) Mantripukhri and 2) City convention centre (see Figure 6.1)

Figure 6.3 Variation of SPT-N values, fine content and factor of safety (FS) with depth for a typical soil profile (near Langol hill)

Figure 6.4a FS against liquefaction at a depth of 1.5m for PGA= 0.16g

Figure 6.4b FS against liquefaction at a depth of 15m for PGA=0.16g

Figure 6.5a FS against liquefaction at a depth of 1.5m for PGA= 0.3g

Figure 6.5b FS against liquefaction at a depth of 15m for PGA =0.3g

Figure 6.6a Contour map of LPI against liquefaction for PGA=0.16g

Figure 6.6b Contour map of LPI against liquefaction for PGA=0.3g

Figure 6.7a Contour map of LSI against liquefaction for PGA= 0.16g

Figure 6.7b Contour map of LSI against liquefaction for PGA= 0.3g

Figure 7.1 Northeastern India (Source: Flash Earth, 13 July 2010)

Figure 7.2 Manipur state map along with grid (0.05°x0.05°) and location of district headquarters

Figure 7.3a Seismic hazard curves at district headquarters of Manipur at rock level.

Figure 7.3b Seismic hazard curves at district headquarters of Manipur (period = 0.3 s) (5% damping)

TH-994_06610404

Figure 7.3c Seismic hazard curves at district headquarters of Manipur (period = 1.0 s) (5% damping)

Figure 7.4a UHRS with 50% probability of exceedence in 50 years (return period= ~100 years) over districts of Manipur (5% damping)

Figure 7.4b UHRS with 10% probability of exceedence in 50 years (return period= ~500 years) over districts of Manipur (5% damping)

Figure 7.4c UHRS with 2% probability of exceedence in 50 years (return period= ~2500 years) over districts of Manipur (5% damping)

Figure 7.5 PGA Contours with 50% probability of exceedence in 50 years (return period= ~100 years) over Manipur

Figure 7.6 PGA Contours with 10% probability of exceedence in 50 years (return period= ~500 years) over Manipur

Figure 7.7 PGA Contours with 2% probability of exceedence in 50 years (return period= ~2500 years) over Manipur

TH-994_06610404

List of Tables

Table 2.1 Some major earthquakes in NE India in the last 1200 years

Table 2.2 Lists of selected attenuation relations

Table 2.3 Level of microzonation map as per TC4-IISMGE (1999)

Table 2.4 Site classifications as per IBC-2006

Table 2.5 Recent microzonation studies

Table 2.6 Recent Studies on microzonation in India

Table 3.1 Fault characteristics

Table 3.2 Regional *a* and *b* values

Table 3.3 Regional velocity model (Mitra *et. al.*, 2005)

Table 3.4 Input parameters in the stochastic finite fault seismological model (Ragukanth and Somala, 2009, Kayal, 2008, Nandy, 2001)

Table 4.1 Regression coefficients for typical D-type (Site-12) and E-type (Site-36)

TH-994_06610404

Table 4.2 . Average regression coefficients for D-Type and E-Type soils

Table 5.1 Distance and Magnitude scaling coefficients (Boore and Atkinson, 2008)

Table 5.2. Regression coefficients (Atkinson and Boore, 2003)

Table 6.1 Liquefiable place in Imphal city

Table 6.2 Liquefaction potential Index based on LPI (Iwasaki et. al., 1982)

Table 6.3 Liquefaction Severity Index by Sonmez and Gokceoglu (2005)

Table 7.1 Manipur districts (population, area) (Source: NEDFI)

Table 7.2 Comparison of PGA with other studies for Manipur 500 year return period

TH-994_06610404

Nomenclature

α	coefficient in Guttenberg Richter relationship, define seismicity
β	coefficient in Guttenberg Richter relationship, large and small earthquake
γ	Shear strain
δ	Standard deviation for site coefficients
η	damping coefficient
λ_m	mean annual rate of exceedance
κ_0	kappa factors
μ	mean value
υ	function of coefficient α and β
$\upsilon_Y(y^*)$	annual frequency of exceeding ground motion
$\Delta\sigma$	stress drop
ρ	crust at the focal depth
χ	Mean rate per unit time interval
$\rho(z)$	travel time weighted averages of density from surface to

TH-994_06610404

	a depth equivalent to a quarter wavelength
σ, σ_χ	Standard deviation
σ_n	total normal stress
σ'	effective normal stress
σ'_v	effective overburden pressure
σ_T,	Coefficient for attenuation relation of Boore and Atkinson (2008)
σ_v	total overburden pressure
σ_{xz}	Normal stress in x-z plane
τ	the shear resistance
ϕ	angle of internal friction
ω	frequency
Δ	near source saturation term

$A(f)$	Fourier amplitude spectrum of ground motion
$AF(f)$	amplification function
$F(f)$	Overall amplification function
$\kappa_{x'}, \kappa_{z'}$	the horizontal and vertical wave numbers
$a_{x'}, a_{z'}$	correlation lengths along-strike and down-dip direction
$\bar{N}$	average standard penetration resistance
$(CSR)_{M_w=7.5,\sigma=1.0}$	the equivalent uniform shear stress due to earthquake having a moment magnitude of M_w=7.5 and overburden pressure (σ'_v) of 1 atm.
$(N_1)_{60cs}$	Adjusted SPT-*N* equivalent to clean sand

TH-994_06610404

$(N_1)_{60}$	the corrected SPT-*N* value
$< R_{\theta\phi} >$	radiation coefficient averaged over an appropriate range of azimuths and take-off angles
a	level of seismicity in a given area
a_1, a_2	are the site coefficients
$A(t)$	ground motion acceleration
a_1 and a_2	regression coefficients for site coefficient
$A_{ij}(t)$	acceleration spectrum of shear wave
a_{max}	peak horizontal acceleration
b	relative occurrence of large and small earthquakes
b_1, b_2, b_3, b_4,….b_K	are the number of events per unit interval
C	scaling factor
c_1, c_2, c_3. M_{ref}, R_{ref} ,	Coefficient for distance scaling.
C_1, C_2 , C_3 , C_4,	Coefficients used in attenuation relationship
C_N	the correction factor for overburden pressure
C_σ	Coefficient for calculating correction factor for overburden pressure.
$D(f)$	characterizes the geometrical and anelastic attenuation in the medium
D_{fault}	the closest distance to fault surface in kms
d_i	thickness of any layer between
D_j	average final slip acting on the j^{th} subfault
e_1, e_5, e_6, e_7, M_h and σ_{TU}	Coefficient for Magnitude scaling.
f_0	corner frequency at the end of the rupture
f_{0j}	dynamic corner frequency
$f_1(M_w)$	magnitude scaling characteristics

$f_2(M_w, r, S)$	distance scaling characteristics
$f_3(F)$	effect of fault mechanism
$f_4(S)$	far-source effect of local site condition
$f_5(H_w,F,M_w,r)$	effect of hanging wall on both average horizontal and vertical ground motion
FC	Fine content
F_c	site coefficient
f_c	corner frequency
F_D	represents distance function
f_m	high frequency fall of the spectrum
F_M	magnitude scaling
F_n	fault no 'n'
FS	*factor of safety*
F_s	Site amplification
$F(z)$	Function of factor of safety
G'	geometric attenuation
g	magnitude dependent of geometrical spreading
G^*	complex shear modulus
G	shear modulus
h_f	focal depth
h	thickness
H	Hurst exponent
K	Number of interval
k	complex wave number
K_σ	correction factor for overburden pressure
L	length of the fault
L_s	Length of individual fault

TH-994_06610404

M	magnitude of the earthquake
M_0	the total seismic moment of all the subfaults
m_b	Body wave magnitude
m_m and m_u	lower and upper bound magnitudes
M_{0i}	Moment magnitude of i^{th} subfault from slip distribution
M_h	"hinge magnitude" for the shape of the magnitude scaling
M_L	Local magnitude
M_s	Surface wave magnitude
M_w	Moment magnitude
N	Number of blows in Standard penetration test
N_{60}	the corrected value for the field process with an average energy ratio of 60% of the SPT hammer
$(N_1)_{60cs}$	Adjusted SPT-N equivalent to clean sand
N_e	the number of earthquakes greater than magnitude (m)
N_i	Standard Penetration Resistance value of i^{th} layer without correction
nl	subfault along the length
N_l	No. of horizontal layer
N_m	magnitude segments
N_r	distance segments
N_{Rj}	cumulative number of ruptured subfaults by the time rupture reaches the j^{th} subfault
N_s	number of sources
nw	subfault along the width
$P(z)$	Probability function
$P(f)$	upper crust attenuation

$p[M=m_j]$	probability density functions for magnitude
$p[R=r_k]$	probability density functions for distance
$P[Y>y^*\|m_j,r_k]$	predictive relationship
p_a	atmospheric pressure taken as 100 kpa
P_i	other parameters (which may be used to characterize the earthquake source, wave propagation, path, and/or local site conditions)
Q	quality factor of the region
r	hypocentral distance
R	distance from the source to the site
R_0	minimum distance of the site from the fault
r_d	stress reduction factor that measures the attenuation of peak shear stress with depth due to non-elastic behavior of soil
r_j	the subfault distance from the site
Δt_{ij}	time delay
R_{JB}	Joyner Boore distance
$S(f)$	source spectral function
S_a	spectral acceleration
S_C, S_D and S_E	(= 0 or1) based on NEHRP *C, D and E* type soils
sl	soil linearity term
T	Duration of sample
T_n	natural period
u	pore water pressure
U, *SS*, *NS*, and *RS*	variables used for, strike-slip, normal-slip, and reverse-slip fault type
V_s	shear wave velocity in the source region

$V_s(z)$	travel time weighted averages of shear wave velocity from surface to a depth equivalent to a quarter wavelength
V_s^{30}	average shear wave velocity in top 30 meters of the soil
v_{si},	shear wave velocity ith layer (m/s)
w_s	weighting factor= $L_s/\sum L_s$, activity indicator for faults
$w(z)$	Function of depth
X	fault rupture length
Y	ground motion parameter
$Y(r,f)$	ground motion
y^*	Ground motion value
y_{br}	rock level motion)
Z_t	Coefficient, zero for interface events and one for intraslab events

AV	Assam valley
BB	Bengal basin
BIS	Bureau of Indian Standards
CPT	Cone Penetration Test
CRR	Cyclic resistance ratio
CSR	cyclic stress ratio
DGA	Design ground motion
DSHA	Deterministic seismic hazard analysis
DST	Department of Science and Technology
EH	Eastern Himalaya,
EPGA	Effective Peak Ground Acceleration

TH-994_06610404

E-W	East west
FRF	Frequency Response Function
GIS	Geographical Information System
GSHAP	Global Seismic Hazard Assessment Program
GSI	Geological Survey of India
HFT	Himalayan Frontal Thrust
HI	hazard Index
IBC	International Building code
IBR	Indo-Burmese ranges,
IMD	Indian Meteorological Department
IST	Indus Suture Thrust
LPI	Liquefaction Potential Index
LSI	Liquefaction Severity Index
MASW	Multi Channel Analysis of Surface Wave
MBT	Main Boundary Thrust
MCE	Maximum considered earthquake
MCT	Main Central Thrust
MMI	Modified Mercalli Intensity
MSF	magnitude scaling factor
MSK	Medvedev-Sponheuer-Karnik
msl	mean sea level
MT	Mishmi thrust,
ND	Naga-Disang thrust
NE	Northeastern
NE–SW	North East-South West
NGA	Next Generation Attenuation

TH-994_06610404

NH	National Highway
PGA	peak ground acceleration
PGV	Peak ground velocity
PI	Peninsular India
PSHA	probabilistic seismic hazard analysis
RIMS	Regional Institute of Medical Sciences
RSR	Response Spectra Ratio
SDOF	single degree of freedom
SMA	Strong Motion Accelerograph
SP	Shillong plateau
SPT	Standard Penetration Test
SRR	Structural Response Recorder
UHRS	Uniform Hazard Response Spectra
ZPA	Zero period acceleration

TH-994_06610404

Publications based on the work in the thesis

a) *Journals*

1. RaghuKanth, S.T.G., Singh, K.D., and **Pallav, K.** (2009), *Deterministic seismic scenarios for Imphal city,* Pure and Applied Geophysics, 166, 641-672.
2. **Pallav, K.**, RaghuKanth, S.T.G., and Singh, K.D. (2010), *Surface level ground motion estimation for 1869 Cachar Earthquake (M_w 7.5) at Imphal City*, Journal of Geophysics and Engineering, 7, 321-331.
3. **Pallav, K.**, RaghuKanth, S.T.G., and Singh, K.D. (2010), *Liquefaction Potential Status of Imphal City.* (**manuscript prepared**).
4. **Pallav, K.**, RaghuKanth, S.T.G., and Singh, K.D. (2010), *Probabilistic Seismic Hazard Assessment of Manipur State.* (**manuscript prepared**).
5. **Pallav, K.**, RaghuKanth, S.T.G., and Singh, K.D. (2010), *Seismic microzonation of Imphal City using Site Coefficients. (***manuscript prepared)**

b) *Conference*

1. Raghukanth, S.T.G., Singh, K.D., **Pallav, K.** (2008), *Microzonation of Imphal city,* In *Seminar on Indo-Myanmar Ranges in the Tectonic Framework of the Himalaya and Southeast Asia,* Manipur University.

Chapter 1

Introduction

1.1 General

In the past, India has experienced a series of destructive earthquakes like, Cacher, 1869 (M_w 7.5); Assam, 1897 (M_w 8.7); Kangra, 1905 (M_w 8.6); Bihar-Nepal, 1934 (M_w 8.4); Assam-Tibet, 1950 (M_w 8.7); Indo-Burmese, 1988 (M_w 7.2); Uttarkashi, 1991 (M_w 6.5); Latur, 1993 (M_w 6.4); Jabalpur, 1997 (M_w 6.0); Chamoli, 1999 (M_w 6.8); Bhuj, 2001 (M_w 7.6); and Kashmir, 2005 (M_w 7.4) etc. The intense damages caused due to recent earthquakes (e.g., Bhuj in 2001, Sumatra in 2004, Haiti in 2010 etc.) have attracted attention of many researchers and engineers towards the seismic safety of densely populated cities such as Imphal city. After the devastating Bhuj earthquake (26 January 2001) which caused severe losses of lives and properties, researchers and engineers in India started more extensive studies in the areas of earthquake science and engineering. In order to accommodate changes in seismic scenarios (after Bhuj earthquake, 2001 etc.), the Bureau of Indian Standard (BIS) revised its code of practice, *Criteria for Earthquake Resistant Design of Structures* IS: 1893 in 2002. In this amendment, the Indian subcontinent (~ 3.2 million km^2) has been divided into mere four seismic zones *viz.*, Zone II, III, IV,

TH-994_06610404

and V (previously five zones i.e., Zone I , Zone II, Zone III, Zone IV, Zone V) and zone factors assigned based on Maximum Considered Earthquake (MCE). In addition, only three broad types of strata *viz.,* rock and hard soil, medium soil and soft soil have been considered for response spectra recommendation, without taken into account the presence of large variations in overlaying soil types. Such small scale (~ 1:1,000,000) seismic zoning maps without consideration of detail microlevel geological and geotechnical site conditions have limited help for planners, administrators, engineers etc. associated with seismic microzonation (with map scales of the order ~ 1:5,000 or 1:1,000), especially for populated urban areas. Seismic microzonation study can assist in 1) estimating of the regional seismic hazard, 2), determining of the local geological and geotechnical site conditions, and 3), assessing probable ground response parameters on the surface on smaller scale (e.g., Ansal, 2004). Seismic microzonation maps can be broadly classified into three levels depending on its purposes and level of accuracy achieved *viz.,* 1) for city and landuse planning usage, 2) estimating possible earthquake characteristics for structural vulnerability studies in earthquake prone areas, and 3) for providing input for earthquake design codes (Marcellini *et. al.,* 1995a, 1995b; Lachet *et. al.,* 1996; Fah *et. al.,* 1997; Ansal *et. al.,* 2003; Ansal, 2002).

Past studies (e.g., Idriss and Sun, 1992; Ansal, 2004) suggest that one of the primary factors that can influence seismic safety of structures is the accurate estimation of the location (or site) specific ground motion. Ground motion characteristics can be influenced significantly by several source and site factors viz., near field effects, directivity, duration, focusing, topographical and basin effects, soil profile, water table etc. (Faccioli, 1991; Ansal, 1994, 1999; Bard, 1994; Chavez-Garcia *et. al.,* 1996; Chin-Hsiung *et. al.,* 1998; Kawase, 1998; Athanasopoulus *et. al.,* 1999; Hartzell *et. al.,* 2001). It may be noted that whilst Manipur state (including its capital, Imphal city) is located in one of the most

seismically active (i.e. Northeast India) regions in the world, to the best of author's knowledge no study has been attempted to assess surface level ground motion (and hence seismic hazard assessment). Thus the present research effort is aimed at systematic study of seismic microzonation of Imphal city to estimate surface level ground motion using both deterministic and probabilistic approaches, and probabilistic seismic hazard assessment of Manipur state.

In the present work an attempt is made to develop a new procedure for studying seismic microzonation of Imphal city (24°48' N, 93°56' E), the capital of Manipur state located at the Northeastern (NE) most part of India and adjacent to Myanmar. The Indian Standard code of practice, IS: 1893 (2002) has identified the NE region of India including Imphal city as a severe seismic hazard zone by placing it in the highest zonal level (i.e. zone V). Hence the present research is directed towards assessment of ground motion variation, considering uncertainties related to source, magnitude, distance and local soil conditions, so as to help planners and engineers for site selection and identification of vulnerable areas, design of earthquake resistant structures, and Manipur State administration in seismic hazard mitigation. The current thesis focuses on 1) development of site coefficients for Imphal city, 2) development of an approach for accurately estimating surface level ground motion probabilistically for Imphal city by making use of site coefficients, and 3) assessment of existing seismic hazard status of Manipur state, by addressing the uncertainties associated with source, medium, and site.

TH-994_06610404

1.2 Thesis Organization

The research work presented in this thesis is written in eight chapters.

1. Introduction
2. Literature review
3. Deterministic seismic scenarios for Imphal city
4. Local site effects on ground motion for Imphal city
5. Probabilistic seismic hazard estimation at surface level for Imphal city
6. Liquefaction potential status of Imphal city
7. Probabilistic seismic hazard status of Manipur State
8. Conclusions and Suggestions for further research

Chapter 1 introduces the research area with brief descriptions on the various chapters.

A detailed literature review of relevant methodologies in seismic microzonation is presented in **Chapter 2**. Lack of strong motion data for NE India is highlighted. The need for synthetic ground motion models which include major sources, paths and site features are brought out in this chapter. Methodologies and procedures associated with site characterization and estimation of ground motion are also discussed. The limitations of IS-1893 (2002) for estimation of ground motion have been critically examined. Based on the literature review it has been concluded that there is a need to adopt probabilistic analysis as an improvement over deterministic analysis for surface level seismic hazard assessment.

TH-994_06610404

In **Chapter 3**, recurrence relationship of magnitude and frequency of occurrence has been established based on Gutenberg–Richter relation by computing *'a'* (a measure of total seismicity rate) and *'b'* (a measure of likelihood of large and small earthquakes) values for each of the seven important seismic zones/blocks *viz.*, Indo-Buremse ranges, Eastern Himalaya, Mishmi thrust, Shillong plateau, Naga-Disang thrust, Bengal basin and Assam valley, identified using a catalogue of past earthquakes and seismo-tectonic map (GSI, 2000). Due to scarcity of strong motion data for NE India rock level acceleration time histories at Imphal city for 1988 Indo-Burmese (M_w 7.2) earthquakes, 1869 Cachar (M_w 7.5) earthquake in Kopilli fault, and a hypothetical event (M_w 8.1) in Indo-Burmese subduction zone have been estimated using finite-fault seismological model (Motazedian and Atkinson, 2005) based on regional parameters *viz.*, stress drop, pulsing percentage, slip distribution, rupture velocity etc.

In **Chapter 4**, seismic susceptibility of Imphal city with respect to synthetically generated ten samples for 1869 Cachar earthquake (M_w 7.5) in Kopili faults and a hypothetical earthquake (M_w 8.1) in Indo-Burmese ranges is presented. Nonlinear site response analysis (Idriss and Sun, 1992) has been carried out and surface level ground motion has been determined for Imphal city for these two earthquake scenario using soil investigation data of 122 boreholes that have been collected (for the present study) from several construction projects in Imphal city. The results are presented in the form of mean and standard deviation of surface level spectral acceleration at Peak Ground Acceleration (PGA) and natural periods of 0.3 s and 1.0 s. Effect of local soils has been modeled in terms of site coefficients (ratio of surface level response to the rock level response) using synthetically generated 700 earthquake time histories (based on various combination of magnitude and distance of faults that can affect the Imphal city). Site coefficients developed in the present study have

been computed at different periods of engineering purposes and these can be used for estimating surface level responses.

In **Chapter 5**, site coefficients computed in Chapter 4 have been used for surface level Probabilistic Seismic Hazard Analysis (PSHA) by incorporating ground motion induced by each of the twenty-seven major faults of potential seven seismic zones present around Imphal city (see Chapter 3). The attenuation relations proposed by Boore and Atkinson (2008) for strike slip, thrust and reverses fault, and Atkinson and Boore (2003) for subduction zone have been used for computing the PGA and response spectra. Uniform Hazard Response Spectra (UHRS) (defined in terms of equal probability of exceedance for all frequencies of ground motion) results are presented in the form of surface level PGA and response spectra for return periods of 500 and 2500 years as recommended by IBC (2006).

As most of the sites in Imphal city come under E-type category (and hence susceptible to liquefaction) as per IBC (2006) liquefaction potential hazard studies using two indices *i.e.,* Liquefaction Potential Index (LPI) (Iwaski *et. al.,* 1982) and Liquefaction Severity Index (LSI) (Sonmez and Gokceoglu, 2005) have been presented in **Chapter 6**, using Factor of Safety (FS) defined as the ratio of CRR (Cyclic Resistance Ratio) to CSR (Cyclic Stress Ratio) as input (Idriss and Boulanger, 2006). The results are presented in the form of liquefaction hazard contour map for Imphal city.

Finally in **Chapter 7**, PSHA is extended for entire Manipur state by estimating annual frequencies of exceedance of ground motion level (expressed in terms of Peak Ground Acceleration (PGA) or spectral acceleration). Based on the PSHA, probabilistic hazard map has been prepared by determining the seismic hazard at 0.05° x 0.05° (~ 5.5 km x 5.5 km) grid size along EW (94°45′E to 92°58′E) and NS (25°42′N to 23°50′N) directions at

rock level. In addition, UHRS have been derived for return periods of 100, 500 and 2500 years for all nine districts headquarters (*viz.*, Senapati, Tamenglong, Churachandpur, Chandel, Imphal East, Imphal West, Ukhrul, Thoubal, Bishnupur) of Manipur state.

A summary of the major conclusions from this thesis is presented in **Chapter 8.** Based on the conclusions important contributions made in the present work are listed below:

- Site coefficients have been developed by considering the uncertainties associated with local site conditions for Imphal city
- A procedure has been proposed for computing the Probabilistic Seismic Hazard at surface level using site coefficients for Imphal city.
- Probabilistic Seismic Hazard map for Manipur state has been prepared.

Few suggestions for further research are also highlighted in the same chapter.

Three appendices are added in the end of this thesis. Appendix A gives the details on general terminology related to Geology, Earthquake engineering and Seismology. Borehole data have been shown in Appendix B. Site coefficients at all 122 sites are presented in Appendix C.

TH-994_06610404

Chapter 2

Literature review

2.1 Introduction

Manipur (Capital: Imphal) is one of the 28 states of India and lies in the easternmost part of India's most seismically active Northeastern (NE) region. Manipur state is located between latitude 23°50'N to 25°42'N and has strategic importance for international trade and commerce with Southeast Asian countries. Various upcoming projects and announcements made by the state government make Manipur an ever developing state. It shares 352 km long international border with Myanmar in the east and 502 kms long state border with Nagaland state in north, Assam state in west and Mizoram state in south (Figure 2.1). As per census 2001, the population of Manipur was 2.29 million and since then the population has increased and is expected to attain 2.79 million in 2011 (DES, 2008-09). It has three National Highway (NH), *viz.*, NH-39 runs towards Myanmar through the town of Moreh in Manipur, NH-53 runs towards Silchar town of Assam, NH-150 its link Manipur to Mizoram; other state highways, such as, Imphal–Sugnu Highway, Tidim Road, Ukhrul road makes Manipur an important corridor for Southeast Asia. There are several major and minor irrigation cum hydropower projects, which include

Sinda, Thoubal and Khuga Multi-purpose projects, Loktak lift irrigation project, Khoupum dam, Imphal barrage and Sekmai barrage projects (Maisnam, 2002), besides various infrastructural projects such as rail link from Manipur to Vietnam, trilateral Highway Project between India, Myanmar and Thailand, digital connectivity of optical fiber cable link between Moreh in Manipur and Mandalay in Myanmar have been proposed (PTI, 2010) makes Manipur more vulnerable in present scenario. To cater the need of an ever developing Imphal city, many infrastructural projects such as Capitol complex, Bir Trikandrajit Flyover, Hospital buildings etc., have also been taken up. As a result of increasing population and developments activities, the seismic vulnerability of Manipur state (and Imphal city) has increased. It may be noted that this NE region of India had experience damaging earthquake in the past (e.g. 1869, 1897, 1950, 1988, etc) and there are speculation that earthquakes of similar/higher magnitude may occur in the future (Kayal *et. al.*, 2006, Cummins, 2007). Further many of the existing infrastructure were designed using the recommendation of IS codes which do not reflect any consideration to local geology, site conditions and recurrence properties earthquakes. To the best of author's knowledge there is no published report on seismic hazard studies of Manipur state /Imphal city. Hence in present research, an attempt has been made to develop a simplified procedure for microzonation of Imphal city and probabilistic seismic hazard assessment of Manipur state. It is expected that such studies are likely to help planners, designers and administration against seismic hazard. As a preamble, a review of literatures have been made in the present chapter to know the seismic status of NE India and its seismicity, strong ground motion, and attenuation relation for stable continent, active region and subduction zones. A note on development of Indian standard has also been presented. Further seismic hazard studies *viz.*, deterministic as well probabilistic approaches, local site

effects, site amplification and lastly microzonation studies are presented in brief.

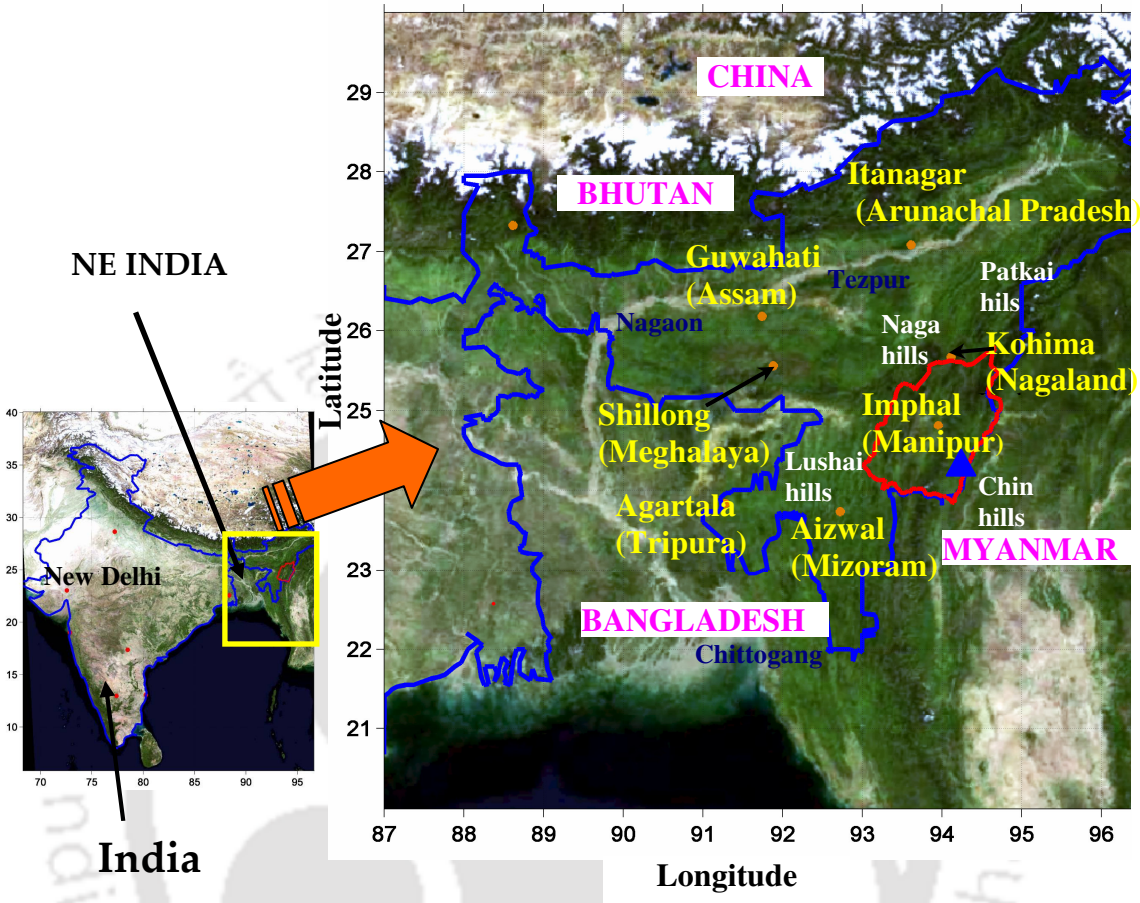


Figure 2.1 NE India along with States and its capital

2.2 Seismic status of Northeast India and adjoining regions

The Indian subcontinent can be broadly classified into three sub-regions, *viz.*, the Himalaya, the Gangetic Plain and the Peninsular Shield (Valdiya, 1976). The northeastern part of India has an exceptionally complex tectonic and geologic setup. It has the Himalayan mountain belt in the north, Mishmi hills in the west, Naga Patkoi mountain range in the south, and the Brahmaputra plain at the middle, along with the Shillong Plateau, the Burmese arc, the

Tripura folded belt, and the Surma Valley, that makes this region among most active regions of the world. The most stunning facet of this region is the sharp bend of Himalaya along the Assam syntaxis that continues towards the east of Myanmar, and joins the Andaman arc-giving rise to a complex plate boundary. Most of the earthquakes in NE India are caused due to the south–north and the west–east movement of the Indian plate (Chen and Molnar, 1990; Nandy, 2001; Kayal, 2008). There are many discrepancies on different types of seismic block present in this region. Goswami and Sarmah (1982) and Nandy (2001) had classified the region into six seismic blocks based on past earthquakes data and tectonic setting of the region *viz.,* Shillong Plateau, Assam Valley, Eastern Himalaya, Mishmi Thrust, Bengal Basin and Indo-Burmese Ranges. Further, Bhattacharya and Kayal (2003) based on seismic parameter and tectonic setting classified this region into five blocks *viz.,* Shillong plateau, Mikir hills, Lower Assam and Western Arunachal Himalaya, Upper Assam and Eastern Arunachal Pradesh and Indo-Burmese ranges. Several studies have been done so far to get an insight of seismic trends, geology, and tectonic setting of the NE India (Dutta, 1964; Tandon and Srivastava, 1975; Gyi, 1973; Verma, *et. al.,* 1976; Khattri and Wyss, 1978; Nandy, 2001; Kayal, 2008) and are still in process to understand the complexity of this region.

Several parts of the northeast India are well known for their seismicity. The first known historic event for Northeastern region occurred near Guwahati around 825-835 A.D. (M_w ~8.0) was reported by Banerji (1923) and Choudhury (1964). The summary of older earthquakes, prior to 18 century A.D. has been reported by Iyengar *et. al.,* (1999). Table 2.1 shows a list of earthquake which occurred in NE region. Oldham (1882) and Oldham (1899) have reported the damages due to two major earthquakes *i.e.,* the 1869 Cachar and the 1897 Great Assam earthquakes. Around 18 large earthquakes (Mw > 7) have

occurred during the last hundred years including the great earthquakes of Shillong (12.06.1897, M_w 8.7) and Assam-Tibet border (15.08.1950, M_w 8.6) (Oldham, 1883; Nandy, 2001; Kayal, 2008). In addition there were earthquakes of smaller magnitudes.

Table 2.1 Some major earthquakes in NE India in the last 1200 years

Date	M_w	Latitude	Longitude	Location
825-835 A.D.	~8.0	-	-	Guwahati, Assam
1548 A.D.	~7.0	-	-	Assam
1596 A.D.	~7.0	-	-	Gajala, Assam
1642 A.D.	~3.0	-	-	Assam
1649 A.D.	~3.0	-	-	Assam
1663 A.D.	-	-	-	Kajali, Guwahati
1697 A.D.	~8.0	27.8	94.5	Sadiya, Assam
1714 A.D.	~4.0	-	-	Sibsagar, Assam
1759 A.D.	~8.0	-	-	Assam
10.01.1869	7.4	25.50	91.00	Manipur
12.06.1897	8.7	25.50	91.00	Shillong, Meghalaya
04.04.1905	7.8	32.10	76.40	Manipur
02.07.1930	7.1	25.80	90.20	Meghalaya
26.06.1941	8.1	12.40	92.50	Srimongal, Bangladesh
23.10.1943	7.2	26.80	94.00	Dhubri, Assam
15.09.1950	8.6	28.38	96.76	Assam
11.12.1967	6.5	17.54	73.84	Assam
19.01.1975	6.2	32.38	78.49	Assam Tibet Border
06.08.1988	7.5	25.12	95.17	Indo-Burmese Border

The high seismicity in the region is attributed to the collision tectonics between the Indian plate and the Eurasian plate in the north and subduction tectonics

along the Indo-Burmese range (IBR) in the east. Subduction, on the other hand, is still continuing in the IBR, which is evidenced by the intermediate to deep focus earthquakes in IBR. Although several devastating earthquakes have occurred in the past (Cacher, 10.01.1869; Shillong Plateau, 12.06.1897; Srimangal, 08.07.1918; Dhubri, 02.07.1930; and Great Assam, 15.08.1950) which severely affected northeast region (Nandy, 2001; Kayal, 2008), few (1869 Cachar and 1988 in IBR) are reported to affect (due to nearer epicentral distance from Manipur) the Manipur/ Imphal city.

2.2.1. Cachar earthquake (M_w 7.5, 1869)

On 10 January 1869, an earthquake of magnitude M_w 7.5 occurred in the Kopili fault of the *Shillong-Mikir massif* with epicenter over the northern border of Jaintia hills, Meghalaya (Nandy, 2001). The felt area was about 6,65,600 sq. km. Intense damage was reported in Guwahati, Cachar, Nagaland, Manipur and Sylhet (Bangladesh). Oldham (1882) deduced an epicentral tract of 5-6 km wide and 32-48 km long, trending nearly in the E-W direction around the intersection of latitude 26°00'N and longitude 92°40'E, at the northern border of the Jaintia hills, Meghalaya. The epicentral tract was located in the Kopili gap area (Nandy, 2001), the area between the Shillong Plateau and Mikir hills. Its focal depth was estimated at 50 km. In Manipur, it is locally known as the great earthquake (*yuharaba achouba*).

2.2.2. Shillong earthquake (M_w 8.7, 1897)

The 12th June, 1897 Shillong earthquake (M_w 8.7) is considered to be the largest intraplate event in the last 200 years. Oldham (1899) postulated that the event occurred on a north-dipping thrust fault. For many years, a gentle north-dipping thrust beneath the Shillong Plateau, linked structurally to the style of Himalayan thrust faulting, was considered to be the source area (Seeber and

Armbuster, 1981; Molnar and Pandey, 1989; Kayal and De, 1991). Bilham and England (2001), based on geodetic and GPS data inferred that the 1897 earthquake was generated due to the rupture on a south dipping 110 km long reverse fault at the northern boundary of the plateau. The fault is named as 'Oldham fault' and its depth extends from 9 km to 40 km towards south. In this event several structures such as Kamakhya temple, situated on top of Nilachal hill, Barnadi bridge, Gate pillars in the boundary walls of Loki Rani's house, Telegraph Club and Old Dak Bunglow, the Commissioner's and Deputy Commissioner's offices and several other small stone bridges built in and around Guwahati were severely damaged (Rajendran *et. al.,* 2004). The then newly built railway station building of brick masonry and an old temple at the steamer *ghat* were also badly damaged (Oldham, 1899). Apart from structural damages caused due to direct shaking and soil amplification, damages due to foundation failures caused by liquefaction was also reported in several parts of Guwahati city. The Medvedev-Sponheuer-Karnik (MSK) intensity of this event at Guwahati city has been estimated to be VIII (Oldham, 1899; Ambraseys and Bilham, 2003).

2.2.3. Srimangal earthquake (M_w 7.6, 1918)

The 8th July, 1918 earthquake (M_w 7.6) occurred in the Bengal basin, also known as the Srimangal earthquake, is one of the largest earthquakes that was recorded by local seismographs, *viz.,* Bombay, Colaba and Calcutta (Kayal, 2008). The epicentre was given at 24°30'N and 91°00'E, and depth at 15 km. The maximum intensity X (Rossi-Forel scale) was reported around Srimangal (24°15'N, 91°42' E) in Sylhet district of Bangladesh. Many tea estates were cleaned out but no casualty was reported (Nandy, 2001; Kayal, 2008).

2.2.4. Dhubri earthquake (M_w 7.1, 1930)

The 2nd July, 1930 earthquake (M_w 7.1) occurred in Dhubri area of Assam. Epicentre of this earthquake was estimated at latitude 25°30'N and longitude 90°00'E. The maximum intensity was reported to be IX (Rossi-Forel scale) around Dhubri town and adjoining area. As reported by observers at different places, it preceded for a period of several seconds by a rumbling sound, which was described as 'an approaching train', 'thunder', 'passing motor car' etc. In this event no loss of life was reported and only a few instances of injuries were reported. Effect of this earthquake was felt for about 322,000 square miles extending from Dhubri to Manipur valley in the east, Patna in the west, Calcutta and Chittagong (Bangladesh) in the south, and Bhutan and Sikkim in the north (Gee, 1934; Kayal, 2008). The local geology and damage pattern depicted the N-S Dhubri or Jamuna fault to be the possible source of this event (Nandy, 2001).

2.2.5. Great Assam earthquake (M_w 8.6, 1950)

On August 15, 1950 one of the devastating earthquakes of the 20th century shook the entire NE India with the epicenter at the tri-junction of India, Burma and Tibet adjacent to the Mishmi Hills of Arunachal Pradesh in India (Tandon, 1954). Tandon (1955) and Brune and King (1967) assigned a magnitude of 8.6 based on instrumentally recorded data. This earthquake was felt over an area of about 2,892,000 sq. km. extending from Varanasi to Rangoon, further at distant places such as Norway and England where Seiches were observed in many lakes (Kvale, 1955). The earthquake intensities at various places are as follows: Intensity scale X at Sadya, Passighat, Dum Duma, Dibrugarh, North Lakhimpur, and Sibsagar; IX at Digboi and Galaghat; VIII at Tezpur, Ganhati, and Shillong; VI at Daca, Calcutta Dhubri, Darjeeling, and Imphal. This event has produced a profound change in the topography and river courses (e.g. Brahmaputra, Dihang, Dihing and Subansiri) of NE India. Severe floods

resulted from this event brought untold devastation and increasing the total casualties in NE India. Widespread collapse of buildings, slope failures, cracks and fissures with water and sand venting / liquefaction were reported (Poddar, 1950). The damages during the earthquake were mainly ascribed to the strong near-source ground motion, surface ruptures and widespread slope failures in the epicentral region. The official reports indicate that about 1,532 people were killed in the Brahmaputra valley during the earthquake (Rao, 1953).

2.2.6 Indo-Burma earthquake (M_w 7.2, 1988)

The Indo-Burma earthquake of 6th August, 1988, (M_w 7.2), occurred in the early morning (6 a.m.) in NE region. Its epicenter was located at latitude 25°07′ N, longitude 95°10′ E, depth 115 km (Kayal, 2008). The tremor was felt all over NE India, Bangladesh and parts of Myanmar. It lasted for about two minutes, and caused loss of human lives, considerable damages to buildings, railway tracts, roads etc. Field survey showed that the maximum intensity reached VIII on the Modified Mercalli Intensity (MMI) scale (Kayal, 2008). Maximum damages were reported in Jorhat, Silchar and Diphu. Landslides, formation of fissures, ejection of sand, mud and water were observed at several places. Chen and Molnar (1990) concluded the cause of the earthquake to be a mixture of strike-slip and reverse-fault mechanisms. Considering the depth and the fault-plane solution it has been inferred that this large earthquake occurred within the subducted Indian plate. The deeper focal depth provided a plausible explanation for the small number of casualties and limited damages (Pearson, 1989). This earthquake occurred caused damages in Imphal city, the capital of Manipur state e.g. some four-storied buildings in both Paona and Thangal markets tilted approximately at 1:240 slope, walls cracked and many doors and windows got jammed (Manichandra, 2007).

2.3 Strong ground motion

Damages due to large and great earthquakes can be minimized by proper planning, design and construction of infrastructure facilities by engineers and planners. This requires accurate estimation of ground motion and forces arising from possible future earthquakes at a site. As such earthquake engineers are interested mainly in strong motion information which is the shaking of the ground near the earthquake source such that structures are affected by maximum dynamic forces. The ground motion created at a point due to shaking can be measured on the surface of earth by three orthogonal components of translation motions. These ground motions depend on three parameters *viz.*, source, path and sites (Singh, 1985; Abrahamson and Silva, 1997; Abrahamson and Somerville, 1996). Several efforts have been made by seismologist, geologist and earthquake engineers to understand these near field effects (Borcherdt, 1970; Field and Jacob, 1995; Shrikhande and Gupta, 2001 etc.) on ground motion. Strong motions data are useful to simulate artificial earthquake motions for a region where data are not available. With the deployment of dense arrays of strong motion instruments (e.g. CVDT, 2008), the databases of quality strong motion records are improving. Details on various strong motion data processing techniques have been reported (Trifunac, 1972; Sunder and Conner, 1982; Sunder and Schumacker, 1982; Novikova and Trifunac, 1994; Shrikhande and Gupta, 2001; Boore *et. al.*, 2002; Raghukanth 2010). However, from engineering point of view it is important to understand the contents of ground motion characteristic (e.g. amplitude, frequency content and duration of motion) which are important for knowing the behavior of structures during earthquake. Although ground motion can be characterized in terms of PGA, in order to specify design basis earthquake to assess performance of structures, response spectrum has been suggested as preferred spectral parameter.

The concept of earthquake response spectrum was introduced by Biot in the year 1932, and has been used since then as a realistic means of characterizing ground motions and their effects on structures (Newmark and Rosenblueth, 1976). Response spectrum describes the maximum response of a linear single degree of freedom (SDOF) system for a particular input motion as a function of the natural frequency (or natural period) and viscous damping coefficient of the system. Response spectra reflect strong ground motion characteristic indirectly since they are filtered by a SDOF structure. Response spectra represent ground motion in terms of frequency domain, providing an insight about how structures made of different construction materials act under a presumed future event. The spectral values of input ground motion are generally influenced by amplitude, frequency content and duration of the motion. This generally incorporates the spectral results from several earthquakes and represents them in a kind of average spectrum (Newmark *et. al.*, 1973) for the purpose of structural design.

It may be noted that strong motion data for NE India is very sparse. The data are available for only seven events *viz.*, M_w 5.9, 1987; M_w 7.2, 1988; M_w 6.1, 1990; M_w 6.4, 1995, in IBR; and M_w 5.2, 1986; M_w 5.8, 1988; M_W 6.0, 1997 in Bengal basin and Shillong plateau). These data were recorded by an array of 45 analog accelerograms in the Shillong plateau and Assam valley area in 1985 under a Department of Science and Technology (DST) project, Kangra array in the Himachal Pradesh region, the Shillong array in the northeastern India, and the Uttarakhand array in the northwest Himalayas. (Chandrasekaran and Das, 1990, 1992, and 1994). It can be seen that out of the seven seismic block surrounding Manipur, only data from 3 blocks are available. Again, these available data are for limited distances and magnitudes (Figure 2.2a,b). The only recorded data available for Imphal city are that of SRR (Structural Response Recorder) for the 6 August, 1988 earthquake (CVDT, 2008). SRR

instrument generates a trace of the response of a laterally oscillating tuned single degree-of-freedom system, with a known damping coefficient η and natural period (T_n) corresponding to local site conditions. As such there is an urgent need of strong motion database covering a wide range of magnitudes (*i.e.*, M_w 4 to 8) and distances for seismic hazard study. In the absence of an ensemble of strong motion data, engineers face a challenging task for estimating design ground motion in NE India. This problem can be overcome largely by stochastic seismological model for NE India (Raghukanth *et. al.*, 2008; Raghukanth and Somala, 2009; Raghukanth, 2010). This method was initially proposed by Boore (1983) and further modified by Motazedian and Atkinson (2005).

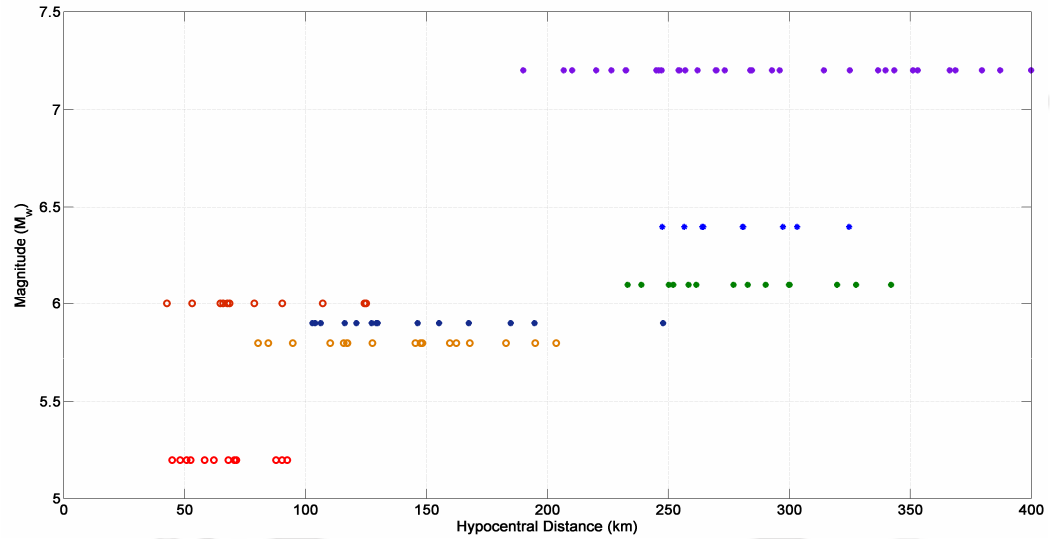


Figure 2.2a Strong motion data for earthquakes in NE India

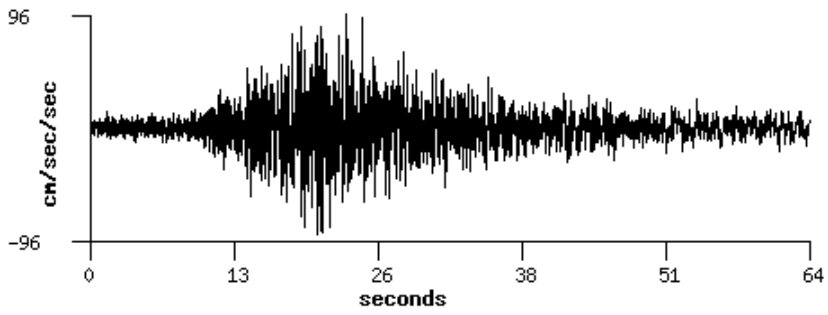


Figure 2.2b Example strong motion record of 1988 earthquake in Indo-Burmese arc (Station: Hajadisa, India, Source: http://db.cosmos-eq.org/)

2.3.1 Estimation of ground motion

In earthquake engineering estimation of seismic hazard is a challenging task that requires accurate design ground motions of a region. However, selecting design ground motion has always been difficult task owing to randomness of earthquake occurrences. Today engineers have recognized that problem of structural design and safety will not be solved by development of sophisticated ground motion simulation models alone. In addition it is necessary to have information about historical seismicity and its temporal and spatial variations. Probabilistic Seismic Hazard Analysis in which ground motion from all possible magnitude and location combinations are considered, can be used for estimating hazard (Cornell, 1968). Although source mechanism models can be used for specifying ground motion in seismic hazard analysis, but uncertainties exist in choosing appropriate source parameter. There has been considerable progress in obtaining crustal models and in developing fast and efficient algorithms for computing the ground motion, but still ambiguity exist in understanding the source process at high frequencies, which is a crucial issue in engineering problems. These problems pose a limitation to the engineers in using source mechanism models (Raghukanth, 2008) in simulating the ground motion prediction. The other problem is the computational cost involved in computing ground motion. In case of scenario earthquakes, the governing equations of motions have to be solved for each sample rupture separately. Moreover, in practice, geometrical details about faults and elastic medium properties are not available. Earthquake may also happen for sites for which there is no information on past seismicity. These reasons have compelled researcher to develop empirical models based on recorded strong motion data, following source mechanism models. These models require very little input such as magnitudes and epicentral distances which are generally known beforehand for a site. However, these models have

to be updated regularly as more strong motion data get accumulated. The following sections briefly reviews such empirical models for estimating ground motion.

2.3.2 Stochastic seismological models

Housner (1947, 1955), an earthquake engineer, was the first to propose the stochastic models for generating samples which resemble past earthquake records in a given region by recognizing random nature of the seismic source mechanisms and the resulting ground motion. The idealization of ground acceleration has been done with white noise and attributes its inconsistent appearance to irregular fault slippage followed by numerous random reflections and attenuation along the propagation path. Based on above model many investigators have proposed stochastic models by incorporating stationary and non-stationary time and frequency domains. The stationary Gaussian process models are an improvement over white noise models. The procedure essentially consists of a deterministic Fourier amplitude spectrum and a set of random phase angles. The Kanai-Tajimi (Kanai 1957; Tajimi 1960) model is one of most popular model in which power spectral density of ground acceleration is interpreted as a response of a damped single degree-of-freedom system subjected to broad-band input at its base. The simulation procedure typically consists of multiplying a deterministic modulating function with a stationary process of known power spectral density. Iyengar and Iyengar (1969) have proposed a more general modulated Gaussian stationary process. The main theme behind these models is to capture the characteristics of high-frequency motion from an average earthquake of specified size at an average site. These stochastic models were developed at a time when details about earthquake source theory and medium propagation were not well known. Through the availability of strong motion data, it became clear to researcher that high frequency ground motion cannot be modeled through deterministic approaches which make the stochastic models more popular in simulating acceleration time histories (Zerva, 1988).

Seismologists recognized the stochastic nature of high frequency ground motion and took on the above non-stationary random process model for simulating ground motion time histories and their peak values. Further, a physical model has been added to describe frequency content of ground motion. Through the Parseval theorem, Hanks and McGuire (1981) associated the root-mean-square (RMS) acceleration of the Strong motion accelerograph (SMA's) to the ω^{-2} source spectra of Brune (1970) modified by anelastic and geometric attenuation. Assuming the acceleration time history as a finite duration, band-limited, white Gaussian noise, a simple relation between PGA and RMS acceleration has been derived. Boore (1983) further extended the study for computing ground motion time histories and response spectra. Boore proposed a seismological model in which Fourier amplitude spectrum of ground motion at a site is derived in terms of source and wave propagation functions represented as a simple equation

$$A(f) = CS(f)D(f)P(f)F(f) \qquad 2.1$$

where, $S(f)$= source spectral function, $D(f)$= characterizes the geometrical and anelastic attenuation in the medium, $P(f)$ = upper crust attenuation and $F(f)$= site amplification function, C = scaling factor. The widely used source spectral function is the single corner frequency model of Brune (1970).

$$S(f) = (2\pi f)^2 \frac{M_0}{1+\left(\frac{f}{f_c}\right)^2} \qquad 2.2$$

Here the corner frequency, f_c, the seismic moment, M_0 and the stress drop, $\Delta\sigma$ are related through

$$f_c = 4.9\times10^6 V_s \left(\frac{\Delta\sigma}{M_0}\right) \qquad 2.3$$

V_s is the shear wave velocity in the source region. The diminution function $D(f)$ is defined as

$$D(f) = G^{'} \exp\left(\frac{-\pi f r}{V_s Q(f)}\right) \quad 2.4$$

Here, G' = geometric attenuation and the second term refers to the anelastic attenuation, accounting for the loss of energy along the wave path. In the above equation r = hypocentral distance and Q is the quality factor of the region defined by

$$Q(f) = Q_0 f^n \quad 2.5$$

The parameters, Q_0 and n have to be determined from past seismic recordings. The high-cut filter in the above model is given by

$$P(f, f_m) = \left(1 + (\frac{f}{f_m})^8\right)^{-1/2} \quad 2.6$$

where f_m controls the high frequency fall of the spectrum. The scaling factor, C is

$$C = < R_{\theta\phi} > \frac{\sqrt{2}}{4\pi\rho V_s^3} \quad 2.7$$

where $< R_{\theta\phi} >$ is the radiation coefficient averaged over an appropriate range of azimuths and take-off angles. The coefficient $\sqrt{2}$ in the Equation 2.7 arises from the product of the free surface amplification and partitioning of energy in orthogonal direction. The parameters in the seismological model has been selected depending on the region under consideration. The spectrum (Equation 2.1) is multiplied with the spectrum of non-stationary windowed white noise and is Fourier transformed into the time domain to generate a synthetic acceleration time history. Peak values of ground motion parameters can be obtained from the above spectrum using random vibration theory directly or by generating synthetic accelerations in time domain. With the help of such a seismological model, it is possible to generate a synthetic strong motion database by calibrating the parameters such as quality factor, stress drop and cut-off frequency to suit a particular region. This approach is helpful

for regions with no reliable strong motion records. However, stochastic seismological model has the disadvantage of representing seismic source as a point. It does not incorporate fault rupture and hence for large magnitude earthquake this model is not suitable. The model was further modified by Motazedian and Atkinson (2005), using the concept of dynamic corner frequency and pulsing subfaults. The simulation methodology takes into account finite-fault effects and is efficient in simulating acceleration time histories with few known sources and medium parameters. In the absence of ground motion data these models are helpful in simulating the synthetic ground motion.

2.4 Ground motion attenuation relationship

Attenuation relationship expresses amplitude of a given ground motion parameter as a function of magnitude & distance and are widely used in conventional seismic hazard analysis. As such attenuation relationships are regional specific. The major requirement for an attenuation relation is that it should represent broadly the seismicity of area and has to be derived from regional strong motion data.

Proper design of earthquake-resistant design of structures and facilities requires accurate estimation of the level of subjected ground shaking. Since the level of shaking is most conveniently described in terms of ground motion parameters, generally, predictive relationship expresses ground motion parameters as functions of magnitude, distance, and other variables, as

$$Y = f(M, R, P_i) \qquad 2.8$$

Here, Y is the ground motion parameter of interest, M the magnitude of the earthquake, R the distance from the source to the site, and P_i are other parameters (which may be used to characterize the earthquake source, wave propagation, path, and/or local site conditions). These relationships are

developed by regression analyses of recorded strong motion databases. Modern attenuation relations typically give natural logarithm of a ground shaking parameter such as acceleration or spectral acceleration as a function of magnitude and distance. There are a large number of attenuation relations that have been reported for different tectonic setups (Table 2.2). The attenuation relation can be classified into three categories based on its region i.e. Shallow active region, Stable region and Subduction zone (Table 2.2).

2.4.1 Shallow active region

Earthquakes that occur at shallow depth *i.e.*, less than 30 km, is known as shallow depth earthquake. Various attenuation relationships had been derived for these regions for computing the ground motion are shown below.

United States, Campbell, (1981);

$$\ln y(g) = -4.141 + 0.868M - 1.09\ln[R + 0.0606\exp(0.7M)] \quad ; \quad \sigma_{\ln PHA} = 0.37 \qquad 2.9$$

United States, Campbell and Bozorgnia, (1994)

$$\begin{aligned}\ln y(gals) = {} & -3.512 + 0.904M - 1.328\ln\sqrt{R^2 + [0.149\exp(0.647M)]^2} \\ & + (1.125 - 0.112\ln R - 0.0957M)F + (0.44 - 0.171\ln R)S_{SR} \\ & + (0.405 - 0.222\ln R)S_{HR}\end{aligned} \qquad 2.10$$

$$\sigma_{\ln PHA} = \begin{matrix} 0.889 - 0.0691M & M \le 7.4 \\ 0.38 & M > 7.4 \end{matrix}$$

United States, Campbell and Bozorgnia, (2003)

$$\ln y(g) = c_1 + f_1(M) + c_4 \ln\sqrt{f_2(M,R,S)} + f_3(F) + f_4(S) + f_5(H_W, F, R) + \varepsilon \qquad 2.11$$

Where the $f_1(M)$ magnitude scaling characteristics, $f_2(M, R, S)$ distance scaling characteristics, $f_3(F)$ effect of fault mechanism, $f_4(S)$ far-source effect of local site condition and $f_5(H_w, F, M, R)$ is effect of hanging wall on both average horizontal and vertical ground motion.

In the Indian context, Sharma (1998) derived an attenuation relation for peak ground acceleration from strong motion acceleration data available for the Himalayan region. Jain *et. al.,* (2000) have worked out an equation from three Central Himalayan earthquakes.

India, Himalayan region, Sharma, (1998),

$$\log_{10}(y) = -1.072 + 0.3903M - 1.21\log_{10}(R + 10^{0.5873M}) \qquad 2.12$$

India, Central Himalayan region, Jain *et. al.,* (2000)

$$\ln(y) = -4.135 + 0.647M - 0.00142R - 0.753\ln(R) \qquad 2.13$$

Recently, for shallow active region, Next Generation Attenuation (NGA) model has been proposed to estimate PGA, Peak ground velocity (PGV), and response spectral ordinates for periods up to 10s (Boore and Atkinson, 2008). The purpose of the NGA project was to develop empirical equations to predict main shock ground-motions in shallow crustal earthquakes in active tectonic regions. The common database used by NGA teams, consists of 3551 available multi-component records from 173 shallow crustal earthquakes worldwide, ranging in magnitudes from 4.2 to 7.9. The generalized attenuation equation proposed by NGA is as follows

$$\ln(y) = F_M(M) + F_D(R_{JB}, M) + F_S(V_{s30}, R_{JB}, M) + \varepsilon\sigma_T \qquad 2.14$$

where F_M is magnitude scaling, F_D represents distance function and F_s is Site amplification, M is moment magnitude and R_{JB} is Joyner Boore distance. Further coming to stable region, some attenuation has been shown and others are listed in Table 2.2.

2.4.2 Stable region

It is defined as regions of continental crust that have not experienced any major seismic events in the past. The following attenuation relations have been proposed for different regions:

Eastern North America, Atkinson and Boore, (1995)

$$\ln(y) = 1.841 + 0.686(M_w - 6) - 0.123(M_w - 6)^2 - \log(R) - 0.00311R; \quad 2.15$$

Eastern North America, Toro *et. al.*, (1997)

$$\ln(y) = -2.904 + 0.926M_w - 1.271\ln(R + 0.06^{0.7M_w}) - 0.00302R; \quad 2.16$$

Peninsular India, Iyengar and Raghukanth, (2004)

$$\ln(y) = 1.7816 + c2(M_w - 6) + c3(M_w - 6)^2 + \ln(R) - c4R + \ln(\varepsilon_{br}) \quad 2.17$$

2.4.3 Subduction Zone

Subduction zone is created when one tectonic plate moves beneath another tectonic plate (e.g. Indo-Burmese Subduction zone). For subduction zone preliminary studies of limited empirical databases have suggested that there are no detectable differences between ground motions among different subduction regions, for a given magnitude and distance (Crouse *et. al.*, 1988; Youngs *et. al.*, 1988; Atkinson,1997). Few relationships on subduction zones are presented below.

Youngs *et. al.*,(1997)

$$\ln y(gals) = 19.16 + 1.045M_w - 4.738\ln(R + 205.5\exp(0.0968M_w)) + 0.54Z_t \quad 2.18$$

Here Z_t is zero for interface events and one for intraslab events

Atkinson and Boore, (2003)

$$\ln Y(g) = c_1 + c_2M + c_3h + c_4R - g\log R + c_5sl\,S_C + c_6sl\,S_D + c_7\,sl\,S_E \quad 2.19$$

H=Here, h denotes focal depth in km, R is defined as $\sqrt{D_{fault}{}^2 + \Delta^2}$, where D_{fault} being the closest distance to fault surface in kms, and Δ, a near source saturation term can be computed by $\Delta = 0.00724 \times 10^{0.507M_w}$, g denotes for interface as well as in-slab events, the value for g are $10^{0.301-0.01M_w}$ (in-slab event) and $10^{1.2\text{-}0.18M}$ (interface events), which is magnitude dependence of geometrical

spreading. S_C, S_D and S_E are NEHRP (National Earthquake Hazards Reduction Program) parameter (= 0 or 1) for *C, D and E* type soils respectively, and *sl* is the soil linearity term (Dobry *et. al.*, 2000; IBC, 2006).

Table 2.2 Lists of selected attenuation relations

Tectonic Environment	**Regions**	**Attenuation Relation**
Shallow active	Western North America	Abrahamson and Silva (1997) Boore *et. al.*, (1997) Campbell and Bozorgnia (1994, 2003) Sadigh *et. al.*, (1993, 1997)
	Europe	Ambraseys *et. al.*, (1996)
	Himalaya region	Sharma (1998)
	Central Himalaya	Jain *et. al.*,(2000)
	Worldwide	Spudich *et. al.*, (1999)
	Worldwide	Boore and Atkinson (2008)
Stable region	Eastern North America	Atkinson and Boore (1995, 1997) Toro *et. al.*, (1997) Campbell (1989,1991,1997,1998)
	Europe	Dahle *et. al.*, (1990)
	Peninsular India	Iyengar and Raghukanth (2004)
Subduction	Worldwide (interface)	Youngs *et. al.*, (1997) Atkinson (1997)
	Worldwide (intraslab)	Youngs *et. al.*, (1997)
	Worldwide (intraslab, Interface)	Atkinson and Boore (2003)
	Worldwide (Undivided)	Crouse (1991a, 1991b)

The strong motion parameters are defined as either the largest horizontal component or the geometric mean (simply as the average) of the two horizontal components, with no attempt to convert between the two. If such a

conversion is necessary, the largest horizontal component can be estimated approximately from the average horizontal component by multiplying by 1.15 (Campbell, 1981; Ansary *et. al.,* 1995). All these engineering models have some limitations that results from unavailability of records, criteria used to select the recordings, theoretical assumptions used to develop the models, and seismological parameters used to define the source, path, and site effects. A review on attenuation relations for different tectonic regions of the world has been presented by Bullen and Bolt (1985) and Campbell (2003).

2.5 Indian standard code (IS: 1893, 2002)

As a step towards disaster mitigation, seismic zone maps have been proposed to mark probable intensity of ground motion in a country, for providing guidelines in design and construction of earthquake resistance structures. In India, Geological Survey of India (GSI) in 1935 proposed its first seismic hazard map, in which three zones *viz.,* severe, moderate, and slight were suggested based on probable damage scenario. Later in 1958-1959, Krishan developed four zones seismic hazard map based on PGA. In 1959, Mithal & Srivastava (Agarwal and Shrikande, 2006) classified earthquakes in India on the basis of thickness of continental shelf using geophysical data and prepared a seismic zone map of three regions as frequent earthquakes, occasional earthquakes & rare earthquakes. Earthquake resistant design of structures has become very essential in India, particularly in view of the intense construction activities all over the country. In view of this IS-1893 was prepared in 1962 to help structural design engineers for earthquake resistance structure. Here a brief overview on development of seismic zoning map of India has been presented.

2.5.1 Seismic zone map during 1962-1970

In 1960, Indian Standard Institution (ISI) constituted a multi-disciplinary committee of engineers, geologists and seismologist to prepare a code of practice to help engineers and designers for designing earthquakes resistant structures. As limited past earthquakes data were available, seismotectonic framework of the country was considered as a basis for the preparation of the zone map. These were improved by preliminary tectonic map prepared by GSI and map of epicenters of past earthquakes prepared by Indian Meteorological Department (IMD). The first zone map in 1962 had seven zones, classified on the basis of intensities in the MMI-Scale. In this the NE India was divided into two Zone i.e. Zone V (IX) and Zone VI (X and above). Manipur was placed in Zone V with an intensity of IX (second highest) in MMI scale.

In 1964, GSI published a new tectonic map for India. About the same time, correlation between magnitude and felt area had been assigned by IMD based on magnitude of earthquake histories. Based on these data modification was done in the narrow zones of MMI, V-VII around the Gujarat region. Although numbers of zones remain the same, it did enhance grades of few regions and reviewed the tectonic of some regions across India. However based on available seismic data and tectonic setup, intensities of Manipur, Tripura and Andaman were enhanced. Isoseismal grade of Satpura and Rewa earthquake were increased by taking into account of the elongated alignment of Narmada rift as a contributing tectonic feature. Isoseismal of Coimbatore earthquake was also drawn. Bellary earthquake of 1843, associated with Dharwarian strike resulted in re-orientation of isoseismal to NW-SE direction. Accounting Oldham's hypothesis of faulted coastline, Isoseismal V was redrawn. Corresponding to the trend of Western Ghat, isoseismal of Kerala region was redrawn. The profile of isoseismics map of entire Northern and northeastern region were modified in the direction parallel to the Himalayan trend. This

amalgamation resulted in reduction of Zones II and Zone III areas in the Northern region, and the extension of Zone Zero in southern part of Peninsula India in comparison to that of IS-1893: 1962.

2.5.2 Seismic zone map during 1970 -2002

After the first revision of IS-1893 in 1966, Koyna earthquake (M_w 6.5, 1967) occurred in Peninsular Shield of India. Hence, second revision of IS-1893 was taken up in 1968 to review seismic zoning map of India based on seismo-tectonic approach by recognizing geological history and tectonic nature of different areas of country. In this revision, numbers of zones were reduced from seven to five. The zones corresponding to MM intensity 'below V' and V in the previous map was changed to a single zone of MM intensity below VI and zones corresponding to MM intensities IX & X were merged to one and termed as MM intensity 'IX and above'. The new seismic zone map had four new separate islets, distinguished as zone V. An islet of zone IV encircling epicentral region of 1967 koyna earthquake was introduced in the new Western Coast seismic zone III. Based on tectonics and seismicity, seismic status of entire Assam, Mizo hills, Tripura, Manipur and northeastern part of Kashmir were enhanced by one grade and placed in intensity of X and above.

In 1984, fourth revision was introduced in which a number of important basic modifications with respect to load factor, field Standard Penetration Test (SPT) N values, base shear and modal analysis were incorporated. The average acceleration spectrum was also modified and a curve of zero percentage damping was incorporated. The earlier concept of different Zero Period acceleration (ZPA) for different damping values was changed. This edition seismically separated the country into five zones based on the probable intensity of damage (MMI) at different places. Again this zonation map was proved inadequate by the Khillari earthquake of 30th Septemeber 1993 and Bhuj earthquake (2001) in India making researcher to re-think the seismic

status of Peninsular India. The committee decided to do a pattern analysis of hazard using a combination of seismotectonics and probabilistic method. Hence another further revision of the code appeared recently in 2002 (IS-1893: 2002), wherein only four zones (Figure 2.3) have been proposed. This code assumes that all of India is susceptible to earthquakes and placed NE India in most severe zone *i.e.,* Zone V with PGA=0.36g. The previous Zone I has been merged with Zone II. The basic zone factors included herein are based on effective peak ground accelerations. Effective Peak Ground Acceleration (EPGA), is defined as 0.4 times the 5 percent damped average spectral acceleration between period 0.1 to 0.3 sec. This is taken as the Zero Period Acceleration (ZPA), for the MCE of the code and service life of structure, in each seismic zone. Smoothen average response spectra are now specified for three types of foundation strata namely, rock or hard soil, medium soil and soft soil (Figure 2.4).

2.5.3 Limitations of macro-zoning

The seismic forces are random in nature, similar to wind loads (IS-875, part 3) which is referred in terms of return period, linked with the design life of structure. In comparison, for seismic loading no such effort has been made in the IS-1893: 2002 to link earthquake return period with the design life. It may be noted that macro-zones of the IS code may be affected by errors associated with damage survey, intensity assessment, and building quality survey. Moreover considering the uncertain nature of earthquake, recommendation of fixed PGA values for different zones, covering a area of more than 3.2 million sq. km. (with a complex tectonic setup) can lead to unsafe/uneconomical design hence not adequate. It may be noted that IS:1893 zones do not reflect local geology, past earthquake data and their recurrence properties of the active faults which are required for any seismic zoning.

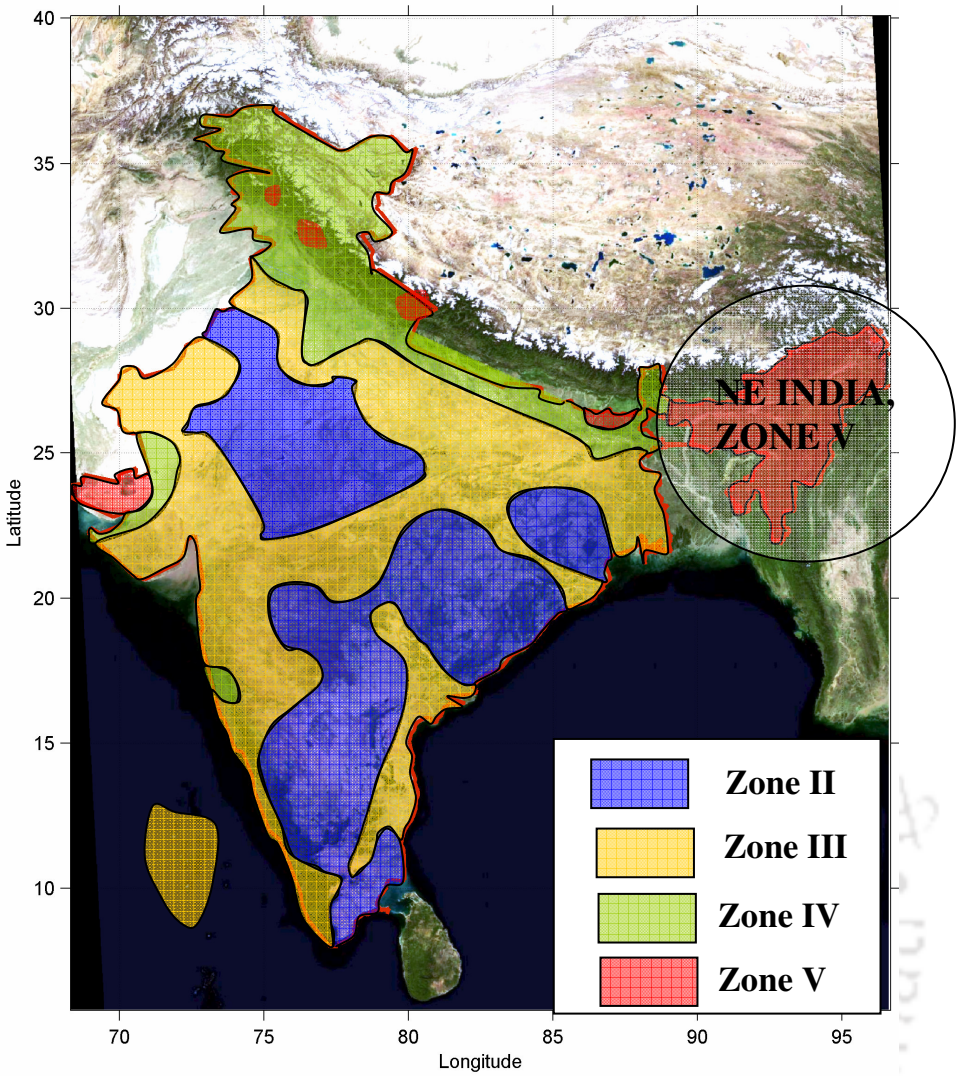


Figure 2.3 Seismic zonation map of India (Adapted from IS: 1893: 2002)

Further (de)amplification of rock level ground motion at surface level due to the presence of soil is not reflected in IS code, as hazard estimation by IS code is based on damage history. As such, the Latur-Khillari event could not be warned of by the code and only after the event the seismicity of region has been upgraded. Now it is believed that no region in India could be considered to be non-seismic. With industrialization and urbanization, seismic threat to Indian cities has to be understood more accurately. It provides neither deterministic nor probabilistic hazard assessment, carried out on a scientific basis. The macro-zonation by IS code fails to give site specific hazard (with return periods) at city level and hence not suitable for sensitive and critical

structures like nuclear power plants, dams, bridges and other important structures etc.

2.6 Seismic hazard assessment

Computation of ground motion for a particular site due to nearby seismic sources can be achieved through deterministic or probabilistic approach. Since uncertainty in occurrence is one of the distinctive features of the earthquake phenomenon, even deterministic seismic hazard assessment has to account for uncertainties to some extent. Both approaches overlap to a large extent and PSHA is in fact are an improvement over its deterministic counterpart. The key steps in Seismic hazard assessment are as follows

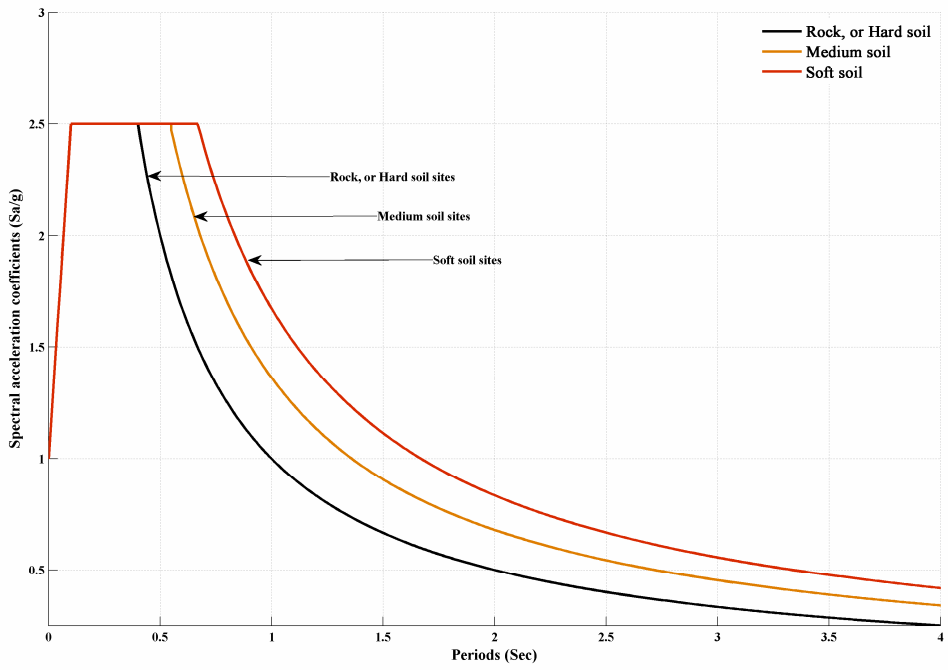


Figure 2.4 Response spectra for rock and soil sites for 5 percent damping

1. *First, identification and characterization of all earthquake sources capable of producing ground motion of sufficiently critical earthquake magnitude at the site. Source characterization includes defining source geometry, seismotectonic characteristics i.e. rate of slip, fault rupture length etc. and possible range of magnitudes. In addition to this the maximum possible magnitude (m_u) has to be fixed or estimated for each source.*

2. *Determination of frequency-magnitude recurrence relationship of regional historical earthquakes for each source.*
3. *Assessment of source to site distance for each source fault. In deterministic seismic hazard assessment the shortest distance between the faults and the site is selected as the controlling distance.*
4. *Calculation of required earthquake ground motion parameters (e.g. PGA) from the predictive attenuation relationship for each source, corresponding to* m_2.

The maximum value of PGA among all the different sources is selected as the deterministic value of PGA for the site. Peak ground acceleration or peak velocity and spectral acceleration are the commonly used parameters characterizing site ground motion. Depending on the chosen life anticipation of a structure, the characterizing magnitude with the same recurrence period is chosen on all the sources. A set of possible values of PGA at the site due to various sources is computed with the help of attenuation relationship. The maximum magnitude of this set of PGA values is chosen as the quantified hazard (Kramer, 2008).

2.6.1 Earthquake data and its completeness

For a given study period available earthquake catalogue may not be complete with respect to all magnitude values. This issue of completeness of dataset has attracted considerable attention of seismologists and earthquake engineers from time to time. It may be noted that information about large magnitude earthquakes are available for historically long periods, only in the last few decades, it has been possible to accurately record lower magnitude earthquakes. Thus it is clear that any catalogue is not likely to be complete with reference to different magnitude values. In 1972 Stepp (Shanker and Sharma, 1997) developed a method which circumvents the above problem of incompleteness data on a quantitative basis. Basically in this method data are

arranged into groups of different magnitude intervals depending on the duration in which each interval may be deemed to be complete for the region under consideration. A statistical procedure for estimation of *b*-value (*b*-value describes the relative likelihood of large and small earthquakes), by the maximum likelihood method considering both extreme and complete catalogues with different threshold magnitudes and incorporating heterogeneities in magnitudes have been proposed by Kijko and Sellevoll, (1989a, 1989b), by assuming Poisson process for occurrence of earthquakes and doubly truncated exponential distribution for earthquake magnitudes.

2.6.2 Recurrence relation

Regional recurrence relations can be established based on earthquake catalog prepared for the region of interest. Recurrence relations are crucial components of seismic hazard analysis. They are the means of defining the relative distribution of large and small earthquakes and incorporating the seismic history into the hazard analysis. A recurrence relation describes the frequency of occurrence of earthquake of particular magnitude in a given period of time. The reciprocal of the annual rate of exceedance for a particular magnitude is commonly referred to as the return period of earthquakes exceeding that magnitude. The most widely used recurrence relationship for frequency-magnitude in seismology has been proposed by Gutenberg and Richter (1944) is given below:

$$\log_{10} N_e = a - bm \qquad for\ m_m \le m \le m_u \qquad 2.20$$

Here N_e is the number of earthquakes greater than magnitude (m) per year or is the annual rate of exceedance of magnitude m, a is the seismicity of the region, and b slope of equation, describes the relative likelihood of large and small earthquakes. m_m and m_u are the lower and upper bound magnitudes

respectively, specific for seismic source. The Gutenberg-Richter relation can be used for both magnitude and intensity as descriptors of earthquake size.

2.6.3 Limitations of deterministic approach

Deterministic Seismic Hazard Analysis (DSHA) (except for the recurrence relation computation) ignores randomness of earthquake occurrences. Therefore, DSHA may lead to uneconomical or unsafe design. It may be noted that DSHA uses finite source model, which is known to be unrealistic for large magnitude values. The randomness in source to site distance (as a result of uncertainties in source location and rupture length) is ignored in DSHA Furthermore, on any given fault, depending on its potential, the future earthquake will have its magnitude distributed as a random variable with an exponential density function. DSHA overlooks this randomness in magnitude and selects a fixed magnitude value corresponding to a desired recurrence period. These limitations paved way for probabilistic approach. However, DSHA studies are helpful in understanding the ground motion for particular scenario earthquake.

2.7 Probabilistic seismic hazard assessment

An improvement in DSHA would be to incorporate all possible uncertainties into the hazard estimation procedure. Such method is called Probabilistic Seismic Hazard Assessment or PSHA. This method provides a framework in which these uncertainties can be identified, quantified, and combined in a coherent manner to provide a more complete picture of seismic hazard. In order to analyse the problems of seismic risk at a site, Cornel (1968) developed a method where point source model and predictive attenuation relation are used to get a closed form analytical solution. In this method Cornel incorporated the influence of all potential sources of earthquakes with average activity rate assigned. The results are presented in terms of PGA versus

average return period. The present practice of PSHA is described in detail in several publications *viz.*, National Research Council (1988), Earthquake Engineering Research Institute (1989), Reiter (1990), Coppersmith (1991) Kramer (2008), McGuire (2004), and Thenhaus and Campbell (2003) and is discussed briefly. The hazard associated with each source zone is estimated by integrating over all magnitudes and distances in terms of mean annual rate of exceedance (λ_m).

$$\lambda_m = \sum_{i=1}^{Ns}\sum_{j=1}^{Nm}\sum_{k=1}^{Nr} \upsilon_i P[Y > y^* \mid m_j, r_k]\, p[M = m_j]\, p[R = r_k]\, dmdr \qquad 2.21$$

where N_s, N_m and N_r are the number of sources, magnitude segments, distance segments respectively. Here, $P[Y>y^*|m_j,r_k]$ is obtained from the predictive relationship (attenuation relationship) and $p[M=m_j]$ and $p[R=r_k]$ are the probability density functions for magnitude and distance respectively.

Merz and Cornell (1973) improved the previous approach by introducing quadratic log frequency versus magnitude relationship. This work was motivated by the observation that the linear magnitude-frequency law, if untruncated, may overestimate the frequency of occurrence of large magnitude events. Cornell and Menz (1975) described a quantitative analysis of the seismic threat on rock sites of Boston city based on the above mentioned procedure. Annual risk associated with the Boston city was represented in terms of the probability that in any given year certain intensity value will be equaled or exceeded. It should be noticed that hazard assessment in the above work were based on a point source model.

The point source model assumption of earthquake is suitable for small magnitude only. For larger earthquakes, the fault rupture length will be significant and may have substantial effect on the resulting hazard assessment. The rupture on a fault during earthquake may propagate close to the site even if the epicenter is far away from the site, so that the effective source to site

distance may be lowered. This physical phenomenon is well captured in the model proposed by Kiureghian and Ang (1977). Hazard estimation model of Kiureghian and Ang assumes a logarithmic magnitude rupture length relationship and hence the two random variables *viz.*, magnitude and source to site distance, will no longer be independent as it was in the point source model. It is indicated that length of rupture zone of a large earthquake has significant escalating effect on the final calculated PGA value. Specifically the point source model may underestimate the actual hazard associated with a site. Due to the advantage of the fault rupture model over point source model it is widely accepted and included in standardized PSHA (e.g. Kramer, 2008). The PSHA may be carried out in the following four steps (Figure 2.5).

1. *Characterization of spatial uncertainty related to the seismic sources. In addition it is required to characterize the uncertainty in spatial description (e.g. point, line area sources) of each source.*
2. *Characterization of uncertainties in magnitude. The distribution of the rate of occurrence of future earthquakes for each source needs to be described as a function of magnitude.*
3. *Determination of uncertainty in ground motion attenuation for the controlling region around the site, to establish relationship amongst amplitudes of ground motion with earthquake magnitude and source to site distance.*
4. *Calculation of the seismic hazard using each combination of inputs determined in Steps 1 through 3, to plot hazard curve expressing the annual probability that a given value of ground motion will be exceeded.*

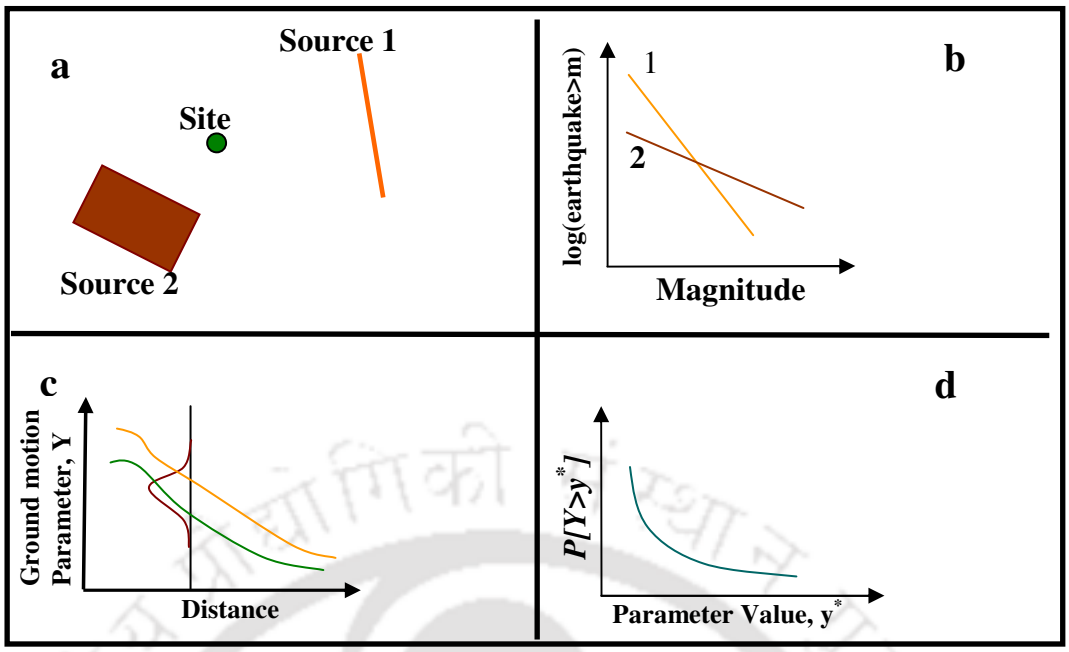


Figure 2.5 Steps of a probabilistic seismic hazard analysis a) Identification and Characterization, b) Recurrence relationship, c) Uncertainty Inherent in predictive relationship, and d) Parameter Exceedance value in particular time

2.8 Deaggregation of seismic hazard

In PSHA, the combination of the relative effects of all sources at a site is computed. In order to highlight the relative contribution of each event to the overall seismic hazard estimation, the concept of deaggregation was introduced. In common practice, overall seismic hazard is deaggregated in terms of at least two variables *i.e.* magnitude (M_w) and source to site distance (R) (Chapman, 1995; McGuire and Shedlock, 1981; Stepp *et. al.*, 1993). This can be done by computing the fractional contribution of each magnitude and distance to the final hazard. Chapman (1995) and McGuire (1995) pointed out that the value of the deaggregation to achieve an optimal earthquake event may be taken as design earthquake. The US Nuclear Regulatory Commission has identified PSHA deaggregation as one of the main elements of the seismic hazard documentation. To understand the relative contribution of seismic sources to the overall hazard Bazzurro and Cornell (1999) introduced deaggregation of the seismic hazard in terms of latitude and longitude, rather

than distance and referred this as geographical hazard deaggregation. Such geographical deaggregation provides spatial distribution of the predominant sources of seismic hazard (Halchuck and Adams, 2004; Halchuck *et. al.*, 2007; Harmsen and Frankel, 2001; Montilla *et. al.*, 2002).

2.9 Hazard estimation in NE India

In India seismic hazard is represented in terms of four zones (IS-1893: 2002). Hazard is then specified in terms of a standard response spectrum shape scaled by the zone factor, which is the expected PGA value. PGA values for these zones are given as 0.1g, 0.16 g, 0.24g and 0.36g for Zones II, III, IV and V respectively (Figure 1.2). It may be noted that the Indian subcontinent suffers from interplate as well as intraplate earthquakes events. The geological disposition of the faults and the seismotectonic setup of the Northeastern India is much more complex than the Indo-Gangetic plains and the southern part of India. For NE region, it has been pointed out that at any site there could be about 10 to 20 faults contributing to ground motion. Hence it is necessary to conduct a detail seismic hazard analysis.

The issue of seismic hazard in India was first addressed by researchers as early as 1956 at the time when three zones (*e.g.*, Severe, Moderate, and Minor) seismic map was proposed (Tandon, 1956). The basis of this map was established on a broad perception of earthquake distribution and seismotectonics of India. Several hazard studies have been attempted for Indian subcontinent e.g. Delhi, Peninsular India, Guwahati, etc., however there are limited studies for NE India in general and Manipur in particular. Khattri *et. al.*, (1984) adapted a probabilistic approach based on historical seismicity, seismotectonics and geology of the region, by dividing Indian subcontinent divided into 24 seismogenic sources and published a map of seismic hazard for northwestern India and its neighborhood region using the PGA attenuation curve of Algermissen and Perkins (1976) (which was

developed for a region in United States). Based on the analysis by Khattri *et. al.,* peak acceleration range of 0.4g - 0.45g was observed in the Manipur region of NE India. Bhatia *et. al.,* (1999) presented the results of PSHA exercise carried out under the Global Seismic Hazard Assessment Program (GSHAP) over India and adjoining regions using the attenuation relation given by Joyner and Boore (1981). PGA range of 0.4g - 0.45 g was estimated in the Manipur region for 10% probability of exceedance in 50 years by Bhatia *et. al*. It may be noted that both Khattri *et. al.,* (1984) and Bhatia *et. al.,* (1999) used a single attenuation relationship for entire India (where different tectonic setups exist), suggesting that the results are questionable.

Das *et. al.,* (2006) also proposed a new attenuation model for pseudo-spectral velocity scaling by using recorded accelerograms in Northeast India. For Imphal city, at 0.04 sec time period, the value of spectral acceleration was found to be 0.43g. However, a single attenuation relation was applied for two entirely different tectonics *i.e.,* shallow active and subduction zone (IBR), hence its validity is doubtful. Parvez *et. al.,* (2003) performed deterministic hazard analysis for entire India and came up with Design Ground Motion (DGA). Near Manipur region the values are found to be in the range of 0.15g to 0.3g. It may be noted that these PGA values cannot be linked with the lifetime of structure (not addressed in DSHA). Jaiswal and Sinha (2007) reported probabilistic based seismic hazard analysis of Peninsular India, based on attenuation relation proposed by Iyengar and Raghukanth (2004). Raghukanth *et. al.,* (2008) estimated ground motion at Guwahati city deterministically for possible future great earthquake using an improved version of the stochastic seismological model (Motazedian and Atkinson, 2005). The analysis was done for particular seismic scenario without mentioning the return period of the event. Vipin *et. al.,* (2009) estimated the peak ground acceleration and spectral acceleration of South India using

probabilistic method. Raghukanth and Dash (2010) reported result by considering the deterministic seismic hazard analysis for entire NE region of India historic earthquake that occurred in the NE region and simulated the ground motion. Among these the Cacher earthquake (M_w 7.5) produced around 0.16g PGA value in Manipur region.

2.10 Seismic microzonation

A Seismic microzonation study consists of three stages: (1) estimating the regional seismic status, (2) exploring the local geology and local soil condition of site, and (3) assessing the expected ground response and ground motion parameters (PGA, spectral acceleration) on the ground surface. The seismic microzonation is graded based on the scale of the investigation (Ansal, 2004). The technical committee on earthquake geotechnical engineering of the International Society of Soil Mechanics and Foundation Engineering (TC4-ISSMGE, 1999) classified the seismic microzonation map into three categories that as shown in Table 2.3.

Study of seismic hazard and preparation of microzonation maps can help in city planning and designing of earthquake resistant structures (e.g. Ansal, 2004). In this the study of expected earthquake ground motions at any site is estimated.

Table 2.3 Level of microzonation map as per TC4-IISMGE (1999)

Level	Scale	Basis to assess ground motion
I	1: 1,000,00 to 1:50,000	historical earthquakes and existing information of geological and geomorphological maps
II	1:1,000,00 to 1:10,000	microtremor and simplified geotechnical studies
III	1:25,000 to 1:5,000	complete geotechnical investigations and ground response analysis

The response of soil layers under earthquake excitation is computed and thus the variation of ground motion characteristics on the ground surface can be shown in the form of seismic hazard map. One of the crucial stages of seismic microzonation is geotechnical site characterization and assessment of site

response which include ground shaking intensity, amplification and liquefaction susceptibility. Use of microzonation study effectively requires an understanding of how inputs to the hazard analysis is developed, the ways in which the analysis may be carried out and the uncertainties associated with almost every parameter of the analysis. Proper handling of uncertainties is one of the major conceptual changes since Cornell introduced the method in 1968. The three factors *i.e.,* source and path characteristics, local geological and geotechnical conditions, and type of structures are the key elements of seismic hazard analysis. Evidently, all these parameter would need analysis of a huge quantity of seismological, geological, and geotechnical data. Microzonation has generally been the most established tool in seismic hazard assessment and is defined by TC4-ISSMGE (1999) as the zonation with respect to ground motion characteristics taking into account source and site conditions (Ansal, 2004). The basic intention of the site response analysis is to estimate the effect of local site conditions in assessing the site amplification with respect to ground shaking. It would be logical to base this decision on all the available results obtained from site characterization based on equivalent shear wave velocity, site response analysis as well as from microtremor measurements conducted in the region. Many parameters such as geological formations, local soil conditions, equivalent shear wave velocity, spectral amplification and their variations are amongst the controlling factors in seismic microzonation studies (Ansal, 2004).

The main purpose of microzonation is to provide local authorities for assessing the seismic risk associated with the landuse as well as to estimate the seismic ground motion to be used in the design of new structures and/or retrofitting of existing ones. The main objective of seismic zonation is to establish a seismic hazard map in a large scale taking into account, earthquake source and local site effects.

2.10.1 Local site effects

Local site conditions describe the soil that lie directly beneath the site surface to basement rock. They are usually defined in terms of surface or near-surface geology, shear-wave velocity, and the depth of sediments beneath the site. Site conditions play a major role in ascertaining the damage potential of incoming seismic waves from major earthquakes. Damage patterns in Mexico City after the 1985 Michoacan earthquake demonstrated decisively the significant effects of local site conditions on seismic response of the ground. The amplified motions had devastating effects on structures with periods close to site periods. In the 1989 Loma-Prieta earthquake, major damage occurred at soft soil sites in the San Francisco-Oakland region where the spectral accelerations were amplified 2 to 4 times over adjacent rock sites (Housner, 1989). Large Damages due to 2001 Bhuj earthquake is reported at Ahmedabad where epicentral distance located at 160 miles. The reason for the large damage is due to site amplification effects in the thick alluvial sand deposits underlying Ahmedabad (Madabhusi and Heigh, 2005). It is clear that any assessment of seismic hazard or seismic risk should incorporate the amplification effects of local soil conditions.

- ***Site coefficients***

To ascertain the effect of earthquake shaking on the ground surface, it is essential to characterize the site by evaluating shear wave velocity. The seismic site characterization for calculating seismic hazard is usually carried out based on the near-surface (30 m) shear wave velocity values. Equivalent velocity for top 30m (V_s^{30}) depth is used for site classification (IBC-2006). The equivalent shear wave velocity up to a depth of 30 m can be computed in accordance as follows:

$$\bar{v}_s = \frac{\sum_{i=1}^{n} d_i}{\sum_{i=1}^{n} \frac{d_i}{v_{si}}} \qquad 2.22$$

where v_{si}, shear wave velocity in feet per second (or m/s), d_i thickness of any layer between 0 and 100 feet (or 30480 mm). Site classification can also be classified based on SPT-N value,

$$\bar{N} = \frac{\sum_{i=1}^{n} d_i}{\sum_{i=1}^{n} \frac{d_i}{N_i}} \qquad 2.23$$

N_i is the Standard Penetration Resistance (SPT) as directly measured in the field without corrections. The classification as per IBC- 2006 is show in Table 2.4. As already mentioned above, local site conditions are typically defined in terms of shear-wave velocity (V_s).

Table 2.4 Site classifications as per IBC-2006

Site class	Soil Profile Name	Average Properties in top 30m	
		Soil shear wave velocity, $\bar{v}_s$ (m/s)	Standard penetration resistance, $\bar{N}$
A	Hard rock	$\bar{v}_s$ >1500	N/A
B	Rock	760< $\bar{v}_s$ ≤1500	N/A
C	Very dense soil and soft rock	360< $\bar{v}_s$ ≤760	$\bar{N}$ >50
D	Stiff soil profile	180< $\bar{v}_s$ ≤360	15< $\bar{N}$ ≤50
E	Soft soil profile	$\bar{v}_s$ <180	$\bar{N}$ <15

Thus, for a specific site, precise correction of the bedrock results will be possible, only when soil data is available including variation of V_s with depth. In the absence of shear-wave velocity (V_s) profiles, the N value has been used

to estimate the V_s through available correlations such as $V_s=97N^{0.314}$ by Imai and Tonouchi (1982) is applicable for all type of soils, where V_s is in m/s.

2.10.2 Site amplification

Site amplifications is the phenomenon in which amplitudes of seismic waves increase significantly when they pass through soil layers near the Earth's surface. As the seismic energy flux passes through soil layer, there is a reduction in the impedance of soil which is compensated by any increase in shaking velocity, yielding site amplification of seismic waves (Kokusho *et. al.*, 2007).

Site amplification is normally measured as the ratio of characteristic of seismic waves or spectral responses at soil versus referenced rock sites (e.g. Safak, 1997). It is a major factor influencing the extent of seismic damage to geotechnical and structural engineering systems. Therefore quantification of site amplification is a key component in mapping seismic hazard in urban areas (e.g., Frankel *et. al.*, 2000). The site amplification for these soil profiles are found by using the quarter-wavelength approximation. The amplification function is of the form.

$$AF(f) = \sqrt{\rho V_s \sqrt{\rho(z) V_s(z)}}$$

where ρ, V_s, $\rho(z)$, and $V_s(z)$ density, shear wave velocity at the bedrock, travel time weighted averages of density and shear wave velocity from the surface to a depth equivalent to a quarter wavelength respectively.

The response of site due to seismic wave can be estimated using three methods *viz.*, linear, equivalent linear and nonlinear analysis. Linear analysis is the simplest one in which it is assumed that the soil deposit consists of one uniform layer with soil stiffness either constant or varying with depth. In equivalent linear analysis, the nonlinear properties of the soil are modeled in terms of equivalent stress-strain properties. A nonlinear analysis usually

incorporates non-linear stress-strain characteristics of the soil. (e.g. GovindRaju *et. al.,* 2004).

2.10.3 Equivalent linear wave propagation

The theory considers the response associated with vertical propagation of shear waves through the linear visco-elastic system (Figure 2.6). The system consists of *N* horizontal layers, Each layer is considered as homogeneous and isotropic and is characterized by the thickness, *h*, mass density, ρ and shear modulus, *G*. The solution to the wave equation (Kanai, 1951) can be obtained through Fast Fourier Transform algorithm (Cooley and Tukey, 1965). The nonlinearity of the shear modulus and damping is accounted by the use of equivalent linear soil properties (Idriss and Seed, 1968; Seed and Idriss, 1970).

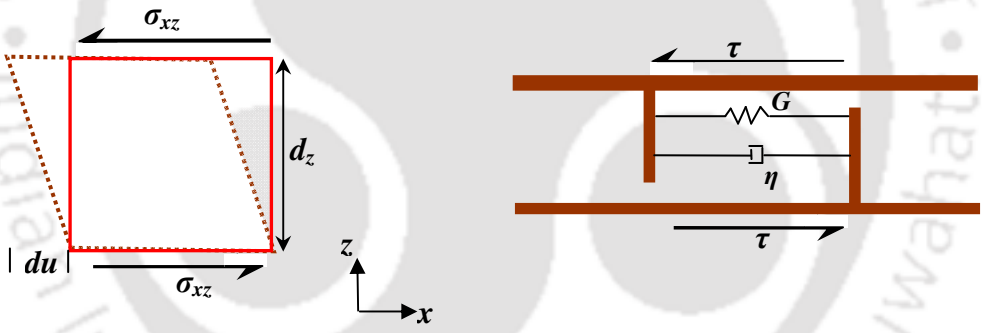


Figure 2.6 Kelvin-Voigt solid subjected to horizontal shearing (Kramer, 2008)

For the purpose of visco-elastic wave propagation, soils are usually modeled as Kelvin-Voigt solids (*i.e.,* materials whose resistance to shearing deformation is the sum of an elastic part and a viscous part) (Figure 2.6). The stress-strain relationship for such model is given as

$$\tau = G\gamma + \eta\frac{\partial\gamma}{\partial t} \qquad 2.24$$

Vertical propagation SH-waves may be represented by a stack of infinitesimal elements of the type as shown in Figure 2.7. One dimensional equation of motion for vertically propagating SH-waves can be written as in Equation 2.25.

$$\rho \frac{\partial^2 u}{\partial t^2} = \frac{\partial \sigma_{xz}}{\partial z} \qquad 2.25$$

Substituting equation (2.25) into equation (2.24) with $\tau = \sigma_{xz}$ and $\gamma = \partial u / \partial z$,

$$\rho \frac{\partial^2 u}{\partial t^2} = G \frac{\partial^2 u}{\partial z^2} + \eta \frac{\partial^3 u}{\partial z^2 \partial t} \qquad 2.26$$

The solution to the wave equation (Equation 2.26) for a harmonic motion of frequency ω is given by:

$$u(z,t) = Ee^{i(kz+\omega t)} + Fe^{-i(kz-\omega t)} \qquad 2.27$$

where the first term represents the incident wave traveling in the negative z-direction (upwards) and the second term represents the reflected wave traveling in the positive z-direction (downwards).

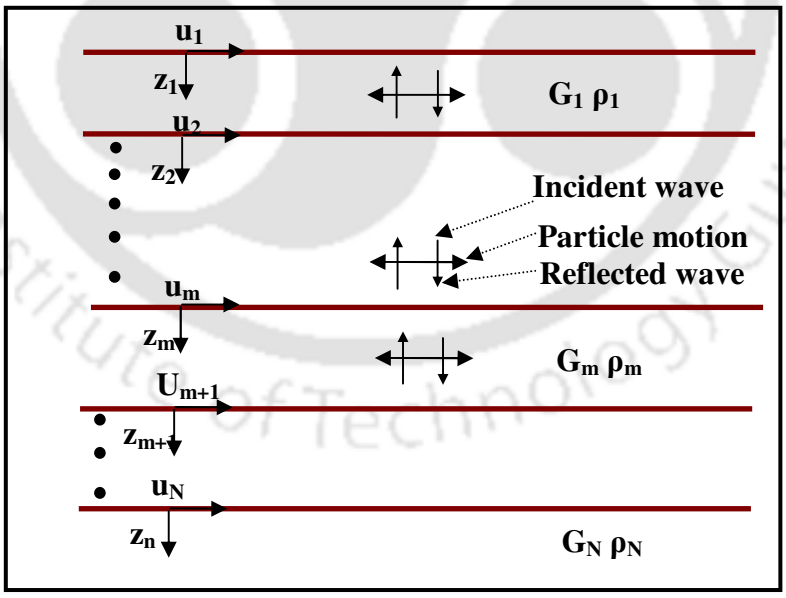


Figure 2.7 One dimension system of vertical wave propagation

2.10.4 Liquefaction potential

Liquefaction refers to the loss of strength in saturated, cohesionless soil due to the build-up pore pressures during dynamic loading. A more precise definition of soil liquefaction is given by Sladen *et. al.,* (1985): *'Liquefaction is a phenomenon wherein a mass of soil loses a large percentage of its shear resistance, when subjected to monotonic, cyclic, or shock loading, and flows in a manner resembling a liquid until the shear stresses acting on the mass are as low as the reduced shear resistance'.* Later Ishihara (1993) presented a more systematic definition of soil liquefaction as *'A state of particle suspension resulting from release of contacts between particles of sand constituting a deposit. Therefore, the type of soil most susceptible to liquefaction is one in which the resistance to deformation is mobilised by friction between particles under the influence of confining pressure'.* It has been recommended by IBC (2006) that for E and F type sites liquefaction potential analysis needs to be performed. Liquefaction is one of the most important reasons of ground failure during the earthquake. Slope failure, foundation failures etc. due to the Nigata Earthquake (M_w 7.5, 1964) in Japan and the Good Friday earthquake (M_w 9.2, 1964) in Alaska, USA, attracted several researcher (Seed and Idriss, 1982; Liao *et. al.,* 1988; Barlett *et. al.,* 1995; Harder, 1997; NCEER, 1997; Youd and Noble, 1997; Chen and Juang, 2000; Cetin *et. al.,* 2002; Juang *et. al,* 2003; Sonmez, 2003; Lee *et. al.,* 2003; Sonmez and Gokceoglu, 2005; Idriss and Boulanger, 2006; Moss *et. al.,* 2006) towards liquefaction-induced damages . The 1999 Kocaeli earthquake in Turkey (M_w 7.4) and the 2001 Bhuj earthquake in Gujarat (India) caused sand boiling; serious lateral spreading and settlement. In NE India past earthquakes *viz.,* 1869 Cachar earthquake, 1897 and 1950 Great Assam earthquake, resulted in liquefaction failure at many places (e.g. Nandy, 2001, Oldham, 1882).

- ***Liquefaction and its mechanism***

Several investigations have been made for understanding the phenomenon of soil liquefaction in the last four decades (Iwasaki *et. al.,* 1982; Seed and

Idriss, 1982; Liao *et. al.*, 1988; Prakash 1982; Prakash and Guo, 1998; Puri *et. al.*, 1996, Prakash and Puri, 2010). The liquefaction phenomena can be divided into two main sets *viz.*, flow liquefaction and cyclic mobility. Flow liquefaction can occur when the static shear stress is greater than the shear strength of the soil in its liquefied state. Cyclic mobility occurs when the static shear stress is lesser than the shear strength of the liquefied soil. It may be noted that This can flow liquefaction cause more severe damage than cyclic mobility as the deformation in flow liquefaction is relatively higher. Both clean sands and sands containing fines have been shown to be liquefiable in field (e.g., Robertson and Campanella 1985; and Holzer *et. al.*, 1989) and in laboratory (e.g., Seed & Lee, 1967 and Koester 1994). Both laboratory base assessment of liquefaction potential (e.g. Roy, 2008) and field based tests (e.g., Robertson and Campanella 1985; and Holzer *et. al.*, 1989) are available at present. Seed and Idriss (1971) proposed a basic 'simplified method' for computing Factor of Safety (FS) (defined as CSR/CRR, where CSR is Cyclic Stress Ratio and CRR is Cyclic Resistance Ratio) (in see Section 6.3.1 for details on CRR and CSR) against liquefaction. This procedure was modified and improved by several researchers (e.g., Seed *et. al.*, 1985; Youd *et. al.*, 2001; Idriss and Boulanger, 2004 and Cetin *et. al.*, 2004). Various relationships have been recommended to determine the CRR (see Section 6.3.1) of clean and silty sand. These relations have been evolved based on the differences between the boundary curves of clean and silty sands when CSR is plotted against corrected SPT blow counts. Youd et. al., (2001) and Cetin *et. al.*, (2004) proposed the most recent equivalent clean sand relations. Youd *et. al.*, (2001) mentioned that corrections based solely on fines content should be used with engineering judgment and caution. However, it has been concluded by Guo and Prakash (1999), Cascante and Santamarina (1996) and Das (2006) that ignoring the presence of fines in sand can result in erroneous interpretation as conservative according to Seed (1985)'s liquefaction assessment chart.

2.11 Seismic microzonation studies

In 1930, the first systematic large scale program to develop seismic zonation maps of an entire country and to develop microzonation maps for large cities was started in the USSR. The development of the microzonation methodology started after the first USSR zoning map appeared in 1937 (Trifunac, 1990). Seismic macro-zoning maps for a larger area such as whole country was attempted by GSHAP, 1999; Adams and Atkinson, 2003; Das *et. al.,* 2006 etc. Such macro-zonation studies reflect the presence of major fault systems or of large seismically active zones in broader scale. It may be noted that the characteristics of strong earthquake ground shaking at a site depends on numerous soil and geological features surrounding the site, however these are not reflected in macro-zonation. The microzoning maps with larger scale are preferred for city area to accommodate such fine details on a local scale (Trifunac, 1990; Todorovska *et. al.,* 1995 etc.).

Several seismic microzonation works have been reported for urban areas *viz.,* Bursa (Topal *et. al.,* 2003), Bucharest (Moldoveanu *et. al.,* 2004), Algiers (Harbi *et. al.,* 2004), Alexandria (El- Sayed *et. al.,* 2004), Beijing (Ding *et. al.,* 2004), Napoli (Nunziata, 2004), Santiago de Cuba (Alvarez *et. al.,* 2004), Sofia (Slavov *et. al.,* 2004), Zagreb (Herak *et. al.,* 2004, Panza *et. al.,* 2004), Greater Bangkok (Tuladhar *et. al.,* 2004), Las Vegas (Luke and Liu, 2008), Bam City (Motamed *et. al.,* 2007) etc. (Table 2.6). Whilst for India, seismic microzonation studies have been carried out for important cities such as Delhi (Parvez *et. al.,* 2006; Neelima, 2006, DST), Dehradun (Mahajan *et. al.,* 2007), Guwahati (Raghukanth *et. al.,* 2008; DST), Haldia (Mohanty and Walling, 2008), Bangalore (Sitharam and Anbazhagan, 2007; Anbazhagan *et. al.,* 2009), Jabalpur (DST), Sikkim (DST). Department of Science and Technology (DST) on a mission mode has taken up around 63 cities for seismic microzonation studies (Bansal and Vandana, 2007).

Table 2.5 Recent microzonation studies

Place	Author	Year
Mexico	Lermo and Chavez-Garcia	1994
Tokyo	Matsuoka and Midorikawa	1995
Bundabeg city	Turnbull	2000
Bursa	Topal *et. al.,*	2003
Bucharest	Moldoveanu *et. al.,*	2004
Algiers	Harbi *et. al.,*	2004
Alexandria	El-Sayed *et. al.,*	2004
Beijing	Ding *et. al.,*	2004
Napoli	Nunziata	2004
Santiago de Cuba	Alvarez *et. al.,*	2004
Sofia	Slavov *et. al.,*	2004
Zagreb	Herak *et. al.,* Panza *et. al.,*	2004
Greater Bangkok	Tuladhar *et. al.,*	2004b
Hanoi, Vietnam	Tuladhar *et. al.,*	2004a
Addis Ababa	Messele H.	2004
Las Vegas	Luke and Liu.	2008
Cologne, Germany	Parolai *et. al.,*	2006
Bam City	Motamed *et. al.,*	2007
Qom, Iran	Kamalian *et. al.,*	2008
Kermanshah City	Sharafi *et. al.,*	2009

The idea of microzonation is to present ground motion parameters on a scale which matches with the scale used in city planning for residential settlements. A method for seismic microzonation of metropolitan area has been presented by Lee and Trifunac (1987) based on the information on the location of active faults and their relative level of seismicity, the three dimensional geometry of the source top station, frequency dependent attenuation and local amplification of seismic wave amplitudes. This methodology has been applied for Los Angeles basin in Southern California and significant variations in peak ground velocity have been observed. Significant amplifications of long period ground motion have also been reported central region of the metropolitan area where there are considerable sediment deposits. Turnbull (2000) investigated

seismic hazard that exists in Bundabeg city of Australia and derived seismic microzonation information for the city. This study considered the effect of ground motion amplification and its associated seismic rick using microtremor measurements with a grid of 1 km. x 1 km. Matsuoka and Midorikawa (1995) performed seismic microzonation study for the Tokyo city by considering three major seismic hazards associated with earthquakes such as ground motion, liquefaction, and slope failure, in a Geographical Information System (GIS) platform. The overall hazard map has been constructed for Tokyo city by overlaying three potential maps. Lermo and Chavez-Garcia (1994) proposed microzonation of Mexico City based on 9 SMA data and 409 microtremor measurements. The synthesis of microtremor data resulted in a detailed map of the dominant period for Mexico City. Wong *et. al.,* (2000, 2002) provided probabilistic ground shaking microzonation maps for American cities *viz.*, .

.Portlan, Pregon, New Mexico, Slat Lake City and Utah. These maps were prepared for ground motion values in terms of peak horizontal acceleration and horizontal spectral acceleration at 0.2 sec and 1.0 sec periods. Their maps showed surface ground shaking by including site response effects of unconsolidated sediments. Moldoveanu *et. al.,* (2004) conducted seismic microzonation of the city of Bucharest based on the records obtained from three major earthquakes and soil layer characteristics near the station sites. Seismic microzonation results have been presented by mapping the control period of response spectra and effective peak acceleration.

For India, preliminary microzonation assessment have been carried out for cities like Jabalpur (DST, 2010), Sikkim (DST, 2010), Delhi (Parvez *et. al.,* 2006); Neelima, 2006), Bangalore (Sitharam and Anbazhagan, 2007; Anbazhagan *et. al.,* 2009), Chandigarh (Kandpal *et. al.,* 2009), Chennai (Boominathan *et. al.,* 2007) Guwahati (Raghukanth *et. al.,* 2008; DST, 2008) and Haldia (Mohanty and Walling, 2008) etc. A pilot project was initiated by DST (2010) to prepare

seismic microzonation map of Jabalpur involving GSI, IMD etc., and Jabalpur engineering college as active participants using deterministic approach. Based on the microzonation map, Jabalpur urban area has been classified into low, medium and high hazard categories. Parvez *et. al.,* (2004) performed a deterministic site specific ground motion modeling based on two soil profiles for Delhi using a hybrid technique (Fah *et. al.,* 1993, 1994) of modal summation (Panza, 1985) and finite-difference method (Virieux, 1984, 1986). The earthquake source for modeling was taken from the earthquakes of 1720 (M, 7.4) and 1960 (M, 6.0) that caused damages in Delhi city.

DST (2010) and Pal *et. al.,* (2008) initiated the work on seismic microzonation for entire Sikkim state. Sikkim has been divided six zones of hazard *viz.*, low (HI: <2.0), moderate (HI: 2.0–4.0), moderately high (HI: 4.0–6.0), high (HI: 6.0–8.0) and very high (HI:≥8.0) with their corresponding average PGA of 0.18 g, 0.23 g, 0.33 g, 0.50 g and 0.82 g respectively, based on surface geology, soil cover, slope, rock outcrop and landslide and peak ground acceleration and predominant frequency.

Neelima (2006) in her work on Delhi city divided the area into four zones based on spectral acceleration computed from data collected on Multi Channel Analysis of Surface Wave (MASW) tests from 118 sites in Delhi and estimated shear-wave velocities. The areas in the south and south central part of Delhi have been found to have very low amplification factor i.e. 1.2. In the western side of the Delhi with older alluvium, an amplification factor ranging from 1.2 to 1.8 has been observed (moderate amplification). However, the amplification factor has been found to be high in the Trans Yamuna region.

Mohanty *et. al.,* (2007) have also reported seismic microzonation map of Delhi based on GIS platform, where Delhi has been divided into 4 zones of hazards based on five thematic maps *viz.,* PGA, soil type, geology, groundwater fluctuation and bedrock depth. The four zones of vulnerability are classified as

very high, high, moderate and less in terms of seismic hazards. Very high seismic hazard zone has been assigned to areas on either side of the Delhi ridge where the maximum PGA of 0.14g to 0.22g g was observed.

Mahajan *et. al.,* (2007) presented variation of shear wave velocity in the upper 30–40 m of soil horizon of Dehradun city. Based on shear wave velocity site amplification has been reported for deterministic scenario. It may be noted that PGA has not been presented.

Raghukanth *et. al.,* (2008) deterministically estimated the ground motion at Guwahati city for an 8.1 magnitude earthquake. The earthquake was simulated synthetically on Oldham fault in the Shillong plateau by stochastic finite-fault simulation method. The peak ground acceleration (PGA) at various locations in Guwahati was computed by site response analysis. The maximum amplification for PGA over Guwahati city has been reported as high as 2.5. The liquefaction potential has also been computed based on the simulated PGA value.

The microzonation map for Guwahati was also reported by DST, (2008). According to the map, Guwahati has been classified into five broad zones of hazard, based on geology and geomorphology of city, basement depth or bedrock formations, soil, shear wave velocity, predominant frequency and surface PGA. The five zones are expressed in terms of different levels of Hazard Index (HI). The zones classified are lows (HI: ≤0.2), moderate (HI: 0.2–0.3), moderately high (HI: 0.3–0.4), high (HI: 0.4–0.5) and very high (≥0.5). The estimated value of PGA was based on deterministic approach.

Mohanty and Walling (2008) prepared seismic microzonation map based on the integration of thematic maps of PGA, predominant (resonance) frequency and elevation map. Based on the tectonic framework of the region surrounding Haldia and the past seismicity, five source zones are delineated that can affect Haldia. The ground motion in terms of PGA from the five

source zones was estimated using the attenuation relationship of Toro *et. al.,* (1997). The site-specific predominant frequency has been estimated employing the Horizontal by Vertical Spectral Ratio (HVSR) technique of Nakamura (1989). The PGA has been estimated from the five potential seismic source zones surrounding Haldia and ranges from 0.09g to 0.19 g.

Table 2.6 Recent Studies on microzonation in India

Place	Author/Agency	Year
Jabalpur,	DST	2010
Delhi	Parvez *et. al.*, Neelima Mohanty *et. al.,*	2004 2006 2007
Dehradun	Mahajan *et. al.*	2007
Sikkim,	DST, Pal *et.al.,*	2010,2008 2008
Bangalore	Sitaram and Anbazhagan	2007
Guwahati	Raghukant *et. al.,* DST	2008 2008
Haldia	Mohanty and Walling	2008
Chennai	Boominathan *et.al.,*	2007
Chandigarh	Kandpal *et.al.,*	2009

Anbazhagan and Sitaram (2008) carried out the microzonation study of Bangalore city. Based on large number of borehole data with SPT '*N*' values site characterization of Bangalore has been attempted using measured shear wave velocity from Multichannel Analysis of Surface Wave. Based on 30 m average shear wave velocity of soil, Bangalore has been classified as "Site class D" as per NEHRP and IBC. Theoretical 1-D site response study showed that the amplification factor falls in the range of 1 to 4.7 and with predominant frequency variation from 3 to 12 Hz.

Boominathan *et. al.,* (2007) used the DSHA approach for seismic microzonation Chennai city. The result of the ground response analysis has been represented by characteristic site period contours ranging from 0.25 – 0.83 s for the city (for the controlling earthquake of M_w 4.4). The Spectral Acceleration Ratio (SAR)

i.e., the ratio of spectral acceleration at the surface to the bedrock contours, for a typical period of 0.5 s has also also plotted. Higher amplification (> 3) has been obtained in the central and southern parts of Chennai city due to the presence of deep soil sites with clayey or sandy deposits.

Based on geotechnical approach, Kandpal *et. al.,* (2009) performed site response studies around Chandigarh using 24 boreholes, each of 30 m depth Shear wave velocities of the subsurface layers were computed and found to be less than 216 to 305 m/s.

In the above studies for India microzonation studies have been attempted considering the deterministic scenario (i.e. based on worse seismic event that affected the city in the past), without no reports of linking PGA values to the design life of the structure (required for economical and safe design).

2.12 Conclusions

NE India was severely affected by earthquakes in the past (e.g. Cachar earthquake, 1869, Shillong earthquake, 1897, Assam earthquake, 1950, Indo-Burma earthquake, 1950 etc.) and due to increase in population and infrastructure in recent time, the risk associated with earthquake hazard has increased in terms of death, injury, infrastructural damage, and economic loss as a whole. To deal with such seismic hazard, engineers, administrations and insurance companies require variation of seismic hazard at micro level as macro-level zonation (e.g. the current zonation recommended by IS: 1893) map may not provide detailed information in such situation. Review of literature shows that regional geology plays an important role on the characteristics of ground motion (e.g. Bell *et. al.,* 1987; Legget, 1987; Hake, 1987; Rau, 1994; Dai *et. al.,* 1994; 2001; Van Roy and Stiff, 2001). Therefore macro-level seismic

zonation map for entire country may not be suitable for detailed seismic hazard assessments of cities. This necessitates the development of microzonation maps for cities for detailed seismic hazard analysis (e.g. Seed and Schnabel, 1972; Ansal, 2004 etc.). This seismic microzonation maps are vital for city planners, designers as well as administrations for placing and planning of critical and important structures like subways, bridges, highways, dam sites, hospitals, nuclear power plants sites etc. It may be noted that many large cities around the world (e.g. Kermanshah, Qom, Bangalore, Delhi etc.) have developed seismic microzonation maps and further improvements based on recent developments in earthquake engineering are being attempted for better results. Tables 2.5 and 2.6 show the details of studied conducted for different city.

A brief literature review on seismic hazard study of India has been presented in this chapter shows that practicing engineers in India uses four basic PGA values (i.e. 0.10g, 0.16g, 0.24g, 0.36g for Zones II, III, IV and V respectively) for the whole country recommended by IS-1893. Using four blanket values of PGAs in designing structures in a large region (~ 3 million sq. km.) such as Indian subcontinent, ignoring geological inhomogeneity, tectonic history, soil conditions etc. is irrational and dangerous. It may be noted that inaccurate estimation of PGA values may lead to unsafe or uneconomical designs. Hence, a seismic hazard assessment/zonation at micro-level based on rigorous and sound engineering approach is a pre-requirement for earthquake resistant design and construction of civil engineering structures.

It has been seen from literature review that most of the studies which have been reported for India are based on deterministic approach (DSHA) i.e. for a particular seismic scenario the ground motion has been estimated (e.g. Parvez *et. al.* 2004, Raghukanth *et. al.,* 2008, DST, 2008) whereas those who have attempted PSHA, conducted their study up to rock level only (e.g. Khatri *et. al,*

1984; Iyengar and Ghosh, 2004). As mentioned in Section 2.6.3, DSHA approach has the main limitation of non-consideration of uncertainties associated with earthquakes, whereas PSHA takes into account of various uncertainties in earthquake parameters like source location, rupture length, distance of source from site etc. Hence it has been inferred that PSHA is a promising method for seismic risk studies (Tuladhar *et. al.,* 2004). In this research a procedure for performing seismic microzonation study at the surface level has been presented by considering uncertainties related to source, source to site distance, and local soil conditions (and hence a probabilistic approach). It may be noted that Sitaram and Anbazghan (2008) and Anbazhagan and Sitharam (2008), also presented a similar procedure for seismic microzonation study of Banglore city. An attempt has also been made to extend PSHA for Manipur state. Preparation of seismic hazard maps of vulnerable cities like Imphal city is expected to raise awareness levels amongst public and governmental agencies for hazard mitigation. Further, these seismic hazard maps will help law enforcers for suitable by-laws in land use planning and construction.

TH-994_06610404

Chapter 3

Deterministic seismic scenario for Imphal city

3.1 Introduction

Previous chapter on literature review shows that the requirement for adopting the seismic microzonation assessment procedures for densely populated Indian city like Imphal. By this ground motion variation can be estimated for future seismic events on small-scale microzonation maps. Before preparing seismic hazard map of any city, it is essential to know the seismotectonics details incorporating identification of sources, seismicity, past earthquakes etc. around the study area. In the present chapter all the information concerning to seismic setups and seismicity in and around Imphal region are discussed. The important seismic sources around Imphal and adjoining areas have been identified and recurrence relations have been established. Based on deaggregation results synthetic ground motion for Imphal city has been simulated by stochastic finite fault model proposed by Motazedian and Atkinson (2005) for two earthquake events *i.e.,* 1869 Cachar earthquake (M_w 7.5) and hypothetical earthquake (M_w 8.1) in IBR, to make up for the lack of strong motion data. These rock level acceleration time histories for 1869

TH-994_06610404

Cachar (M_w 7.5) earthquake and hypothetical M_w 8.1 event in the IBR have been used as an inputs in subsequent chapters for microzonation study of Imphal city.

3.2 About Imphal city

Imphal city (24°48' N, 93°56' E), the capital of Manipur state forms the central part of the oval shaped Imphal valley. Compared with other cities of India, the development growth of Imphal city has been very slow for various political (unstable law and order) and geographical (limited and unreliable outside connectivity) reasons. However, in the recent years, an increase in population density in and around Imphal has been observed. As per 2001 census the population of Imphal city is about 0.25 million (10 % of the entire state's population) which is about 26.04 % growth from the last census of 1991. The population density in Imphal city is registered at 7,202 persons per sq. km which is much higher than the state density of 97 persons per sq. km. It has been estimated that the population will continue to grow in Imphal with a decadal growth rate stabilizing at around 10% for the next few decades (City development plan, http//:manipur.nic.in). The physiographic character of Imphal city has considerable influence on its population growth pattern. Major growth has taken place in the central area, and towards the south along the highways which is shown in Figure 3.1 and 3.2 (plotted using images taken from Google Earth/flash earth after geo-referencing with a minimum four points). The growth at the outskirts of Imphal city has been limited due to agricultural landuse. The city is below the high flood level of Imphal, Nambul and Kongba rivers. Imphal city encompasses several important national road networks *viz.*, Maosongsang-Imphal-Sibong road (National Highway (NH) 39), and Imphal-Oinamlong Road (NH 53), Parbung-Imphal-Jessami road (NH 150); river networks *viz.*, Nambul, Imphal and Kongba rivers; Tulihal airport; educational institutions *viz.*, Regional Institute of Medical Sciences (RIMS),

Manipur University (MU), state administrative blocks, *viz.* Manipur state assembly, High court, Manipur secretariat, Head post office, various government departments etc; Hospitals viz., RIMS, Jawaharlal Nehru (JN) hospital, Sija hospital etc., Sports complex, viz., Khuman Lampak multipurpose stadia, Sports Authority of India (SAI) complex etc; historical places, *viz.*, Museum, palaces, temples etc.

In spite of the fact that several earthquakes have occurred in the past, there is a lack of proper documentation of the damages caused by earthquakes in Manipur that happened prior to 1869. Probably the earliest documented earthquake is that of 10th January 1869 which caused widespread damage in Imphal city. In the literature this is referred to as the '1869 Cachar earthquake' (Oldham, 1882). The 6th August 1988 earthquake which occurred in Indo-Burma region also caused notable damages in Imphal city. These events occurred at a time when the population as well as infrastructure facilities in Imphal were limited in nature. Due to increase in the population in recent times, the local government has taken up several important infrastructural building programmes *viz.*, construction of BT flyover (Bir Tikendrajit), ongoing construction of city sewerage system, city convention centre, capitol buildings, high court, widening of roadways, rail link from Manipur to Vietnam, trilateral Highway project between India, Myanmar and Thailand, digital connectivity of optical fibre cable link between Moreh in Manipur and Mandalay in Myanmar (PTI, 2010) etc. As such the vulnerability of Imphal city to damaging earthquakes has increased.

If the aforementioned earthquakes of 1869 and 1988 (see Section 2.2) were to repeat in future, they are likely to cause severe damages to infrastructures as well as increased human causalities. In view of this it is pertinent to understand the seismic hazard of Imphal city to large earthquake events.

TH-994_06610404

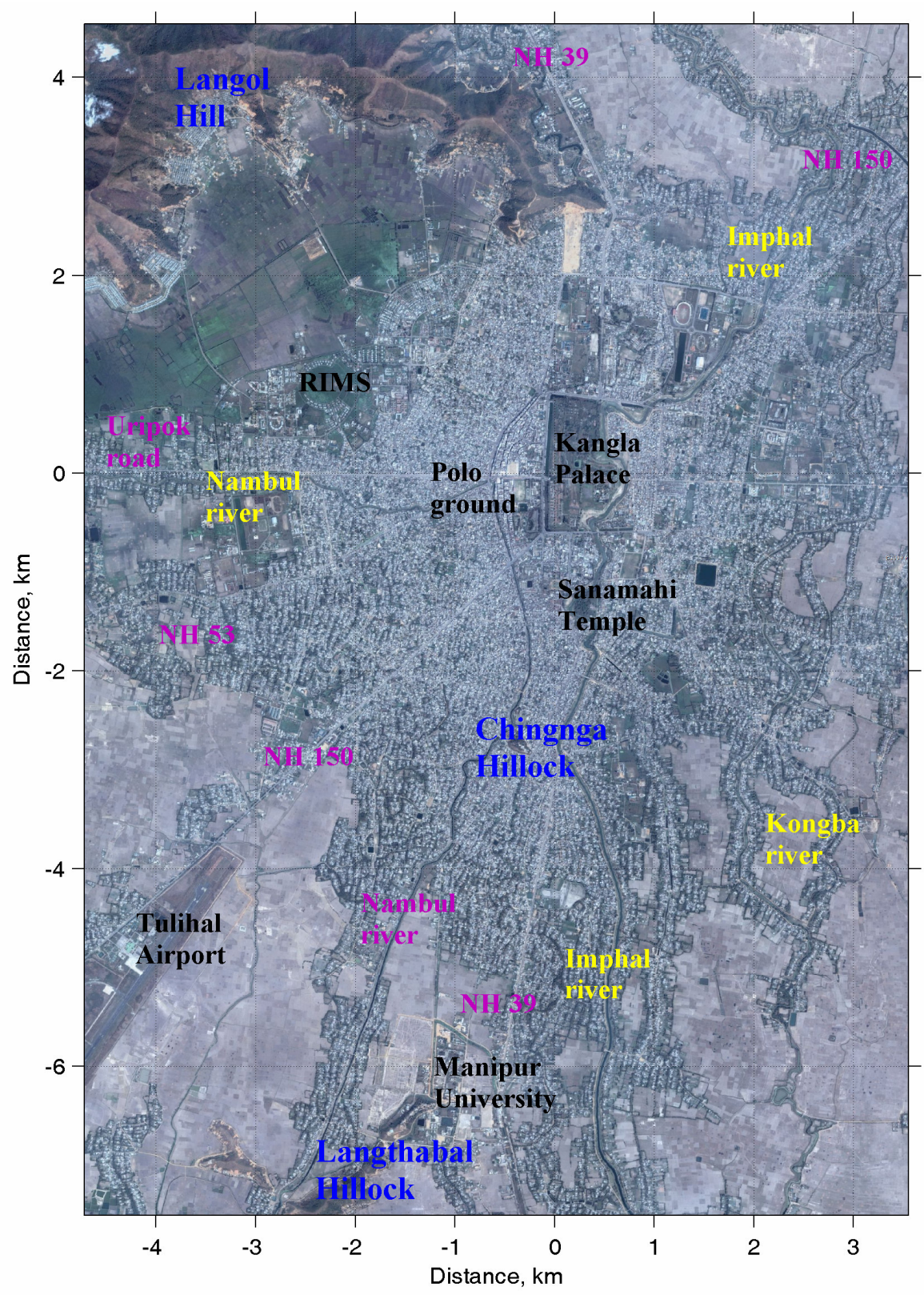


Figure 3.1 Imphal city with important places, rivers and transportation network (Origin (0 km, 0 km) corresponds to latitude of 24.81^0 & longitude of 93.94^0, at Kangla palace, Source: flashearth.com)



Figure 3.2 An ever developing Imphal city

3.3 Seismic status of Imphal city

The past seismicity data shows that NE region has experienced more than 2000 earthquakes of magnitude, $M_w \geq 4.0$, in a period of 140 (1866-2007) years. These earthquakes have their origin to both the crustal as well as the subduction zone, both of which are close to Imphal (< 300 km). In seismic hazard assessment, the first step is to identify the probable seismic sources around a given site, and hence seismotectonic features in a broad region around Imphal have been identified and prepared from the seismotectonic atlas of India (GSI, 2000). Figure 3.3a shows that almost the entire region around the Imphal city is surrounded by faults. These faults attribute to tectonic activity in the region, which is mainly due to the interaction between north-south convergence along the Himalayan boundary, and east-west convergence along the IBR (discussed in Chapter 2). Based on the seismotectonic features and geology NE India is broadly divided into seven seismic zones. These are 1) Indo-Burmese Ranges (IBR), 2) Eastern Himalaya (EH), 3) Mishmi Thrust (MT), 4) Shillong Plateau

(SP), 5) Naga-Disang thrust (ND), 6) Bengal basin (BB), and 7) Assam Valley (AV) (Goswami and Sarmah, 1982 and Nandy, 2001).

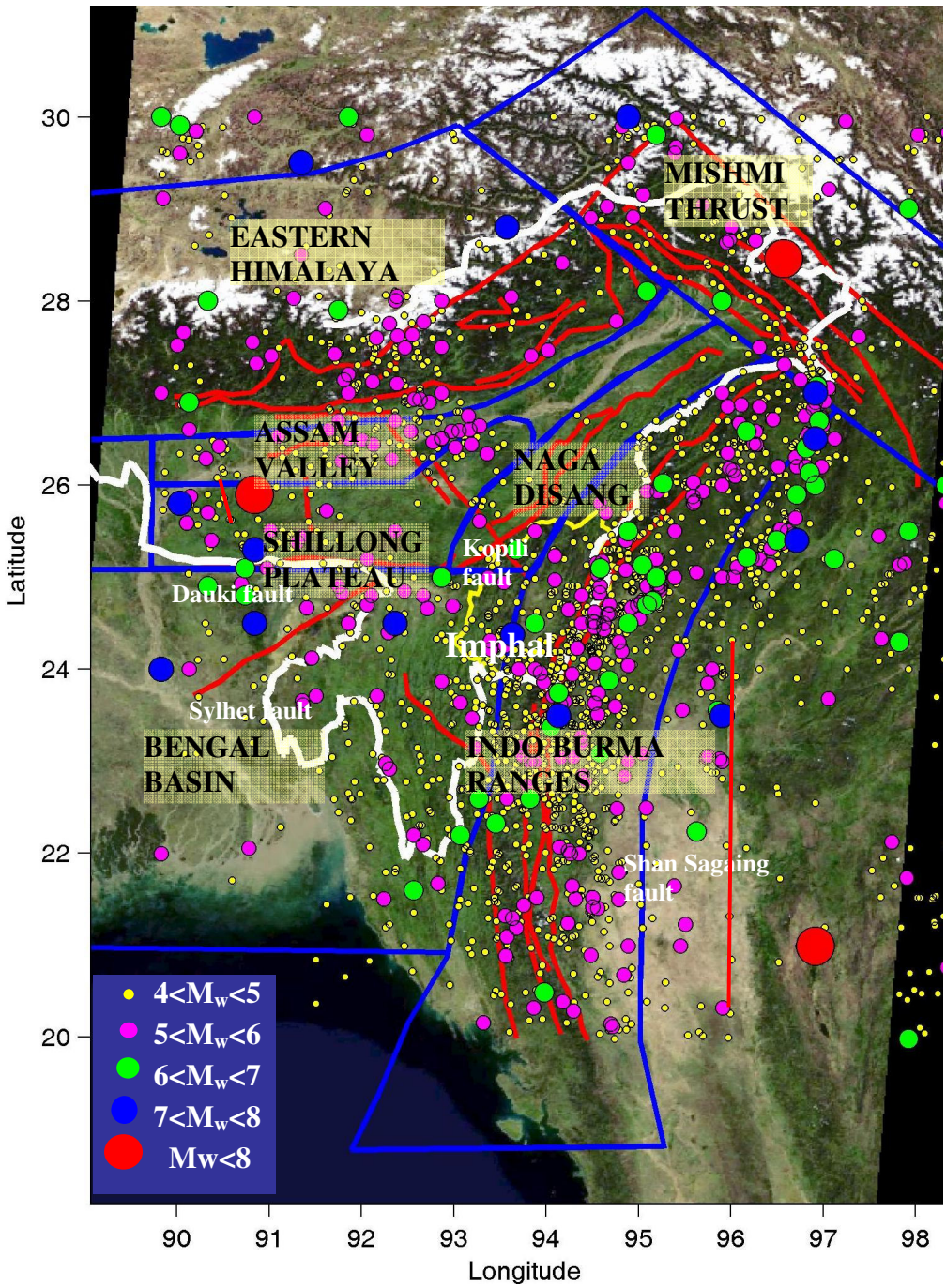


Figure 3.3a Seismotectonic map of NE India along with epicenters (1866-2007)

Brief descriptions of these seven zones are described in the following subsection (3.3.1-3.3.7). Among these tectonic blocks IBR, ND, SP and BB, are

closer to Imphal city, which makes the city more susceptible to the earthquakes originating in these seismic zones.

3.3.1 Indo-Burmese Ranges

The Indo-Burmese ranges are situated in a diverse tectonic environment with leaning subduction towards its western part, Sagaing fault on the eastern part, Mishmi thrust in the north, and the Andaman spreading ridge towards south. The Burmese arc is convex in westward direction having approximately 1100 km long plate boundary running in north-south direction. The Sagaing fault that runs parallel to the Indo-Burmese ranges separates the Shan plateau to farther east (Figure 3.3a). The ranges in IBR are Arakan-Yoma, Chin and Naga hills which pass through northeast direction to join with the Himalayas. In the southern direction, the ranges continue into the Andaman and Nicobar islands and have width of around 150 km in its central part. Several theories have been proposed about the evolution of the IBR *viz.,* 1) Eastward subduction of Indian plate in the Eurasian plate (Mitchell and McKerrow, 1975), 2) Sea-floor spreading (Curray and Moore, 1974; Curray *et. al.,* 1979 and Mitchell, 1981), 3) spreading under the Andaman Sea (Tapponnier *et. al.,* 1982) etc. It is generally agreed that IBR is a subduction zone characterized by high seismicity (Satyabala, 2003). The focal depth of earthquake events gradually increasing towards the east with depth between 30-45 km beneath the Bengal basin and it gradually increases to 40-160 km beneath the IBR. The eastern boundary fault (Kabaw fault) and Sagaing faults are two major discontinuities identified in the Indo-Burmese region. The Kabaw fault is a major tectonic break between the Indo-Burmese ranges and the Burmese Basin. Several damaging earthquakes have occurred in the past within the IBR (Le Dain *et. al.,* 1984; Satyabala, 2003) as discussed in Section 2.2.

3.3.2 Eastern Himalaya

Major thrust/fault systems are on both sides of the entire length of the Himalayan arc including the northeastern Himalaya *viz.,* the Indus Suture Thrust (IST), the Main Central Thrust (MCT), the Main Boundary Thrust

(MBT) and the Himalayan Frontal Thrust (HFT). Further, the northeastern Himalaya may also be subdivided into four major units from north to south *viz.,* the Trans-Axial Himalaya, the Central Himalaya, the Lesser Himalaya and the Outer Sub-Himalaya (Kayal, 2008). At the MBT, the Indian plate is under constant thrust by the Lesser Himalaya at shallow angles (Gansser, 1964; Fitch, 1970; Molnar *et. al.,* 1973; Ni and Barazangi, 1984; Baranawaski *et. al.,* 1984); at the Burmese ranges the Indian plate dips at angles of 30°-60° and is seismically active down to depths of 150-200 km (Ni *et. al.,* 1989; Kayal, 1996). The Burmese plate which lies between the Burmese arc and Sagging fault is compressed northward by the leaning subduction (Mitchell and McKerrow, 1975; Curray *et. al.,* 1979; Ni *et. al.,* 1989; Curray, 1989). These movements makes Eastern Himalaya zone as one of the most tectonically active regions in the world. Though definite ages of various fold movements in the northeastern Himalaya are not known, intensive fold movements in the Trans Himalaya region started during Cretaceous and still continue (Chang Ta, 1963).

3.3.3 Mishmi Thrust

The Mishmi thrust also known as the eastern Himalaya syntaxis, located at the trijunction region of the Indian plate, the Eurasian plate, and the Burmese plate, connects the MBT in the Himalaya with the Burmese arc (Curray, 1989). The major discontinuities identified in the Mishmi block are the Mishmi thrust, Lohit thrust, and Po Chu faults (Nandy, 2001). Chandra (1978) suggested that the Himalayan edge of the Assam syntaxis was formed due to the deformation of the Indian plate within the angular wedge comprised of the Indus- Tsangpo suture zone and aseismic lineaments in the eastern part of NE India. These syntaxis zones are also the locations of high stress concentrations due to the influence of seismic forces associated with both the Eastern Himalayas and Burmese ranges. The Mishmi block is considered as a special zone of seismic activity with block tectonics (Gansser, 1966; Dutta, 1964). The great 1950 Assam earthquake occurred within this syntaxis region. Armijo *et.*

al., (1989) suggested that the 1950 earthquake involved right-lateral slip which is consistent with their hypothesis that right-lateral slip on the Jiali-Po-Qu fault zone in southeast Tibet around the eastern Syntaxis is connected with the right-lateral strike slip motion on the Sagaing fault. The Mishmi hills occur at the junction of the northeastern Himalaya and the Indo-Burmese ranges. The Himalayan arc takes a sharp turn of about 90° and meets the Indo-Burmese ranges. The frontal Mishmi thrust overrides the Quaternary sediments of the Mishmi foot hills and finally truncates the Indo-Burmese fold belt and associated thrust system (Acharyya *et. al.,* 1986).

3.3.4 Shillong Mikir Massif

The Shillong-Mikir massif forming a NE propagation of the Indian shield occurs as a pivot to the west of the Naga hill and to the south of the Eastern Himalayas (Kayal, 2008). It is considered as a part of the peninsular India, which moved to the east along the Dauki fault with an average elevation of about 1000 m above sea level. In south Shillong-Mikir massif (or Shillong) plateau is limited by the 320 km long E-W Dauki fault system and to the west by the Jamuna and Dhubri faults. Within the plateau region, the contact between the tertiary sediments to the southwest and the Archaean gneiss to the northeast is demarcated by the 100 km long NW-SE trending Dapsi thrust, a northwest extension of the Dauki fault (Kayal and De, 1991; Nandy, 2001, Kayal, 2008). Oldham (1899) reported that a 20 km long NW trending fault, called Chedrang fault was formed by the great Shillong earthquake of 1897 within the Shillong plateau (about 10 m vertical displacement was observed during the earthquake). The Mikir hills are detached from the plateau by the NW-SE tending Kopili fracture zone called the lineament (a linear topographic feature). This 300-400 km long Kopili lineament crosses the Assam valley and reaches to the MBT. The lineament also transverses to the Himalayan trend, running parallel to the Bomdila lineament in the Arunachal Himalaya. This active tectonic feature is known as Kopili gap and lies between the Shillong Plateau and the Mikir hills. The NW–SE-trending Kopili fault separates Shillong plateau from its fragmented Mikir hills. This fault was responsible for

the damaging 1869 Cachar earthquake (Oldham, 1882; Nandy, 2001). Locally it is known as the great earthquake (*yuharaba achouba*). *Cheitharol Kumpapa* (the royal chronicle of the kings of Manipur) records that the aftershocks of this event was continued for the next three days and then alternately for about 10 days (Sarangthem, 2005; Ningthoukhongjam, 2005). Evans (1964) inferred right-lateral strike-slip movement on this fault and suggested that 200 km or more of right-lateral displacement occurred on this fault since Miocene to separate the plateau from the Indian shield. Evans suggested that the Dauki fault to be a tear fault extending only through the upper crust. Many researchers (e.g. Murthy *et. al.,* 1969; Desikachar, 1974; Dasgupta, 1977; Rao, 1983; Hiller and Elahi, 1984; Khan *et. al.,* 1988), on the other hand, emphasized vertical displacement across the fault. Molnar (1987) suggested of a rupture involving large thrust faulting on a plane dipping gently northward. Kailasam (1979) reported a relative uplift of the Shillong Plateau of the order of 2.5 cm in 70 years. The Shillong Plateau, Mikir massif and the Brahmaputra valley together is called *Foreland Spur* (Evans, 1964). Recently, Bilham and England (2001) suggested 'pop-up tectonics' for the Shillong Plateau bounded by two reverse faults, the north dipping Dauki fault to the south and WNW-ESE tending, south dipping deep seated 'Oldham fault' at the boundary of the plateau and the Brahmaputra valley. From the geodetic observations it has been argued that the Shillong Plateau rose violently by at least ~ 10 m during the 1897 great earthquake, due to a burried reverse fault and named it Oldham fault which is approximately 110 km in length and dipped steeply away from the Himalaya.

3.3.5 Naga Disang Thrust

The Naga hills situated in the northeast part of the IBR consist of an entire Tertiary sequence of Eocene (around 56 million) to Pliocene (around 5 million) rocks and is called a *Belt of Schuppen* (Evans, 1964). Having more than eight overthrusts along which the rocks moved northwestwards relative to the basements *ancient crystalline rock*. In this thrusts form a complex pattern of one thrust overriding the other. This elongated belt having a width of around 14

km presents a homogeneous pattern of overthrust masses. The northwestern edges resemble closely the upper Assam alluvial boundary for over 350 km, and finally end near Halflong to the south. The northwestern margin of the Belt of Schuppen is called the Naga Thrust which is made up of a series of different thrusts. The total horizontal movement of the thrusts exceeds 200 km (Evans, 1964). Khattri and Wyss (1978) termed the upper Assam valley *aseismicity* as the *Assam Gap* with possibility for a future large earthquake. In this *Assam Gap* since 1548 there has been no record of any medium or large earthquake (Bapat *et. al.*, 1983). A survey performed on microearthquakes concluded that the elongated zone is *aseismic* or very low active (Kayal, 1987; Kayal and De, 1991). Kayal (1989 and 1996) and marked it as an *Aseismic Corridor*. The corridor runs parallel to the Naga thrust in the east and ends at the Dauki fault to the south. The deadly Killari earthquake (M_w 6.3, 1993) in the so called stable region of peninsular India makes it difficult to call any part of the Indian sub-continent as *aseismic* (Kayal, 1998). The recent digital network data shows some earthquake activities along the Kopili fault/Mikir hills region and it is speculated that in near future some damaging earthquakes may occur in this regions.

3.3.6 Bengal Basin

The *Bengal Basin* is one of the largest linear troughs in the world formed by the accumulation and subsequent compression of sedimentary rock strata in the basin. It is situated at the western foreland part of the Indo-Burmese mobile belt that contains thick deposit of tertiary sediments under the cover of Ganga–Brahmaputra alluvium (Nandy, 2001). It is of interest to note that it contains nearly 15 km thick sediments (Evans, 1964; Talukdar, 1982). Several significant stages in the geological history can be identified to this region, i.e., collision of Indian plate with Eurasian plate, uplift and erosion of the Himalaya in the Tertiary–Quarternary, transport of the eroded materials by the Ganges and Brahmaputra rivers, and deposition of the sediments in the newly formed Bengal geosynclines (Curray and Moore, 1971; Johnson *et. al.*, 1976; Curray *et. al.*, 1982). This basin occupies eastern part of West Bengal,

TH-994_06610404

entire Bangladesh and NE part of the Bay of Bengal. The Sylhet fault is the most active fault in this region. The area is getting smaller with time as a consequence of the eastward subduction of the Indian plate beneath the Andaman-Burmese arc (Curray *et. al.,* 1979). The most interesting tectonic zone is the *Eocene Hinge* zone of the Bengal basin. This narrow elongated zone separates the thick Post-Eocene sediments in the east from the shelf zone of the west (Evans, 1964). The Hinge zone is atleast 500 km long. Its width varies from 25 km in the north to 110 km in the central part and 35 km in the south. Curray *et. al.,* (1982) suggested that the Hinge line represents the boundary between the continental crust and the young oceanic crust that extends southwards into the Bay of Bengal. Based on surface wave analysis of teleseismic events, Brune and Singh (1986) have advocated continent like crust beneath the Bay of Bengal.

3.3.7 Assam Valley

The Assam valley which lies in between the Shillong Plateau and the eastern Himalayan tectonic domains, flanks the Shillong-Mikir massif with its basement gently sloping towards northeast as well as towards southeast (Dasgupta, 1977). The sedimentation on the Assam-Shillong shelf begins with the deposition of the Jaintia Group which has a large spread in the upper Assam sub-surface and in the Mikir hills. Its upper region that lies between the Himalaya and Naga hills is a plain land spreading over 100 km in width and 300 km in length. This block is having both thrust as well as strike-slip movements (Nandy, 2001). Khattri and Wyss (1978) and Khattri *et. al.,* (1983) surmised that this area is truly aseismic and not a seismic gap in real sense between great 1897 and 1950 events as these two events belong to two distinctly different tectonic domains having their characteristic tectonic evolution and characteristic contemporary tectonic activity. Mukhopadhyay (1984) has however, inferred that the tectonic stress over the Assam gap has been taken up by the thrust of the Eastern Himalaya and the northern part of the Indo-Myanmar arc lying on either side of the upper Assam valley leaving it aseismic.

TH-994_06610404

3.4 Damage due to past earthquakes

A detailed seismicity of NE India has been presented in Chapter 2. Here only the damages which incurred in and around Imphal city are presented. Although earthquake history of NE India is about 1200 years old (Iyengar, 1999), the report of damages in this region is available for only ~ 200 years. The first earthquake damage was documented by Oldham (1882) for the 1869 Cachar earthquake. The 1869 Cachar earthquake (M_w 7.5) occurred in the Kopili fault of the Shillog-Mikir massif with epicenter near the northern border of Jaintia Hills, Meghalaya (Oldham, 1882; Nandy, 2001). The earthquake caused extensive damage to buildings in Imphal. Land fissures, liquefaction phenomena and sand venting were reported. Four persons died in Imphal and many were injured when a two-story building of the Maharaja's palace at Imphal collapsed (Oldham, 1882). The temple of Shree Govindaji was severely damaged. A four-story building in the royal palace of Imphal collapsed (Oldham, 1882). Cracks developed on the brick walls of the queen mother's palace. The courtyard of the temple of Lainingthou Nongshapa (traditional local deity) at Kangla fissured and sandy fluid erupted. Muddy fluid was also erupted from the old rivulets, e.g., Singhtha turel, Luwang turel, Tu-Khong turel (*turel* means river). The idols in the palace temple suffered damages due to structural collapse. The banks of the Imphal, Thoubal, Nambul and Iril rivers subsided, blocking the flow of rivers, which further led to the rise of water levels. Damage was also observed to the brick arch bridge (*Thong Nambonbi*) near the polo ground. Traffic became disrupted due to the settlement and fissuring of roadways (Sarangthem, 2005; Ningthoukhongjam, 2005). During the 1897 great Assam earthquake, no damage was reported in Imphal city. The 1918 Srimangal earthquake (M_w 7.5) occurred on Sylhet fault of Bangel basin showed no report on structural damage in Imphal city. The Shillong plateau and Bengal basin tectonic blocks are seismically active and show sporadic seismicity when compared to the Indo-Burmese ranges. Recently Kayal *et. al.,* (2006) observed intense seismic activity in the epicentral

TH-994_06610404

region of the 1869 Cachar earthquake along the Kopili fault, and speculated a large impending earthquake in this region.

In the earthquakes that followed *viz.*, 1947, 1950 and 1988 earthquakes, damages were also observed in Imphal city (Manichandra, 2007). In the 1947 earthquake which occurred in the eastern Himalaya (M_w 7.9) there were reports of wall cracking, rolling of cooking pots, movements of beds etc. in Imphal city. During the 15th August 1950 earthquake (M_w 8.6), which occurred in the Mishmi tectonic block, wall cracks appeared in many buildings, temple bells rang due to structural shaking, sloshing of Loktak (the biggest fresh water lake in eastern India) water surface was observed (Ningthoukhongjam, 2005). It has been reported that the entire IBA is characterized by high seismicity with the focal depth of events gradually increasing towards the east (Kayal, 2008). The dip angle obtained from focal mechanism solutions of past events in the Indo-Burma region showed a slope from an initial 30-45 km to about 70–100 km depth towards east (Satyabala, 2003). In the 6th August, 1988 earthquake which occurred in the subduction zone several four-story buildings in both Paona and Thangal markets in Imphal city tilted by about 25–50 mm (1:240), walls cracked, many doors and windows got jammed (Manichandran, 2007). After the 26th December 2004 Sumatra and Andaman earthquakes there are speculation amongst several seismologists that stress adjustments are taking place in the NE region with every possibility of occurrence of large magnitude earthquakes in the IBA (Cummins, 2007).

It can be observed from the above discussion that Imphal has been affected by earthquake events originating in the Shillong plateau as well as IBA. The control region around Imphal is inhomogeneous as regards its tectonic background. Hence to understand the seismicity of these seven seismic zones/blocks recurrence relations need to be established by assembling historic earthquake data of the region.

3.5 Earthquake catalogue

As it can be seen from above sections that Imphal city is embedded in a severe seismic region. The seismic activity of all seven seismic blocks has been

quantified in term of standard (*a, b*) values of Gutenberg-Richter frequency-magnitude recurrence relationship. The earthquake data used in this study comprises of a record 140 (1866-2007) years from all the seismic blocks.

A total of 3230 earthquakes of magnitudes greater than 4 have been collected from IMD (http://www.imd.gov.in/section/seismo/dynamic/welcome.htm), DST (2008), ISC (http://www.isc.ac.uk/) and USGS website (http://neic.usgs.gov/). To assemble the data into an earthquake catalogue different magnitude values reported in the literature are converted into moment magnitude (M_w) numbers. Pre-instrumented data (available in MMI scale) have been converted using an empirical relation, M_w= (2/3 MMI+1) (Raghukanth and Iyengar, 2006). Local magnitudes (M_L) data reported by IMD have been converted to M_w following the approach of Idriss (1985). For events from ISC, USGS catalogues with surface (M_S) and body (m_b) wave magnitudes, the following relations given by Scordilis (2006) have been used to convert into M_w (Equation 3.0 a-c).

$$M_w = 0.67M_s + 2.07, \text{for}\,(3.0 \le M_s \le 6.1) \quad 3.0a$$

$$M_w = 0.99M_s + 0.08, \text{for}\,(6.2 \le M_s \le 8.2) \quad 3.0b$$

$$M_w = 0.85m_b + 1.03, \text{for}\,(3.5 \le m_b \le 6.2) \quad 3.0c$$

For estimation of the recurrence parameters it is assumed that the sample data series to be temporally statistically independent. The declustering approach given by Gardner and Knopoff (1974) and further modified by Uhrhammer (1986) has been used to remove time-dependent events (e.g. aftershocks and foreshocks) from the earthquake catalogue. The procedure essentially removes a space and time window after each main shock. A total of 1034 aftershocks and foreshocks have been removed from the above main catalogue and the same is used in obtaining the regional recurrence relationship.

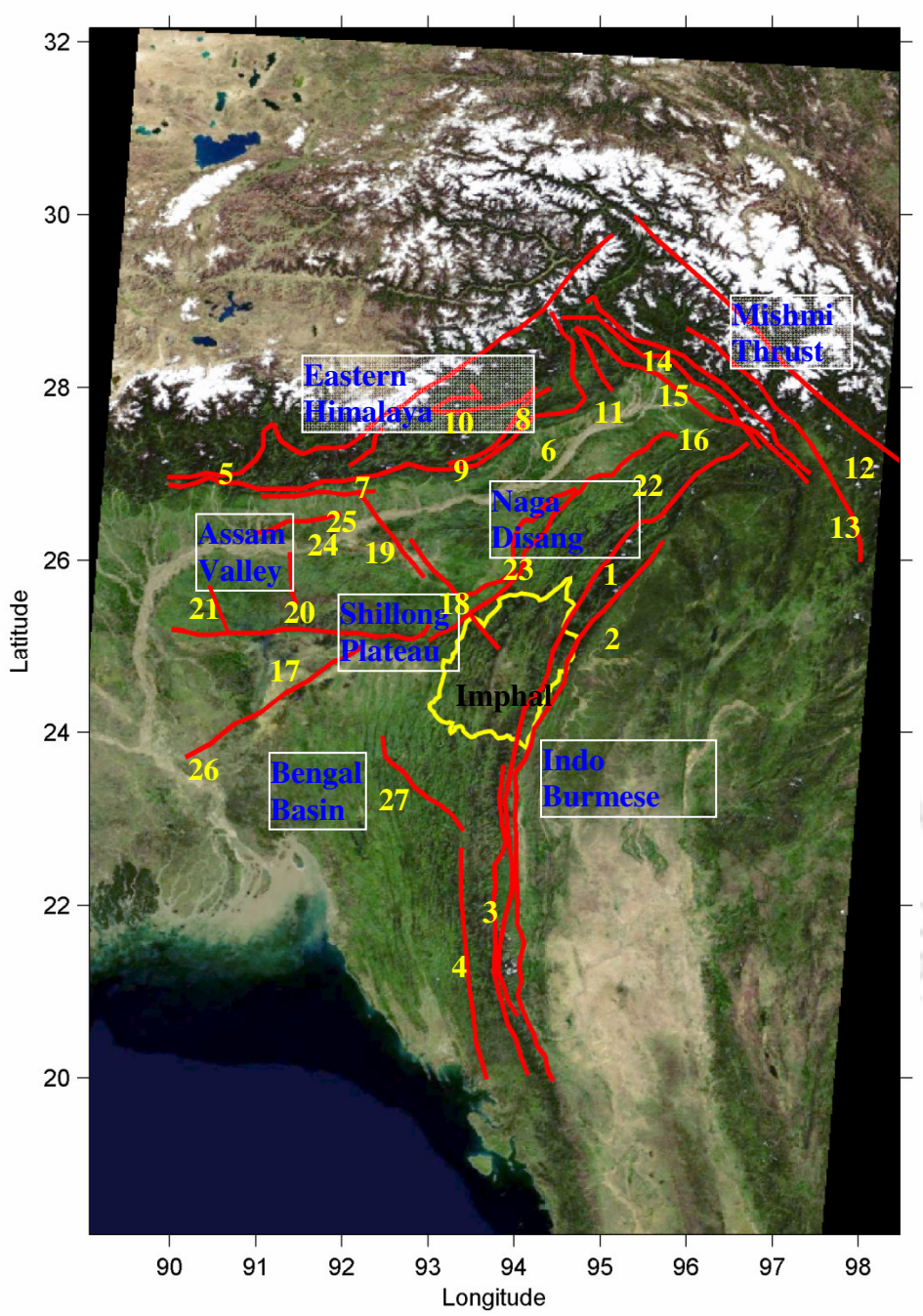


Figure 3.3a Fault map along with fault numbers

3.5.1 Regional recurrence

A total of 27 major faults were identified from all seismic blocks/regions *viz.*, IBA, EH, MT, SP, ND, BB and AV (fault lengths lesser then 5.0 km are not considered in this study) given in Seismotectonic Atlas of India (GSI, 2000) (Figure 3.3b). Since the size of fault is finite, the maximum possible magnitude (m_u) due to a fault must be limited to a logical value. Here m_u is based on

historical seismicity data. In the absence of reliable data *e.g.* fault rupture length, fault rupture area and fault slip rate, the present study mainly depends on the historical data for evaluating m_u value. A historical window of 1866-2007 (140 years) having 2196 events (without aftershock and foreshock) of magnitudes greater than 4.0 in the region are considered in the present study for estimating the regional *a* and *b* values. It is well known that earthquake catalogue contains high number of smaller magnitude events of recent earthquakes (generally detected with the help of instruments). On the other hand larger earthquakes are rare but even without instruments their occurrence would be known from general regional history. These point to the limitation that any regional catalogue can be treated as complete at different magnitude levels with differing periods of representative history. Quantification of completeness of a catalogue is essential to arrive at reliable (*a*, *b*) values in the Gutenberg–Richter recurrence relationship. The measure of completeness of the historical data has been estimated by the method proposed by Stepp (1972). In this, the earthquake catalogue is arranged into magnitude intervals of $4 \le m < 4.9$; $5 \le m < 5.9$; $6 \le m < 6.9$; $7 \le m < 7.9$ and $m > 8$ and in time intervals of 10 years. The average number of events per year for each magnitude interval is determined. For a particular magnitude range if b_1, b_2, b_3, b_4,….b_K are the number of events per unit interval then fair estimate of the mean rate per unit time interval of the sample is given by Equation 3.1a.

$$\chi = \frac{1}{K}\sum_{i=1}^{K} b_K \qquad 3.1a$$

and its variance is calculated by Equation 3.1b

$$\sigma_{\chi}^2 = \frac{\chi}{T} \qquad 3.1b$$

Here the occurrence of earthquake is assumed to follow a Poisson distribution. If χ were to be a constant, then σ_χ varies as $\frac{1}{\sqrt{T}}$, where *T* is the duration of the sample. The deviation of standard deviation of the sample mean from the parameter value indicates the length up to which a particular magnitude range

TH-994_06610404

can be taken as complete. It is seen from Figure 3.4 that standard deviation shows stability in shorter time windows for smaller earthquakes and in longer time windows for the larger magnitude earthquakes. The tangent lines of $\frac{1}{\sqrt{T}}$ is drawn through the stable values of standard deviation of various magnitude ranges. The completeness test results shown in Figure 3.4 reveal that the earthquake catalogue is complete within time window of 1866-2007 (140 years).

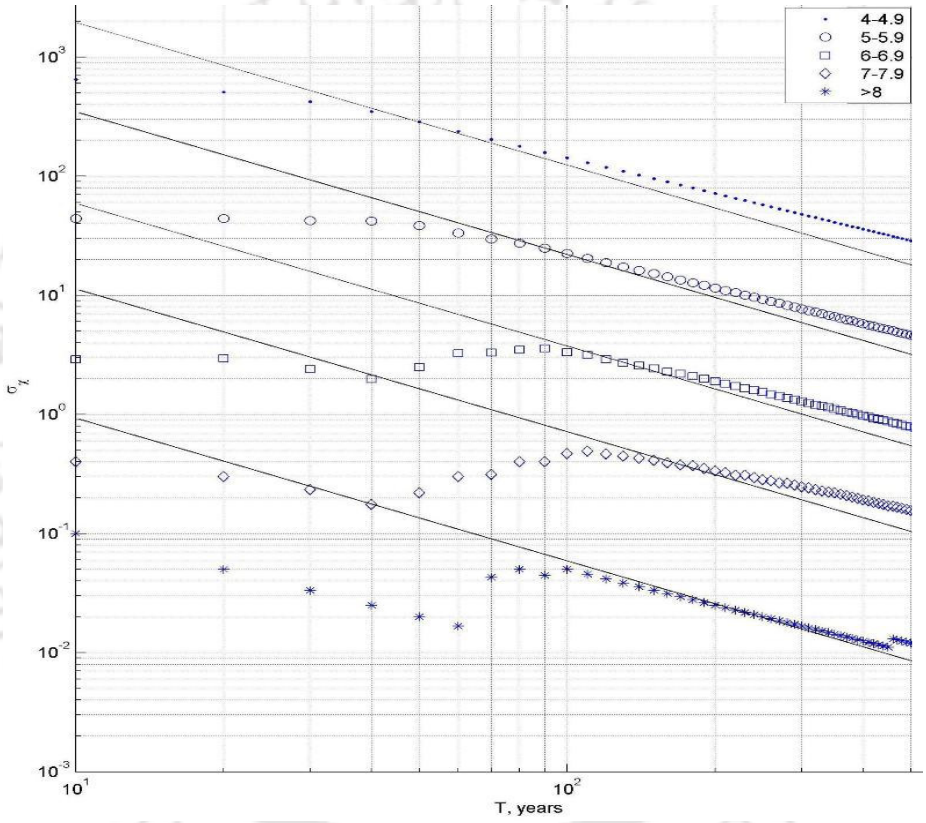


Figure 3.4 Variation of σ_x versus time interval and magnitude.

The Gutenberg–Richter relationship used for obtaining the regional parameters (e.g. *a* and *b* values) can be expressed as,

$$\log_{10} N_e = a - bm \qquad for\ m_m \le m \le m_u \qquad 3.1c$$

where N_e is the number of earthquakes greater than magnitude (m) per year or the annual rate of exceedance of magnitude m. The parameter a characterizes the general level of seismicity in a given area during the study period *i.e.,* the

higher the *a* value, the higher is the seismicity; and *b* slope of equation, describes the relative likelihood of large and small earthquakes.

The high value of *b* indicates a greater proportion of smaller events and a low value of *b* indicates a greater proportion of larger events. The computer program written by the Kijko and Sellevoll, (1989a, 1989b) (HN2, Release 2.08) has been used to determine the *a*, *b* and maximum magnitude value. The recurrence relationships of all seven seismic regions which control seismic hazard of Imphal city are shown in Figure 3.5. It can be observed that IBR, EH, MT and SP have magnitudes greater than 8.0 and hence are treated as the controlling seismic zones in this region (Figure 3.5). It can be seen that the highest magnitude earthquake associated with AV is 6.0. Figure 3.5 also shows that the IBR is having highest frequency of low magnitude (< M_w = 6) earthquake whereas ND is having very low occurrence of low magnitude earthquake among all seismic sources. Further for each region, *a* and *b* values are estimated (Table 3.2). Table 3.2 suggests that IBR (which is located less than 100 km from Imphal city) has the highest values for both *a* (= 20.10) and *b* (= 0.87), hence most active zone.

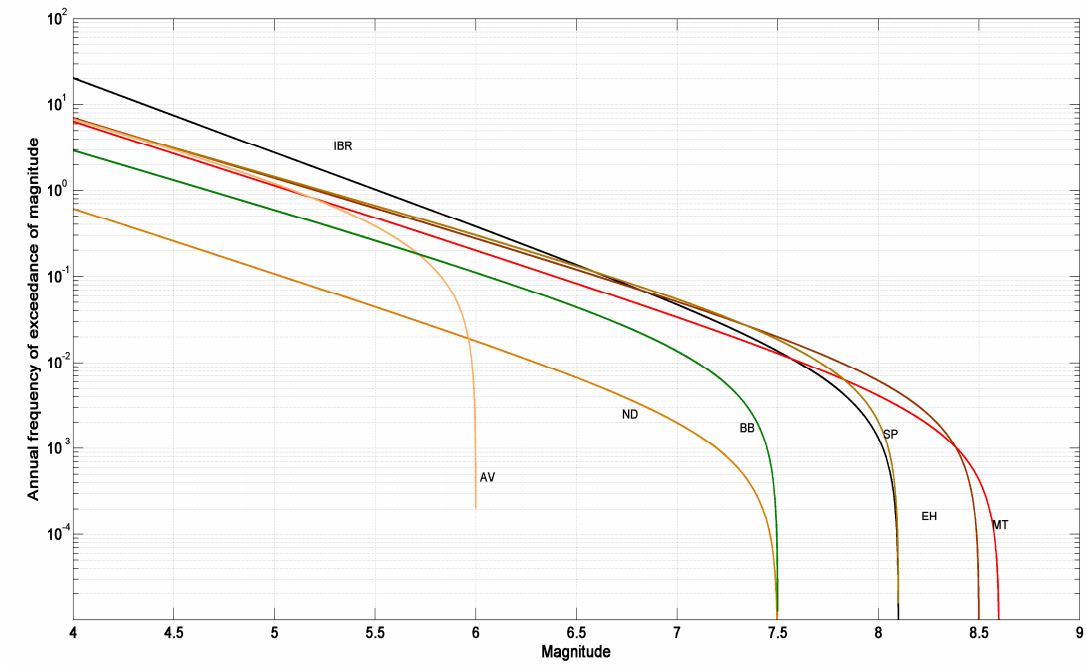


Figure 3.5 Regional magnitude-frequency relationships

Table 3.1 Fault characteristics

Fault	Fault Region	m_u	Length	Weight	Lamda
1	Indo Burmese Ranges	8.1	771.95	0.3236	6.5861
2		8.1	872.13	0.3656	7.4416
3		8.1	441.75	0.1852	3.5133
4		8.1	299.84	0.1257	2.5584
5	Eastern Himalaya	8.5	735.76	0.3669	2.5757
6		8.0	706.16	0.3522	2.4721
7		6.0	69.04	0.0344	0.2417
8		6.0	139.76	0.0697	0.4893
9		6.0	168.75	0.0842	0.5908
10		6.0	89.96	0.0449	0.3149
11		6.0	95.83	0.0478	0.3355
12	Mishmi Thrust	8.6	600.15	0.2907	1.5914
13		6.5	388.62	0.1882	1.0305
14		6.5	384.01	0.1860	1.0183
15		6.5	324.42	0.1571	0.8603
16		6.0	367.57	0.1780	0.9746
17	Shillong Plateau	7.0	342.93	0.4214	1.1213
18		7.5	182.25	0.2239	1.2130
19		6.5	140.74	0.1729	0.5959
20		6.0	67.94	0.0835	0.4602
21		8.0	79.94	0.0982	0.2599
22	Naga-Disang Thrust	7.5	440.35	0.6588	0.4018
23		7.5	228.10	0.3412	0.2082
24	Assam Valley	6.0	115.22	0.4466	0.3767
25		6.0	142.77	0.5534	0.4865
26	Bengal Basin	7.5	269.81	0.6186	1.1813
27		7.5	166.35	0.3814	1.1175

TH-994_06610404

3.5.2 Deaggregation

Any point in the given region will be affected by ground motion originating from any of the twenty seven faults (Table 3.1). However, it can be seen from the Figure 3.4 that these faults have different lengths, orientations and seismic activity rates. To compute ground motion due to an event information regarding the magnitude of the event and the site-to-source distance are required. The magnitude of a future event on any fault can be treated as a random variable since the fault of interest has potential to produce an earthquake of magnitude m in the interval (m_m, m_u) according to its individual recurrence properties, which are again not known.

Table 3.2 Regional *a* and *b* values

Sr. No.	Seismic regions	*a*-value	*b*-value
1	Indo-Buremese Range (IBR)	20.10	0.86
2	Eastern Himalaya (EH)	7.02	0.70
3	Mishmi Thrust (MT)	6.40	0.75
4	Shillong Plateau (SP)	6.81	0.67
5	Naga-Disang Thrust (ND)	0.61	0.75
6	Bengal Basin (BB)	2.93	0.69
7	Assam Valley (AV)	6.81	0.67

To evade this difficulty heuristic principle of conservation of seismic activity is invoked. According to this principle, the number of earthquakes per year with $m > m_m$ in the region should be equal to the sum of possible number of events (N_e) due to all faults in the region. Here, m_m can be fixed at 4.0 since events of still lower magnitudes are not of engineering importance (Iyengar and Ghosh, 2004, Raghukanth and Iyengar, 2006). It is also assumed that N_e may be taken to be proportional to the length of the fault (Iyengar and Ghosh, 2004). This gives the weighting factor $w_s = L_s/\sum L_s$ as an activity indicator for fault 's' .The weight assigned to each fault is given in Table 3.1. By making use of Equation 3.2 (Kramer, 2008), the regional recurrence is deaggregated into individual fault recurrence as shown in Figure 3.6.

$$\lambda_m = w_s \nu \frac{\exp[-\beta(m-m_m)]-\exp[-\beta(m_{\max}-m_m)]}{1-\exp[-\beta(m_{\max}-m_m)]} \qquad 3.2$$

where, $\upsilon = \exp(\alpha - \beta m_0)$, $\alpha = 2.303a$; $\beta = 2.303b$. Here it may be mentioned that *b*-value of a fault has been taken to be equal to the regional *b*-value. From the Figure 3.6 it can be seen that Fault no. 5 (EH), Fault no. 12 (MT) and Fault no. 21 (IBR and SP) control earthquakes of higher magnitudes ($M_w > 8.0$).

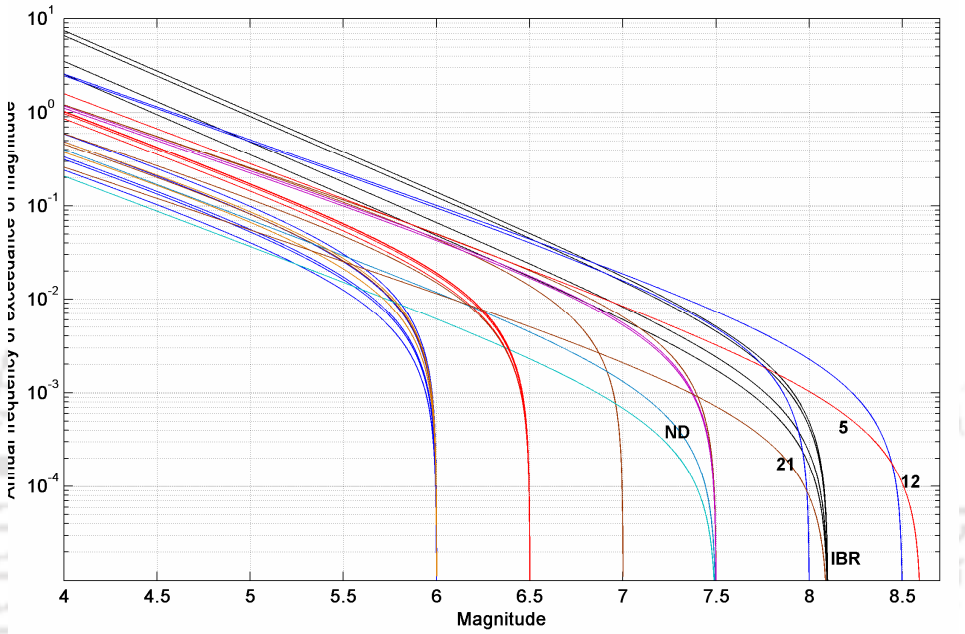


Figure 3.6 Deaggregation of regional hazard in terms of fault recurrence

3.6 Ground motion simulation

Due to unavailability of strong motion records of past earthquakes that caused damages to Imphal city ground motions are simulated by analytical models. In this approach features of source and path are modelled as primary system parameters and the effect of local top soil condition is treated as a secondary modification. First rock level ground motion for the 1988 Indo-Burmese earthquakes is simulated by stochastic finite fault approach of Motazedian and Atkinson (2005) which is based on the concept of dynamic corner frequency and pulsing subfaults. In the present approach, the fault is divided into N′ number of subfaults and the subfaults are represented as point sources. The rupture front spreads radially from the nucleation point and triggers the sub-

faults when it reaches their center. The sub-fault acceleration time histories are propagated to the observation point by considering specified distance-duration curves and attenuation model.

The Fourier amplitude spectrum of ground motion [$Y(r,f)$] due to the j^{th} subfault at a site is derived from the point source seismological model (Boore, 1983), expressed as

$$Y_j(r,f)=\left(\frac{\mathrm{M_0}D_j}{\sum_{j=1}^{N}D_j}\right)\left(\frac{N'(2\pi f)^2\sum_f\left(\frac{f^2}{1+(f/f_0)^2}\right)^2}{\left(1+\left(f/f_{0j}\right)^2\right)\sum_f\left(\frac{f^2}{1+(f/f_{0j})^2}\right)^2}\right)^{1/2}\left(\frac{\sqrt{2}<\mathrm{R}_{\theta\phi}>}{4\pi\rho\mathrm{V_s}^3}\right)\left(G'e^{\frac{\pi f r_j}{\mathrm{V_s}Q}}\right)\left(F(f)e^{-\pi f\kappa_0}\right) \quad 3.3$$

where, M_o is the total seismic moment of all the subfaults, G' refers to the geometric attenuation, r_j is the subfault distance from the site, V_s is the shear wave velocity and Q is the quality factor of the region. D_j is the average final slip acting on the j^{th} subfault, f_{0j} is the dynamic corner frequency (Motazedian and Atkinson, 2005) and $F(f)$ represents site amplification due to propagation of earthquake waves from the source region toward the surface. The term $\exp(-\pi f\kappa_0)$ is a high cut filter which takes care of the rapid spectral decay at high frequencies (Anderson and Hough, 1984). $<R_{\theta\phi}>$ is the radiation coefficient averaged over an appropriate range of azimuths and take-off angles and ρ is the density of the crust at the focal depth. The dynamic corner frequency, f_{0j}, the seismic moment, M_o and the stress drop, $\Delta\sigma$ are related through the following equation

$$f_{0j}=4.9\mathrm{x}10^6(\mathrm{N_{Rj}})^{-1/3}(\mathrm{N}')^{1/3}\mathrm{V_s}\left(\frac{\Delta\sigma}{\mathrm{M_0}}\right)^{1/3} \quad 3.4$$

where, N_{Rj} is the cumulative number of ruptured subfaults by the time rupture reaches the j^{th} subfault. The corner frequency at the end of the rupture, f_0 is obtained by substituting $N_{Rj} = N'$ in Equation 3.4. To account for realistic model of earthquake rupture, Motazedian and Atkinson (2005) introduced the concept of pulsing area where the cumulative number of active subfaults, N_{Rj}

(see in Equation 3.4) increases with time at the initiation of rupture, to attain a constant magnitude at some fixed percentage of the total rupture area referred to as percentage pulsing area. This pulsing area parameter determines the number of active subfaults during the rupture of i^{th} subfault. These active subfaults are used in Equation 3.4 for computing the dynamic corner frequency. In the present study, the finite fault seismological model is implemented in the time domain through numerical simulation process suggested by Boore (1983). First, a Gaussian stationary white noise sample, at distance *r*, of length equal to the strong motion duration (Boore and Atkinson 1987) is simulated using Equation 3.5.

$$T=1/f_c + 0.05\, r \tag{3.5}$$

Second, this sample is multiplied by the modulating function of Saragoni and Hart (1974) to introduce the non-stationarity and then Fourier transformed into the frequency domain. This Fourier spectrum is normalized by its root-mean-square value and multiplied Fourier amplitude (derived from Equation 3.3). Third, the resulting function is transformed back into the time domain to get a sample of subfault acceleration time history. This way acceleration time histories are simulated for all the subfaults and are summed up with a time delay Δt_i, to obtain the ground motion acceleration $A(t)$ due to the entire fault as

$$\mathrm{A}(t) = \sum_{i=1}^{N} \mathrm{A}_i(t + \Delta t_i) \tag{3.6}$$

In the present study, the geometrical attenuation term G' in Equation 3.3, for NE India, is taken to be equal to 1/R for R < 100 km and equal to 1 / (10√R) for R > 100 km (Singh *et. al.*, 1999). Recently Raghukanth and Somala (2009) calibrated the above finite fault seismological model for NE India. In which the range of stress drop, pulsing percentage and the quality factor for Indo-Burma, Shillong plateau and Bengal basin tectonic blocks have been derived from the strong motion data of seven events in NE India. The Quality factor has been

derived from events originating in Indo-Burma tectonic domain as $Q = 431f^{0.73}$. The shear wave velocity model in Imphal region for rock type sites as reported by Mitra *et. al.,* (2005) is shown in Table 3.3. Based on the average shear wave velocity in the top 30 meters of the soil, sites can be classified as A: (V_{30} > 1.5km/s); B: (0.76 km/s < V_{30} ≤ 1.5km/s); C: (0.36 km/s < V_{30} ≤ 0.76 km/s); D: (0.18 km/s < V_{30} ≤ 0.36 km/s) type sites (IBC, 2006). Since the average shear velocity is 1.25 km/s (Table 3.3), the rock site in Imphal can be classified as B-type site. Figure 3.7 shows the presence of such site in Imphal city. Since modification between bedrock and B-type sites is a linear problem in one dimension and hence for such sites, amplification [$F(f)$] can be found directly by the quarter-wavelength method of Boore and Joyner (1997). Chandler *et. al.,* (2006) compiled a database of kappa factors estimated for various parts of the world.

Table 3.3 Regional velocity model (Mitra *et. al.,* 2005)

Depth (km)	V_s (km/s)
0.1	1.25
0.2	2.75
2.2	3.6
24	3.75



Figure 3.7 B-type rock site near Chingmeirong in Imphal city

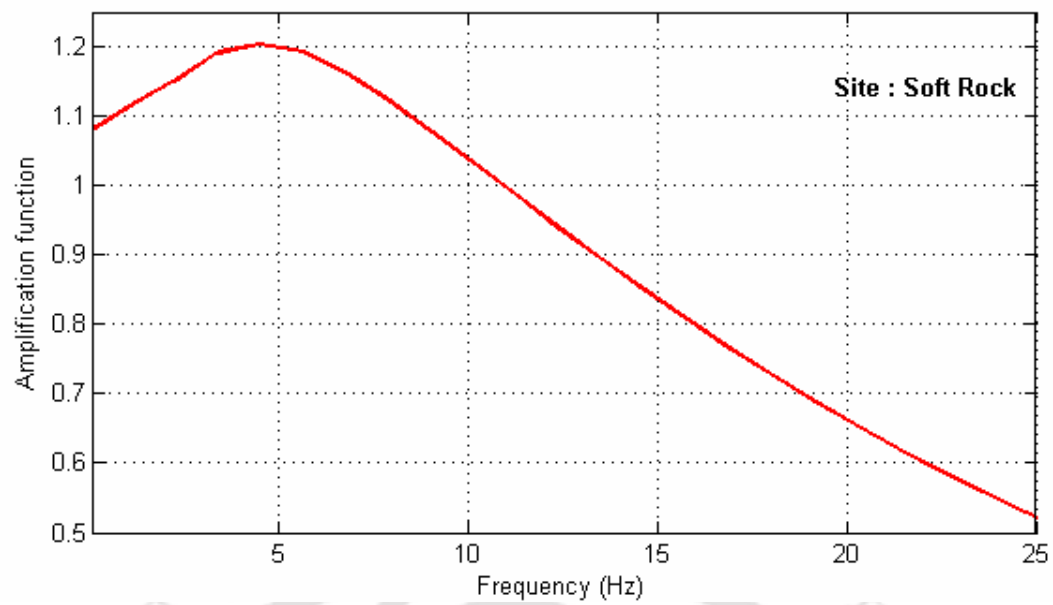


Figure 3.8 Amplification function for soft rock sites

They proposed an empirical equation for estimating the kappa factors from the average shear wave velocity in top 30 meters of the soil ($V_{s,30}$) as

$$\kappa_0 = \frac{0.057}{V_{s,30}^{0.8}} - 0.02 \qquad 3.7$$

Given $V_{s,30}$ in a region, Equation 3.7 can be used for estimating kappa factor. By substituting the $V_{s,30}$ as 1.25 km/s, the average kappa factor for soft rock site in Imphal city is obtained as 0.03. The overall amplification function ($F(f)e^{-\pi f \kappa_0}$) for soft rock sites estimated from quarter wavelength method is shown in Figure 3.8. This amplification function has been used for simulating rock level ground motion at Imphal city.

Computation of ground motion by the stochastic finite fault method demands slip distribution on the rectangular fault plane. Mai and Beroza (2002) studied the finite-fault slip distributions of several past earthquakes and proposed a random field model for characterizing the spatial complexity of earthquake slip. This model has been used in this study to generate possible scenarios of slip distribution for each event. In this approach, the power spectrum of earthquake slip in wave-number domain is modeled by the anisotropic von Karman spectral density (PSD) as

$$P(\kappa) = \frac{a_{x'} a_{z'}}{(1+\kappa^2)^{H+1}}, ; \qquad 3.8$$

where the wave number (κ) is defined as

$$\kappa = \sqrt{a_{x'}{}^2 \kappa_{x'}{}^2 + a_{z'}{}^2 \kappa_{z'}{}^2}$$

In the above expressions, H is the Hurst exponent, $\kappa_{x'}, \kappa_{z'}$ are the horizontal and vertical wave numbers, and $a_{x'}, a_{z'}$ are the correlation lengths along-strike and down-dip directions respectively. By modeling 44 slip models of past earthquakes, Mai and Beroza (2002) derived regression equations between the correlation lengths along-strike and dip directions with magnitude as

$$Log(a_{x'}) = -2.6 + 0.53 M_w$$
$$Log(a_{z'}) = -1.8 + 0.37 M_w \qquad 3.9$$

Based on their analysis, Mai and Beroza (2002) obtained Hurst component (H) as 0.75. It can be observed from Equation 3.9 that the correlation length along the strike ($a_{x'}$) and dip ($a_{z'}$) of the fault plane increases with increasing magnitude of the earthquake. Given the magnitude of an earthquake, the correlation lengths in strike and dip direction can be determined from the above scaling relations (Equation 3.9). The correlation lengths are then substituted in Equation 3.8 and the power spectrum of earthquake slip is simulated from the von Karman distribution PSD in wave-number domain. Assuming phase as a random variable uniformly distributed between 0 and 2π, slip on the rupture plane is simulated as a random field by the spectral representation method of Shiozuka and Deodatis (1996). From the spectral representation procedure, one can simulate several realizations of the moment field by replacing the sequences of random phase angles. The hypocenter in each case is taken near the regions of maximum slip release (Mai *et. al.,* 2005). This sample slip field on the fault plane is discretized into subfaults of size 1 km x 1 km and the seismic moment of each point source is computed using

Equation 3.10. The moment of i^{th} subfault (M_{0i}) is computed from the slip distribution as follows

$$M_{0i} = \frac{M_0 D_i}{\sum_{i=1}^{N} D_i} \qquad 3.10$$

where, D_i is the average final slip acting on the i-th subfault. M_0 is the total seismic moment of all the subfaults. Since the moment distribution on the rupture plane is modeled as random field one can generate an ensemble of time histories at the surface by numerical simulation. To cover all possible peculiarities in the slip distribution, ten samples of slip field are generated for each event. The slip distribution, stress drop and pulsing area are treated as random field and random variables in the simulation. These three simulated seismic parameters are combined using the Latin Hypercube sampling technique (Iman and Conover, 1980) to establish 10 sets of random seismic parameters. In Figure 3.9 a sample of the slip field generated for the M_w 7.2, event is shown.

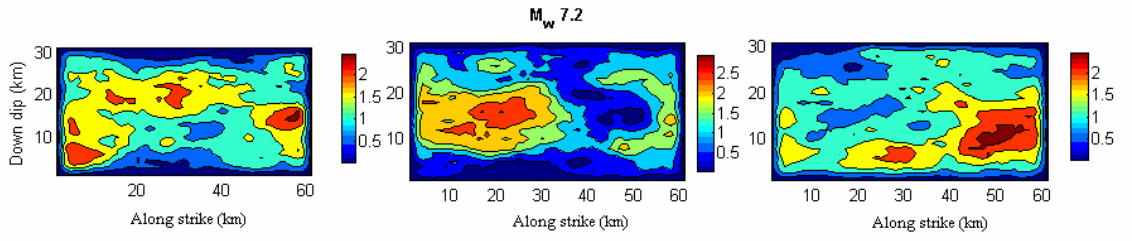


Figure 3.9 Sample slip field on rupture plane for 1988 earthquake

3.7 Comparison with the SRR data of 6th August 1988 earthquake

Before simulating ground motion for significantly damaging earthquakes, ground motion simulation methodology is validated against the available SRR data of the 6th August 1988 earthquake (M_w 7.2). This event produced 33 strong motion acclerograms in the Shillong array and another 80 structural response recorder (SRR) data at different places in NE India (CVDT, 2008). Raghukanth and Somala (2009) modeled these 33 strong motion records and have obtained parameters such as, stress drop, pulsing area percentage and quality factor.

These have been used as input parameters for the present simulation and are shown in Table 3.4.

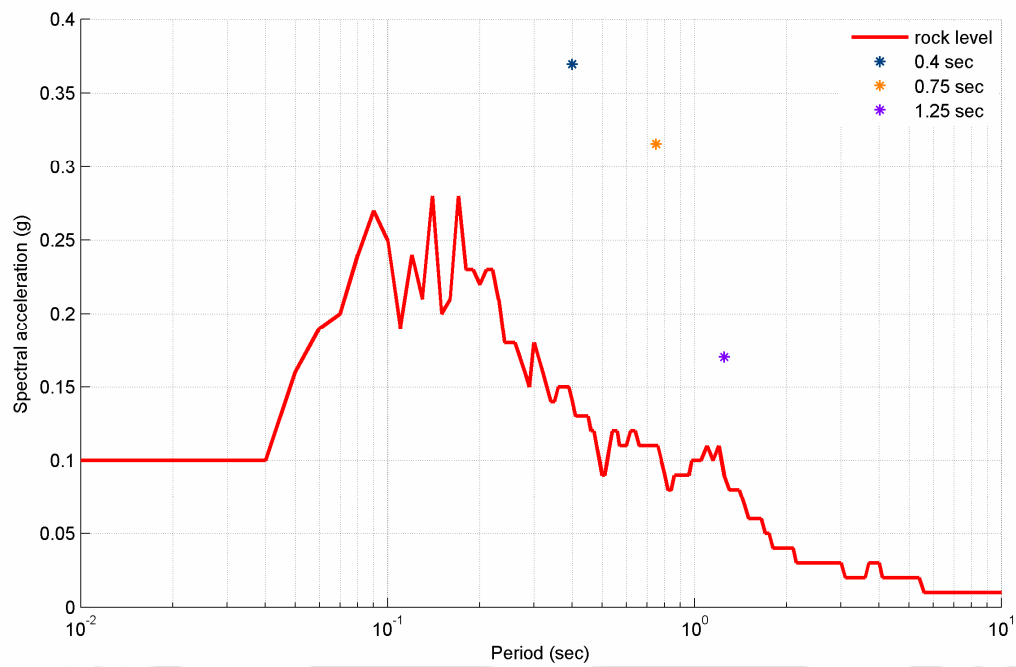


Figure 3.10 Comparison of simulated response spectra with SRR data of 1988 earthquake in Indo-Burmese Ranges

Since the key input source and region parameters are known for this event, stochastic finite-fault model can be used directly for simulating the rock level ground motion in Imphal city. Here rock level acceleration time histories have been generated for Imphal city, corresponding to 10 sample realization of the slip field. The mean rock level PGA is obtained as 0.1g.

As mentioned earlier, the 1988 event produced four SRR data (obtained through four sets of instruments with $\eta = 0.05$; 0.1 and $T_n = 0.4$ s; 0.75 s and 1.25 s) at Imphal city. Spectral acceleration $S_a(\eta, T_n)$ for 5 % damping obtained from the SRR data are compared with the present estimates in Figure 3.10. It can be observed from Figure 3.10 that the recorded data lies above the estimated response spectra of rock level. It may be noted that as this SRR data were recorded at certain soil profile above rock level, direct comparison with the present rock level values of *Sa.* This consideration of local soil effects is presented in Chapter 4. It may be noted from the previous section that EH,

MT, SP and IBR are the controlling seismic zones in the region of interest. It may be observed that as EH and MT are far away (> 400 km) from Imphal city their contribution to seismic effect at Imphal city may be considered as comparatively small.

Table 3.4 Input parameters in the stochastic finite fault seismological model (Ragukanth and Somala, 2009, Kayal, 2008, Nandy, 2001)

Parameter	**1988 Indo-Burma**	**1869 Cachar**	**Hypothetical (Indo-Burma)**
Magnitude, M_w	7.2	7.5	8.1
Location: Latitude Longitude	 25.1 95.1	 26.1 92.6	 27.1 92.5
Depth to top of the fault (km)	80	5	60
Stress drop (bars)	100	50-100	50-100
$Q(f)$	$431f^{0.73}$	$221f^{0.89}$	$431f^{0.73}$
Site effects [F (f)]	Quarter wavelength	Quarter wavelength	Quarter wavelength
Kappa factor	0.03	0.03	0.03
Fault dimensions (km)	60 x 30	85 x 40	180 x 75
Fault orientation Strike(^{0}) Dip (^{0})	 284 45	 130 60	 55 58
Pulsing percentage	25-60	25-60	25-60
Rupture velocity	0.8β	0.8β	0.8β
Slip distribution	Random field	Random field	Random field

And hence for site response analysis, rock level acceleration time histories for the 1869 Cachar (M_w 7.5) earthquake (Kopili fault in Shillong plateau) and a hypothetical Mw 8.1 event in the Indo-Burma subduction zone have been estimated by a stochastic finite-fault model at Imphal city.

3.8 Synthesis of ground motion during the 1869 Cachar Earthquake (M_w 7.5)

The input source and path parameters used in the finite fault seismological model, for simulating ground motion due to this event are shown in Table 3.4 The magnitude, location of the fault and depth have been taken from Kayal (2008) (see Table 3.4). The strike and dip of the Kopili fault has been taken as reported by Kayal *et. al.,* (2006). The rupture dimensions have been estimated from magnitude based on the relations (Equation 3.9) proposed by Mai and Beroza (2002). The slip distribution, stress drop and pulsing area are treated as random field and random variables in the simulation. A total of 10 samples of these three parameters are generated using stochastic seismological model. The slip field generated for the M_w 7.5 event is shown in Figure 3.11. Figure 3.12 shows the acceleration time histories simulated at Imphal city. The peak ground acceleration (PGA) varies between 0.1 to 0.2g.

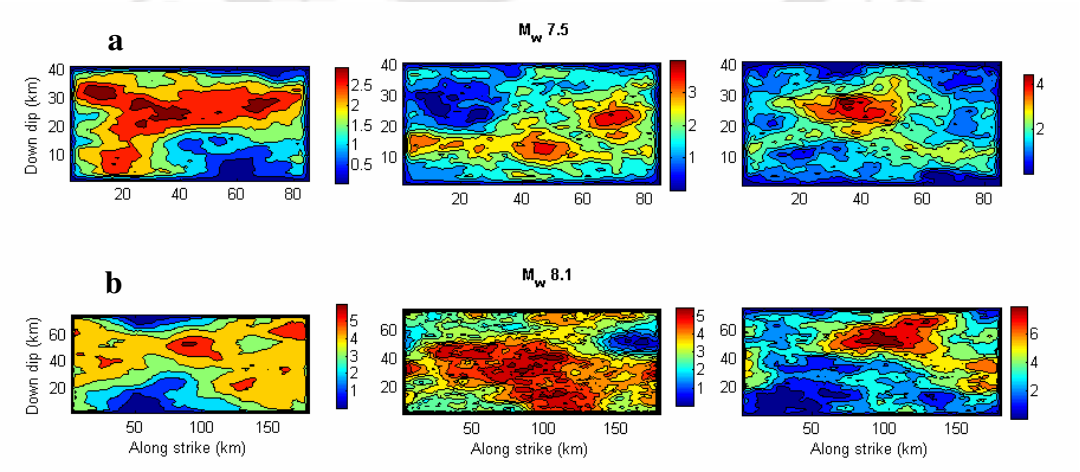


Figure 3.11 Sample slip field on rupture plane (a) 1869 Cachar earthquake (M_w 7.5) and (b) hypothetical earthquake in IBR (M_w 8.1)

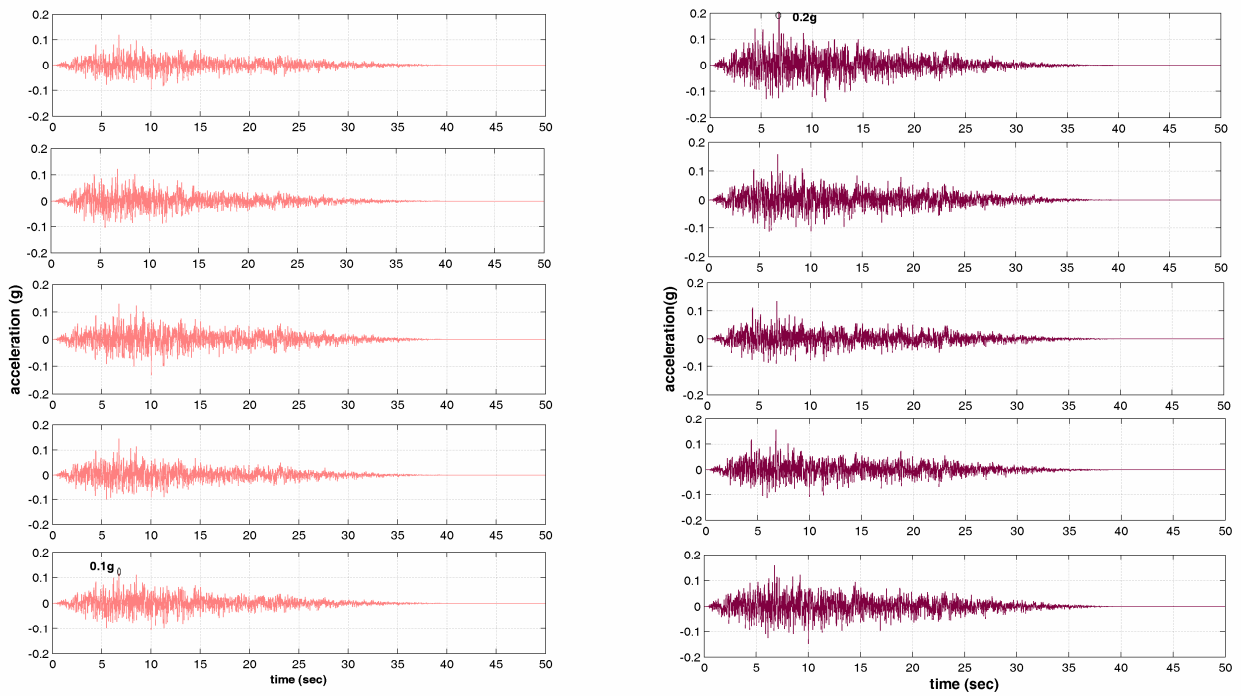


Figure 3.12 Synthesis of ground motion due to 1869 Cachar earthquake (M_w 7.5)

3.9 Synthesis of ground motion for hypothetical earthquake in of M_w 8.1 in IBR

As pointed out earlier, seismologists have speculated a great earthquake in IBA after the 26 December Indonesian 2004 event (Cummins, 2007). Any great earthquake in the IBA may likely cause immense damages to life and property in Imphal city. Hence it is necessary for engineering purposes to determine the possible ground motion affecting for such a future event. Due to the unavailability of reliable fault parameters like fault rupture length, rupture area and slip rate, the probable maximum magnitude (M_u) of the IBA has been estimated (using frequency magnitude relation) based on historical seismicity data considering threshold magnitude as 4.0. The input parameters in the finite fault seismological model for this event are shown in Table 3.4. Ten samples of acceleration time histories and corresponding response spectra at

rock level have been simulated from the finite fault seismological model (Figure 3.13). The PGA varies from 0.11g to 0.3g.

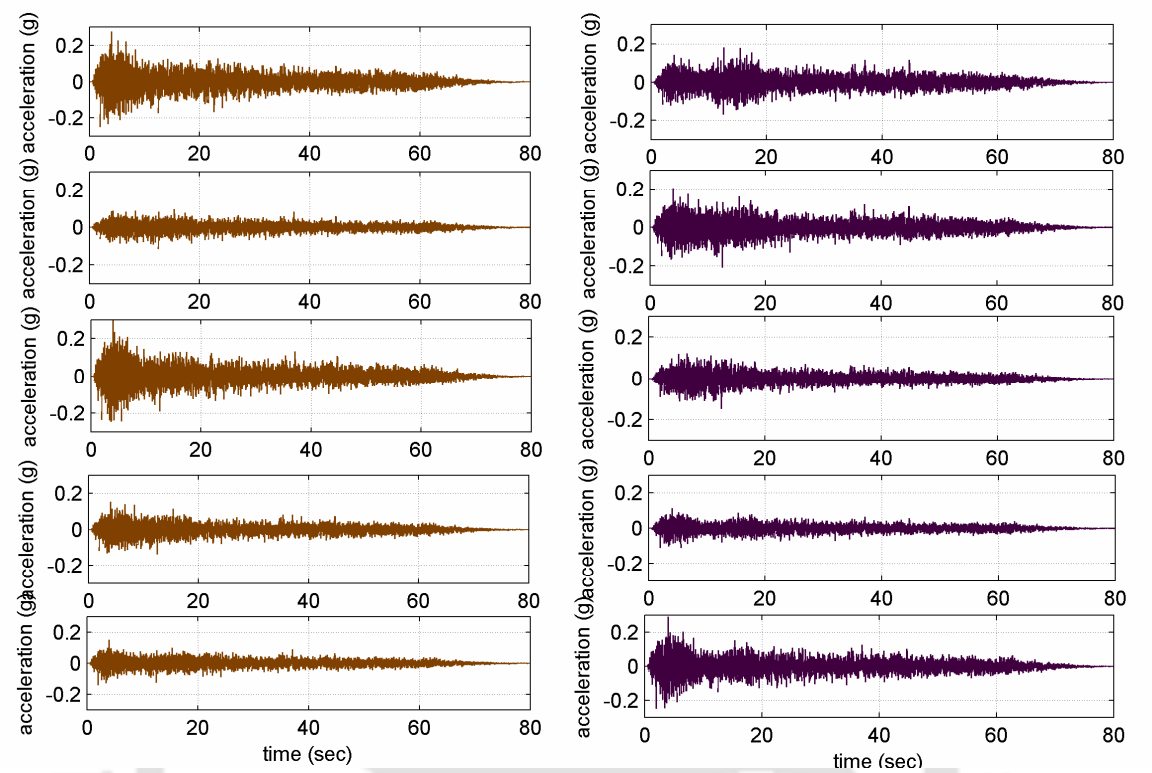


Figure 3.13 Synthesis of ground motion due to a hypothetical earthquake (M_w 8.1) in the Indo-Burmese Ranges

3.12 Conclusions

In terms of seismicity Imphal city lies in the NE region of India which is regarded as one of the most seismically active regions in the world. By constructing a catalogue of past earthquakes and seismo-tectonic map, seven potential seismic zones/blocks *viz.*, Indo-Burmese ranges (IBR), Eastern Himalaya (EH), Mishmi thrust (MT), Shillong plateau (SP), Naga-Disang thrust (ND), Bengal basin (BB) and Assam valley (AV), that can affect the seismicity of Imphal city/Manipur state have been identified. Recurrence relationship of magnitude and frequency of occurrence has been established based on Gutenberg–Richter relation and seismic parameters, *a* and *b* have been computed considering the aforementioned seven seismic blocks. It has

been seen that the seismic blocks EH, MT, IBR and SP control higher magnitude (> 7.5 M_w) earthquakes whilst BB, ND and AV control earthquakes of lower magnitudes. Deaggregation analysis showed that the entire faults of IBR, Fault no. 5 of EH, Fault no. 12 of MT and Fault no. 21 of SP (see Table 3.1) are the main contributing faults which control large earthquakes. As a remedy for the scarcity of strong motion data rock level acceleration time histories at Imphal city for 1988 Indo-Burmese (M_w 7.2) earthquakes, 1869 Cachar (M_w 7.5) earthquake in Kopilli fault, and a hypothetical M_w 8.1 event in Indo-Burmese subduction zone have been estimated deterministically using the methodology of finite-fault seismological model (Motazedian and Atkinson, 2005) with regional parameters *viz.*, stress drop, pulsing percentage, slip distribution, rupture velocity etc. (Nandy, 2001; Kayal, 2008; Raghukanth and Somala, 2009) as inputs. The simulated rock level S_a results of 1988 earthquake in IBR have been compared with that of the available SRR data and it has been found that SRR values are on the higher side. The difference in the results may be due the absence of local soil effects in the present model. Effect of local soil effect on S_a is addressed in the next Chapter 4.

TH-994_06610404

Chapter 4

Local site effects on ground motion for Imphal city

4.1 Introduction

Past earthquake *viz.,* Negata (1964), Mexico (1985), San-Fransico (1989), and Bhuj (2001) have demonstrated that local soil can have significant influence on seismic damages. So in any seismic hazard analysis it is essential to incorporate the effect of local soil on ground motion for site characterization. As Imphal is a typical example of a city located in a valley formed due to the deposition of alluvial-fluvial deposits by three major rivers *viz.,* Imphal river, Kongba river and Iril river, it is relevant to study the effects of local soil layers in the estimation of surface level ground motions. In the present chapter information about the geography, geology and geotechnical details for Imphal city are discussed. Soil investigation data of 122 boreholes that have been collected from several construction projects in Imphal city for the present study is presented in Figure 4.1. In this chapter rock level time history for 1869 Cachar earthquake and hypothetical earthquake of M_w 8.1 in IBA estimated by stochastic finite fault model (Chapter 3) have been used as an input for site response analysis. The results are presented in the form of mean peak ground

TH-994_06610404

acceleration (PGA) contour map and standard deviation contour map at PGA and natural periods of 0.3 s and 1 s. Further, effect of local soil on surface level ground is model in terms site coefficients (defined as the ratio of surface level response to the rock level response).

4.2 Geography and Geology of Imphal valley

The Imphal valley (also known as Manipur valley) has a NNW-SSE orientation with a gentle tilting slope towards the south, measuring 798 m above mean sea level (msl) at the extreme north and 746 m above msl at the south.

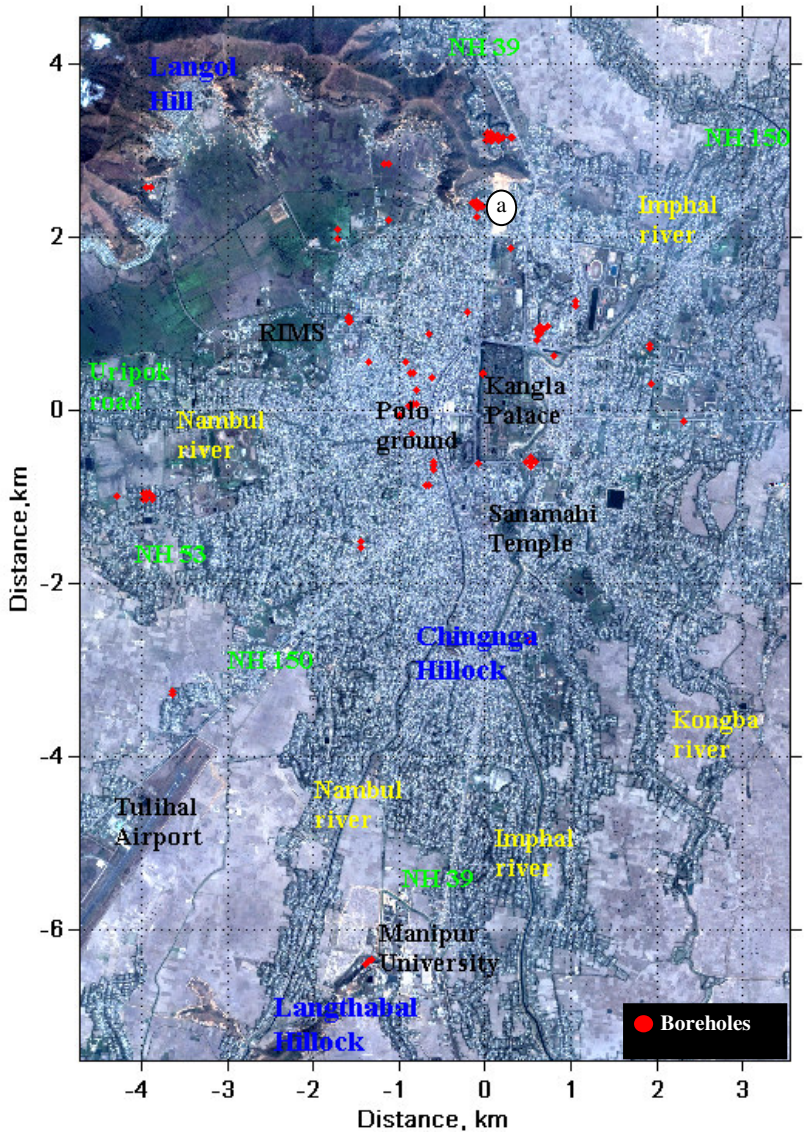


Figure 4.1 Imphal city along with boreholes location

The saucer like Imphal valley is surrounded by a series of mountain chains (Patkai hills on the north and north-east and the Manipur hills, Lushai hills, Naga hills and Chin hills on the south) running from north to south, forming an integral part of Indo-Burmese ranges (Laiba, 1992; Ibotombi, 2000). Brunnschweiler (1974) suggested that the structural and tectonic pattern near Imphal valley is transitional between the NE–SW tending pattern of Naga–Patkai Hills and N-S trend of Mizoram and Chin Hills. These hills comprise of geologically young rock formations due to tertiary upward displacement of the Himalayas from the shallow bed of the Tethys Sea. The rocks are mainly of tertiary and Cretaceous sediments with minor igneous and metamorphic rocks. Ibotombi (1998, 2000) reported that around 70% of the state is underlying with Flysch sediments of Tertiary age. Further, Disang and Barail flysch sediments lie beneath much of the central part of Manipur state. The Disang which is overlain by the Oligocene Barail formation contains abundant carbonaceous matter. The Barail is succeeded by predominantly argillaceous Surma and Tipam formations (Nandy, 1980). In the east of Manipur, igneous rocks of the Ophiolite zone are infringed into the Disang assemblage. Topographically Manipur comprises of a ridge and furrow terrain where sediments derived from surrounding ridges are deposited in the furrows (Ibotombi, 1998, 2000). In the Imphal valley, lenses of argillaceous sediments were deposited in the Assam-Arakan trough. Geomorphologically, Singh (2004) listed from the work of Agarwal and Shukla that the valley area can be classified into five units: 1) moderate to high structural cum Denudational hills, which can be seen as the hills and mountains surrounding the valley, 2) residual hills composing of hillocks and hills which are scattered in the valley (e.g. Langol hill, Chingna hill, etc.), 3) piedmont plain features along the foothills, 4) older alluvial plains of alluvium deposits near foothills of Imphal valley, and 5) younger alluvial plains having lower elevation than the older alluvial plains and mostly flat. The basements of the alluvium plain of Imphal

valley are considered to be made up of Disang shales. Imphal valley is surrounded by four major river basins *viz.*, the Barak river basin (Barak Valley) to the west, the Manipur river basin in central Manipur, the Yu river basin in the east, and a portion of the Laniye river basin in the north (Haokip, 2007). The river basins have eight major rivers: the Manipur, Imphal, Iril, Nambul, Sekmai, Chakpi, Thoubal and Khuga. All these rivers originate from the surrounding hills and deposit their sediment load in the Loktak Lake (Laiba, 1992) located in Imphal valley. The Imphal valley is sandwiched between Thoubal thrust on the east side and Churachandpur-Mao thrust (which partly forms the tectonic contact between the Disangs and Berails) on the western side.

There is a lack of geological information on Imphal city and a detailed geological report is still awaited. The valley is almost flat filled with fluvio-lacustrine dark grey to black clay, silt and sand alluviums. The predominant sediments are clay and mixture of clay and sand, whilst silt and sand forms lensoids and bands within clay. The alluvium profile (and hence bed rock profile) has not been mapped, however some drilling data of the Central Ground Water Board suggest that the average thickness of alluvium is at least ~150-200 m. It is suggested that the basement to be more or less consists of the Disang sediments. The stretching of the basement faults led to the development of isolated hillocks, as remnant of horsts. This forms the basis of tectonic origin and formation of Imphal valley (Ibotombi, 2000). However, this is in contrast to the erosional origin, which suggests that the valley was formed when river borne sediments filled up a lake, the present Loktak lake at the southern part of the valley being the part of the original lake that engulfed the entire valley once. Fluvio-lacustrine origin with subsequent earthquakes is also suggested as another theory (Laiba, 1992).

TH-994_06610404

4.3 Local soil condition

Imphal is a city located on the banks of Imphal, Nambul and Kongba rivers that have left several palaeoseismic channels over which present human settlement exists. Sands, clays, silts etc. of fluvio-lacustrine origin are the main constituents of Imphal valley, whereas ferruginous red soils are found near isolated foot hill regions. Alluvial soils occur near the river banks. Clayey soils in the valley region are rich in humus. In the low lying areas of Imphal city viz., Lamphelpat, Takyelpat, Prompat, Kakwapat (*pat* means lake) etc., virgin soils like clayey loam, dark clayey, and boggy type soils are found (Laiba, 1992).

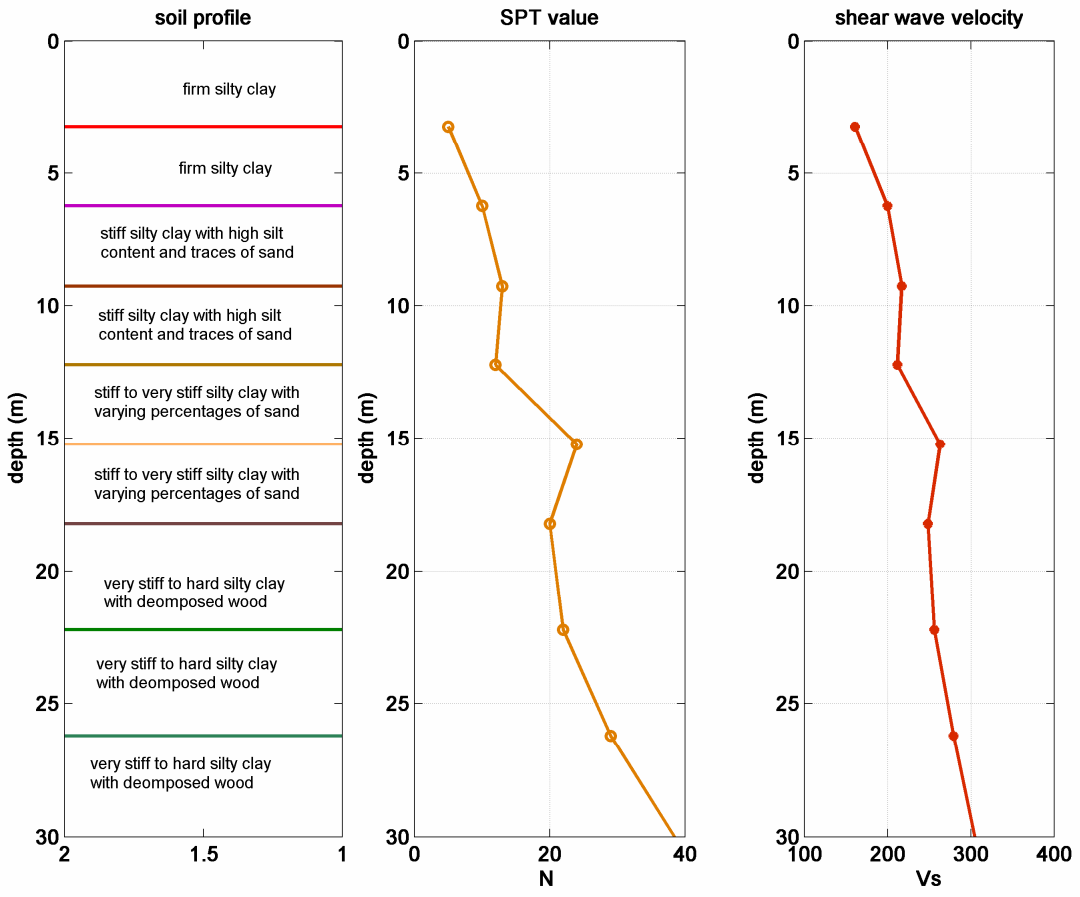


Figure 4.2 Soil profile, SPT-N value at a site near Langol hill

It may be noted that local soil plays an important role in soil amplification (see Section 2.10.2). It is therefore essential to take into account the local soil properties for obtaining the surface level ground motion. Moreover, as evident

from damages during past earthquakes, Imphal city is also susceptible to soil liquefaction. Hence estimation of surface ground motion calls for an extensive geotechnical investigations regarding the shear wave velocity, Cone Penetration Test (CPT) and other material properties distribution with respect to depth. Unfortunately, shear wave velocity profiles and CPT data are not readily available for Imphal city. However, SPT-N data and soil characteristics, at several sites situated at various parts of the city are available. In the absence of shear wave velocity and CPT data, this available limited information can be used for estimating surface ground motion. A detailed soil investigation data has been obtained from various construction projects, which are through Standard Penetration Tests (SPT) at 122 different locations in Imphal city. These locations are scattered over an area of about 11.5 km × 8 km along the NH-39 and NH-53 as shown in Figure 4.1. The SPT–N values have been measured at 1.5 m depth intervals. For many important construction sites, the SPT has been carried out up to a depth of 30 m, however for most sites the depths range from 6 to 20 m. Based on SPT results it has been observed that the soil deposits in Imphal city comprises mostly of silty clay and clayey along with organic matters (i.e. clay, silt, clayey sand, silty sand, clayey silt, sandy clay, silty clay etc.) deposited in different layers. These are typical alluvial/fluvial deposits which are generally loose in density. Indeed the SPT data indicates that the SPT–N values even at 25-30 m depth below ground surface are very low, mostly of the order of 15 to 20, excluding few places where it is about 30 to 40. Majority of these boreholes are located around the Kangla palace area that houses several commercial and administrative establishments, in addition to the sides of NH-39, NH-53 and NH-150 roads. The subsurface soil condition and SPT–N profile at a typical borehole located to the east of Langol hill (near NH 39) are presented in Figure 4.2. To have an idea about the site condition according to international practices, the average standard penetration resistance ($\bar{N}$) at all the boreholes is computed by the following expression (IBC 2006).

$$\bar{N} = \frac{\sum_{i=1}^{n} d_i}{\sum_{i=1}^{n} (d_i / N_i)} \qquad 4.1$$

where, d_i and N_i are the thickness and SPT-N value of each layer, n is the total number of soil layers. It may be noted that IBC (2006) requires soil data upto 30m depth. In present study, as all the soil data are not upto 30m depth for site classification, the mean SPT value estimated from those the boreholes for which SPT values are available upto 30m depth has been used as additional data for the remaining depth upto 30 m. Out of 122 boreholes in Imphal city, considered in the present analysis, 114 boreholes are classified as E-type ($\bar{N}$ < 15), and the remaining 8 belong to D-type (15 < $\bar{N}$ < 50). As per IBC (2006) E-type sites are susceptible to liquefaction of soil and failure. Therefore it can be said that as most parts of Imphal city are vulnerable to liquefaction induced failure. The detailed soil data collected from sites at Imphal city are given in Appendix B.

4.4 Soil amplification

As V_s (shear-wave velocity) are not mapped for Imphal city, in the present work shear wave velocities have been computed from the N-values using the empirical relation $V_s=97N^{0.314}$ of Imai and Tonouchi (1982), where N is SPT N-value and V_s is in m/sec. It is assumed that the top soil layer (i.e. alluvial/fluvial deposits) is underlain by rock. Besides, at each borehole location for SPT, soil samples were collected at different depths. Based on tests such as visual observation, particle size analysis, plasticity characteristics etc., the soil for different layers have been classified as clayey, sand etc. Modification of acceleration time history between soft rock and soil site is a non-linear problem in one dimension and hence for such sites, amplification can be directly found by the nonlinear site response analysis. The nonlinear behavior of the soil *i.e.*, reduction of shear modulus and increase of damping ratio with shear strain are accounted by using equivalent linear soil properties mode. For this purpose, shear modulus reduction versus shear strain curves

and damping ratio versus shear strain curves proposed by Vucetic and Dobry (1991) for different types of soil *i.e.,* clay, sand and rock have been used in the present analysis. Nonlinear site response analysis has been carried out using the computer program SHAKE91 of Idriss and Sun (1992). The simulated acceleration time history at rock level from finite fault seismological model for Imphal city has been used as input in SHAKE91 to generate surface level time histories.

4.5 Comparison with the SRR data of 6th August 1988 earthquake

Among the simulated rock level time histories (Chapter 3) samples, the acceleration time history which has a PGA close to the mean value (0.1g) has been selected for estimating the surface level ground motion at 122 locations at Imphal city.

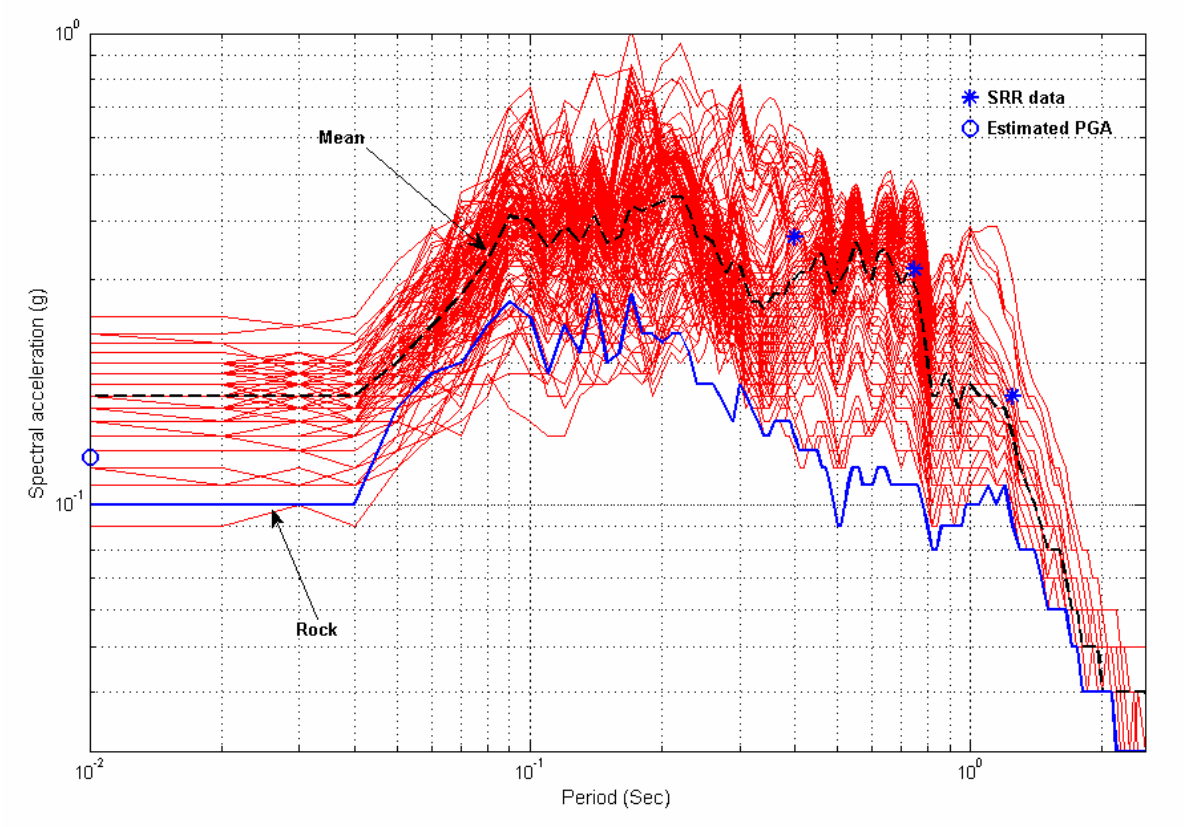


Figure 4.3 Surface level response spectra at Imphal city due to 6th August 1988 earthquake (5 % damping)

The results of nonlinear site response analysis (Idriss and Sun, 1992) are plotted in the form of surface level response spectra for all the 122 borehole locations (Figure 4.3). The rock level response spectra is also shown in Figure 4.3. In Figure 4.3, SRR data for 5% damping are also plotted for comparison. Since the soil condition at the instrument site is not known, direct comparison with the simulated data is not possible. However, it can be observed from Figure 4.3 that the recorded data lies in between the estimated response spectra, which indicates that the methodology is able to estimate the ground motion with reasonable accuracy.

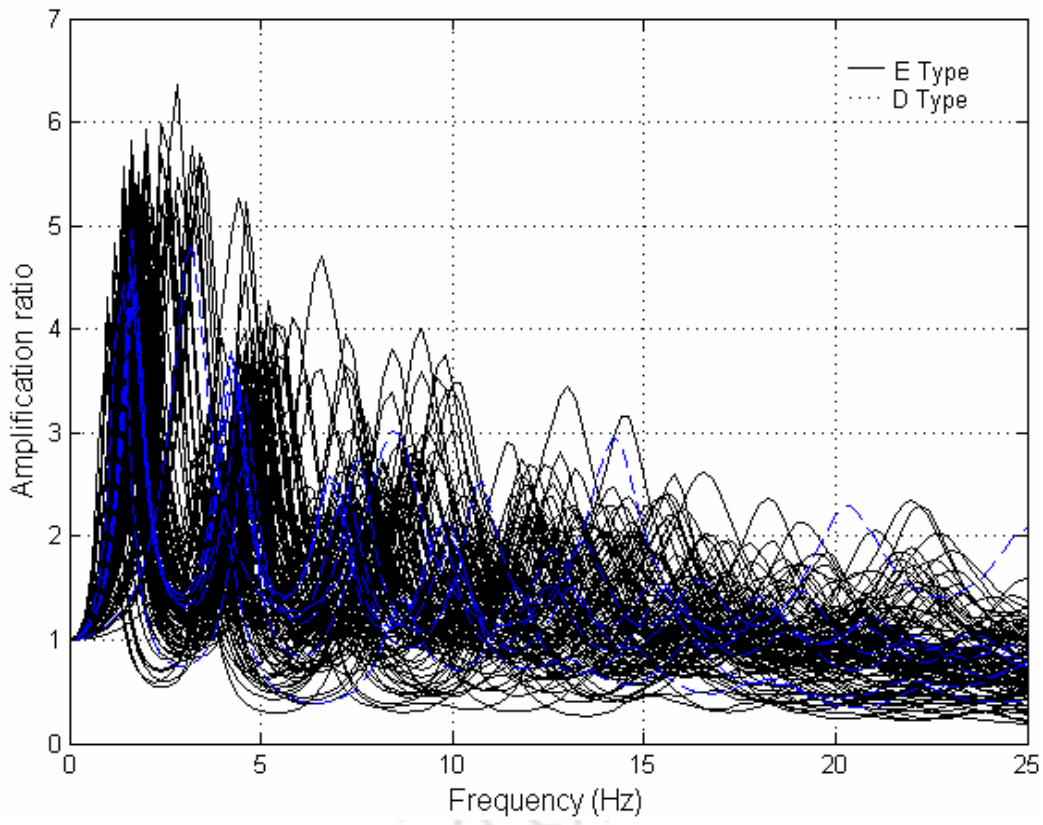


Figure 4.4 Frequency response functions of soil profiles in Imphal city

The frequency response functions (FRF) defined as the ratio of acceleration at the ground surface, computed through SHAKE91, to the acceleration at the bedrock level; for all the soil profiles are shown in Figure 4.4. It can be seen that maximum amplitude occurred in the range of 1-3 Hz. And hence, the first natural frequency of the soil deposits can be inferred in the range 1-3 Hz. After

validating the simulation approach adopted in the present work, the study has been conducted for the two earthquake events i.e. 1869 Cachar (M_w 7.5) and hypothetical earthquakes (M_w 8.1) that may affect the Imphal city in the future.

4.6 Ground motion during the 1869 Cachar Earthquake (M_w 7.5)

In Figure 4.5, simulated accelerogram and it response spectrum both for underlying rock layer and soil surface are shown for one sample acceleration time history of 1869 Cachar earthquake which originated at Kopili fault is presented. It can be seen that the ground motion amplitude gets amplified (0.16g to 0.2g) due to the effect of soil. For the borehole shown in Figure 4.1, response spectra for all 10 samples with mean (μ) and mean ± standard deviation (σ) are shown in Figure 4.6.

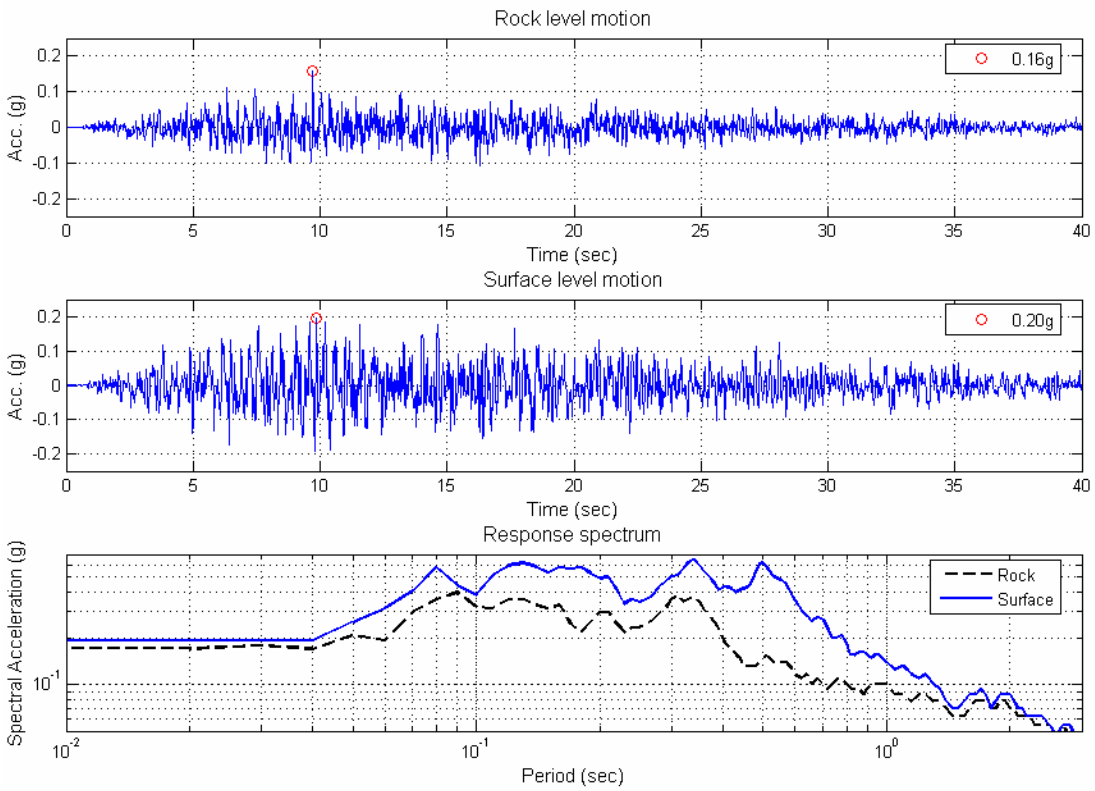


Figure 4.5 Surface level ground motion at a borehole (Figure 4.1) in Imphal city

Almost for all the 10 samples of time histories amplifications have been observed. In a similar fashion, nonlinear site response analysis is carried out at

all the 122 locations and the corresponding surface level acceleration time histories have been computed for all the ten earthquake time history samples, then the mean as well as standard deviation contours have been plotted for different periods (PGA, 0.3 s and 1.0 s) of ground motions (Figures 4.7a-c). At rock exposures in places like Langol hill, Langthabal hillock and Chingnga hillock, it is assumed that there is no amplification. Therefore in these areas the mean PGA is taken same as that of the rock (i.e. 0.12g) and standard deviation (σ) as zero. Figures 4.7a and 4.7b show respectively the variation of mean and standard deviation of PGA in Imphal city. Mean PGA at Langol hill, Regional Institute of Medical Sciences (RIMS) and Kangla are 0.14g, 0.18g and 0.22g respectively with corresponding standard deviations of 0.005, 0.02, and 0.025.

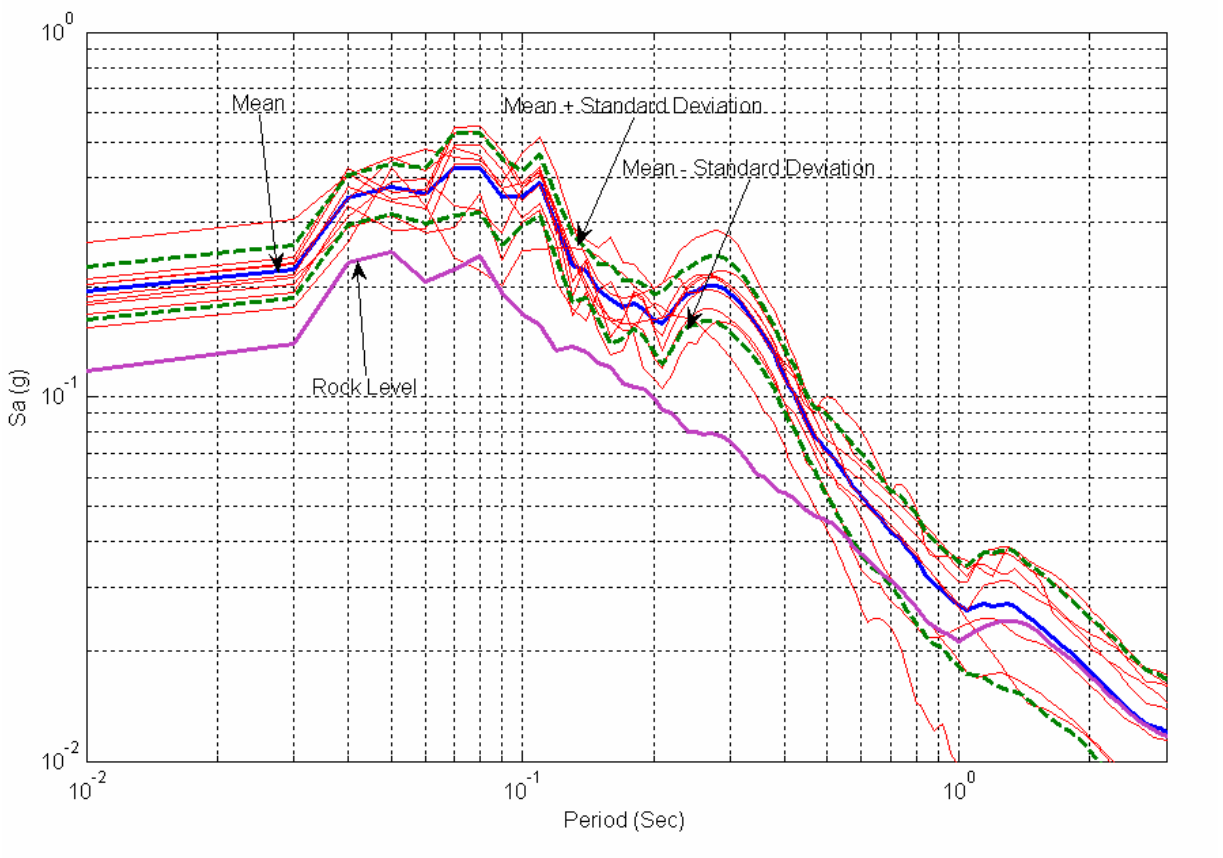


Figure 4.6 Response spectra for one bore hole along with μ and μ ± σ due to 1869 Cachar earthquake

The occurrence of maximum PGA at Kangla area agrees well with the damages reported during 1869 earthquake (Oldham, 1882). Mean surface level

PGA range in the vicinity of Manipur University and Tulihal airport is 0.12g to 0.14g with corresponding standard deviation of 0.005 at both the location.

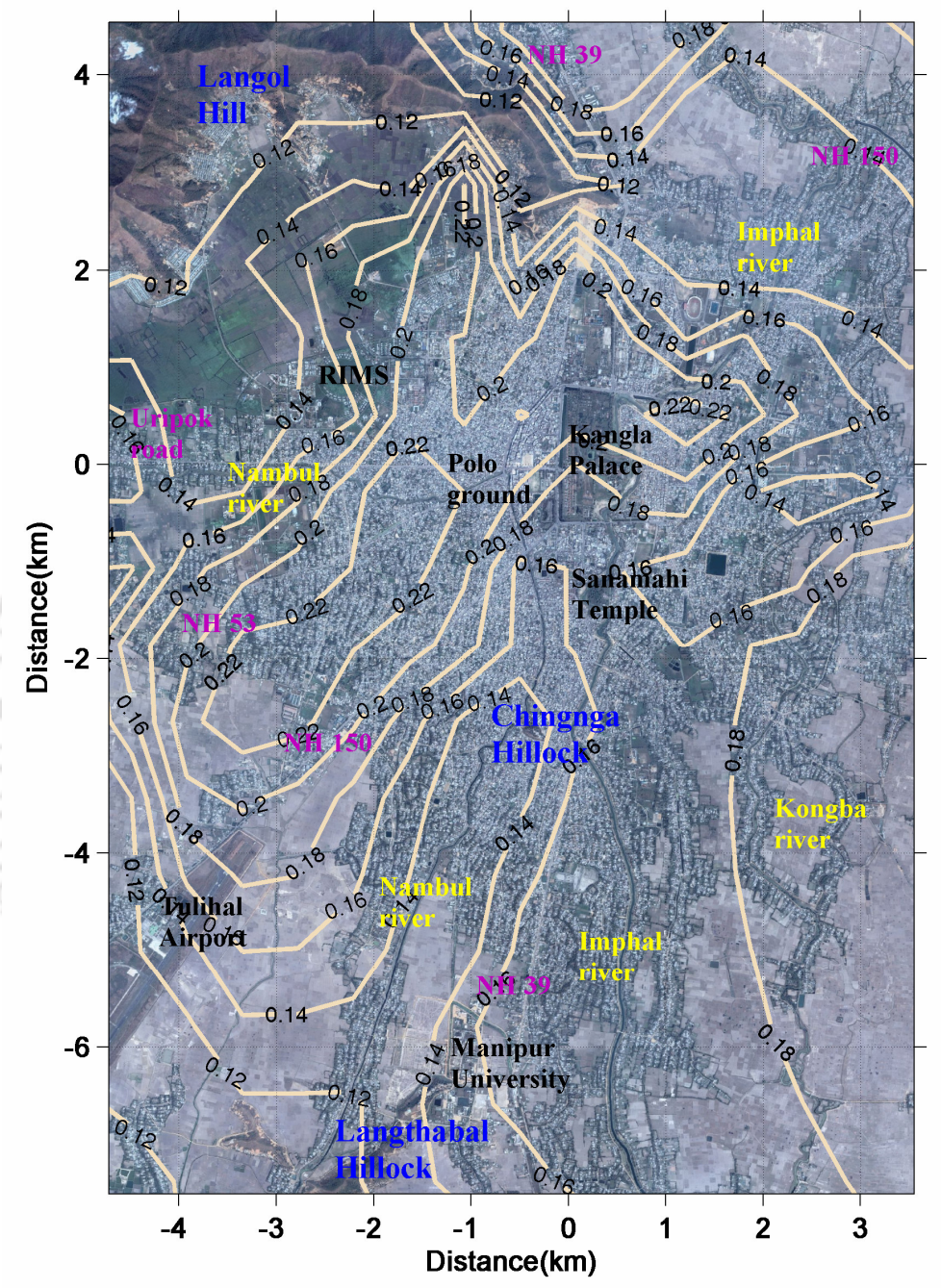


Figure 4.7a Mean Surface level PGA due to 1869 Cachar earthquake

IBC (2006) defines response spectra in terms of short period (0.3 s) and long period (1 s) seismic coefficient and hence the contour map has been plotted for these periods. Figures 4.8a-b and 4.9a-b show the spatial variation of mean and

standard deviation of spectral acceleration at 5% damping for natural time periods of 0.3 s and 1 s respectively.

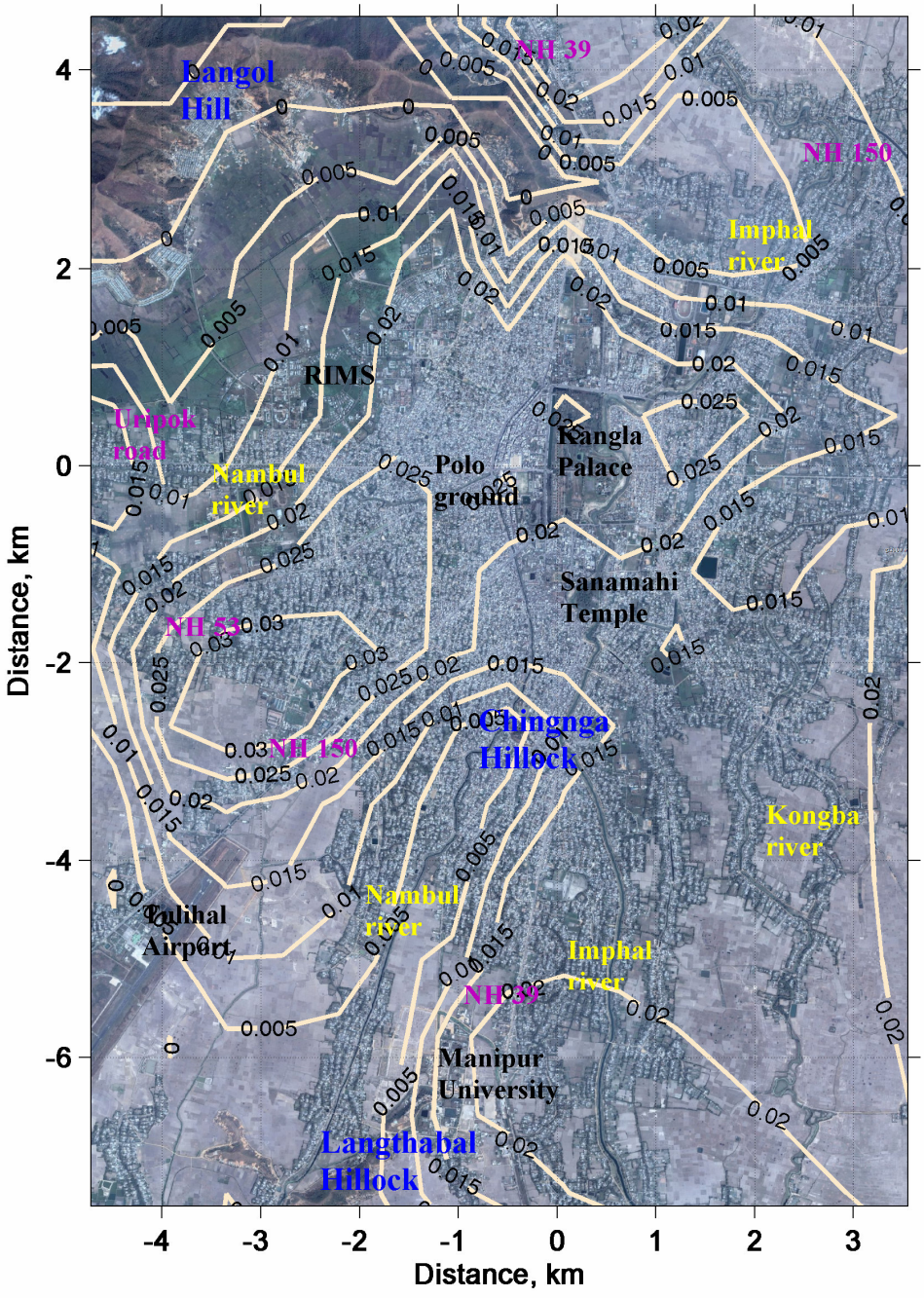


Figure 4.7b Standard deviation of surface level spectral acceleration at PGA due to 1869 Cachar earthquake

From Figures 4.8a and 4.9a, it can be noted that for 0.3 s, maximum mean surface level PGA value of 0.2g occurs at Kangla area and for 1 s it occurs around Manipur University, Sanamahi temple, etc., area. Thus the maximum surface level acceleration affect can be expected for 3 storey (~ 0.3 s natural

period) and 10 storey building (1.0 s natural period) near Kangla and Manipur University area respectively. The same has been compared with the Indian building code response spectra (IS: 1893, 2002).

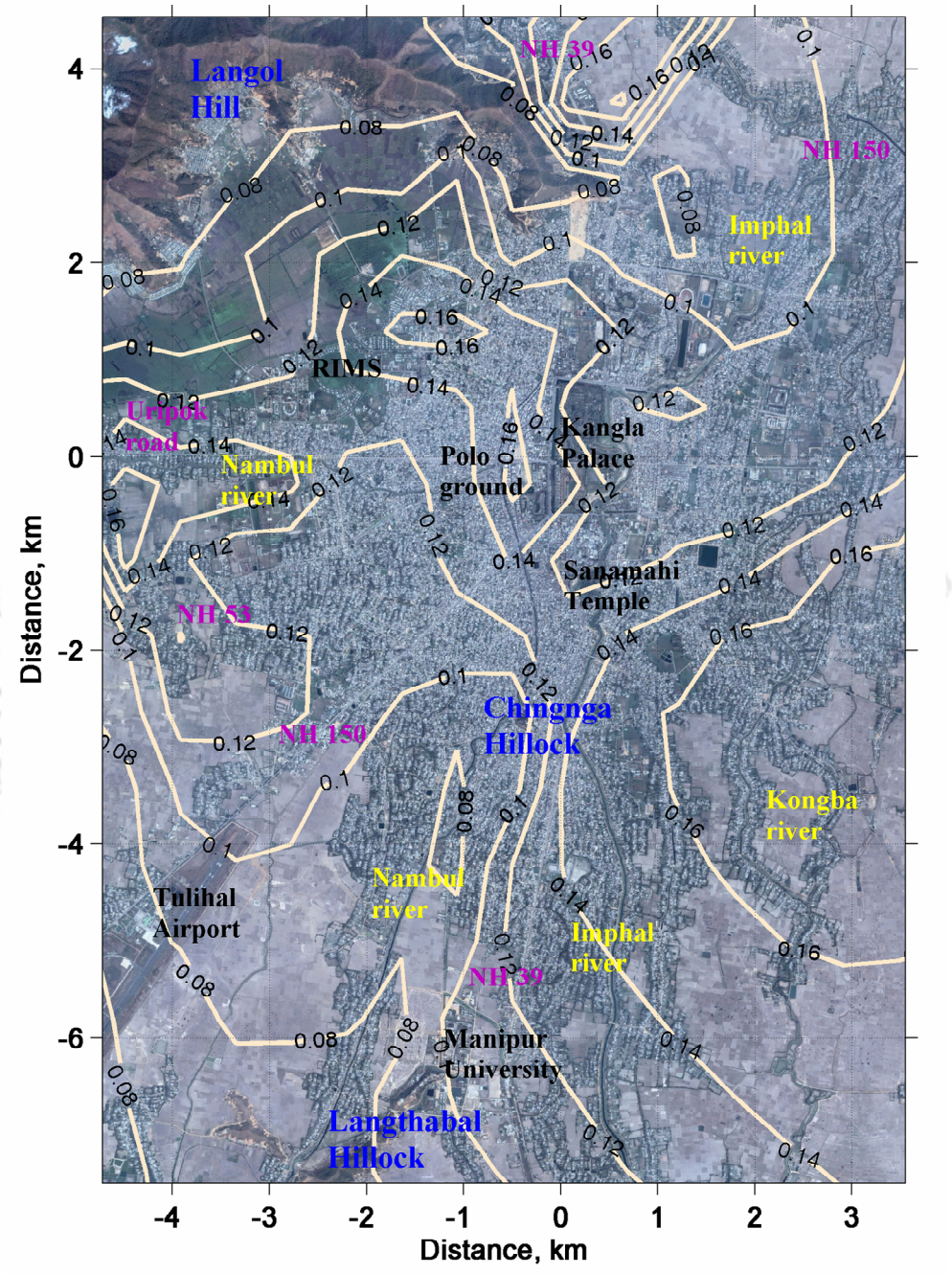


Figure 4.8a Mean Surface level spectral acceleration at 0.3 s (5 % damping) due to 1869 earthquake

From Figure 4.10 it can been seen that amplification of rock level ground motion at surface level can be observed for most area of Imphal city due to simulated 1869 Cachar earthquake. A comparison of the present result (Figure

4.10) with response spectra proposed by IS: 1893 shows that IS: 1893 overestimates the effects of ground motion for 1869 earthquake event and hence it is conservative.

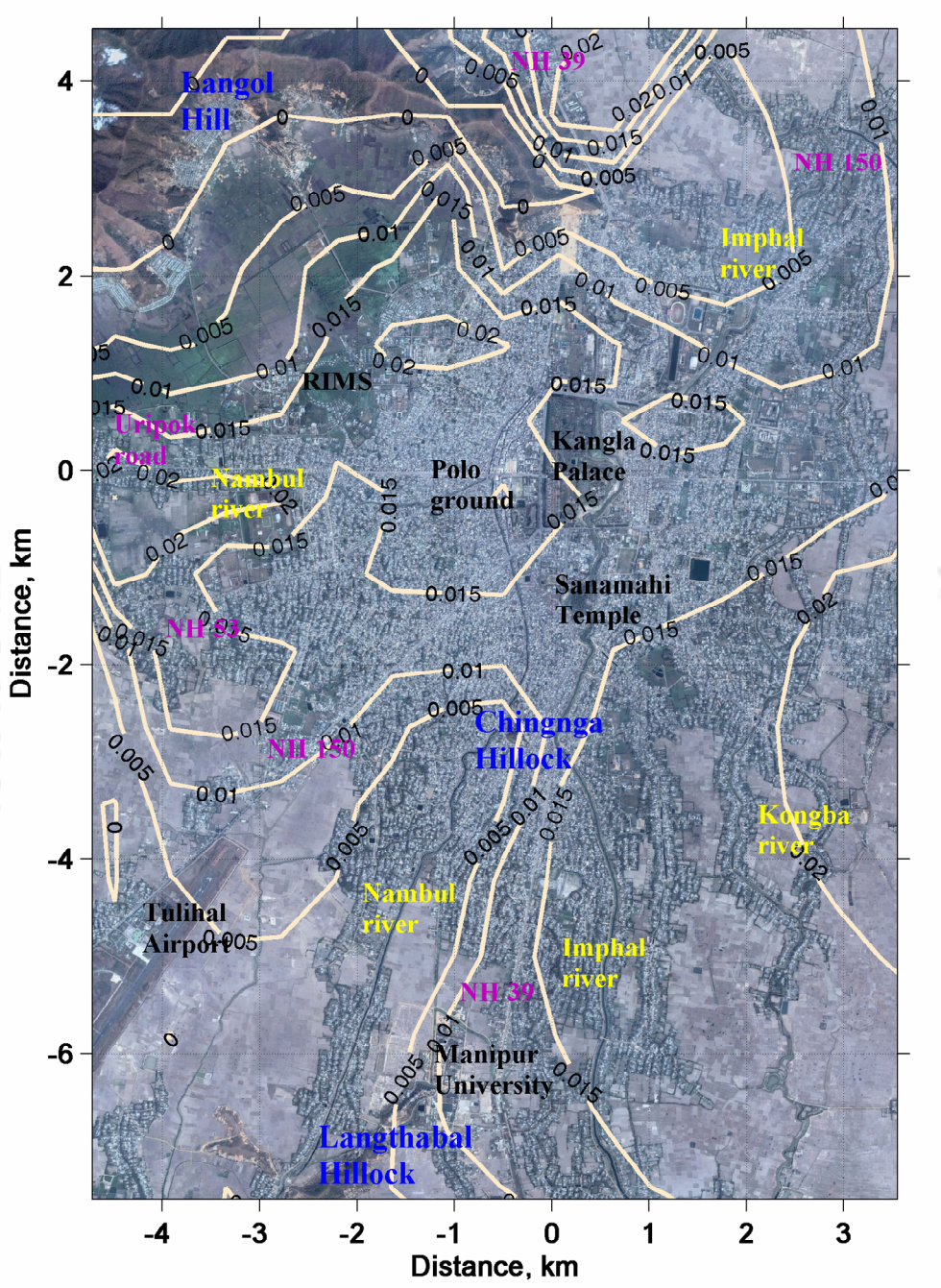


Figure 4.8b Standard deviation of surface level spectral acceleration at 0.3 s due to 1869 Cachar earthquake

Although the PGA at rock level is almost uniform, surface level PGA exhibits striking variation i.e. varying from 0.14 g to 0.24 g. It is alarming to note that around the central part of the city *viz.,* north and south part side of Kangla

palace, where important commercial and administrative establishments are located, there are higher values of amplification with the mean surface level PGA being of the order of 0.18g-0.22g.

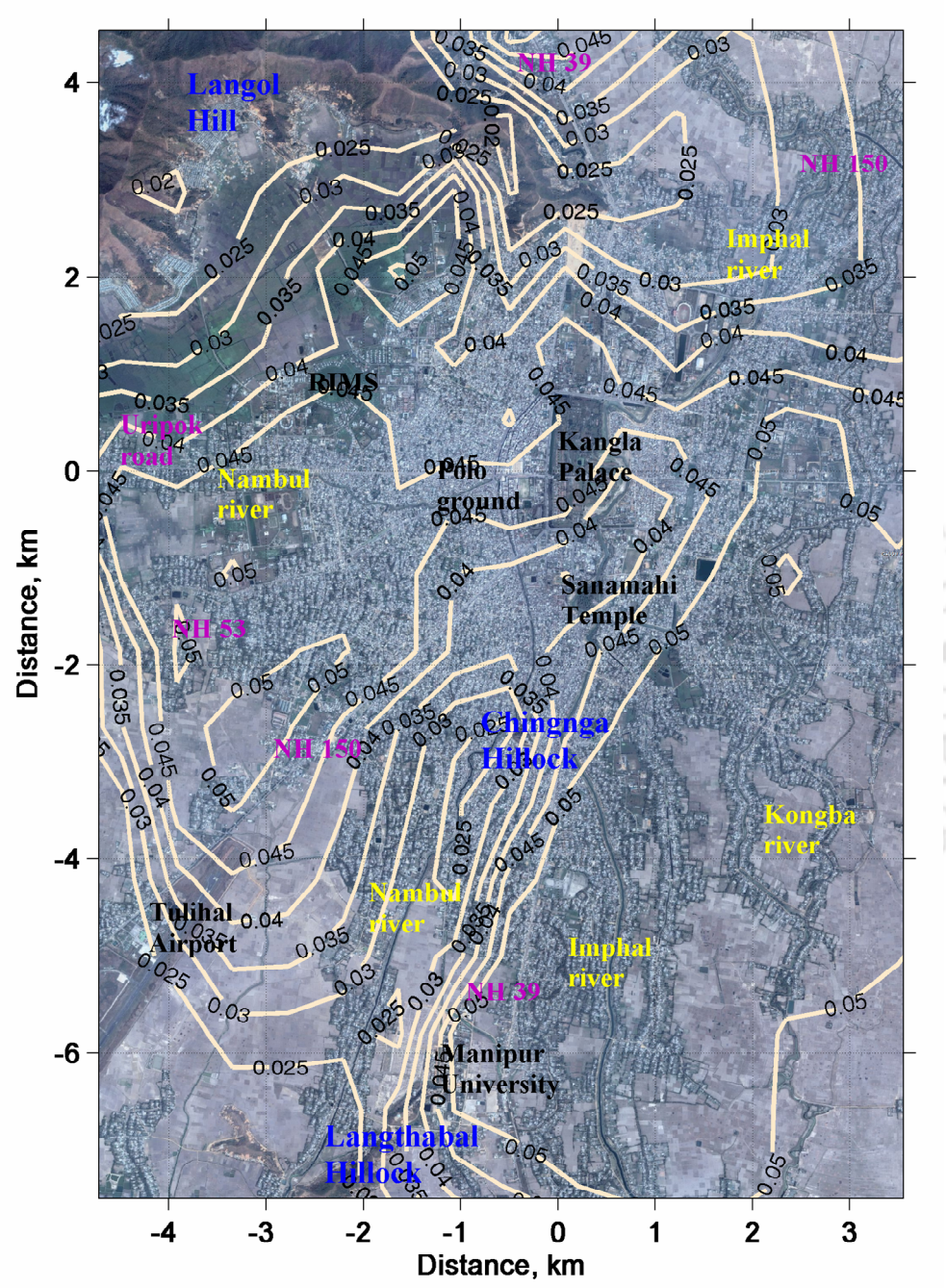


Figure 4.9a Mean Surface level spectral acceleration at 1.0 s (5 % damping) due to 1869 earthquake

The occurrence of maximum PGA at Kangla area agrees with maximum damages reported for 1869 earthquake (Oldham, 1882).Of course, in 1869 the populations as well as the infrastructures were less, so the damages were

comparatively lesser. However, if a future large earthquake in this Kopili region was to occur as speculated by Kayal *et. al.,* (2006), it is likely to have relatively high damage for structure not designed for 0.22g.

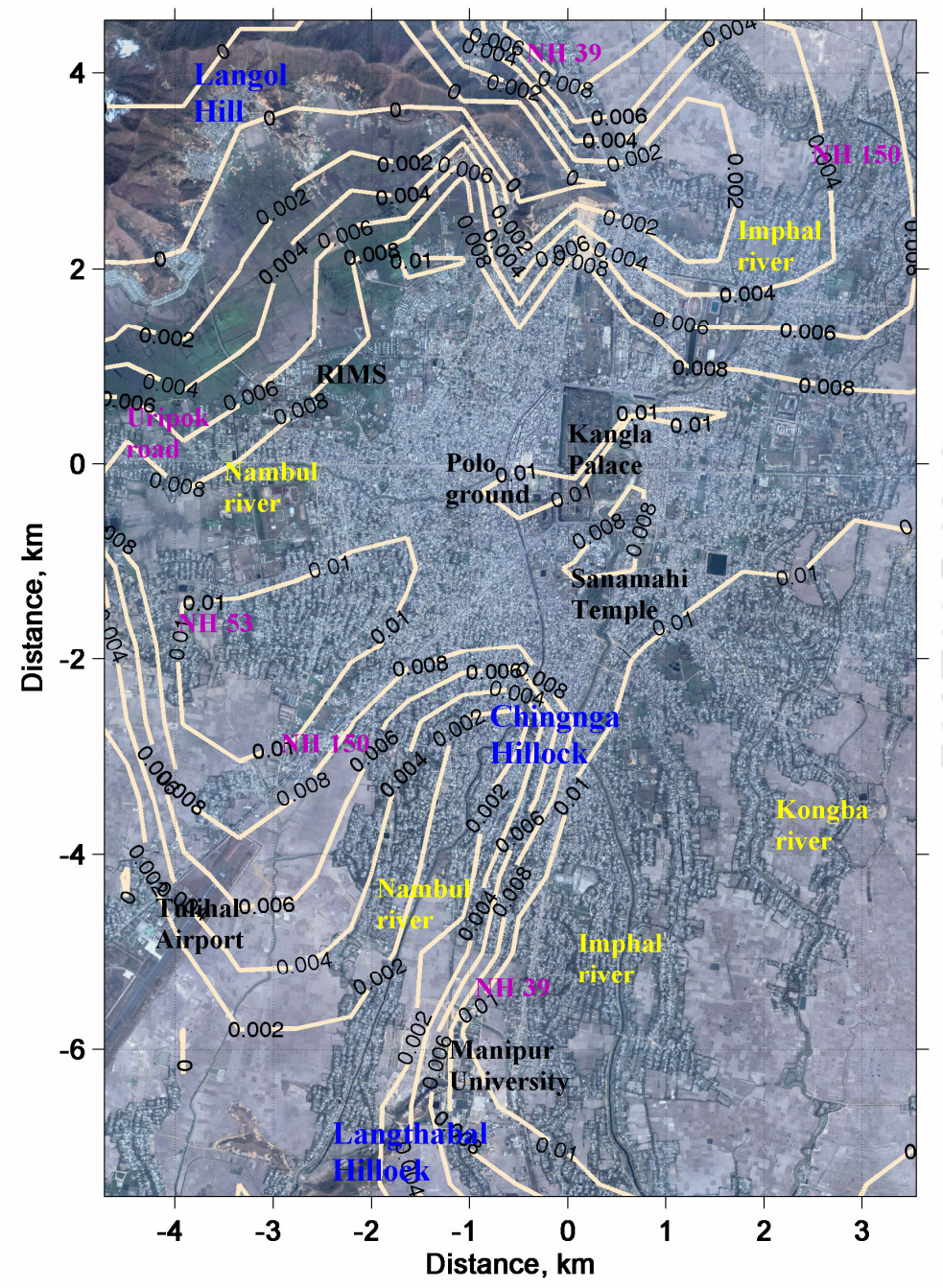


Figure 4.9b Standard deviation of surface level spectral acceleration at 1.0 s due to 1869 Cachar earthquake

4.7 Ground motion due to hypothetical M_w 8.1 earthquake in the Indo-Burmese Ranges

As discussed in recurrence relationship (Section 3.5.1) that the IBR is the most active seismic zone in NE India that can affect to Imphal city (less than 100 km) and hence play a significant role in seismic hazard analysis for this city. A great earthquake in IBA has been speculated by seismologists after the 26th December Indonesian event (Cummins, 2007). Future great earthquake in the IBA is likely to cause great loss of life and immense damages to infrastructures in Imphal city.

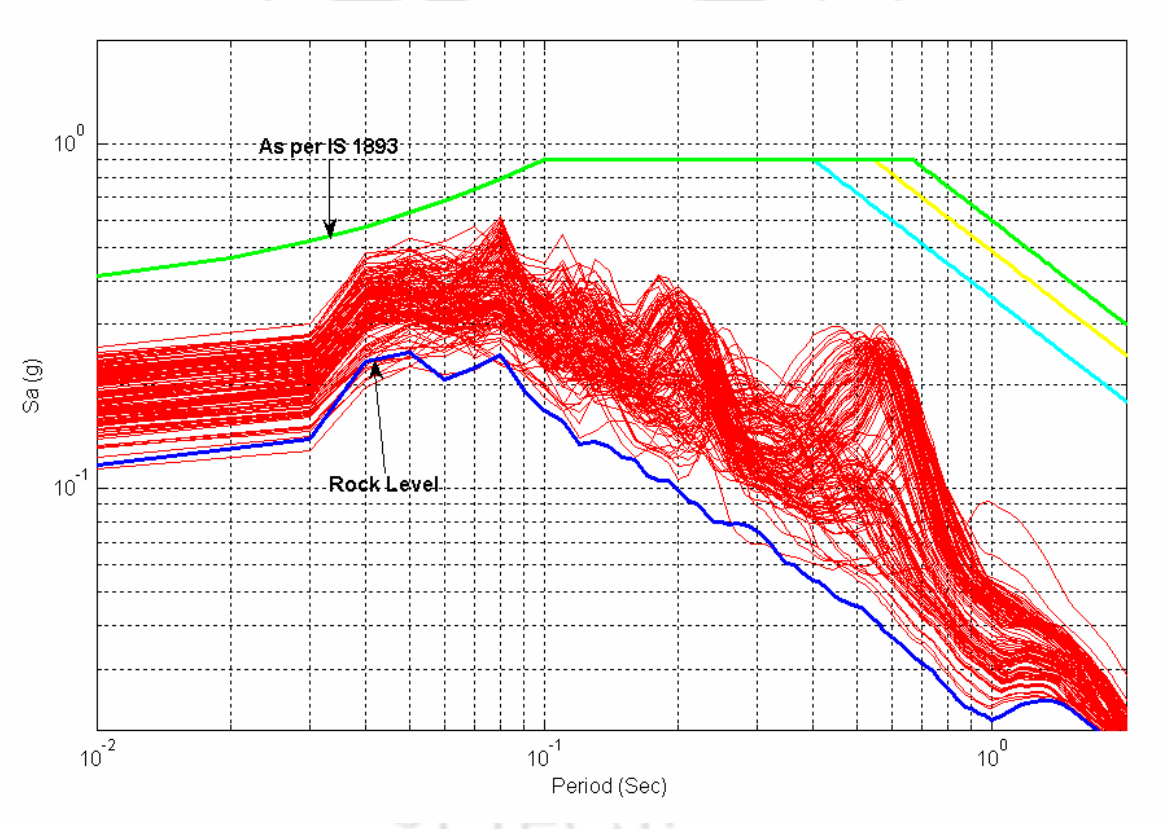


Figure 4.10 Mean response spectra for all sites due to 1869 Cachar earthquake (5 % damping)

Hence possible ground motion due to a hypothetical earthquake in IBR has been considered (Section 3.9). Figure 4.11a shows the surface level PGA distribution for the M_w 8.1 hypothetical event in the IBA. Mean surface level PGA of 0.45g has been observed in several areas surrounding the Kangla palace and to the east of Langol hill. It may be noted that the maximum

surface level PGA has increased to 0.5g (~ 100% increase) for M_w 8.1 event from 0.24g for the 1869 event (Figure 4.7a). The standard deviation around the central places *viz.*, Kangla palace, polo ground and RIMS are 0.12, 0.1, and 0.14 respectively (Figure 4.11b).

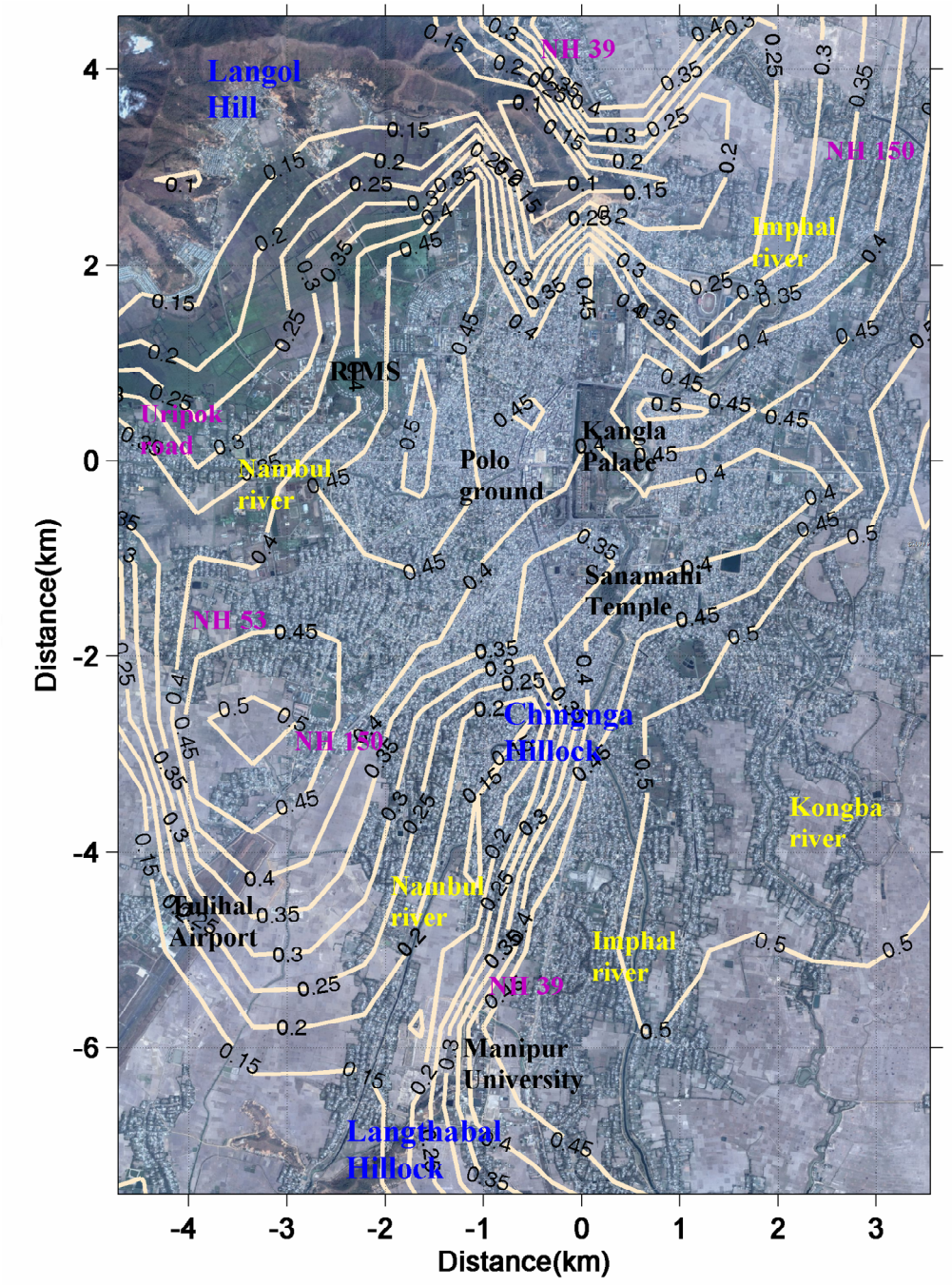


Figure 4.11a Mean surface level PGA due to hypothetical earthquake (M_w 8.1) in IBR

As mentioned earlier that these are important centers and densely populated areas of Imphal city and hence can get affected significantly. In Figures 4.12a

and 4.12b, the spatial distribution spectral acceleration at 0.3 s and 1.0 s are shown for Imphal city.

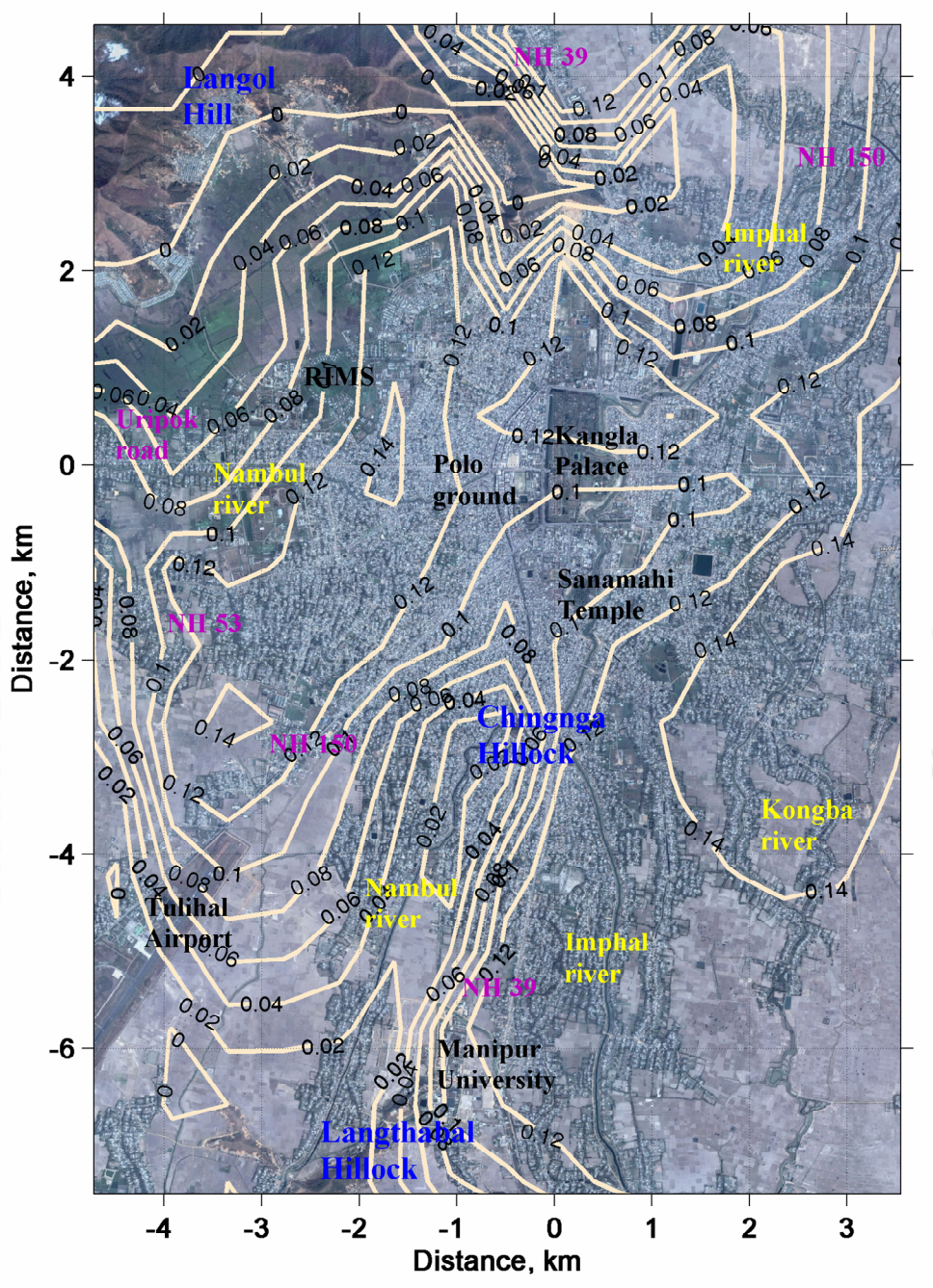


Figure 4.11b Standard deviation of PGA due to hypothetical earthquake (M_w 8.1) in IBR

For 0.3 s time period it can be seen that maximum mean surface level spectral acceleration of 0.27g occurs to the east of Langol hill (Figure 4.12a), whereas near Kangla palace, RIMS and Sanamahi temple area the mean spectral acceleration is around 0.175g. The corresponding standard deviation at these

locations is 0.05. Near Tulihal airport the spectral acceleration is 0.15g with standard deviation of 0.04. For 1.0 s natural period the maximum surface level spectral acceleration is found to be 0.055g which occurs near Kangla palace area with standard deviation values at PGA being 0.14 (Figure 4.13a,b). Further near RIMS, Tulihal airport, Manipur University and Sanamahi temple the mean spectral value is 0.035g with standard deviation of 0.08 in all these locations. At 0.3 s and 1.0 s period standard deviation are 0.04 and 0.016 near Kangla palace area and reduces towards Tulihal airport to 0.02 and 0.008 respectively (Figure 4.12b, 4.13b). Surface level response spectra for M_w 8.1 (5% damping) is shown in Figure 4.14. The Figures show comparison with IS-1893: 2002 response spectra. It can be seen that spectral acceleration for some site the responses are underestimated by the code of practice for this particular hypothetical events.

4.8 Determination of site coefficients

The above analysis gives an idea about the variation of ground motion in Imphal city. To make it simpler for estimating the site response in Imphal city for application purpose, the soil sites in Imphal are modeled in term of site coefficients defined as the ratio of surface level response to rock level response at different period as shown below (Equation 4.2).

$$F_c = \frac{Surface\ level\ response}{Rock\ level\ response} = \frac{S_r}{r_{br}} \qquad 4.2$$

For estimating site coefficient at each site in Imphal city, around 700 synthetic ground motions have been generated for different combination of magnitude and distance from the faults under consideration. Ten samples at a regular interval of magnitude of 0.5 and distance of 20 kms distance between 5-8.5 magnitude and 5-200 km distance have been considered for analysis. The PGA of simulated 700 time histories at various ranges of magnitude and distance

are shown in Figure 4.15. It can be observed that mean PGA is relatively low at lower magnitudes (less than 6.0) and at larger distances (greater than 90 km).

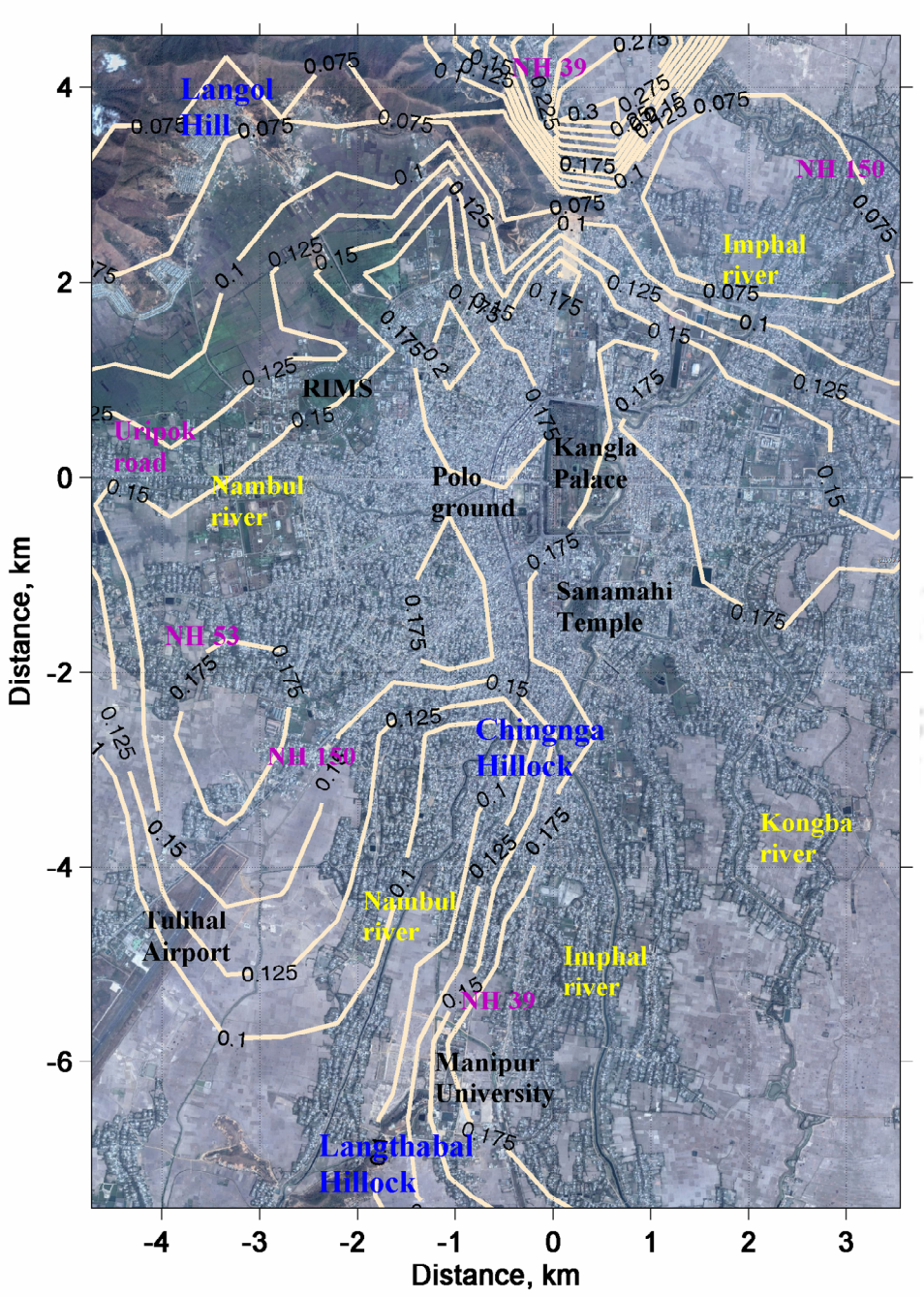


Figure 4.12a Mean surface level spectral acceleration at 0.3 s (5% damping) due to hypothetical earthquake (M_w 8.1) in IBR

For each site, site response analysis has been performed for all the 700 time histories (generated through SHAKE 91) and correspondingly 700 site coefficients are estimated for one site for all periods of engineering interest

(PGA to 3.0 s) and by statistical regression single site coefficient are developed. Similar procedure has been opted for all the sites in Imphal city.

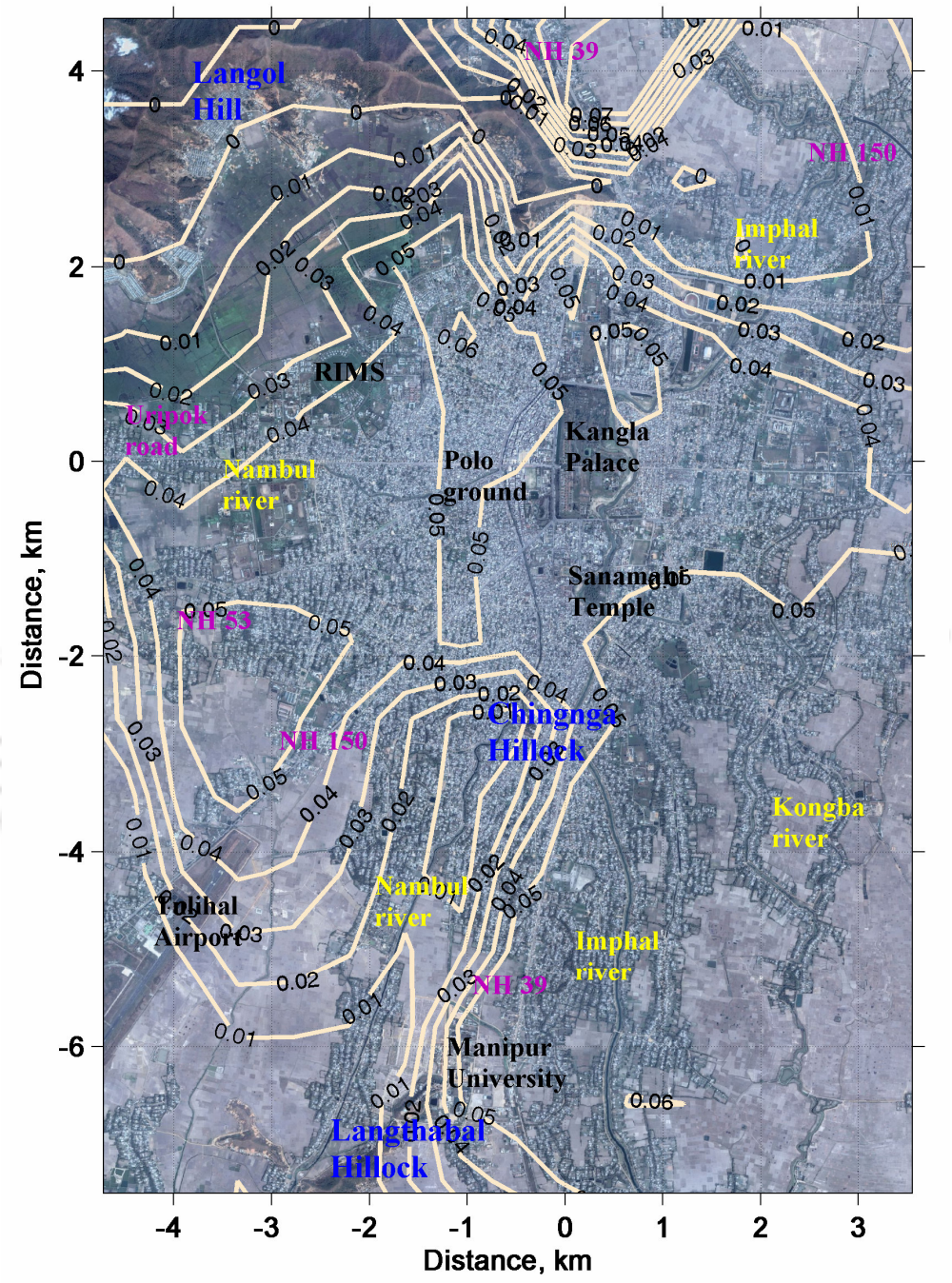


Figure 4.12b Standard deviation of surface level spectral acceleration at 0.3 s due to hypothetical earthquake (M_w 8.1) in IBR

These site coefficients are expected to help design engineers in getting the surface level response for Imphal city. The site coefficient for a soil site category (D, E) at a selected period has been determined as the ratio of the

spectral acceleration value at that period to the corresponding value at a reference site or rock level.

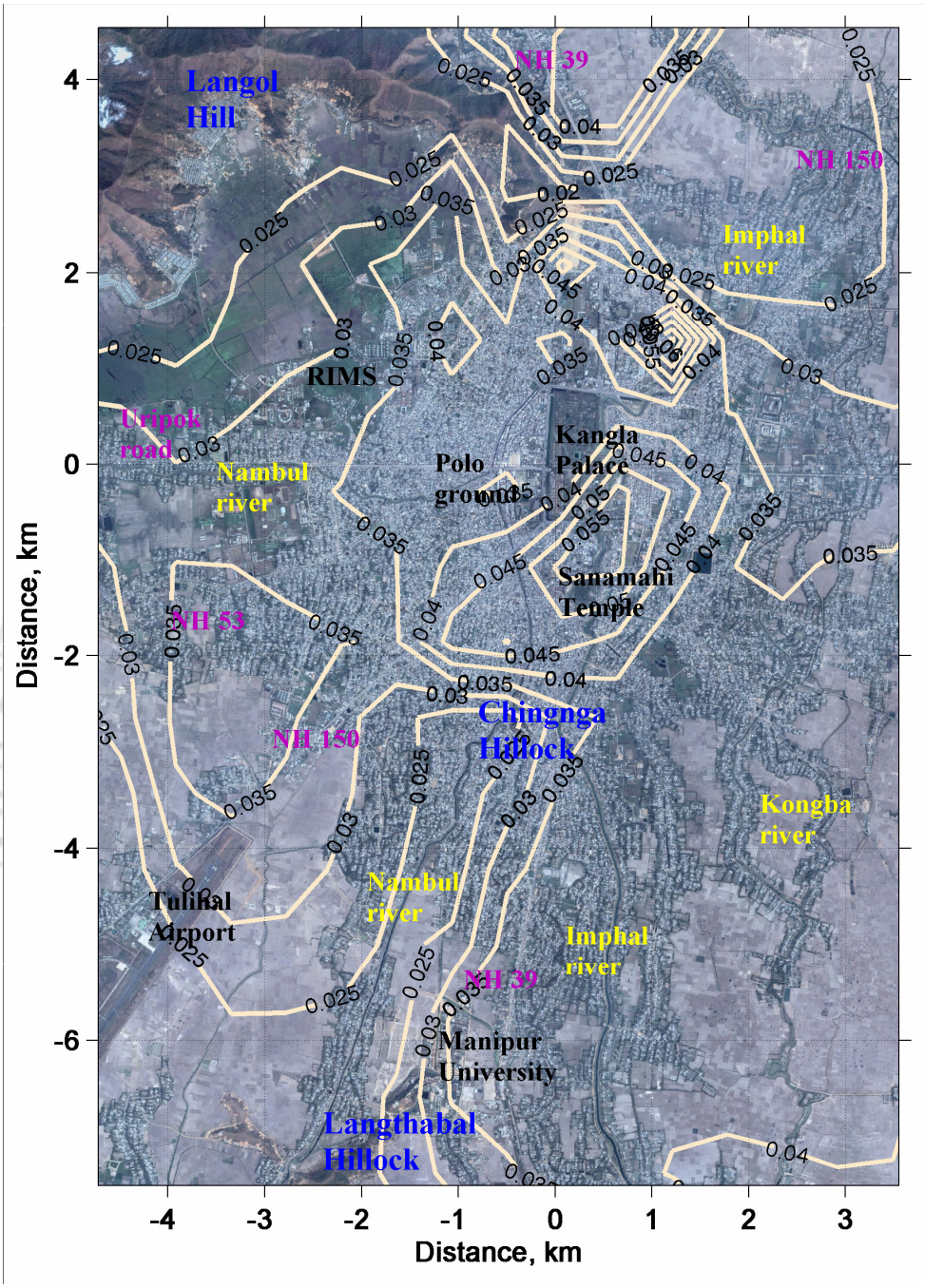


Figure 4.13a Mean surface level spectral acceleration at 1 s (5% damping) due to hypothetical earthquake (M_w 8.1) in IBR

In this study, the reference site is taken as B-Type rock site which are found as hillock in Imphal (e.g. Chingmirong, Langol etc). From the 700 response spectra established for each of the two soil categories present in Imphal city, the site coefficients at various selected periods are calculated

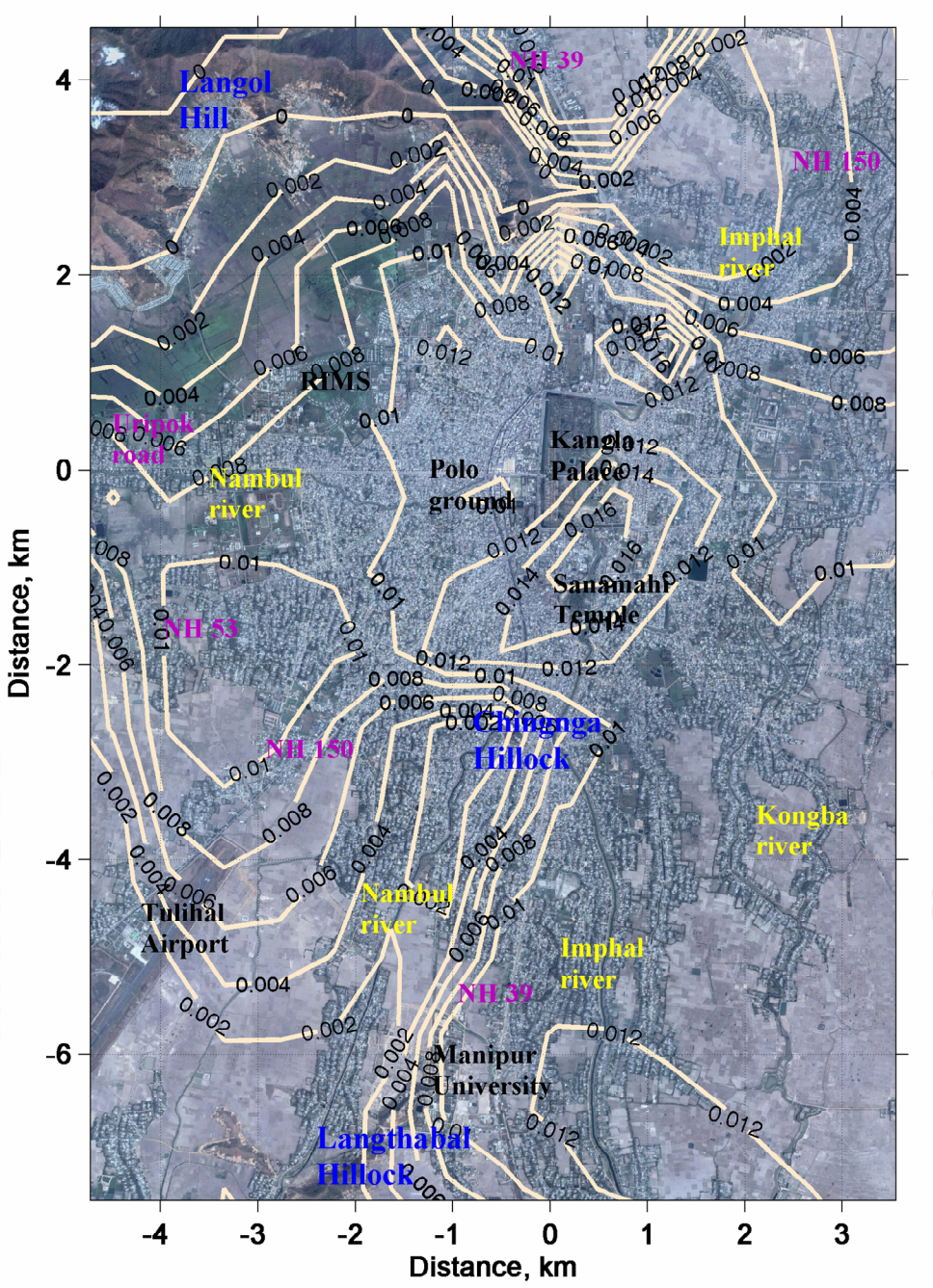


Figure 4.13b Standard deviation of surface level spectral acceleration at 1.0 s due to hypothetical earthquake (M_w 8.1) in IBR

As the site coefficient (F_c) is not a constant value (varies with rock level motion) for a particular site, regression analysis has been used to obtain an empirical relation of the form $\ln(F_c) = a_1 \times r_{br} + a_2 + \delta$ between site coefficient (F_c) and rock level motion 'r_{br}' (Figure 4.16 & 4.17).

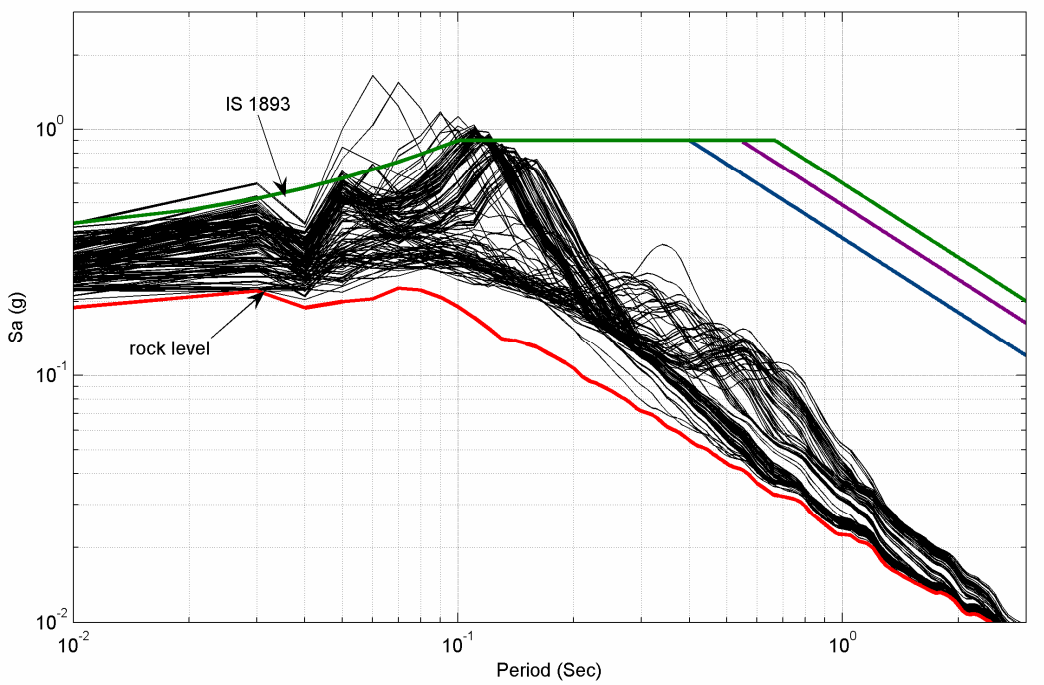


Figure 4.14 Mean Response spectra for all sites due to hypothetical earthquake in IBR (M_w 8.1) (5 % damping)

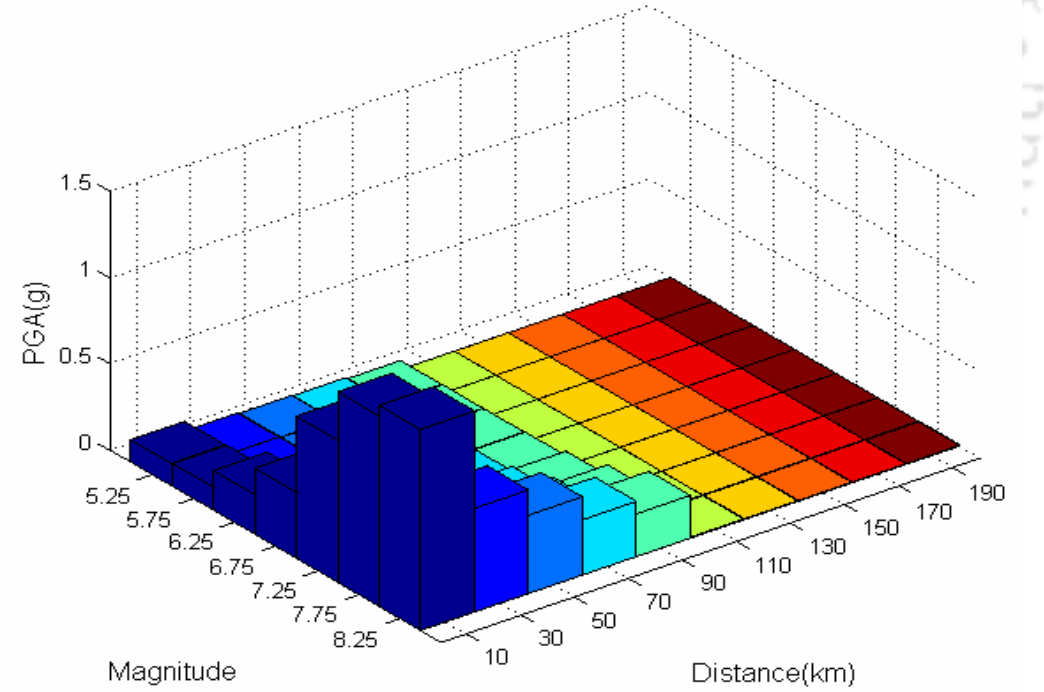


Figure 4.15 Mean PGA distribution

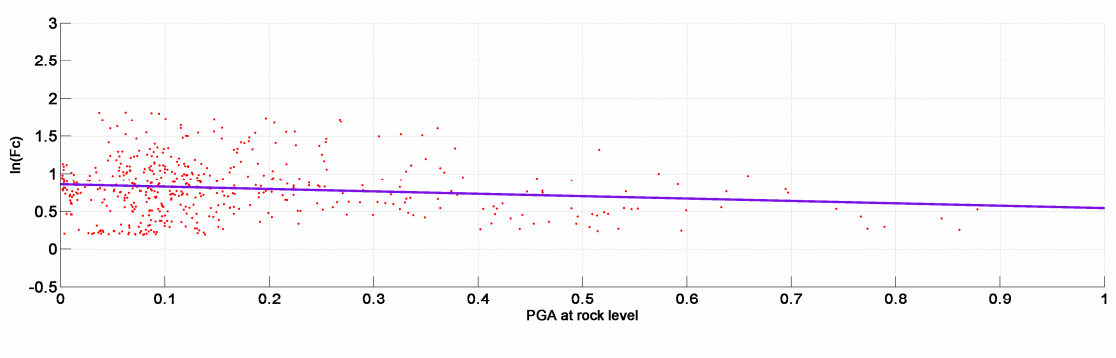


Figure 4.16 Site coefficients for surface level ground motion corresponding to zero period for a typical D-Type soil

The distribution of site coefficients corresponding to zero natural period are plotted with respect to the corresponding bedrock following fit is

$$\ln(F_c) = a_1 \times r_{br} + a_2 + \delta \qquad 4.3$$

where a_1 and a_2 are regression coefficients and δ is the standard deviation. Similarly regression analysis has been performed for various natural periods and the variation of a_1, a_2 and standard deviation are plotted in the form of contour map at zero period (PGA), 0.3 s and 1.0 s respectively.

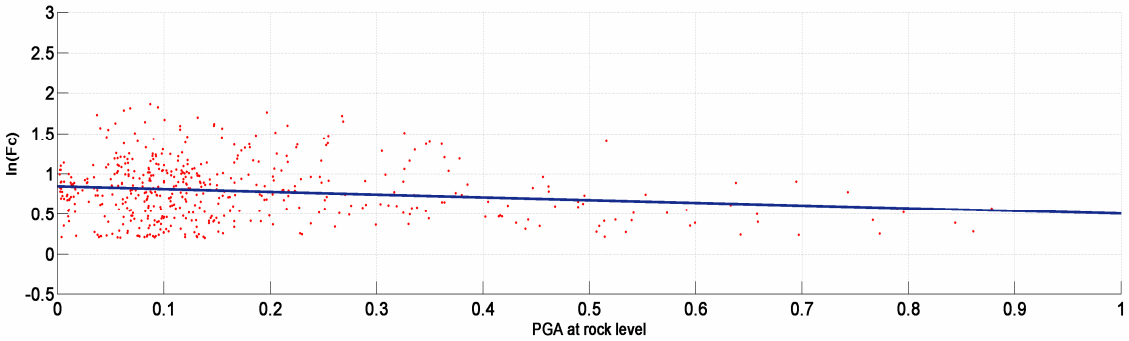


Figure 4.17 Site coefficients for surface level ground motion corresponding to zero period for a typical E-Type soil

For two typical type of sites present in Imphal city *viz.*, site-12 (D-type) and site -36 (E-type) (see Appendix C), the values of a_1, a_2, and δ are shown in Table 4.1. These values can be used to compute the surface level response at different periods. Further Figures 4.18a-c show the spatial variation of a_1 , a_2 and

standard deviation in Imphal city at PGA. Using a_1, a_2, and δ, values, it is possible to obtain surface level spectral acceleration by using Equation 4.4

$$s_r = r_{br} F_c ; \qquad 4.4$$

Table 4.1 Regression coefficients for typical D-type (Site-12) and E-type (Site-36)

Period	F_c for *D*-type site (Site-12)			F_c for E-type Site (site-36)		
	a_1	a_2	δ	a_1	a_2	δ
PGA	-0.1940	0.4384	0.1464	-0.5714	0.4851	0.1498
0.0300	-0.1398	0.4327	0.1484	-0.5579	0.4863	0.1501
0.0400	-0.2025	0.4393	0.1464	-0.5715	0.4852	0.1498
0.1000	-0.3108	0.4306	0.1307	-0.8697	0.4581	0.1555
0.2000	-0.3276	0.5779	0.1342	-0.5310	0.4622	0.1282
0.3000	-0.0428	0.3422	0.1239	-0.4141	0.5727	0.1154
0.4000	-0.1490	0.4407	0.1243	-0.3084	0.4232	0.1298
1.0000	0.3080	0.3801	0.1143	-0.0558	0.6763	0.1804
2.0000	0.0607	0.1618	0.1180	0.3532	0.2332	0.1546
3.0000	-0.2362	0.1652	0.1347	-0.0951	0.1950	0.1681

The surface level ground motion has been calculated (see Equation 4.4) for 0.36g rock level acceleration value (PGA=0.36g, IS: 1893) using site coefficients for PGA and plotted in the form of contour map (Figure 4.19). It may be noted that IS code recommends PGA value of 0.36g for all three type of the site *viz.*, rock or hard soil sites, medium soil sites and soft soil sites and is silent on the effects of soil types on PGA.

TH-994_06610404

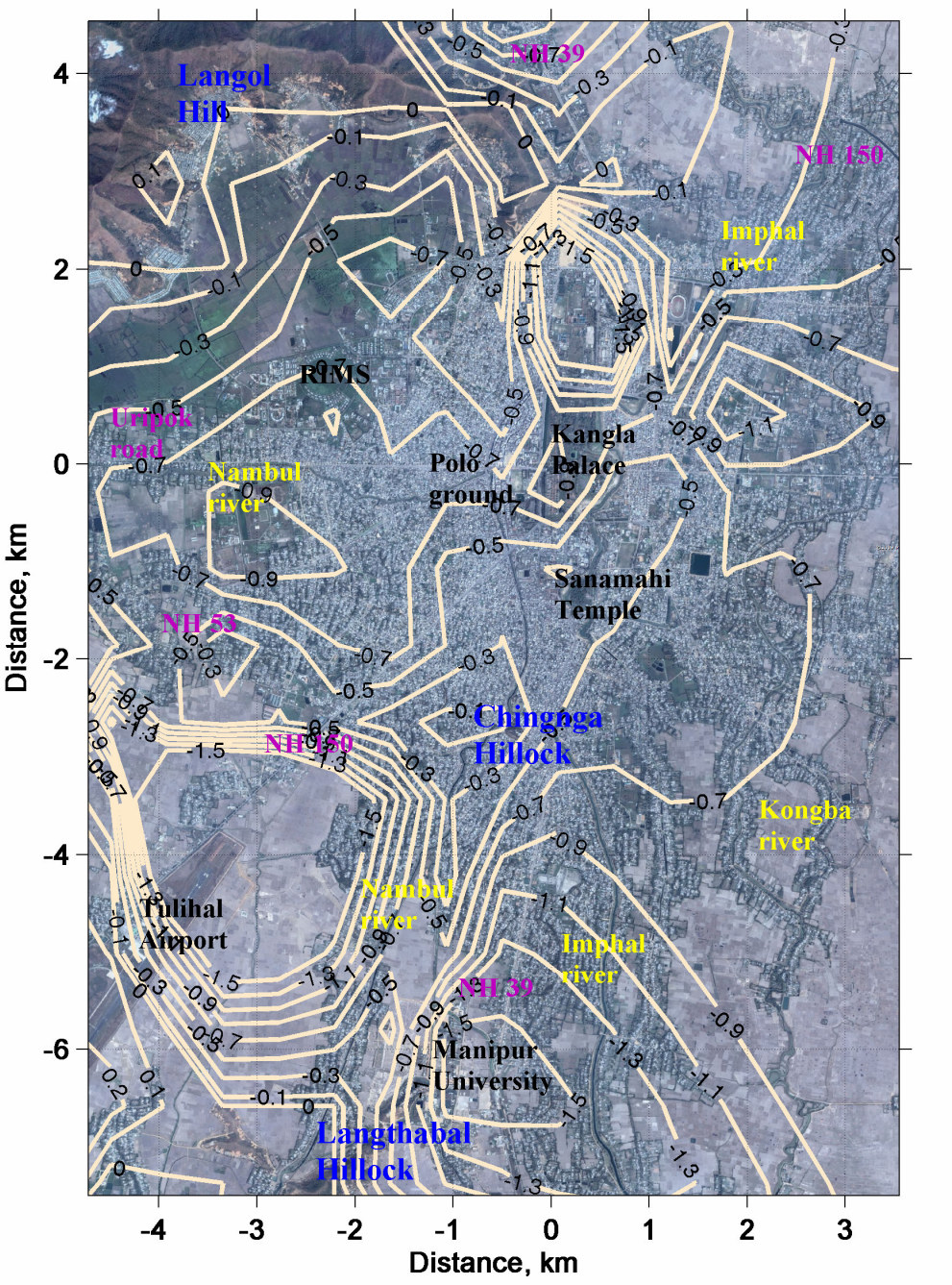


Figure 4.18a Coefficient a_1 at PGA in Imphal city

Figure 4.19 show the variation of PGA, with maximum value of 0.7g near Polo ground and Manipur University areas. This study shows that by making use of site coefficient it is possible to easily compute surface level responses. Further average values of a_1, a_2 and δ for two types of sites i.e., D and E-type soils is presented (Table 4.2). This table may be used for quick reference for

generating the site coefficients for any D and E-type site in Imphal city. Appendix C presents a_1, a_2 and δ for all 122 sites in Imphal city.

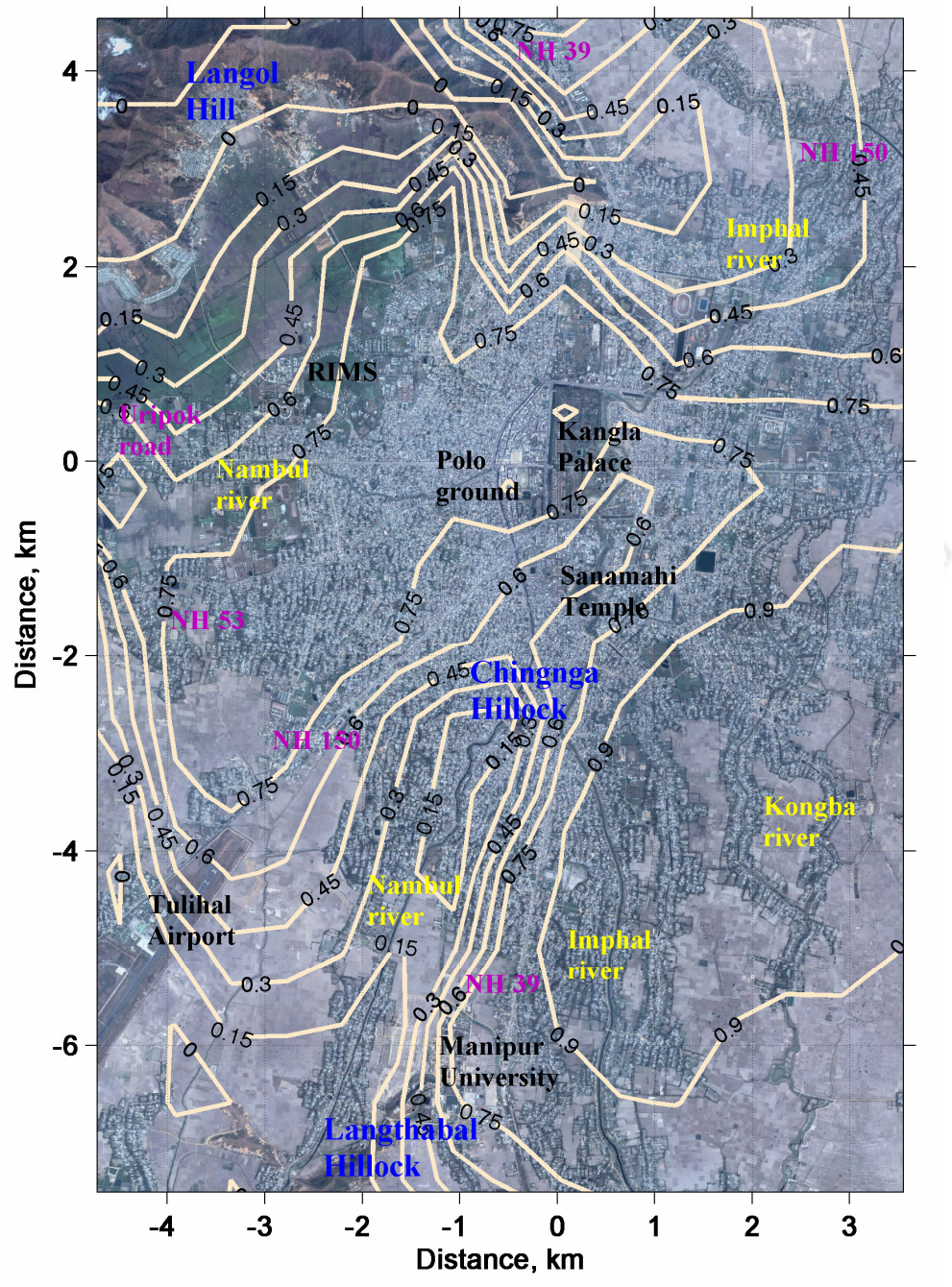


Figure 4.18b Coefficient a_2 at PGA in Imphal city

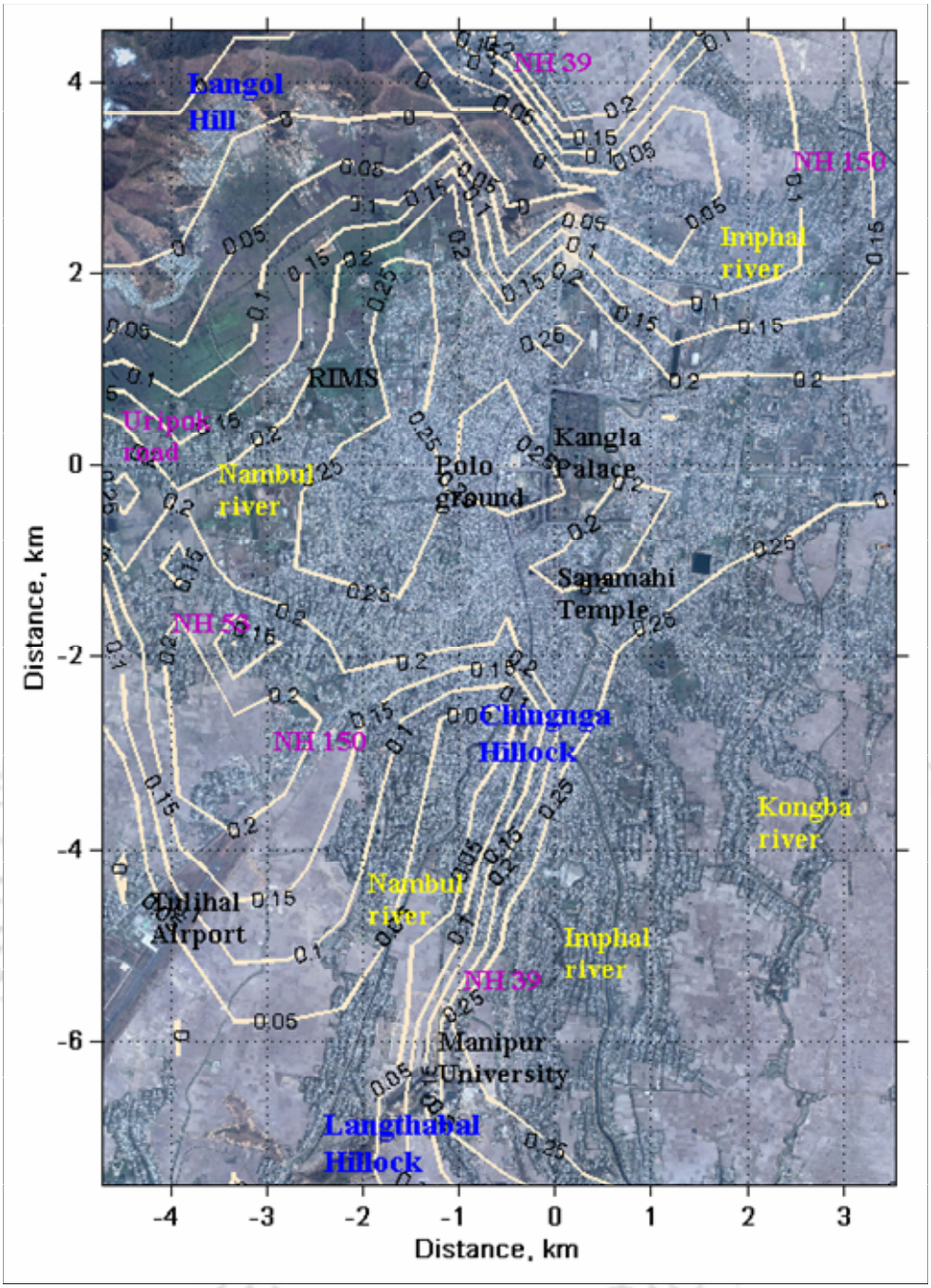


Figure 4.18c Standard deviation at PGA in Imphal city

4.9 Conclusions

Effect of local soils on seismic susceptibility of Imphal city with respect to synthetically generated ten samples for 1869 Cachar earthquake (M_w 7.5) in Kopili faults and a hypothetical earthquake (M_w 8.1) in Indo-Burmese ranges, has been presented. Soil data collected from 122 boreholes located in Imphal

city have been used as inputs in the non linear site response analysis (Idriss and Sun, 1992) and surface level response are simulated for these two scenario earthquake.

Table 4.2 .Average regression coefficients for D-Type and E-Type soils

Period	F_c for D-Type			F_c for E-type		
	a_1	a_2	δ	a_1	a_2	δ
PGA	-0.3065	0.5651	0.1913	-0.6254	0.6784	0.2204
0.0300	-0.2830	0.5648	0.1933	-0.6182	0.6800	0.2223
0.0400	-0.3075	0.5652	0.1913	-0.6254	0.6784	0.2204
0.1000	-0.5640	0.5413	0.1767	-0.7886	0.6379	0.2047
0.2000	-0.6609	0.6308	0.1677	-0.7639	0.7343	0.2143
0.3000	-0.1006	0.5635	0.1735	-0.3020	0.6205	0.2009
0.4000	-0.1627	0.6066	0.1598	-0.4191	0.7035	0.2041
1.0000	-0.3406	0.4341	0.1569	+0.0833	0.6157	0.2058
2.0000	-0.1430	0.1840	0.1478	+0.0837	0.2437	0.2082
3.0000	-0.2193	0.1848	0.1652	-0.3011	0.2249	0.1927

The shear wave velocity (V_s) has been obtained from SPT-N values through empirical relation proposed by Imai and Tonouchi (1982). The methodology has been compared with the SRR data of the 6th August 1988 earthquake. The results are presented in the form of mean and standard deviation of surface level spectral acceleration at Peak Ground Acceleration (PGA) and natural periods of 0.3 s and 1.0 s. It has been observed that at important places around Kangla palace the amplification for PGA is around 2.0. Based on mean surface level spectral response analysis (for 5 % damping) it has been found that IS: 1893 overestimates S_a for scenario 1869 Cachar earthquake, whilst for M_w 8.1 in IBR for corresponding periods of 0.01 s – 0.1 s, IS: 1893 underestimates *Sa* at few locations in Imphal city. Site coefficients developed in the present study

have been computed at different periods of engineering purposes and these can be used for estimating surface level responses.

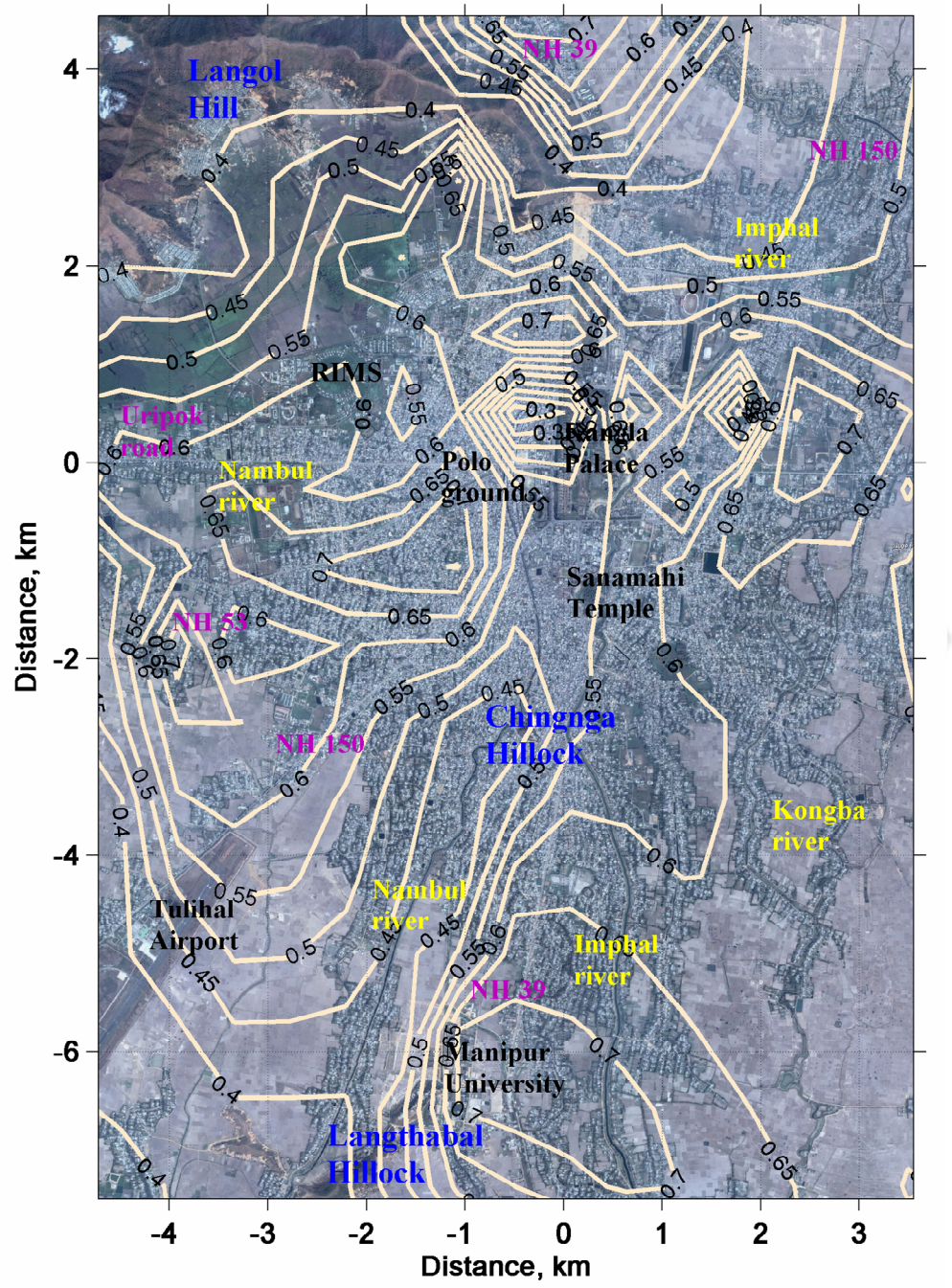


Figure 4.19 Ground motion at PGA in Imphal city for 0.36g (using site coefficients)

Chapter 5

Probabilistic seismic hazard estimation at surface level for Imphal city

5.1 Introduction

Safe design of earthquake resistance structures is possible only if the forces acting on it due to future earthquakes can be estimate. As earthquakes are low probability events with high levels of risk to the society, hence underestimation of seismic hazard will put a risk to the inhabitants and infrastructures whilst its overestimation will prove to be economically expensive. It may be noted that the current trend of designing structures using IS code recommended response spectra which do not recognize seismo-tectonic and earthquake return period aspects have become questionable. This spectra has been modified only by a zone factor representing the peak ground acceleration (PGA) of unidentified probability of occurrence. As discussed in Chapter 2 that this approach is neither related to seismo-tectonic details of the region nor the non-uniform levels of hazards of the suggested response spectrum. So as per the prevailing design practice in India anticipated design

life of structures cannot realistically match with existing earthquake hazard level (in terms of return periods) and hence leading to uneconomical and unsafe design/construction practices. In this context, Probabilistic Seismic Hazard Analysis (PSHA) has addresses engineering safety issues with associated risk levels. In PSHA the parameters associated with the seismic phenomena *i.e.* magnitude of future events, source to site distance and attenuation are treated as random variables. PSHA can be used to obtain response spectrum, with a specific probability of exceedance in a time frame of T years. Such a response spectrum with the same return period or risk level at all frequencies is known as uniform hazard response spectrum (UHRS). In this chapter fault map (see Figure 3.4) and seismic parameters established in Chapter 3 have been used as inputs in the present analysis. The site coefficients developed in Chapter 4 are used to estimate the probabilistic seismic hazard at surface level using PSHA proposed by Cornel (1968). The results are presented in form of seismic hazard curves for Imphal city at surface level. Also UHRS maps have been prepared for 500 year and 2500 years return periods for Imphal city.

5.2 Attenuation relationship

The empirical attenuation relations provide a means for estimating ground motion parameters (i.e. PGA, Peak Ground Velocity (PGV) etc.) from limited source information such as magnitude, epicentral distance and local site conditions. The PGA at a site depends strongly on the magnitude of an event and the corresponding hypocentral distance. The pattern of decay of PGA with distance is a property depending on the quality factor (see Section 3.6) appropriate for the region. The current practice is to obtain the attenuation relation by empirical methods based on instrumental data (accelerogram etc.). It may be noted that as there is no such reported attenuation relationship for the two different seismo-tectonic setups of NE India region. So in order to

compute PGA at Imphal city, attenuation relations proposed by Boore and Atkinson (2008), known as NGA (Next Generation Attenuation), for strike-slip, thrust & reverse fault and Atkinson and Boore (2003) relation for subduction zone are used. The NGA attenuation has been used on the 23 (out of 27 major faults indentified for NE region) major faults present in EH, SP, MT, BB and AV and whereas for the remaining 4 faults in IBR, subduction zone attenuation has been used. Brief descriptions of these attenuations relations are presented below in the following two subsections.

5.2.1 EH, SP, MT, ND, BB and AV attenuation

In order to estimate ground motion for Shallow active region (e.g. Shillong plateau, Eastern Himalaya etc.), the Next Generation Attenuation (NGA) (http://peer.Berkeley.edu/ products/ nga_project.html, 2008) has been proposed by Boore and Atkinson (2008) as a part of the NGA projects. The attenuation for ground-motion models predicts PGA, PGV, and response spectral ordinates for periods up to 10 s. The generalized attenuation equation is as follows

$$\ln(y) = F_M(M) + F_D(R_{JB}, M) + F_S(V_{s30}, R_{JB}, M) + \varepsilon\sigma_T \qquad 5.1$$

where F_M is magnitude scaling, F_D represents distance function and F_s is Site amplification, M is moment magnitude and R_{JB} is Joyner Boore distance. Here the variables are M, R_{JB}, and V_{S30}. The distance and magnitude scaling functions are given by:

$$F_D(R_{JB}, M) = [c_1 + c_2(M - M_{ref})]\ln(R / R_{ref}) + c_3(R - R_{ref}) \qquad 5.2$$

where,

$$R = \sqrt{R_{JB}^{\,2} + h^2}\,; \qquad 5.3$$

and c_1, c_2, c_3. M_{ref}, R_{ref} and h are the coefficients which are given in Table 5.1

$$a)\ For\ M \le M_h \qquad 5.4$$
$$F_M(M) = e_1 U + e_2 SS + e_3 NS + e_4 RS + e_5 (M - M_h) + e_6 (M - M_h)^2,$$

$$b)\ For\ M > M_h \qquad 5.5$$
$$F_M(M) = e_1 U + e_2 SS + e_3 NS + e_4 RS + e_7 (M - M_h)$$

where *U*, *SS*, *NS*, and *RS* are variables used for, strike-slip, normal-slip, and reverse-slip fault type, respectively. As these details are unspecified for NE India, these are taken as zero (Boore and Atkinson, 2008). M_h, the 'hinge magnitude' for the shape of the magnitude scaling, is a coefficient. As the shear wave profile is not known hence, the site amplification terms are ignored in this study. The final coefficients used in the present work are c_1, c_2, c_3. M_{ref}, R_{ref}, e_1, e_5, e_6, e_7, M_h and σ_{TU} as shown in Table 5.1.

5.2.2 IBR subduction zone attenuation

The attenuation relationship proposed by Atkinson and Boore (2003) for subduction zone is given as

$$\log Y = C_1 + C_2 M_w + C_3 h_f + C_4 R - g \log R \qquad 5.6$$

here, h_f denotes focal depth in kms, R is defined as $\sqrt{D_{fault}{}^2 + \Delta^2}$, where D_{fault} is the closest distance to fault surface in kms, and Δ, a near source saturation term which can be computed by $\Delta = 0.00724 \times 10^{0.507 M_w}$, $g = 10^{0.301 - 0.01 M_w}$ denotes the magnitude dependent geometrical spreading for in-slab event (Indo-Burmese subduction zone is classified as an in-slab event). The attenuation is based on historical global subduction database (including the recent in-slab and interface events from online database of Seismological Society of America (SSA)) proposed by Crouse (1991a, 1991b) and Youngs *et. al.,* (1997). The subduction zone attenuation relation has been established (Equation 5.6) by analyzing the strong motion data using maximum likelihood regression method. The coefficients develop in this analysis and used in the present work are shown in Table 5.2. Further these parameters are used as inputs in PSHA.

Table 5.1 Distance and Magnitude scaling coefficients (Boore and Atkinson, 2008)

Periods (Sec)	Distance Scaling Coefficients (M_{ref}=4.5 and R_{ref}=1.0km for all periods				Magnitude Scaling Coefficients					
	c_1	c_2	c_3	h	e_1	e_5	e_6	e_7	M_h	σ_{TU}
PGA	-0.6605	0.1197	-0.01151	1.35	−0.53804	0.28805	-0.10164	0.00	6.75	0.566
0.04	-0.7036	0.1300	-0.01151	1.35	-0.36881	0.12173	-0.14305	0.00	6.75	0.583
0.1	-0.7081	0.11170	-0.01151	1.68	0.20109	0.04697	-0.15948	0.00	6.75	0.608
0.2	-0.5830	0.04273	-0.00952	1.98	0.57180	0.52729	-0.12964	0.00102	6.75	0.596
0.4	-0.6443	0.04394	-0.00626	2.24	0.39220	0.78610	-0.07843	0.02262	6.75	0.603
1.0	-0.8183	0.10270	-0.00334	2.54	-0.46896	0.67880	-0.18257	0.05393	6.75	0.647
2.0	-0.8285	0.09432	-0.00217	2.73	-1.22652	0.77989	-0.29657	0.29888	6.75	0.702
3.0	-0.7844	0.07282	-0.00191	2.83	-2.24656	0.77966	-0.45384	0.67466	6.75	0.702

Table 5.2. Regression coefficients (Atkinson and Boore, 2003)

Periods (sec)	C_1	C_2	C_3	C_4	Std. Dev
PGA	-0.04713	0.6909	0.01130	-0.00202	0.27
0.04	0.50697	0.63273	0.01275	-0.00234	0.25
0.1	0.43928	0.66675	0.01080	-0.00219	0.28
0.2	0.51589	0.69186	0.00572	-0.00192	028
0.4	0.005445	0.7727	0.00173	-0.00178	0.28
1.0	-1.02133	0.8789	0.00130	-0.00173	0.29
2.0	-2.39234	0.9964	0.00364	-0.00118	0.30
3.03	-3.70012	1.1169	0.00615	-0.00045	0.30

5.3 Probabilistic seismic hazard analysis

The present methodology of PSHA proposed by Cornell (1968) and Algermissen *et. al.*, (1982) are based on the following four steps: 1) identification of source, 2) assessment of earthquake recurrence and magnitude distribution, 3) selection of attenuation model for ground motion and 4) calculation of seismic hazard. PSHA estimates the probability of exceedance of ground motion parameters at a site due to all possible future earthquakes. Assuming that the number of earthquakes occurring on a fault follows a stationary Poisson process, the probability that the control variable Y exceeds level y^*, in a time frame of T years is given by

$$P(Y > y^*, in\, T\ years) = 1 - \exp[-\upsilon_Y(y^*)] \qquad 5.7$$

where $\upsilon_Y(y^*)$ is the annual frequency of exceeding ground motion level y^*.This may alternatively be expressed as:

$$\upsilon_Y(y^*) = \sum_{i=1}^{N} \lambda_{m_i} \sum_{M=m_m}^{m_u} \sum_{R=r_m}^{r_u} P[Y > y^* \mid m, r] p_m(m)_i \, p_r(r \mid m)_i \, dmdr \qquad 5.8$$

here N_s is the number of sources, $\lambda_{(m)i}$ is the frequency of earthquakes on seismic sources 'i' above a minimum magnitude (m_m, in the present case is 4.0); $P[Y \geq y^* \mid m,r]$ is the probability for as given earthquake magnitude M_i at a distance R_i from the site, the ground motion exceeds a value y^*; $p_m(m)_i$ represents the probability density function associated to the likelihood of magnitude of events (m_m <Mi <m_u) occurring in source 'i'; $p_r(r \mid m)_i$ is the conditional probability density function used to describe the randomness of epicenter locations within each source. The functional form of $p_m(m)_i$ is derived from the unbounded Guttenberg-Richter (1954). $p_m(m)$ is the truncated term (Cornell and Vanmarcke, 1969) which relates m_m and m_u is given by

$$p_M(m) = \frac{\beta \exp[-\beta(m - m_m)]}{1 - \exp[-\beta(m_u - m_m)]}; \quad m_m \le M \le m_u \qquad 5.9$$

here β=2.303*b*,(b value is taken from Chapter 3) the function $p_r(r|m)_i$ for source-to-site distance is computed conditionally on the earthquake magnitude and is obtained by discretization of the cumulative distance probability relationship using a suitable step size.

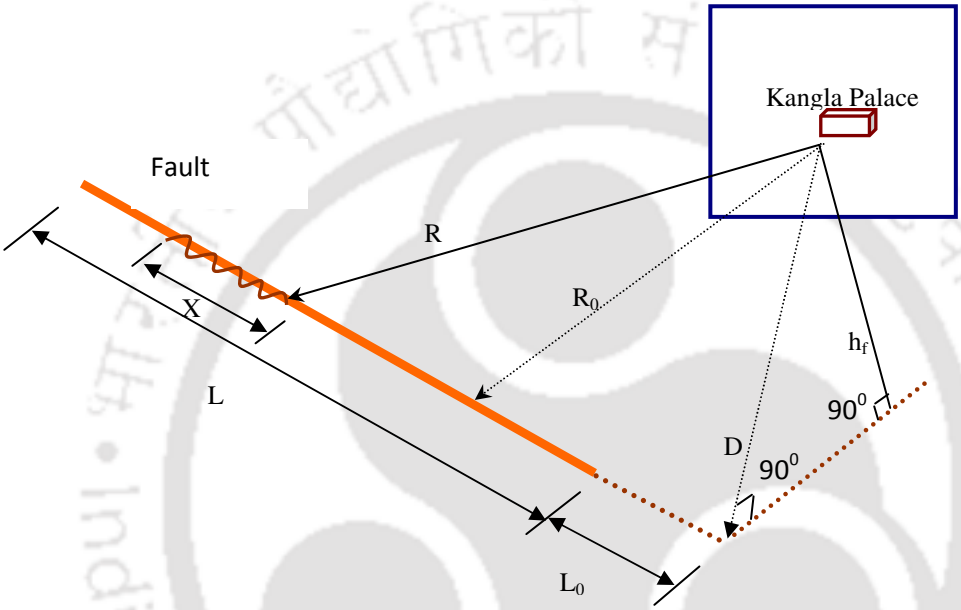


Figure 5.1 Fault rupture model

The return period for the same can be found out by inversing the annual probability of exceedance of corresponding ground motion. Figure 5.1 shows the schematic fault rupture model used in the present work with typical source, sites and distance details along with the rupture length. L, X, h_f, R_0 and R are the length of the fault, fault rupture length, focal depth, minimum distance of the site from the fault, and minimum distance of the site from the fault rupture respectively.

5.4 Seismic hazard curves at Imphal city

Seismic hazard curves at Imphal city have been obtained from the combined mean annual rate of exceedance, υ_{y^*} for different specified ground motion

values corresponding to two category of seismic setups *viz.*,1) strike-slip, normal and reverse faults (SP, AV, EH, ND, MT, BB) and 2) subduction zone (IBR). These seismic hazard curves are first obtained individually for all the seven zone faults and combined to estimate the aggregate hazard of each zones at the site. The zonal hazards are then combined to get the aggregate hazard at Imphal city. The seismic hazard curves for PGA at rock level obtained from the above mentioned method are shown in Figure 5.2 along with the individual contributions of all the seven zones fault.

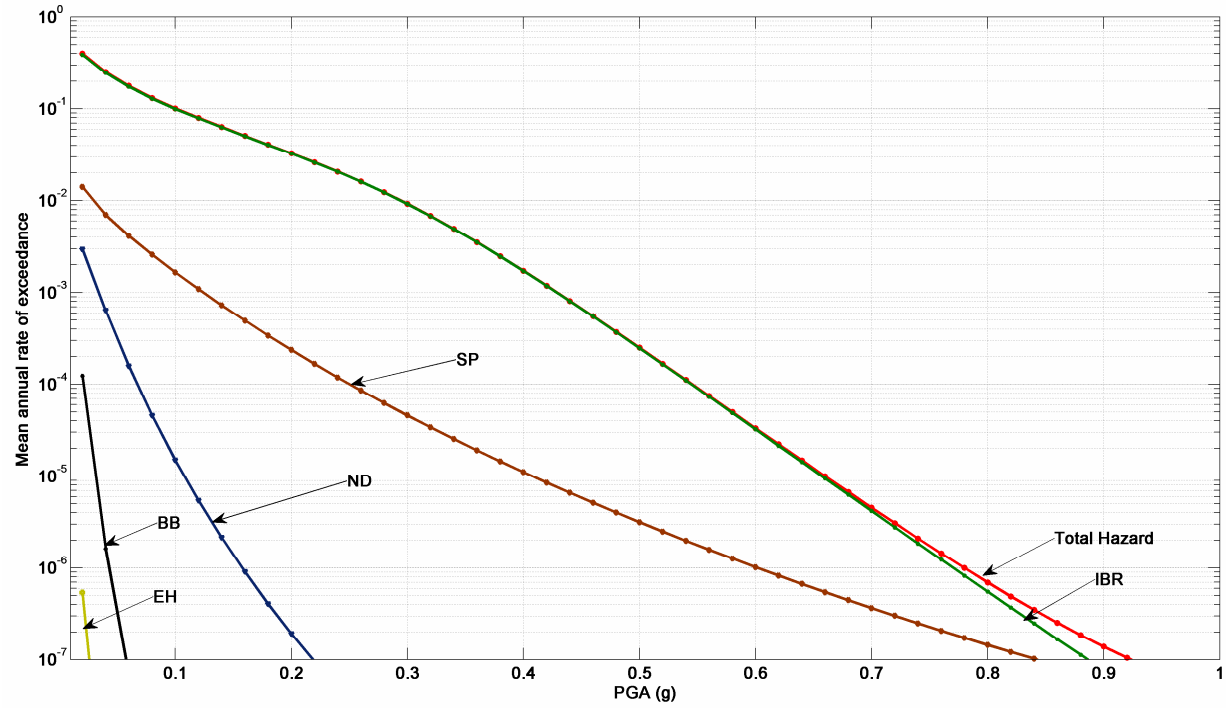


Figure 5.2 Seismic hazard curves for Imphal city at rock level

It can be seen from the Figure 5.2 that the hazard at Imphal is mainly controlled by IBR and Shillong plateau. The contributions from other zones are relatively low level this may be attributed to their location at larger distance. Further hazard curves are obtained at all the frequencies of engineering interest (Figure 5.3).

5.5 Uniform hazard response spectra

Although scaling of response spectra to desired PGA levels for designing structure has been conventionally adopted by practicing engineers and designers, it can lead different probability of exceedance over the frequency range of civil engineering structures. As discussed in Section 5.1, this can produce uneconomical and unsafe structure. Hence, it is desirable to have design response spectrum with equal probability of exceedance over the entire

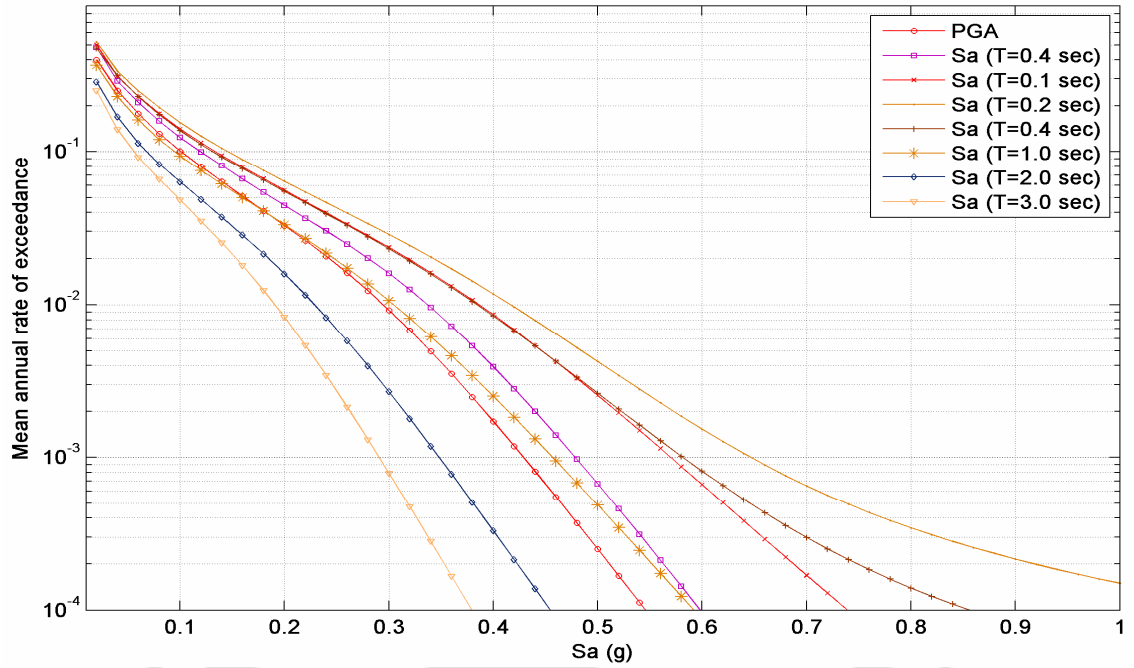


Figure 5.3 Seismic hazard curves for Imphal city at rock level for eight frequencies

frequency range of interest. These design spectra are known as uniform hazard response spectra (UHRS). For finding UHRS, seismic hazard curves of S_a are computed for a range of frequency values as shown in Figure 5.3. From these hazard curves, response spectra for a specified probability of exceedance over the entire frequency range of engineering interest are obtained. IBC (2006) prescribes design forces based on S_a corresponding to 10 and 2% exceedance probability in 50 years. These correspond to 475 (~ 500) and 2475 (~ 2500) year return periods respectively. Figure 5.4 shows UHRS for Imphal city at

standard return periods of 500 and 2500 years. The corresponding PGA values are also shown. Based on the comparison with S_a values recommended by IS: 1893 (2002), it can be seen that IS code overestimates the value and is on conservative side for periods from 0.2 s to 0.7 s, whilst for long period (> 1.0 s) IS: 1893 S_a values are on the lower side.

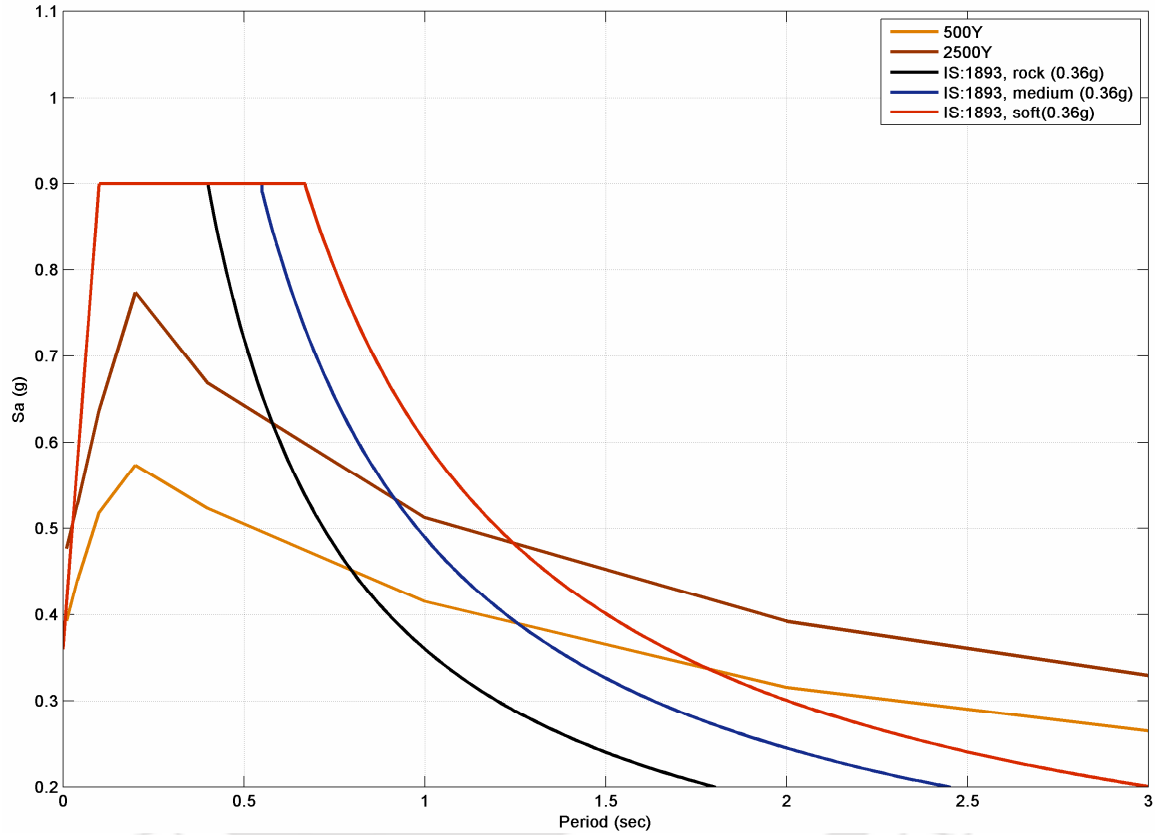


Figure 5.4 Comparison of IS-1893 with Uniform Hazard Response Spectra for 500 and 2500 year return periods at rock level

5.6 Surface level hazard map for Imphal city

The surface level hazard has been estimated for 500 and 2500 years return period at Imphal city using site coefficients developed in Chapter 4. Here computed UHRS at rock level have been multiplied by site coefficients estimated at different periods at all sites in Imphal city. The results are shown (Figures 5.5a-c) in the form of contour plots at PGA, 0.3 s (Short period) and

1.0 s (Long period)for 500 and 2500 year return periods, as suggested by IBC (2006).

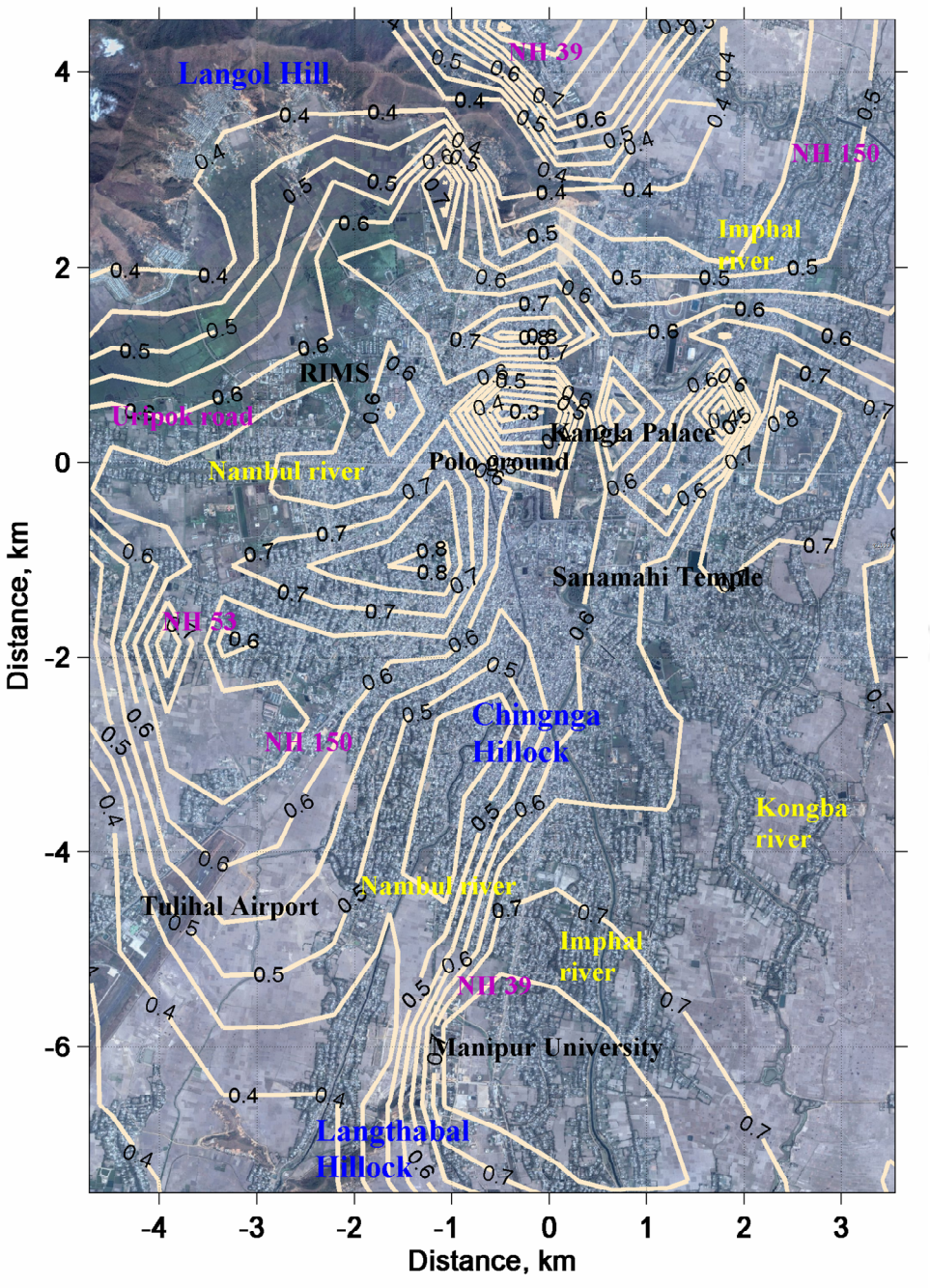


Figure 5.5a PGA contours with 10% probability of exceedence in 50 years (Return period =~500 years) over Imphal city.

Figure 5.5a shows the variation of spectra acceleration at PGA for 500 year return period in Imphal city. The maximum *Sa* value attained is 0.8g near Polo ground whereas the *Sa* maximum values observed near polo ground and

Kangla palace for 0.3 s & 1.0 s are 1.2g and 0.9g respectively (Figures 5.5b-c). Further it can been seen that at these location S_a exceeds the value given in IS: 1893 (0.36g) hence structures designed using IS: 1893 recommended value are vulnerable seismic hazard.

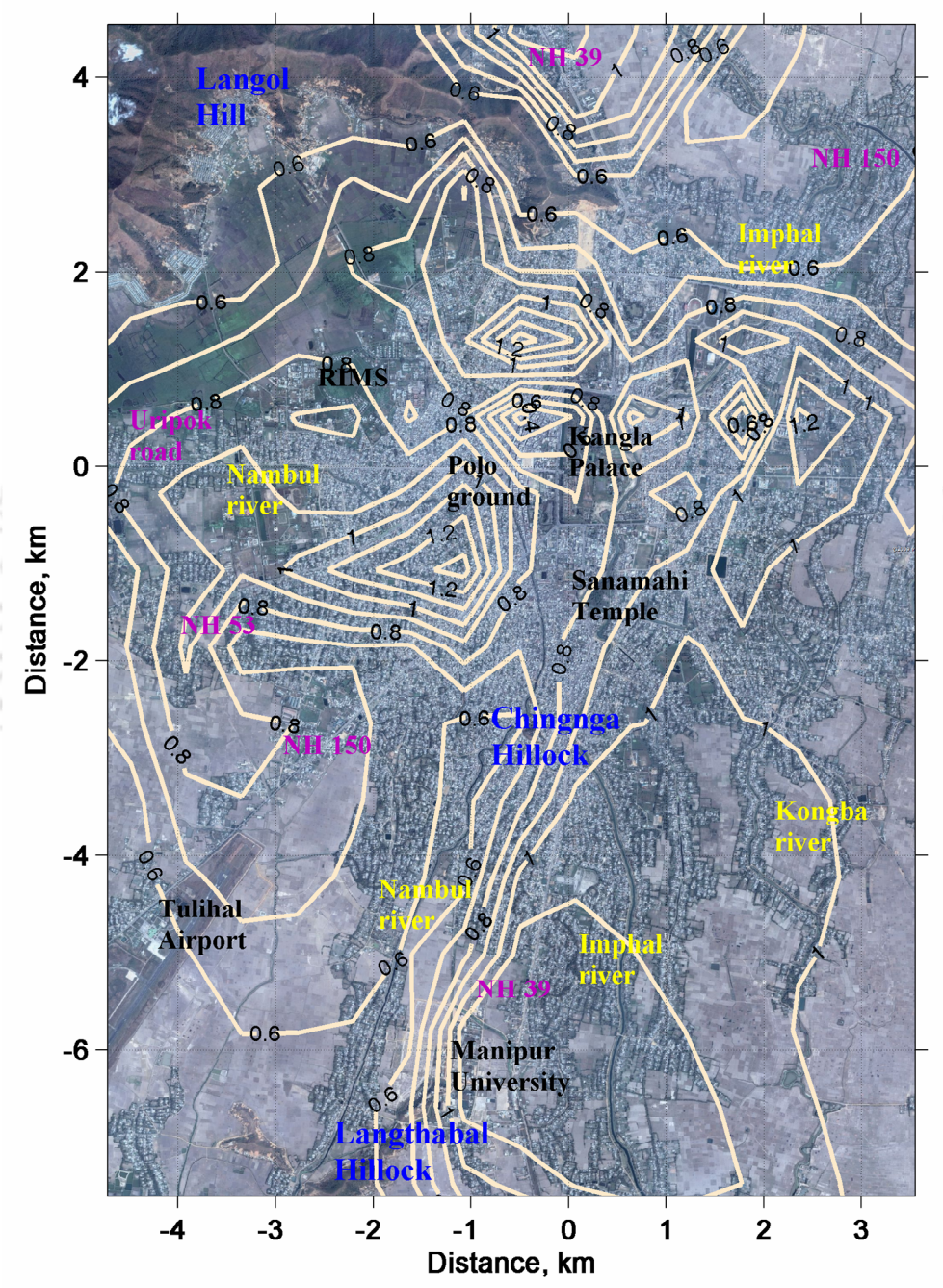


Figure 5.5b Short period spectral acceleration at 0.3 s with return period of 500 years over Imphal city (5% damping)

Figure 5.5b the shows UHRS variation in Imphal city shows for 0.3 s return period. It can be seen that almost entire Imphal is prone to seismic hazard (S_a > 0.36 g). In Kangla palace, Polo ground, RIMS and Sanamahi temple areas spectral acceleration values reach around 0.8g to 1.2g.

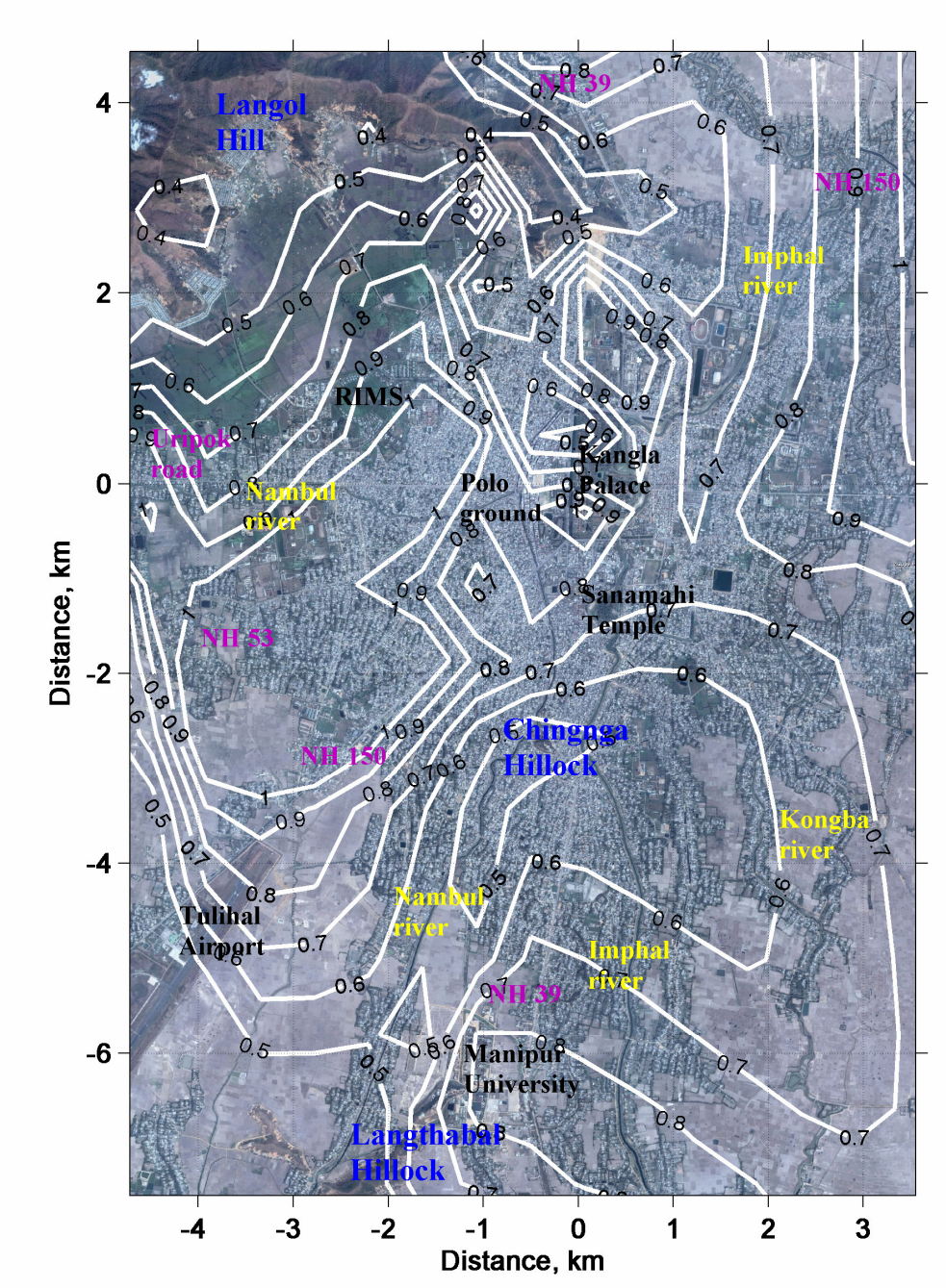


Figure 5.5c Long period spectral acceleration at 1.0 s with return period of 500 years over Imphal city (5% damping).

Whereas at the outskirts of Imphal city *i.e.,* near east of Langol hill, Langthabal hill and Tulihal airport the spectral acceleration varies between 0.6g-0.8g. Variation of UHRS for 500 year return period at 1.0 s is shown in Figure 5.5c. It can be seen that maximum value (i.e., 1.0g) of spectral acceleration is observed near polo ground and Kangla palace area.

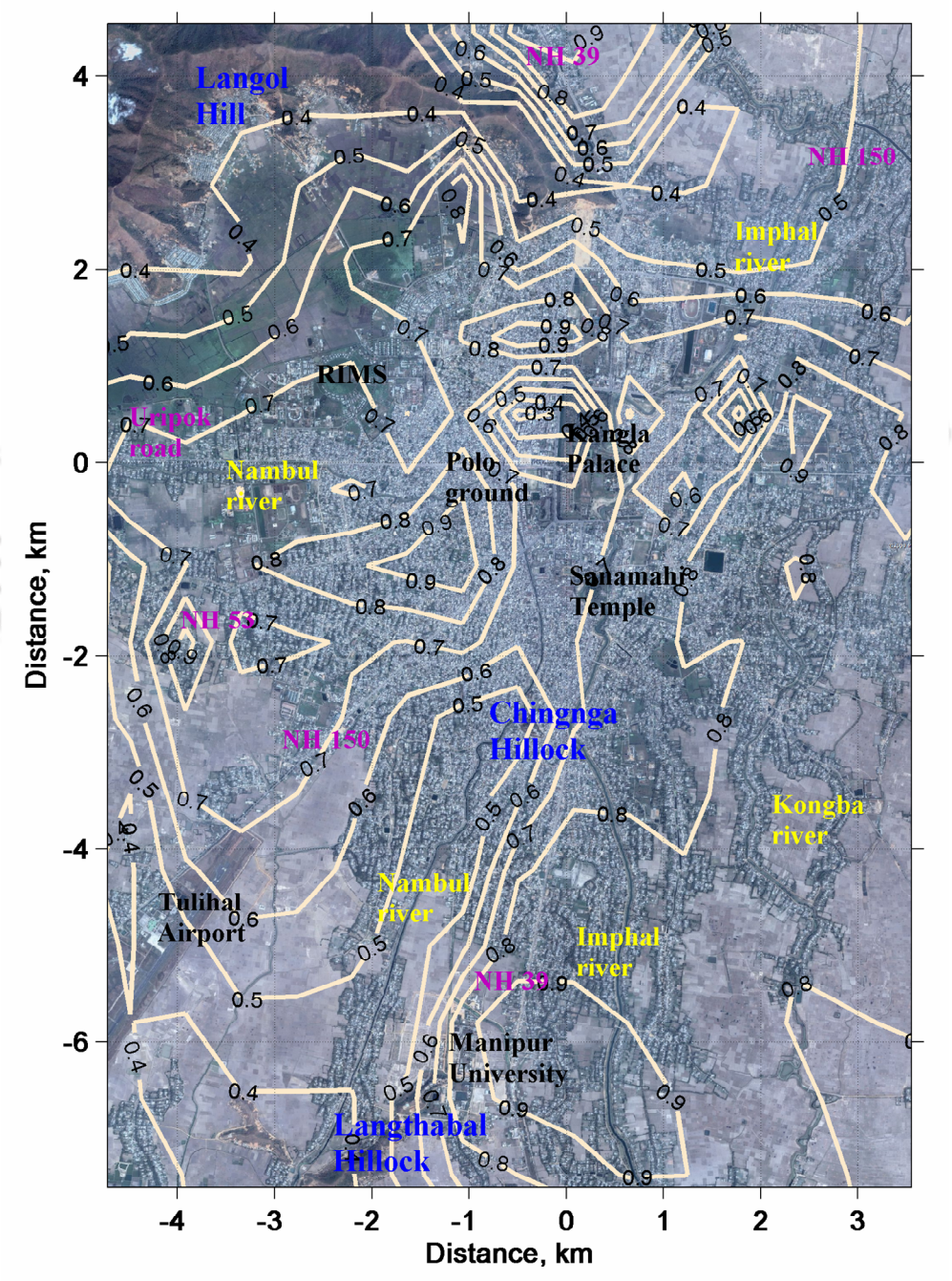


Figure 5.6a PGA contours with 2% probability of exceedence in 50 years (Return period= ~2500 years) over Imphal city.

It may be mentioned that although in most of the codes e.g. IBC, lesser amplification is suggested at longer periods (as compared to shorter periods), there are reports in the literature (Bazurro and Cornel, 2004; Wang *et. al.*, 2006) where soil gets amplified at long periods. The reason behind such amplification in the present case may be due soft soil deposits and presence of high water table level in the Kangla palace area etc.

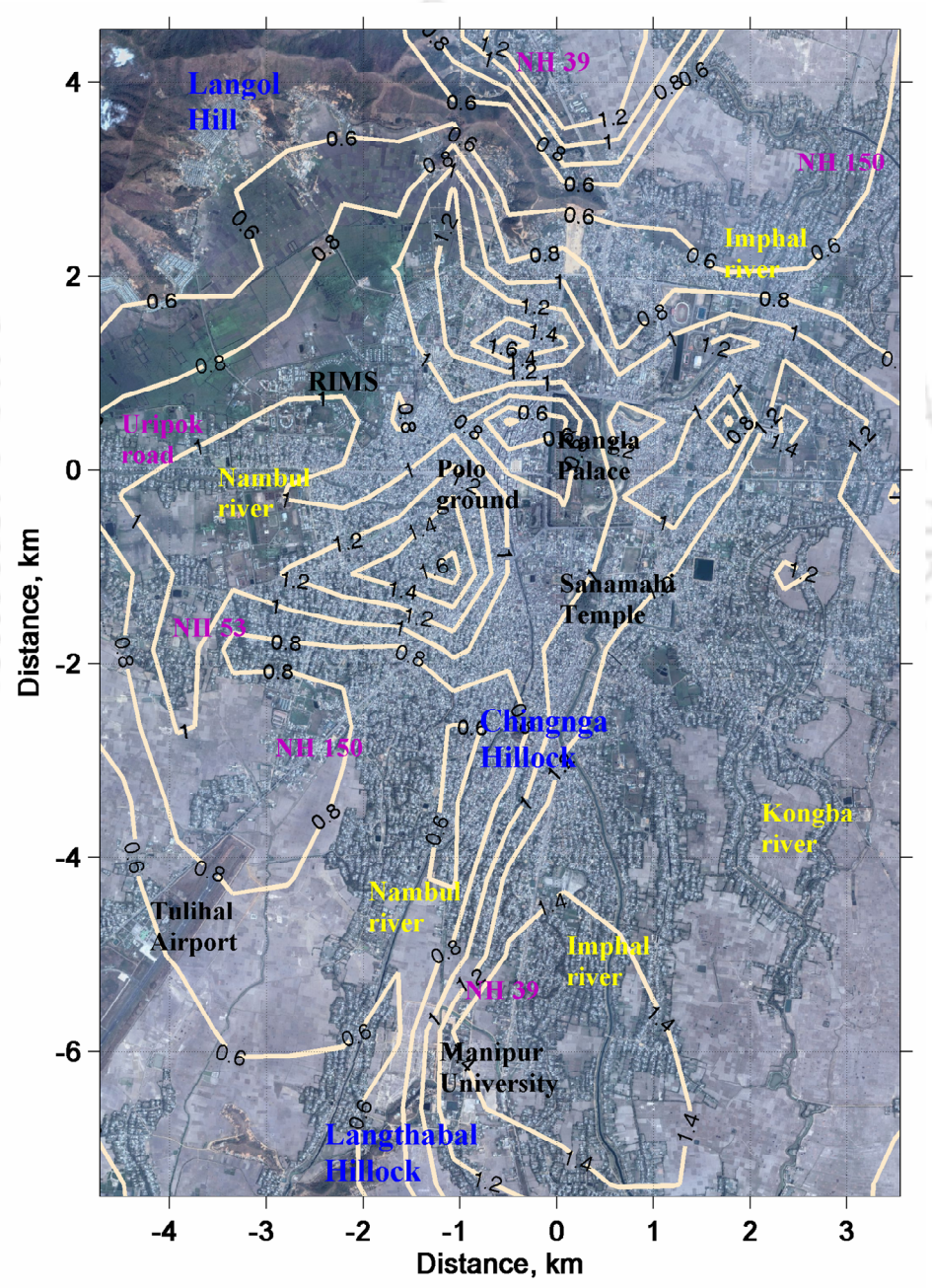


Figure 5.6b Short period spectral acceleration at 0.3 s with return period of 2500 years over Imphal city (5% damping)

UHRS maps have also been plotted for 2500 years return periods at PGA, 0.3 s and 1.0 s (Figures 5.6a-c). From Figure 5.6a, it can be observed that maximum value S_a (0.5g) is observed near Kangla palace area whereas at nearby locations *i.e.,* Polo ground area there is a drastic increase in the S_a value to 0.9g.

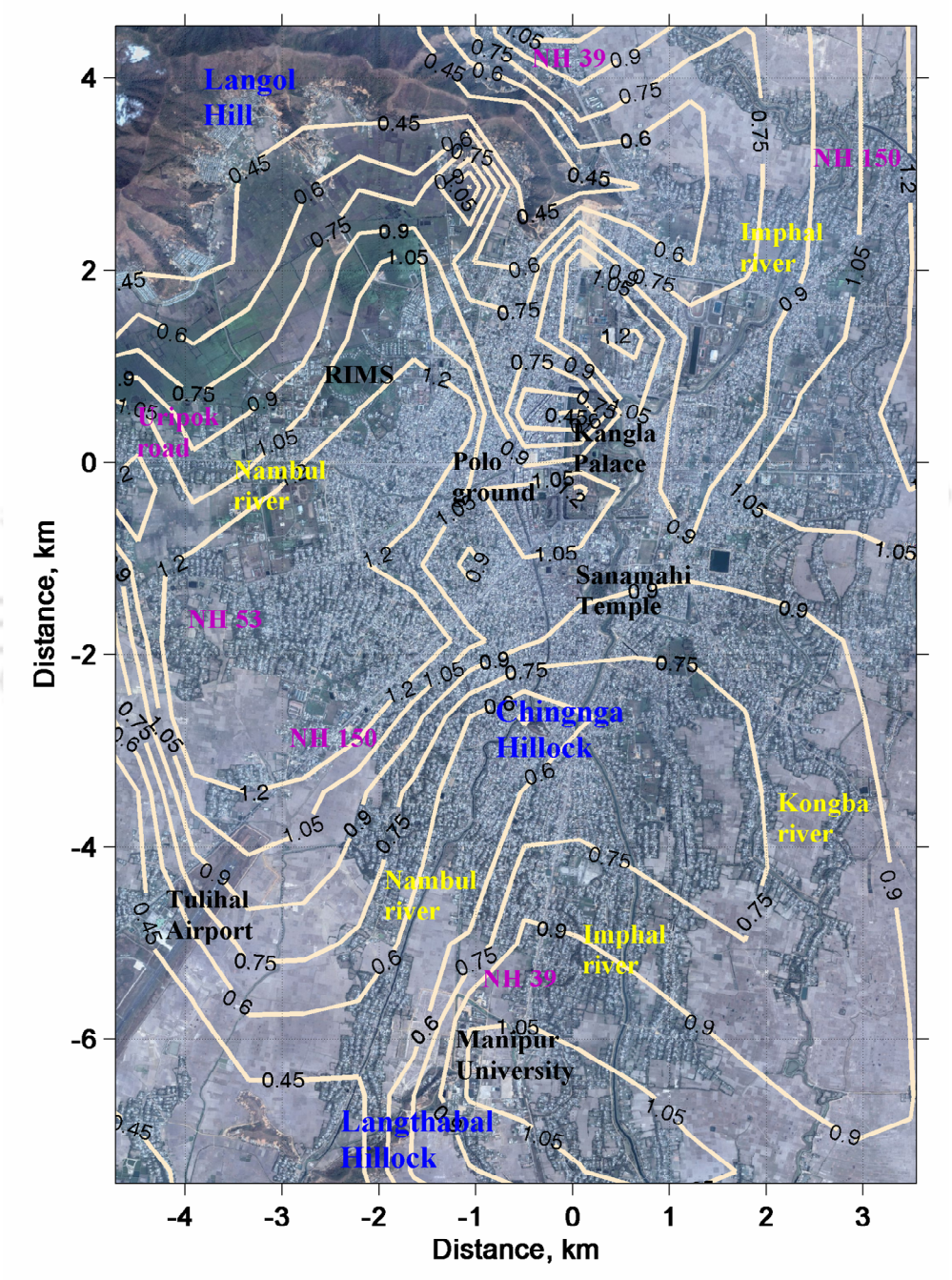


Figure 5.6c Long period spectral acceleration at 1.0 s with return period of 2500 years over Imphal city (5% damping).

Figure 5.6b shows UHRS variation at surface level at time period of 0.3 s in Imphal city, for 2500 year return period. It can be seen that maximum value of S_a attained is 1.6g near Polo ground and towards north of Kangla palace areas. UHRS at surface level for 1.0 s time period has been shown in Figure 5.6c for 2500 year return period. Maximum S_a value (1.2g) has been observed at RIMS, near Nambul river and NH-150 area (Figure 5.6c).

Surface level UHRS are plotted for all 122 sites for 500 and 2500 years return periods in Figures 5.7 and 5.8 respectively. It can be seen from Figures 5.7 and 5.8 that that almost at all the 122 sites amplifications of rock level ground motion have been observed at surface levels. Comparing the present results with S_a recommended by IS: 1893 (2002) it can be found that the IS-1893 underestimates the spectra acceleration value at many locations in Imphal city which is quite a threat to this city from future hazard. It has been seen that predicted mean surface level UHRS (for 500 return period) overestimates S_a recommended by IS: 1893 for longer period (> 1.0 s), whereas for periods greater than 0.2 s, IS: 1893 S_a values are underestimated for 2500 return period.

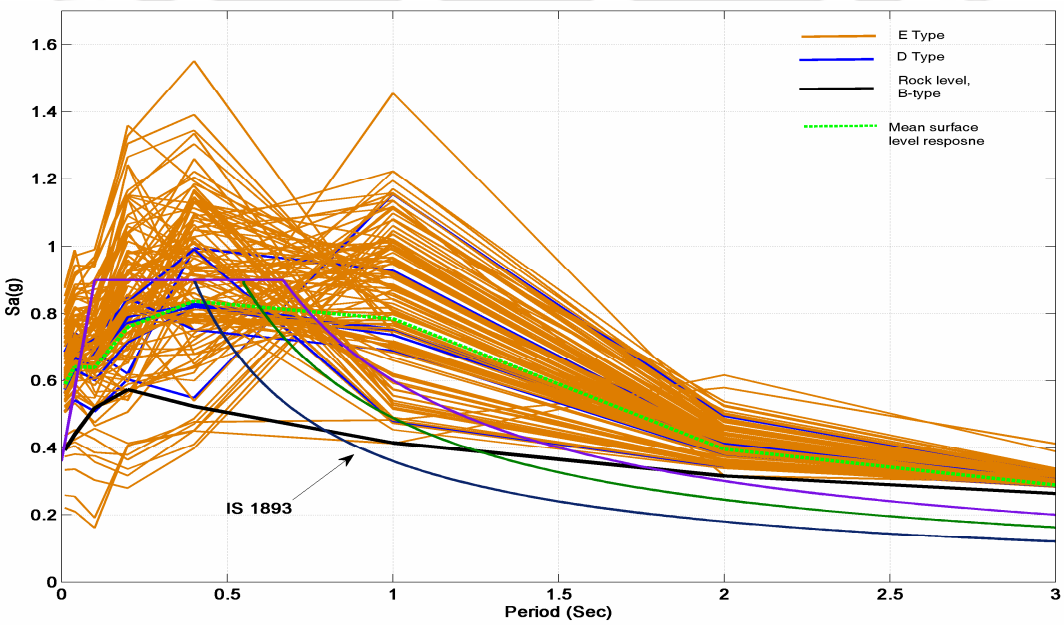


Figure 5.7 UHRS at surface level for 500 year return period for all sites in Imphal city (5% damping)

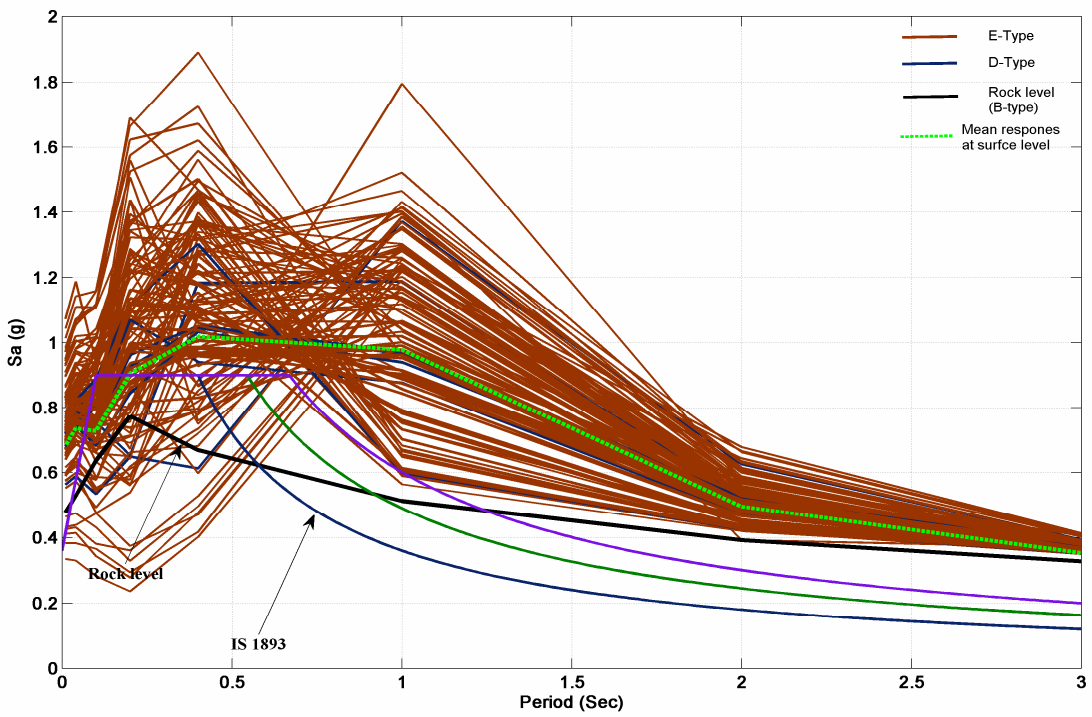


Figure 5.8 UHRS at surface level for 2500 year return period for all sites in Imphal city (5% damping)

5.7 Conclusions

The present article investigates seismic hazard at surface level using site coefficients developed in Chapter 4 at Imphal city using Probabilistic Seismic Hazard Analysis (PSHA). PSHA has been performed by incorporating site coefficients ground motion induced by each of the twenty-seven major faults of potential seven seismic zones present around Imphal. The attenuation relations proposed by Boore and Atkinson (2008) for strike slip, thrust and reverses fault, and Atkinson and Boore (2003) for subduction zone have been used for computing PGA and response spectra, for various uncertainties associated with location, magnitude, recurrence of earthquakes and local site conditions. Uniform Hazard Response Spectra (UHRS) (defined in terms of equal probability of exceedance for all frequencies of ground motion) results are presented in the form of surface level PGA and response spectra for return periods of 500 and 2500 years as recommended by IBC (2006). For 500 years return period, it has been observed that maximum surface level UHRS values

are observed near Kangla and Pologround areas for PGA, 0.3 s and 1.0 s time periods. Whereas for 2500 years return period, it has been observed that maximum surface level UHRS values are observed near Kangla and Pologround areas for PGA, 0.3 s time periods, and at RIMS, near Nambul river and NH-150 for 1.0 s time periods. It has been seen that predicted mean surface level UHRS (for 500 return period) overestimates S_a recommended by IS: 1893 for longer period (> 1.0 s), whereas for periods greater than 0.2 s, IS: 1893 *Sa* values are underestimated for 2500 return period.

TH-994_06610404

Chapter 6

Liquefaction potential status of Imphal city

6.1 Introduction

A detailed seismic hazard status of Imphal city using state of the art DSHA and PSHA have been presented in the previous chapters. It has been shown in Chapter 4 that most of the sites in the Imphal city come under E-type category of soil as per IBC (2006). For such type of soils (*i.e.* E category) IBC recommends liquefaction studies to be carried out. In addition it is observed that water table is relatively high in Imphal city due to various factors such as good rainfall, presence of rivers *viz.*, Imphal, Nambul, Kongba, etc. Figure 6.1 & 6.2 show location of two typical boreholes at Mantripukhri and Chingmirong along with water tables respectively. Liquefaction is one of the most important reasons of ground structures failure during the earthquake. Liquefaction failure can results in fissures, differential movements and loss of strength of soil. In view of this, liquefaction potential status of Imphal city has been evaluated by means of two indices *i.e.* deterministic index LPI (Liquefaction potential

index) and probabilistic index LSI (Liquefaction severity index), for 1869 Cachar event (M_w 7.5, PGA=0.16g) which occurred along the Kopili fault and probable future great earthquake (M_w 8.1, PGA=0.3g) in the Indo-Burmese subduction zone. The PGA values have been taken from Chapter 3 for the two events. Computation of LPI and LSI requires factor of safety against liquefaction (*FS*) of each soil layer as an input. The *FS*s have been obtained based on SPT-N values using the procedure proposed by Idriss and Boulanger (2006). These *FS*s are used as input parameter for evaluating the LPI and LSI indices.

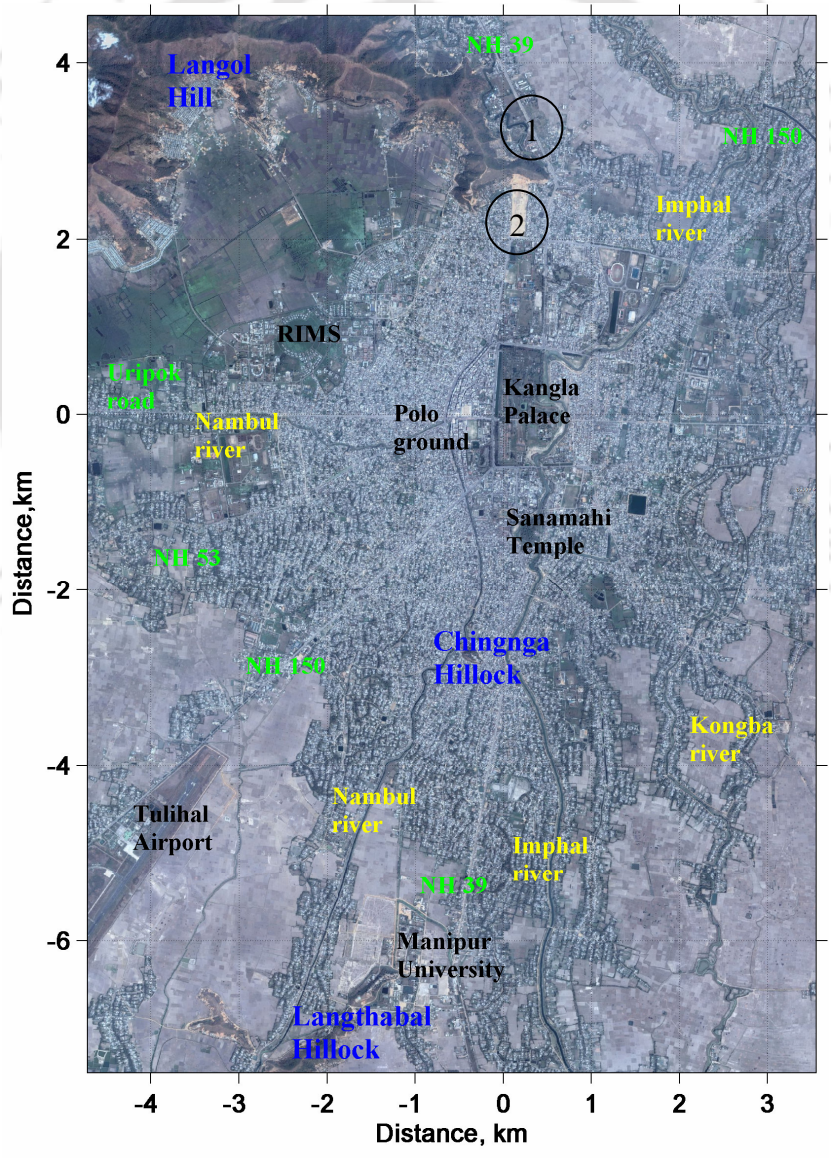


Figure 6.1 Imphal city

6.2 Methodology

Till date to the best of author's knowledge, detail studies on liquefaction hazard of Imphal city due to scenario earthquakes have not been performed. The ground motion results computed in the previous chapter are used as input parameters for the present study. The liquefaction hazard status of Imphal city for 1869 Cachar event (0.16g) along the Kopili fault and probable future great earthquake (0.3g) in the Indo-Burma subduction is performed. First, the factor of safety (FS) against liquefaction for each layer of soil has been computed using soil properties and ground motion as input parameters using method proposed by Idriss and Boulanger (2006). These methods are based on SPT-N values proposed initially by Seed and Idriss (1971). The brief descriptions of methods are presented below.

6.2.1 Semi-empirical approach

The semi-empirical method suggested by Idriss and Boulanger (2006) is based on an updated and improved technique of Seed *et. al.,* (2003) for evaluating the liquefaction potential of soil deposits. Here the liquefaction of soil deposits is expressed in terms of Factor of Safety (FS), which is a ratio of Cyclic Stress Ratio (CSR) to Cyclic Resistance Ratio (CRR). At locations where earthquake loading exceeds the soil resistance, FS less than 1.0, liquefaction is likely to occur. The *FS* against liquefaction is expressed as

$$FS = \frac{CRR}{(CSR)_{M_w=7.5,\sigma=1.0}} \qquad 6.2$$

In this $(CSR)_{M_w=7.5,\sigma=1.0}$ corresponds to the equivalent uniform shear stress due to earthquake having a moment magnitude of M_w=7.5 and overburden pressure (σ'_v) of 1 atm.

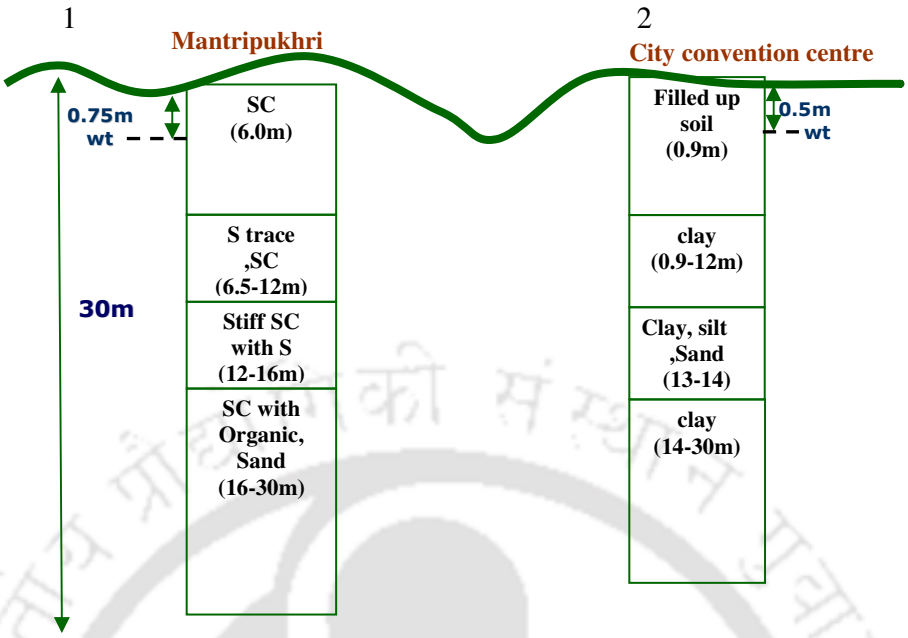


Figure 6.2 Soil profiles at two locations 1) Mantripukhri and 2) City convention centre (see Figure 6.1)

The induced cyclic stress ratio is calculated as per the simplified procedure given by Seed and Idriss (1971), using the following expression

$$(CSR)_{M_w=7.5,\sigma=1.0} = 0.65\left(\frac{\sigma_v a_{\max}}{\sigma'_v}\right)\frac{r_d}{MSF}\frac{1}{K_\sigma} \quad 6.3$$

$$\ln(r_d) = -1.012 - 1.126\,\mathrm{Sin}\left(\frac{z}{11.73} + 5.133\right) + \left[0.106 + 0.118\,\mathrm{Sin}\left(\frac{z}{11.28} + 5.142\right)\right]M_w \quad 6.4$$

$$MSF = 6.9\exp\left(\frac{-M_w}{4}\right) - 0.058 \le 1.8 \quad 6.5$$

where, a_{max}, σ_v and σ'_v are peak horizontal acceleration, total overburden pressure and effective overburden pressure respectively. The stress reduction factor (r_d) that measures the attenuation of peak shear stress with depth due to non-elastic behavior of soil is calculated using the equation (Equation 6.4) given by Idriss (1999) and Golesorkhi (1989). An earthquake having a moment magnitude M_w, is corrected through the

magnitude scaling factor (MSF, Equation 6.5) to adjust the value of CSR to the equivalent uniform shear stress induced by an earthquake having a moment magnitude.

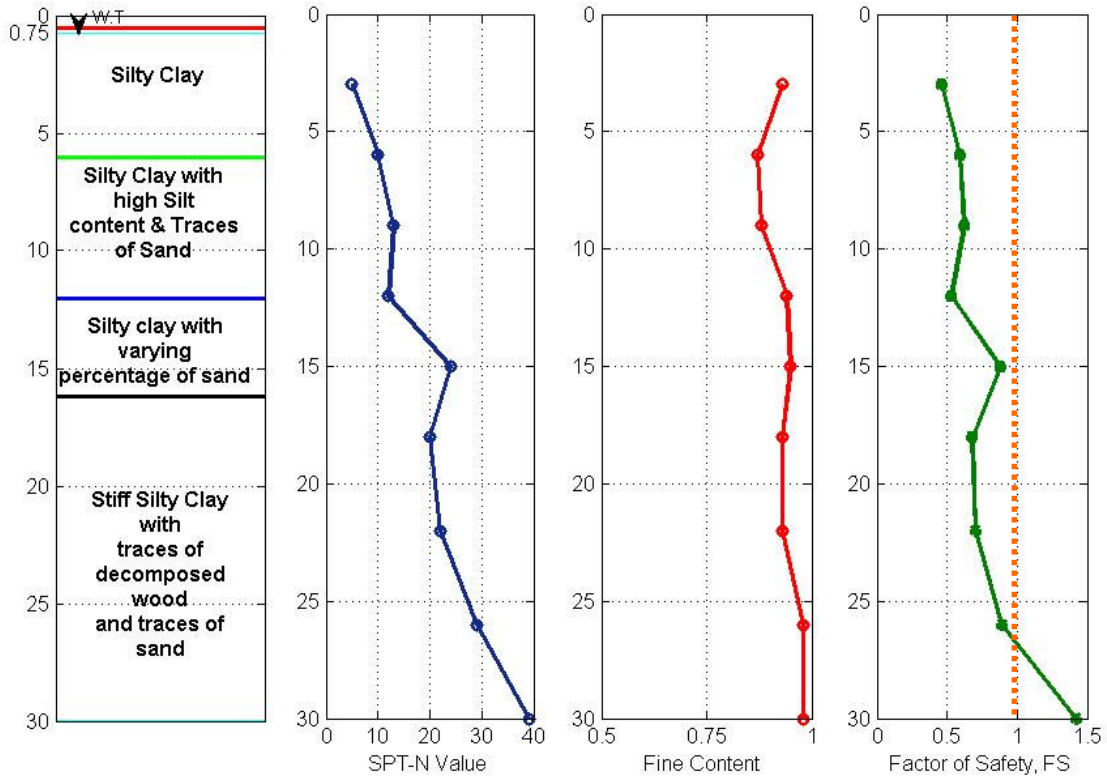


Figure 6.3 Variation of SPT-N values, fine content and factor of safety (FS) with depth for a typical soil profile (near Langol hill)

As liquefaction resistance increases with increasing confining stress, the correction due overburden pressure (K_σ) is applied in such a way that the values of CSR correspond to an equivalent overburden pressure of 1 atmosphere. The expression for the same is shown in Equation 6.6.

$$K_\sigma = 1 - C_\sigma \ln\left(\frac{\sigma'_v}{p_a}\right) \leq 1.0 \qquad 6.6$$

where, the C_σ can be calculated as

$$C_\sigma = \frac{1}{18.9 - 2.55\sqrt{(N_1)_{60}}} \leq 0.3 \qquad 6.7$$

Here p_a is the atmospheric pressure taken as 100 kpa. $(N_1)_{60}$, is the corrected SPT-*N* value = $C_N N_{60} < 37$, N_{60}= the corrected value for the field process with an average energy ratio of 60% of the SPT hammer. C_N is the correction factor for overburden pressure given by

$$C_N = \left(\frac{p_a}{\sigma'_v}\right)^{0.784-0.0768\sqrt{(N_1)_{60}}} \leq 1.7 \qquad 6.8$$

As seen in above equation (Equation 6.8) C_N and $(N_1)_{60}$ are determined by means of iterative procedure.

Idriss and Boulanger (2006), suggested the following equations for determining the CRR based on SPT-N results, for a cohesionless soil with any fine content (FC) as

$$CRR = \exp\left[\frac{(N_1)_{60cs}}{14.1} + \left(\frac{(N_1)_{60cs}}{126}\right)^2 - \left(\frac{(N_1)_{60cs}}{23.6}\right)^3 + \left(\frac{(N_1)_{60cs}}{25.4}\right)^4 - 2.8\right] \qquad 6.9$$

$(N_1)_{60cs}$ = Adjusted SPT-*N* equivalent to clean sand given by

$$= (N_1)_{60} + \exp\left(1.63 + \frac{9.7}{FC+0.1} - \left(\frac{15.7}{FC+0.1}\right)^2\right) \qquad 6.10$$

Assembling these two parameters i.e. CSR and CRR, FS can be worked out for every depth of boreholes. Using Equation 6.2 the FS value is estimated at all the depths for 122 sites in Imphal city.

Figure 6.3 shows a plot of FS with depth at one particular location near Langol hill area (Mantripukhri). Further for depth of 1.5m (shallow foundation level) the variation of FS and 15m depth (deep foundation level) are plotted for both 1869 Cachar earthquake and hypothetical earthquake in IBR, in Imphal city. In Figures 6.4a-b and 6.5a-b shows FS for 1.5m and 15m depth for both the events respectively.

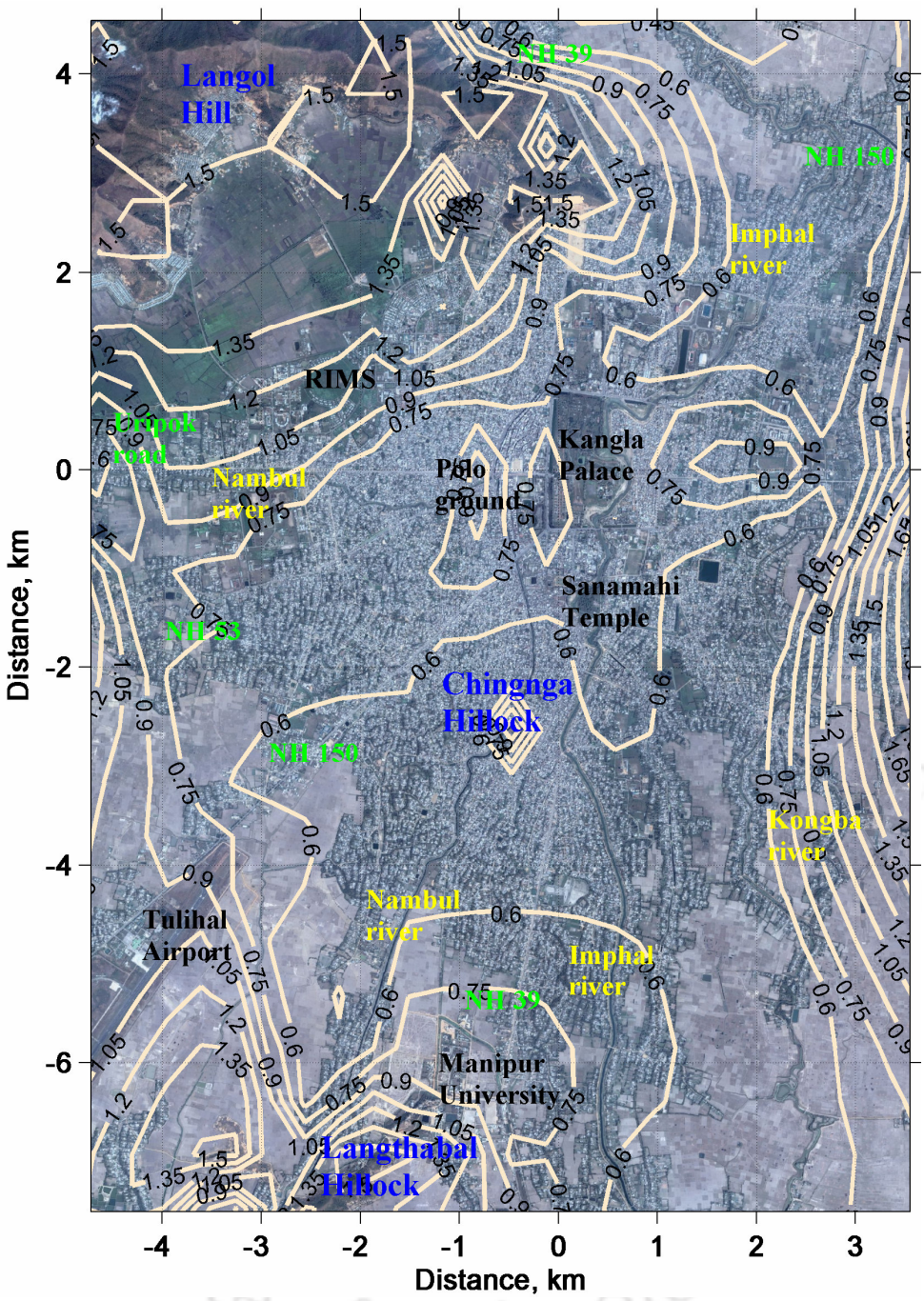


Figure 6.4a FS against liquefaction at a depth of 1.5m for PGA = 0.16g

It can be seen that from Figure 6.4a that the Kangla palace, Polo ground and Sanamahi temple area are liquefiable (FS < 1.0) at depth of 1.5m, whereas near RIMS and Tulihal airport area are at border (FS ~ 1.0) of for 1869 Cachar earthquake event. Areas near Langol hill, Manipur University and Mantripukhri area are safe against liquefaction (FS > 1.0) at depth of 1.5m for the same event.

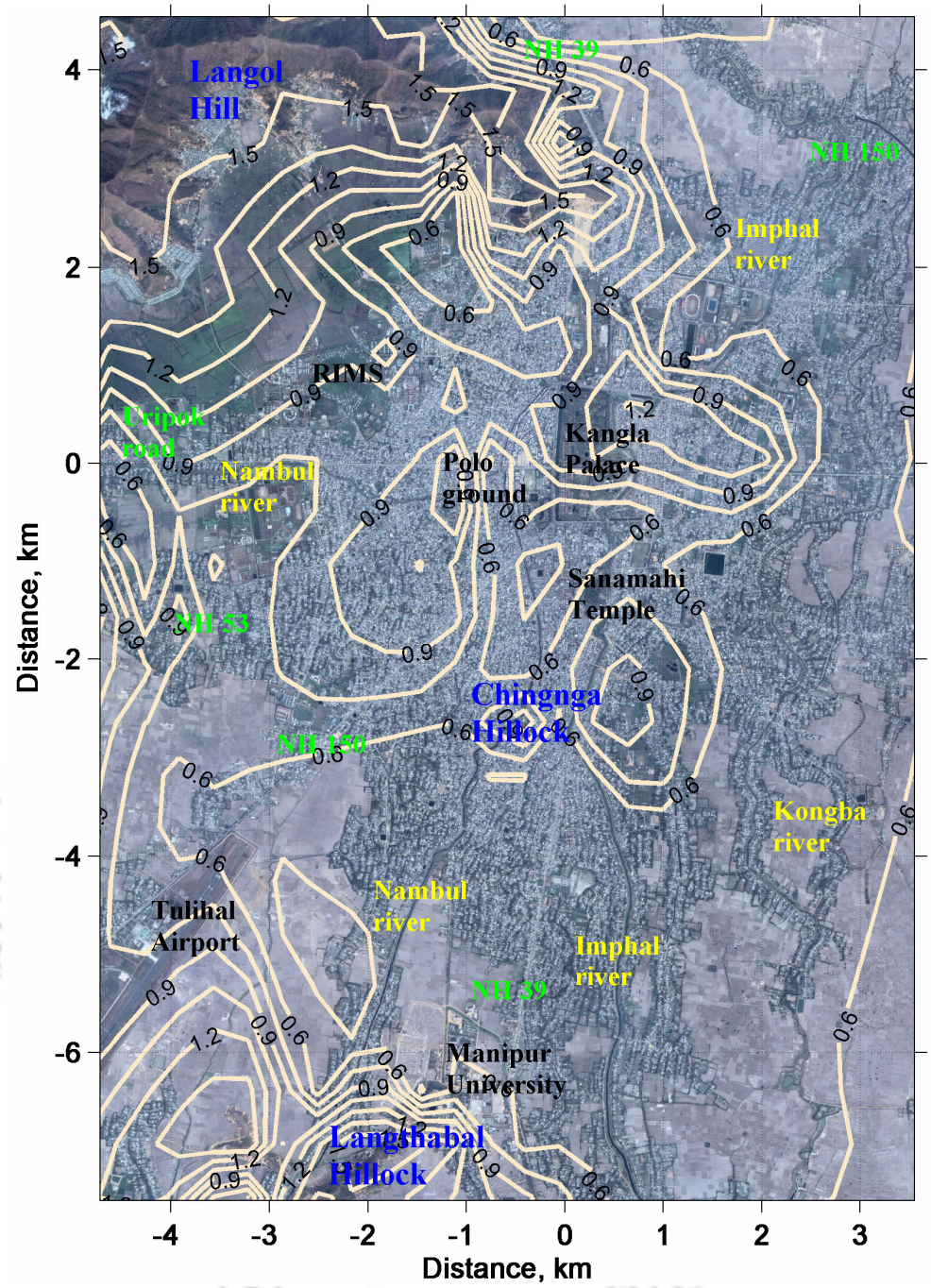


Figure 6.4b FS against liquefaction at a depth of 15m for PGA= 0.16g

In Figure 6.4b it can be observed that entire Imphal city is safe against liquefaction at 15m depth except for few places like Kangla palace, RIMS and some areas close to Tulihal airport which are at the verge of liquefaction for 1869 Cachar earthquake event.

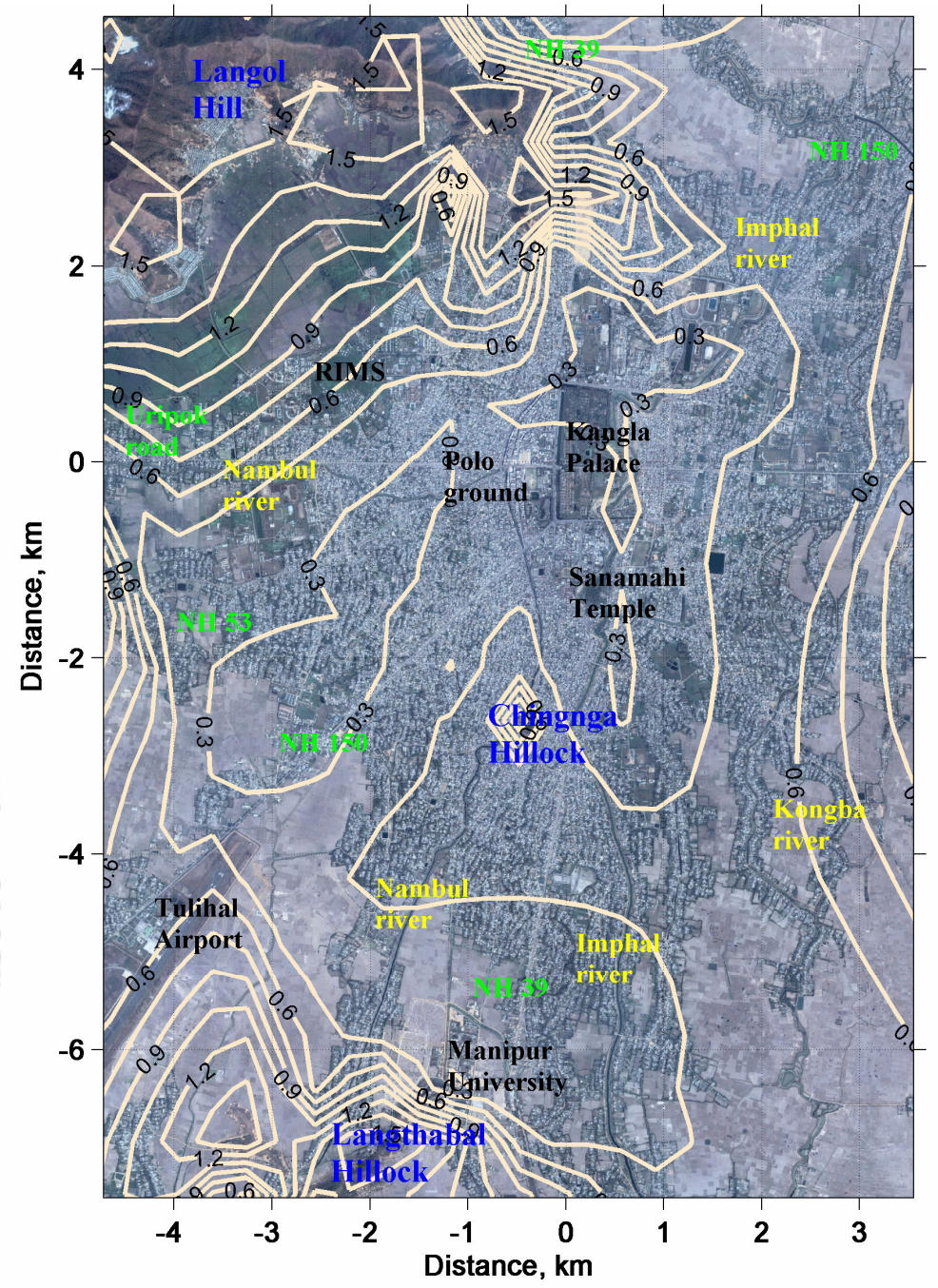


Figure 6.5a FS against liquefaction at a depth of 1.5m for PGA= 0.3g

Factor of safety against hypothetical earthquake in IBR (0.3g) at depth 1.5m and 15m are shown in Figures 6.5a-b for Imphal city. This particular event shows that central places *viz.*, Kangla palace, Polo ground and Sanamahi temple areas are vulnerable to liquefaction failure at 1.5m and 15m depth. Areas near Langol, Langthabal hill and Mantripukhri are safe

against liquefaction. Table 6.1 shows the liquefaction potential status of important locations in Imphal city.

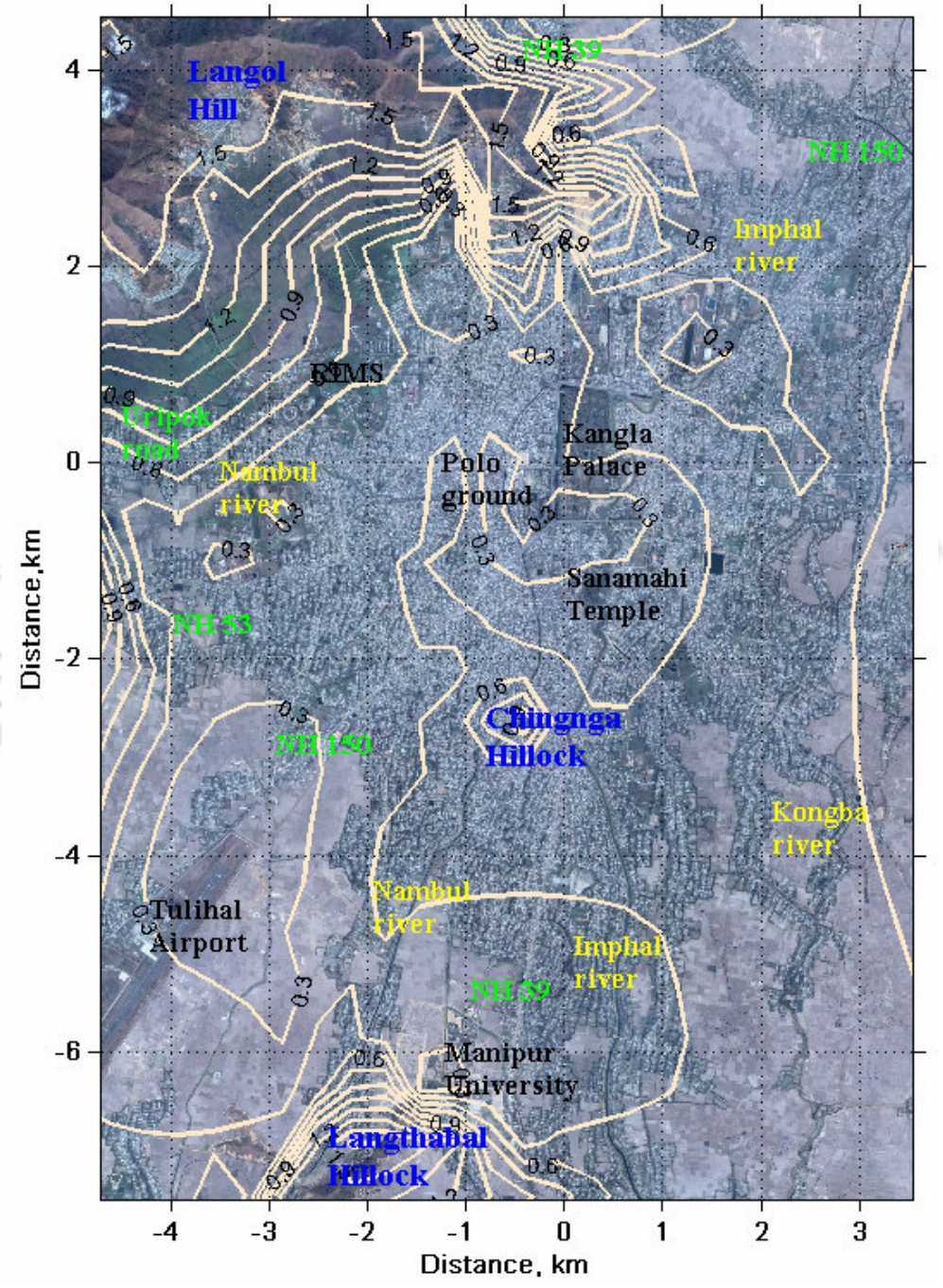


Figure 6.5b FS against liquefaction at a depth of 15m for PGA= 0.3g

Table 6.1 Liquefiable place in Imphal city

Location	1869 Cachar earthquake (0.16g)		Hypothetical earthquake in IBR (0.3g)	
	1.5m depth	15m depth	1.5m depth	15m depth
Kangla Place	Liquefiable	Liquefiable	Liquefiable	Liquefiable
RIMS	Non liquefiable	Liquefiable	Liquefiable	Liquefiable
Near Langol hill	Non liquefiable	Non liquefiable	Non liquefiable	Non liquefiable
Manipur University	Liquefiable	Liquefiable	Liquefiable	Liquefiable

6.2.2 Liquefaction Potential Index

The susceptibility of a site against liquefaction can be expressed as a combined effect of layer wise liquefaction potential over the entire depth of soil under consideration. The study on liquefaction potential is presented in this section using liquefaction Potential Index (LPI) proposed by Iwasaki and Co-workers (1982). Liquefaction potential index (LPI) is defined as liquefaction potential of site in terms thickness, depth and FS value of each layer. Based on above-mentioned parameters, Iwasaki expressed LPI by the following equations.

$$\mathrm{LPI} = \int_0^{20} \mathrm{F(z)\,w(z)\,dz} \qquad 6.11a$$

$$F(z) = 1 - FS; \quad for\ FS < 1.0 \qquad 6.11b$$

$$F(z) = 0; \quad for\ FS \geq 1.0 \qquad 6.11c$$

$$w(z) = 10 - 0.5z; \quad for\ z < 20m \qquad 6.11d$$

$$w(z) = 0; \quad for\ z > 20m \qquad 6.11e$$

where z is the depth from ground level in m.

Table 6.2 Liquefaction potential Index based on LPI (Iwasaki *et. al.*, 1982)

LPI	Category
0	Very low
0<LPI≤5	low
5<LPI≤15	High
LPI<15	Very High

If the FS values are less than 1.0, the soil layer is treated as liquefiable else non-liquefiable. This susceptibility against liquefaction is categorized into four classes as very low, low, high and very high depending on the value of LPI (Table 6.2). The advantage of this method is that it provides a special value for the entire soil column of the sites instead of having several FS values for different layers of soil. Figures 6.6a-b show the variation of LPI in Imphal for PGA = 0.16g and PGA = 0.3g events. For both the events, LPI is greater than 15 for entire Imphal city and hence based on the LPI classification suggested by Iwasaki *et. al.*,(1982) (Table 6.2) Imphal city is highly susceptible category to liquefaction failure.

6.2.3 Liquefaction Severity Index

In order to incorporate uncertainties pertaining to sites (and hence soil) for specific seismic events on liquefaction potential of Imphal city, the method proposed by Sonmez and Gokceoglu (2005) has been followed. The method is briefly discussed below.

$$LSI = \int_0^{20} P(z)w(z)dz \qquad 6.12a$$

where,

$$P(z) = \frac{1}{1+\left(\frac{FS}{0.96}\right)^{4.5}}; \quad for \quad FS \le 1.411 \qquad 6.12b$$

$$P(z) = 0; \quad for \quad Fs > 1.411 \qquad 6.12c$$

The P(z) is the probability function of liquefaction at particular depth z, which is further integrated over the depth to get the severity index for the site. Equation (6.12b) has been taken from the work of Chen and Juang (2000) and Juang *et. al.,* (2003).

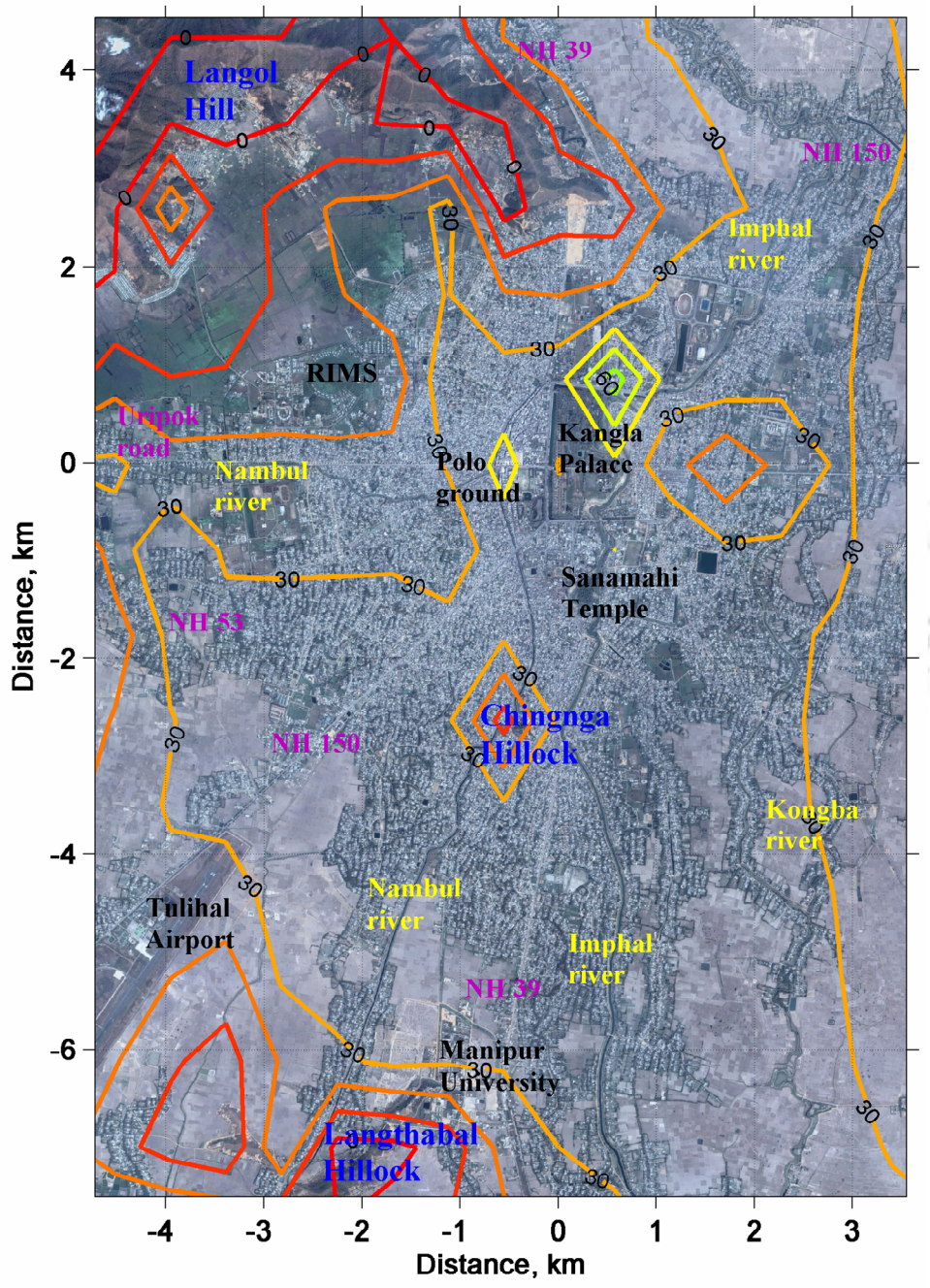


Figure 6.6a Contour map of LPI against liquefaction for PGA= 0.16g

The constant 1.411 is the threshold value of the FS, which is reported as open for discussion (Sonmez and Gokceoglu, 2005).

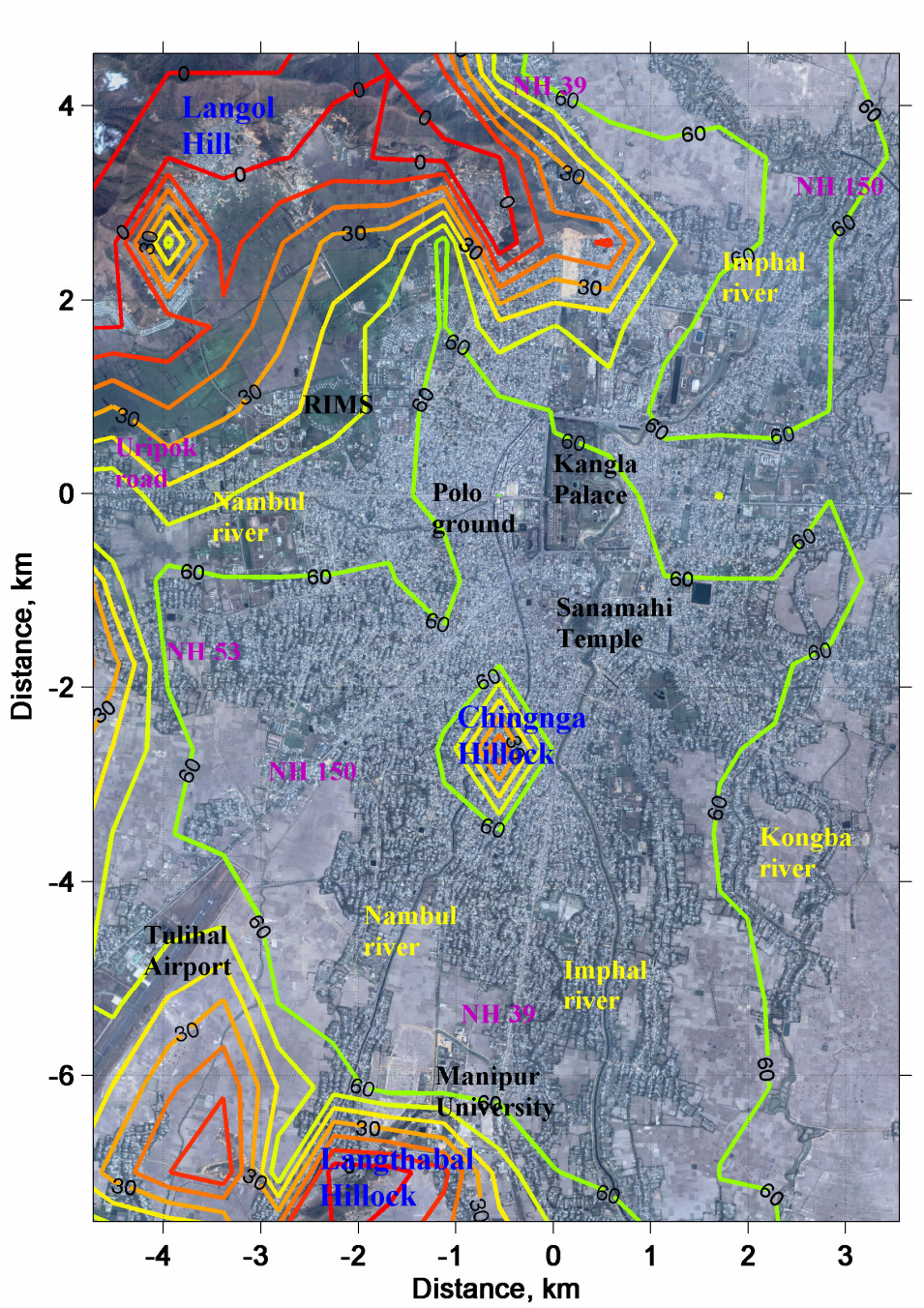


Figure 6.6b Contour map of LPI against liquefaction for PGA= 0.3g

The limiting values for LSI and its severity classes are shown in Table 6.3. Figures 6.7a-b shows that for 1869 Cacher earthquake (0.16g), Kangla palace, RIMS, Polo ground, Tulihal airport and Sanamahi temple areas comes under 'High' severity index whereas, towards Langol hill the LSI reduces to 'very low' severity index as per Table 6.3.

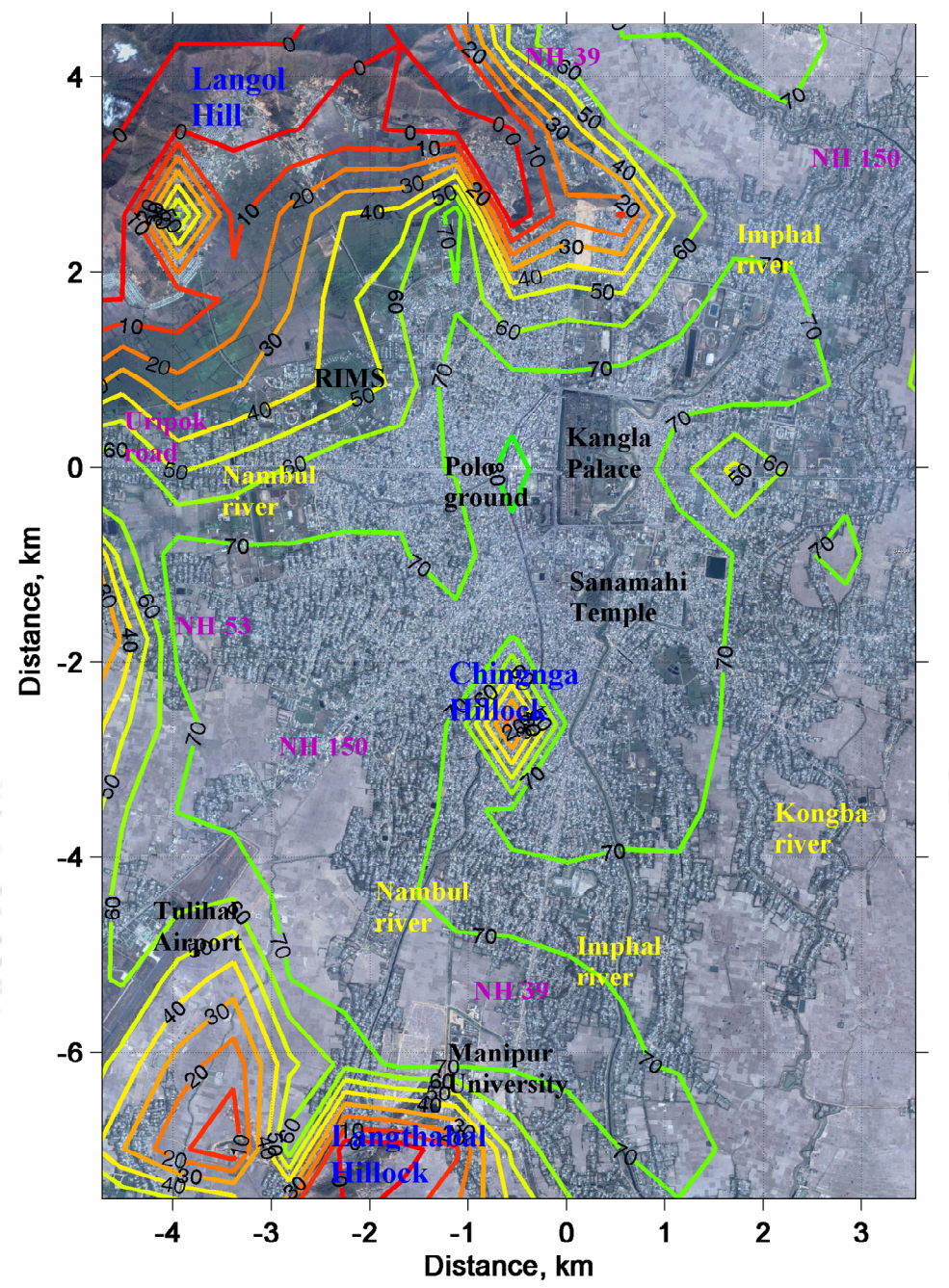


Figure 6.7a Contour map of LSI against liquefaction for PGA= 0.16g

Further for hypothetical event of PGA= 0.3g, severity index in areas like Kangla palace, Polo ground, Tulihal airport and Sanamahi temple are enhanced by one category to 'very high', compared to that of 1869 earthquake.

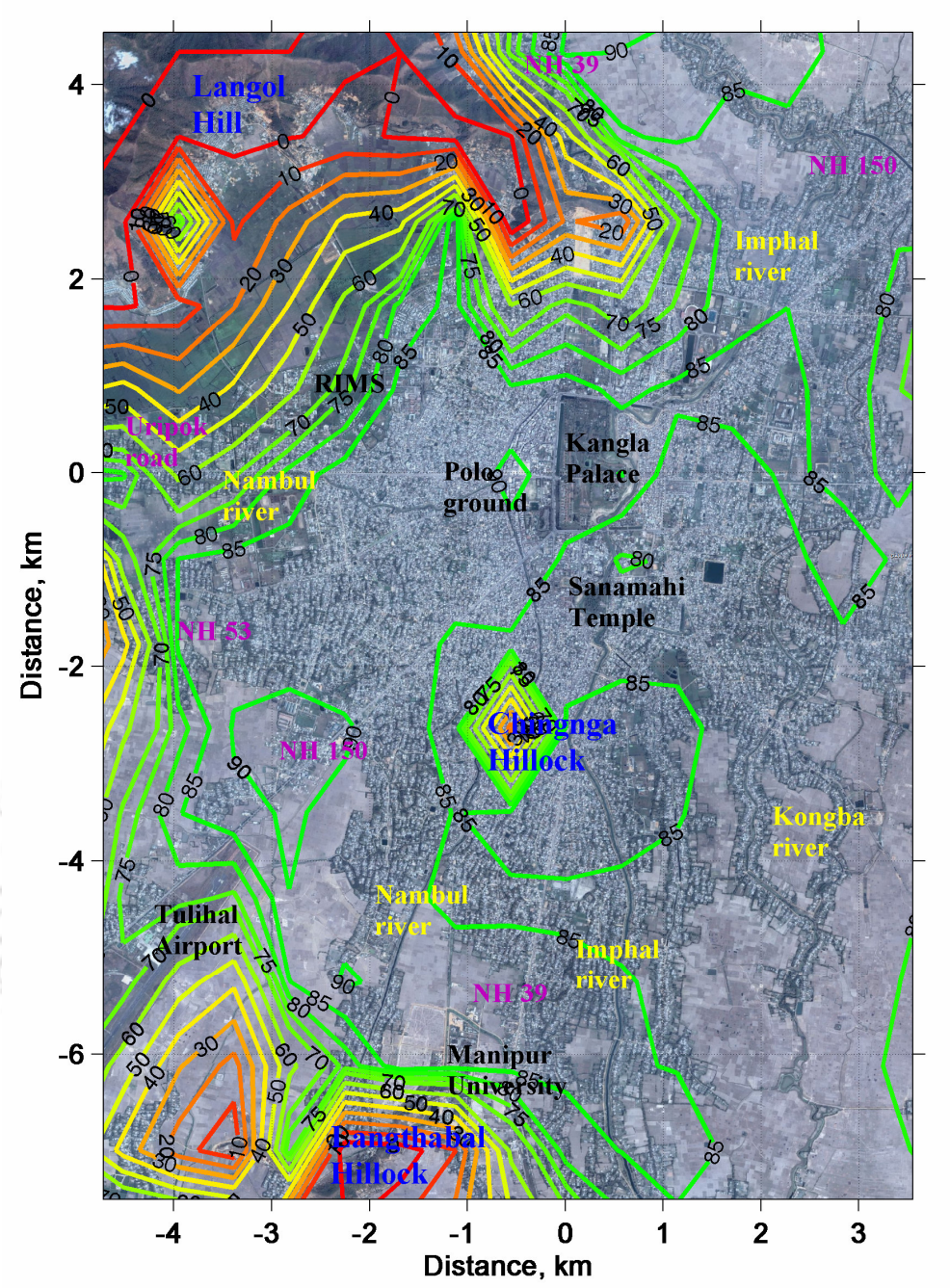


Figure 6.7b Contour map of LSI against liquefaction for PGA= 0.3g

6.3 Conclusions

The geologic setup of Imphal city makes the area prone to liquefaction. It has been established as per IBC (2006) that most of site in Imphal city belongs to E-Type category. It is suggested that for such sites, site-specific studies are recommended. Hence, liquefaction potential hazard studies

using two indices 1) Liquefaction Potential Index (LPI) (Iwaski *et..al.*, 1982), and 2) Liquefaction Severity Index (LSI) (Sonmez and Gokceoglu, 2005) have been presented using Factor of Safety (FS) (=CRR (Cyclic Resistance Ratio) / CSR (Cyclic Stress Ratio) as input (Idriss and Boulanger, 2006), for Imphal city.

Table 6.3 Liquefaction Severity Index by Sonmez and Gokceoglu (2005)

LSI	Particular classes
0	Non-liquefied
0<LSI<15	Very low
15≤LSI<35	Low
35≤LSI<65	Moderate
65≤LSI<85	High
85≤LSI<100	Very High

The results are presented in the form of liquefaction hazard contour map for Imphal city. It has been observed based on FS studies that for both 1869 Cachar and hypothetical earthquakes Kangla Palace, RIMS and Sanamahi Temple area are under highest category (Very High) and Mantripukhri, Uripok and Langol hill areas fall under the next level (High) of liquefaction failure. As per LPI studies, entire Imphal city has 'very high' potential (LPI > 15) of liquefaction failure. Based on LSI studies it has been observed that Kangla palace, Polo ground, Tulihal airport and Sanamahi temple areas fall under 'high' class of LSI for 1869 Cachar earthquake event (PGA = 0.16 g), whereas for hypothetical event of PGA= 0.3g, severity indices in those areas have been enhanced by one category to 'very high'.

Chapter 7

Probabilistic seismic hazard analysis of Manipur state

7.1 Introduction

The key elements for seismic hazard analysis have been discussed in the previous chapters. In the present chapter probabilistic seismic hazard analysis has been extended for entire Manipur state (Figure 7.1). Here, annual frequencies of exceedence of ground motion level, typically stipulated by peak ground acceleration or by spectral acceleration, for Manipur state has been estimated from each of the twenty-seven major faults (see Figure 5.1) that exist around Manipur state using the regional recurrence obtained previously in Chapter 3. Attenuation relations proposed by Boore and Atkinson (2008) for strike-slip, thrust & reverse fault and Atkinson and Boore (2003) for subduction zone, have been used for computing peak ground motion. As the shear- wave velocity profiles of Manipur are not readily available for hilly districts of Manipur, site specific hazard (seismic microzonation) studies are not attempted. Hence probabilistic seismic hazard map has been prepared by determining the seismic hazard at 0.05° x 0.05° (Figure 7.2) grid size along EW

TH-994_06610404

(94°45′E to 92°58′E) and NS (25°42′N to 23°50′N) directions at rock level. The uniform hazard response spectra have been derived for return period of 100, 500 and 2500 years for all nine districts headquarters of Manipur state.

Manipur, one of the eight states of the NE part of India lies between latitude of 23°50′N to 25°42′N and longitude of 92°58′E to 94°45′E, located at the eastern most part of India and adjacent to Myanmar, plays an important strategic corridor (e.g. Trans Asian International Highway) for India's 'Look East Policy' (e.g. Oinam, 2007). Its shares long international border with Myanmar in its east and state border with Nagaland state in north, Assam state in west and Mizoram state in south (Figure 7.1). The state is geographically classified into two regions *viz*., the peripheral hills and the central open valley, having a total area around 22,327 sq. km., out of which 20,089 sq. km. (90% of total area) is covered by hills and only 2238 sq. km. (10% of total area) accounting for a smaller valley. The hilly region comprises of five districts namely Senapati, Tamenglong, Churachandpur, Chandel and Ukhrul whereas central open valley encompasses four districts *viz.*, Imphal east, Imphal west, Bishnupur and Thoubal (Figure 7.2, Table 7.1). As per census 2001, the population of Manipur was 2.29 million, ranks 4th among northeastern Indian states with population density of 103 per sq. km. as against 82 per sq. km. in 1991 and since then the population has increased and is expected to reach 2.79 million in 2011 (DES, 2008-09). The valley area is thickly populated with a density of 631 persons per sq. km. as against 44 persons per sq. km. in the hills.

7.2 Seismic hazard curves

The seismic hazard curves have been obtained by (using seismic parameter *viz., a* and *b* value estimated in Chapter 3 and attenuation relationship from chapter 5) computing mean annual rate of exceedance $\upsilon_Y(y^*)$ for different specified ground motion values *y**.



Figure 7.1 NE India (Source: Flash Earth, 13 July 2010)

The procedure for carrying out seismic hazard to obtained the seismic hazard curves are as follows; 1) identifying of seismic sources around Manipur (see Chapters 3 and 5), 2) evaluating earthquake recurrence and magnitude distributions (see Chapter 3), 3) estimating ground motion using attenuation model (see Chapter 5), and 4) computation of seismic hazard curves for all the

twenty-seven faults to estimate the aggregate hazard at the site. For Manipur there are two categories of seismic setups, 1) strike-slip, normal and reverse faults (SP, AV, EH, ND, MT, BB) and 2) subduction zone (IBR).

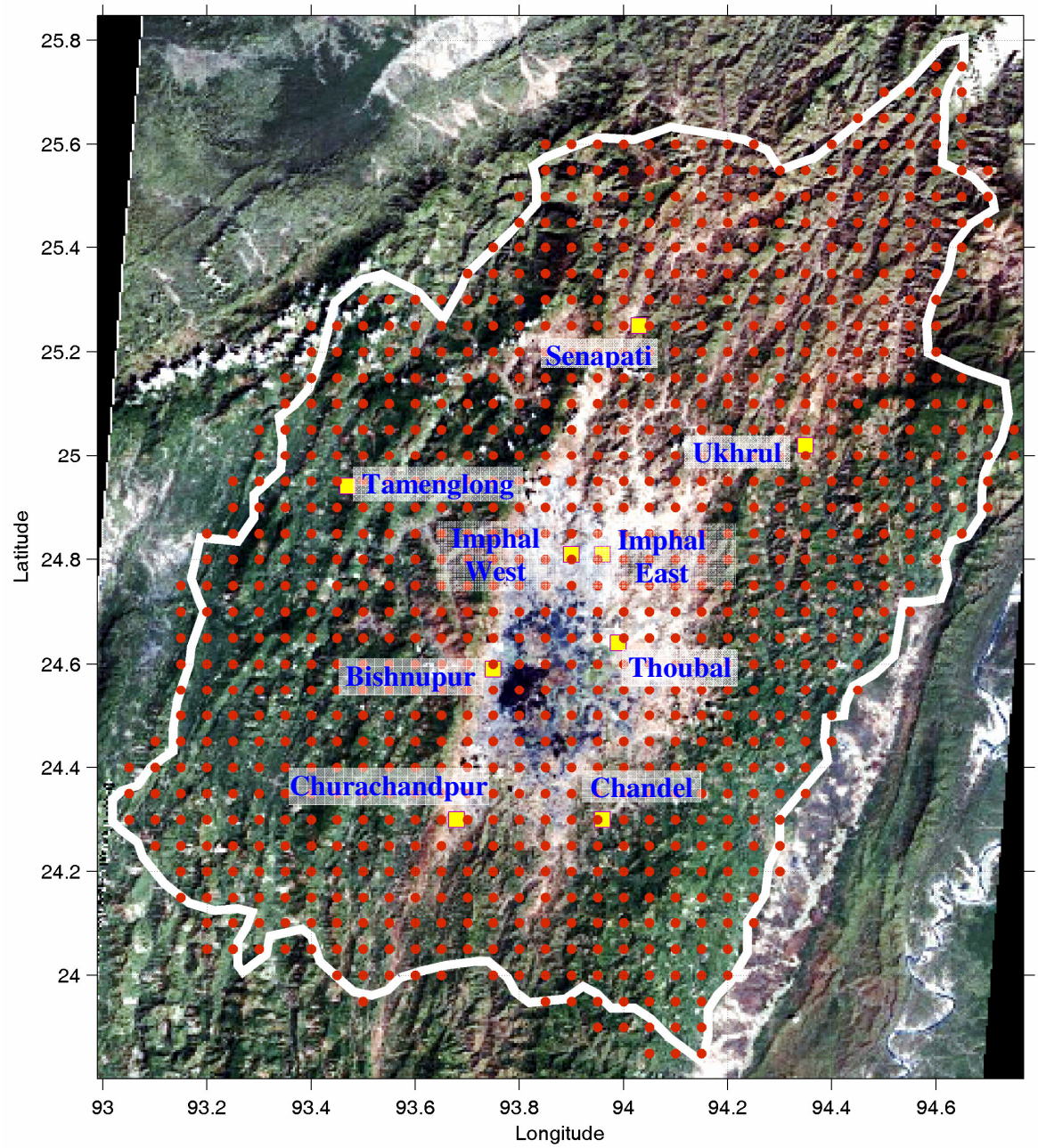


Figure 7.2 Manipur state map along with grid (0.05°x0.05°) and location of district headquarters

The seismic hazard curves at all the grid point (0.05° x 0.05°) of Manipur have been obtained as combined effect of these seismic setups. The hazard curves

are also drawn for all nine district headquarters of Manipur *i.e.* Senapati, Tamenglong, Churachandpur, Chandel, Imphal east, Imphal west, Ukhrul, Bishnupur and Thoubal at PGA, 0.3 s and 1.0 s (Figures 7.3a-c).

Table 7.1 Manipur districts (population, area) (Source: NEDFI)

Hilly districts			**Central open valley districts**		
Districts	**Area (in sq.) km.)**	**Population**	**Districts**	**Area (in sq. km.)**	**Population**
Senapati	3217	2,836,21	Imphal East	709	3,948,76
Tamenglong	4391	1,114,99	Imphal	519	4,443,82
Churachandpur	4570	2,279,05	Bishnupur	496	2,083,68
Chandel	3313	1,183,27	Thoubal	514	3,641,40
Ukhrul	4544	1,407,78	**Valley Total**	**2238**	**14,117,66**
Hill Total	**20089**	**8,821,30**			
Manipur	**Total Area**	**22327**	**Total Population**		**22,938,96**

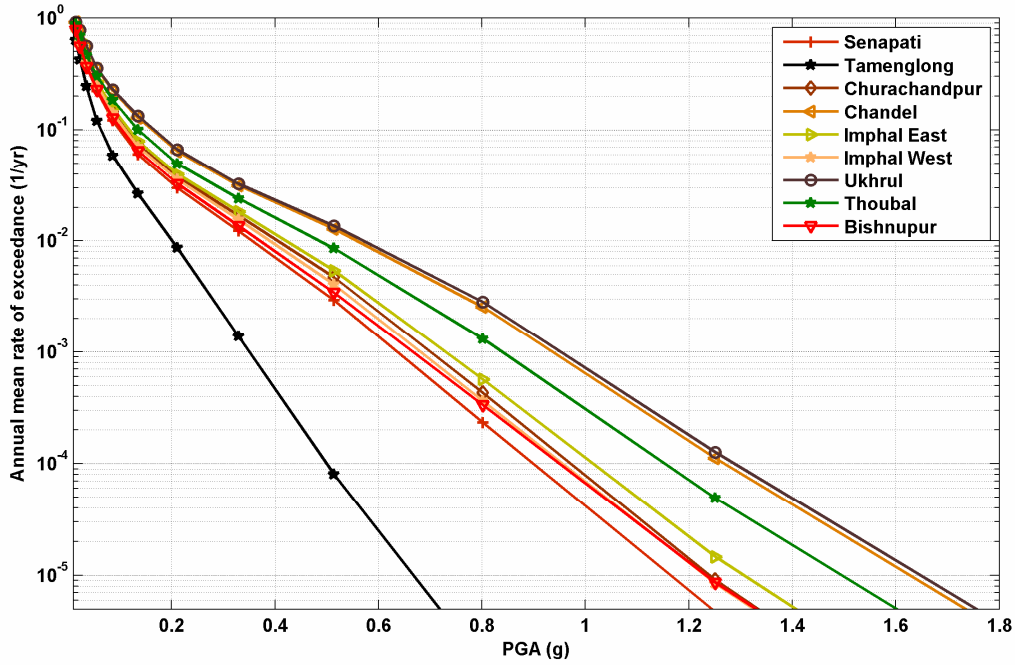


Figure 7.3a Seismic hazard curves at district headquarters of Manipur at rock level.

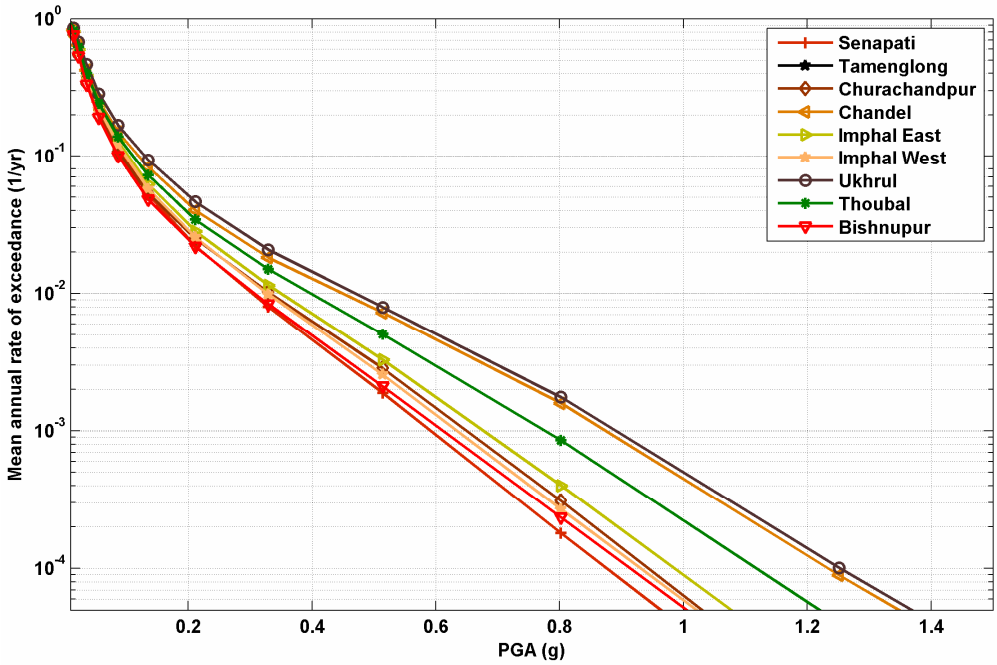


Figure 7.3b Seismic hazard curves at district headquarters of Manipur (period = 0.3 s) (5% damping)

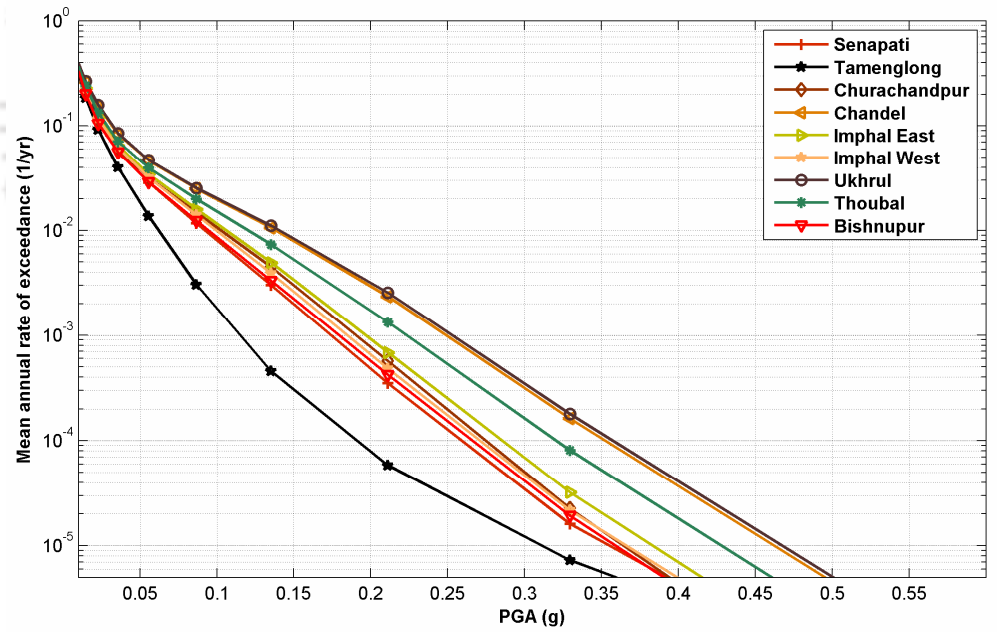


Figure 7.3c Seismic hazard curves at district headquarters of Manipur (period = 1.0 s) (5% damping)

7.3 Uniform hazard response spectra

Conventionally, PGA has been used to characterize ground motion, however, in recent times, preferred parameter for design of engineering structures has

become spectral acceleration (S_a), because in the conventional practice of scaling normalized response spectral shape to the design PGA level leads to different probabilities of exceedance over normal frequency range (~ 0.5 Hz – 25 Hz) of civil engineering structures. The present approach is to use design response spectra with equal probability of exceedance over the entire frequency range of interest. Such design spectra are known as uniform hazard response spectra (UHRS). For finding UHRS, seismic hazard curves of S_a are computed for a range of frequency values. From these hazard curves, response spectra for a specified probability of exceedance over the entire frequency range of engineering interest are obtained.

IBC (2006) prescribes design forces based on S_a corresponding to 10% and 2% exceedance probability in 50 years. These correspond to 475 (~ 500) and 2475 (~ 2500) year return periods respectively. In addition to that UHRS is also shown for 50% probability of exceedence in 50 years (Return Period ~100 years).

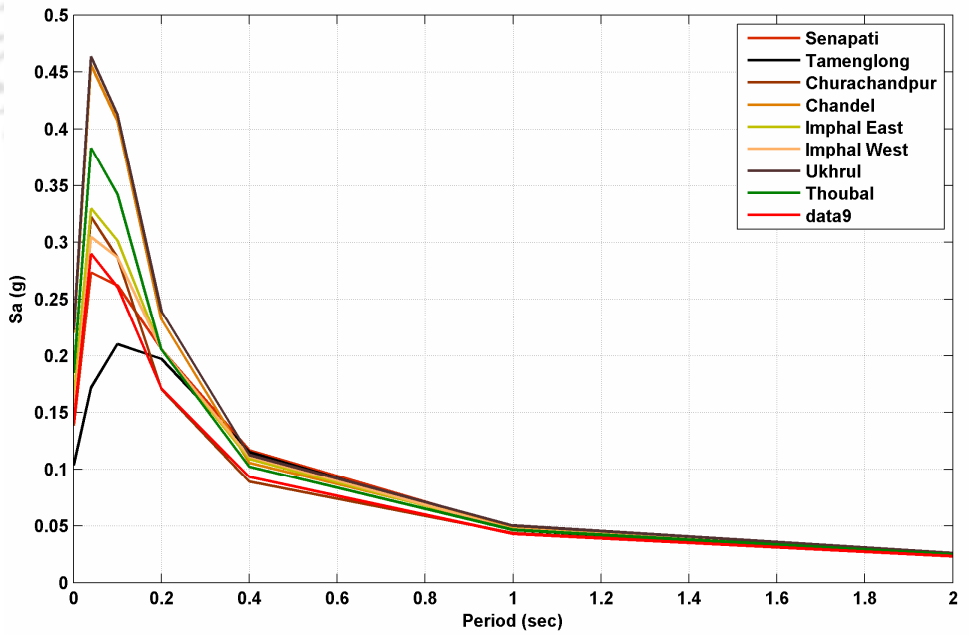


Figure 7.4a UHRS with 50% probability of exceedence in 50 years (return period= ~100 years) over districts of Manipur (5% damping)

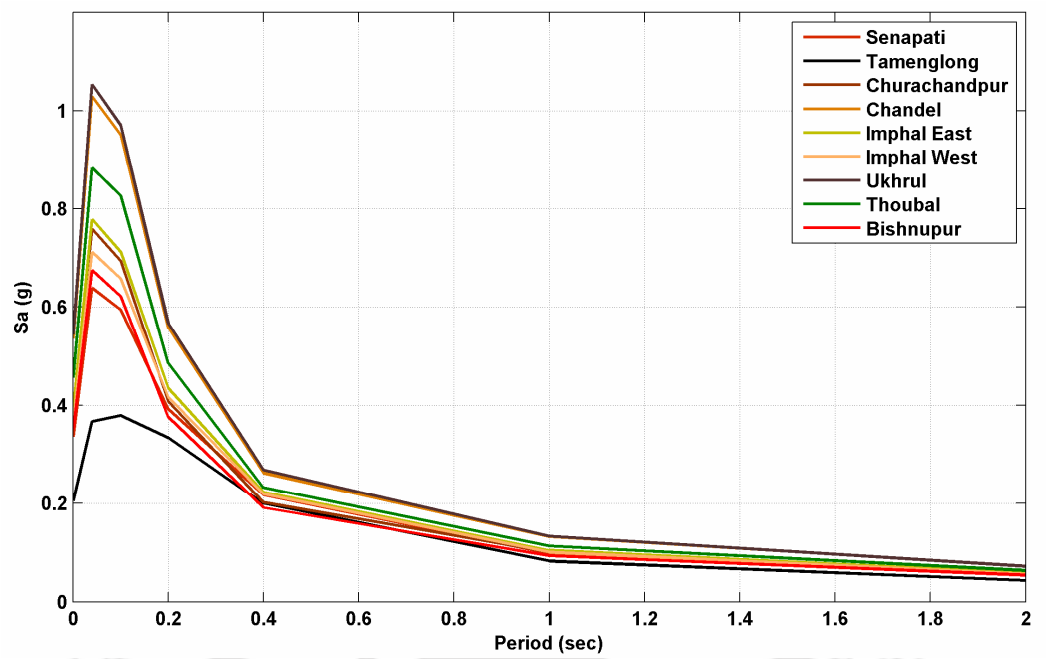


Figure 7.4b UHRS with 10% probability of exceedence in 50 years (return period= ~500 years) over districts of Manipur (5% damping)

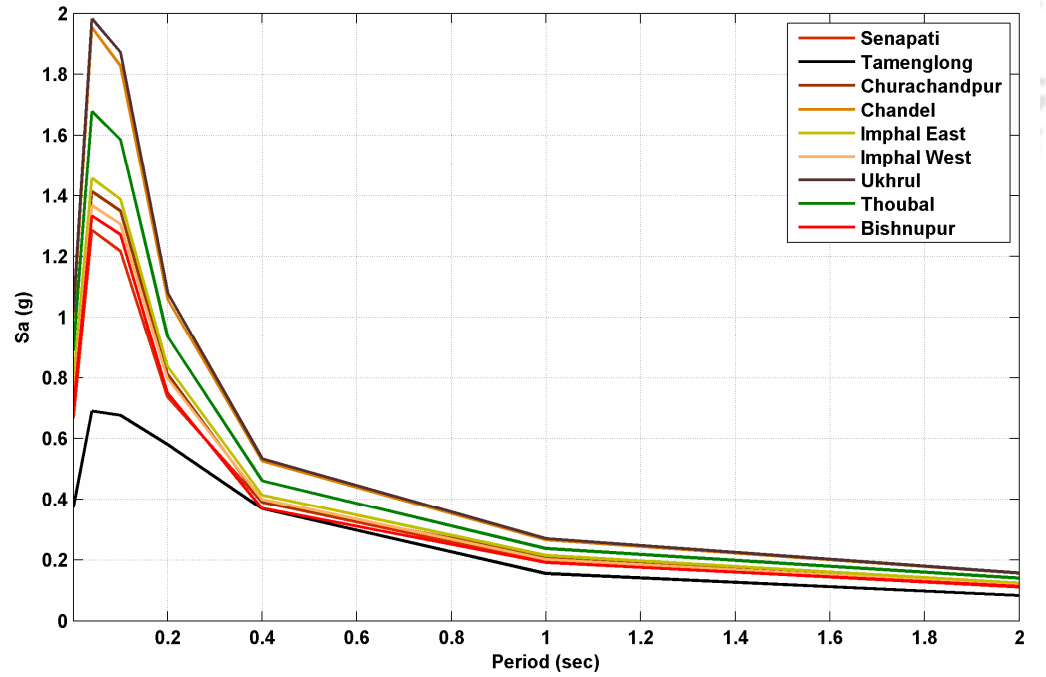


Figure 7.4c UHRS with 2% probability of exceedence in 50 years (return period= ~2500 years) over districts of Manipur (5% damping)

In Figures 7.4a-c UHRS for all nine districts of Manipur corresponding to the standard return periods of 100, 500 and 2500 years are presented. The corresponding PGA values are also shown

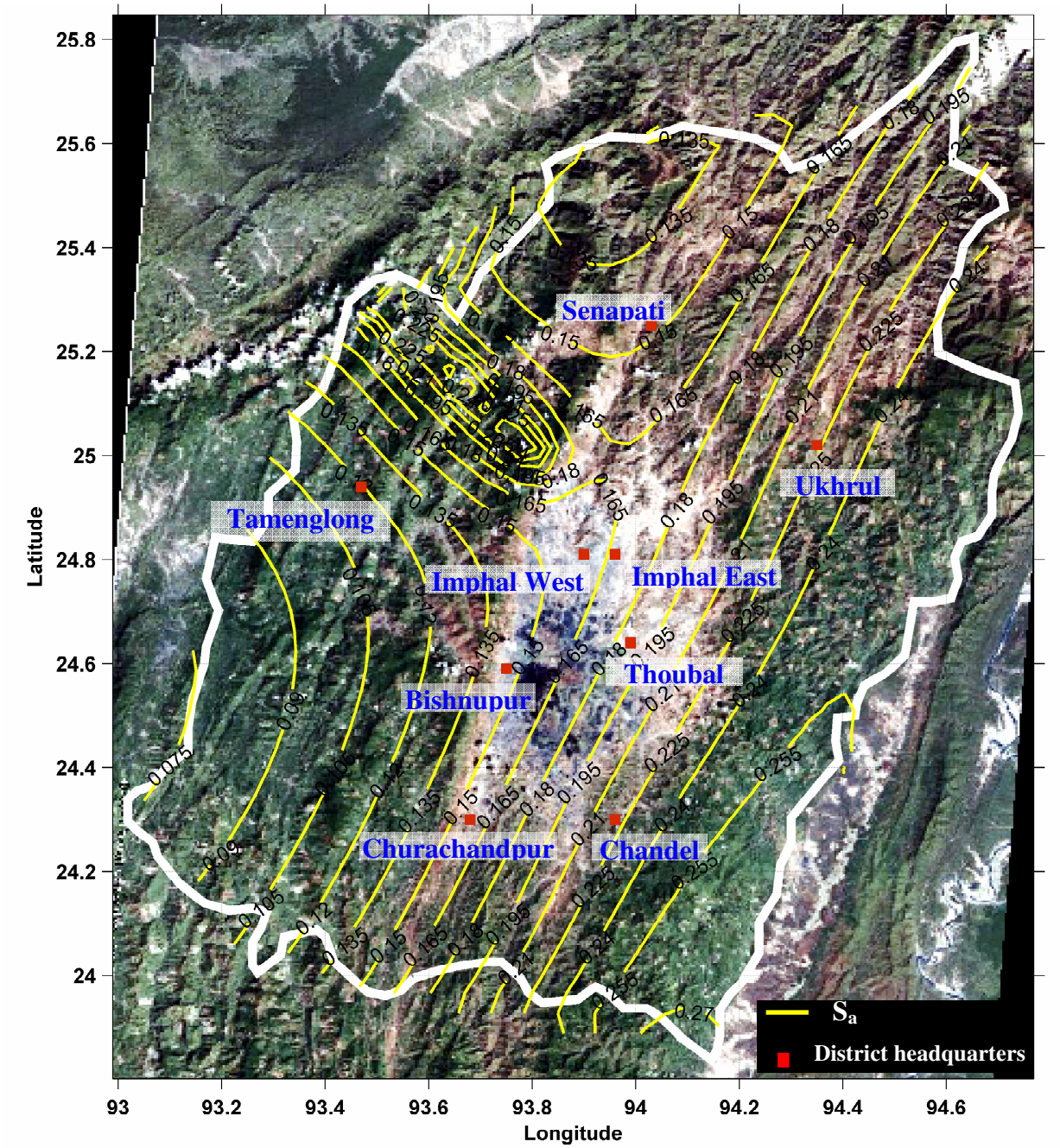


Figure 7.5 PGA contours with 50% probability of exceedence in 50 years (return period= ~100 years) over Manipur

Further, the seismic hazard maps of Manipur for return periods of 100, 500 and 2500 years at PGA are shown in Figures 7.5-7.7. From Figure 7.5 it has been observed that for hill districts the range of PGA values are 0.135g-0.165g, 0.1g-0.12g, 0.12g-0.16g, 0.19g-0.25g, 0.21g-0.24g near Senapati, Tamenglong, Churachandpur, Chandel and Ukhrul district respectively. Whereas for open

valley area (Imphal east, Imphal west, Bishnupur and Thoubal districts) the PGA range is found to be 0.135g-0.195g.

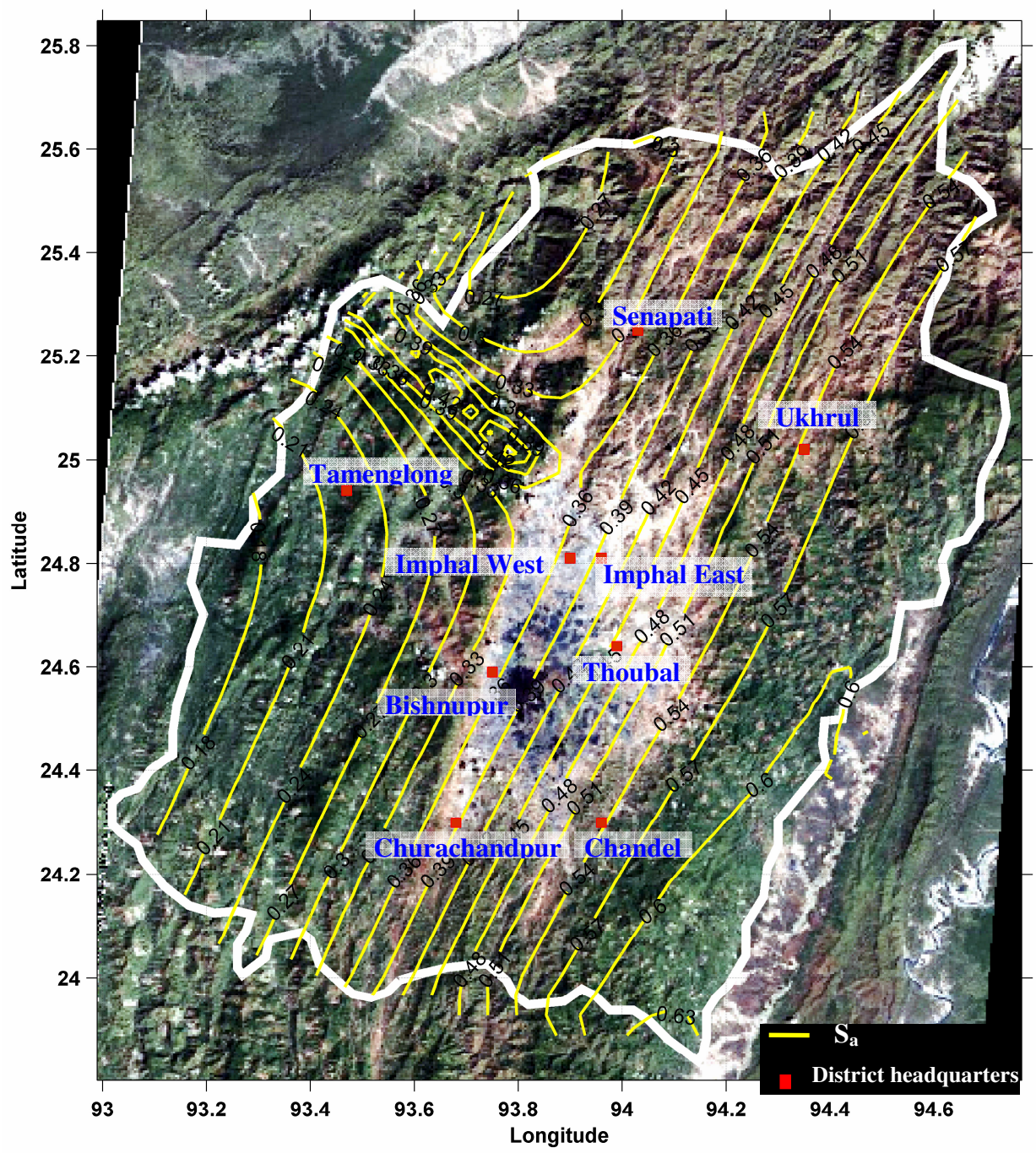


Figure 7.6 PGA contours with 10% probability of exceedence in 50 years (return period= ~500 years) over Manipur

It may be noted that Indian code of practice (IS-1893, 2002) considers the entire NE India as one seismic zone (Zone V) with PGA value of 0.36g, without specifying any return period. Here it can be observed that for return period of

100 year, the present computed values are within recommended value (*i.e.* 0.36g) by IS: 1893.

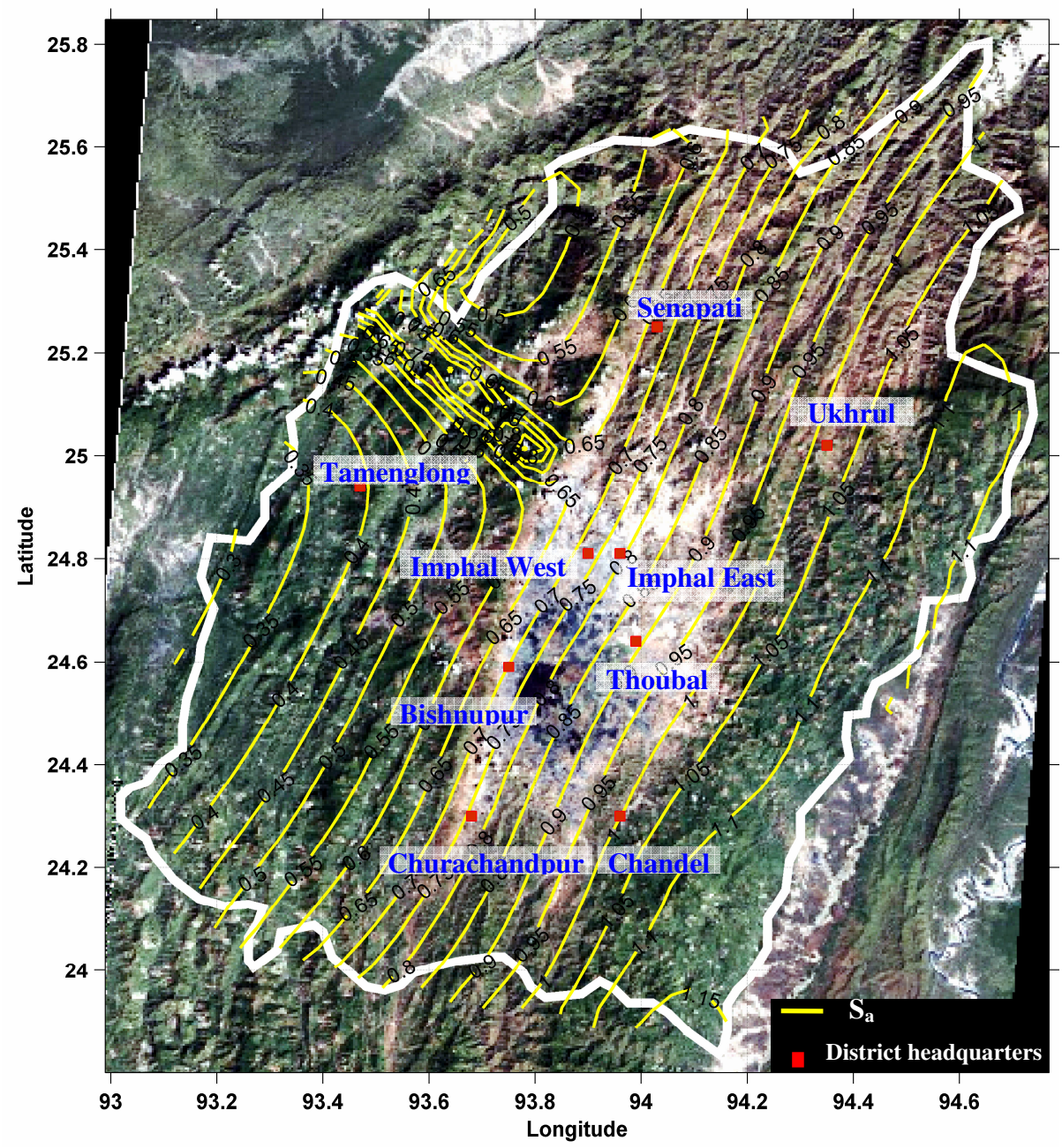


Figure 7.7 PGA contours with 2% probability of exceedence in 50 years (return period= ~2500 years) over Manipur

However for return period of 500 years, PGA varies from 0.50g-0.60g for Ukhrul, Chandel districts, and 0.35g-0.50g for Imphal east, Imphal west, Churachandpur and Thoubal, and 0.2g-0.35g in Senapati, Tamenglong and

Bishnupur (Figure 7.6) districts. It is also seen that Chandel which is close to IBR has higher PGA (0.6g) value as compared to Tamenglong (0.18g) which is away from IBR (Figure 7.6). It can be seen that the present values exceed the recommended value of 0.36g given by IS: 1893 except near some district headquarters *viz.,* Tamenglong and Senapati district headquarters. Similarly, contour map has been drawn for 2500 year return period and the variation ground-motion parameter is found to be between 0.4g - 1.1g for all the districts of Manipur (Figure 7.7).

7.4 Comparison with other studies

To the best of author's knowledge no previous engineering studies has been made to understand seismic hazard dedicated to Manipur state. As such comparison is made with similar PSHA studies at rock level carried out by Khatri *et. al.,* (1984), Bhatia *et. al.,* (*1999*) and Das *et. al.,* (2006) for 500 year return period. Table 7.2 shows a comparison of PGA values of the present study with that of Khatri *et. al.,* (1984), Bhatia *et. al.,* (1999), and Das *et. al.,* (2006) for 500 year return period. It may be seen that although the average value (i.e. 0.48g) agrees well with previous work of Khatri *et. al.,* (1984), Bhatia *et. al.,* (*1999*), and Das *et. al.,* (2006), there is a large variation in the ground motion in the present study. It may be noted that Bhatia *et. al.,* (*1999*) and Das *et. al.,* (2006) adopted a smaller scale (i.e. 0.5° x 0.5°, and 0.1° x 0.1° respectively), however in the present study a larger scale (0.05° x 0.05°) has been opted for Manipur state *i.e.,* scale adopted is 10 times finer and 2 times finer than the studies of Bhatia *et. al.,* (1999) and Das *et. al.,* (2006) respectively. It may also be mentioned that the attenuation relation adopted by Khatri *et. al.,* (1984) and Bhatia *et. al.,* (1999) corresponds to United States (Algermissen & Perkins, 1976; Joyner and Boore, 1981 respectively). However Das *et. al.,* (2006) used a single attenuation relation for two entirely different tectonics *i.e.,* shallow active and subduction zone (IBR) (see Section 2.9). It has been seen in

literature review that the Indian subcontinent is divided into three different group of seismicity *viz.*, active, stable and subduction zone. So using a single attenuation relation for entire country may not be realistic. As NE region is having two different seism-tectonic setups, developing single attenuation for both the setups will be erroneous.

Table 7.2 Comparison of PGA with other studies for Manipur 500 year return period

Ground motion Parameter	Khatri et. al., (1984)	Bhatia *et. al.*, (1999)	Das *et. al.*, (2006)	Present study (Manipur)
PGA	0.4g	0.4g	0.43g	0.18g-0.6g

7.5Conclusions

The present chapter investigates seismic hazard at Manipur, a state of NE India using probabilistic seismic hazard analysis. Based on the PSHA, probabilistic hazard map has been prepared by determining the seismic hazard at 0.05° x 0.05° (~ 5.5 km x 5.5 km) grid size along EW (94°45'E to 92°58'E) and NS (25°42'N to 23°50'N) directions at rock level. The NGA attenuation relations proposed by Boore and Atkinson (2008) for strike-slip, thrust & reverse fault and Atkinson and Boore (2003) for subduction zone, have been used for computing spectral acceleration hazard curves. In addition, UHRS have been derived for return periods of 100, 500 and 2500 years for all nine districts (*viz.*, Senapati, Tamenglong, Churachandpur, Chandel, Imphal East, Imphal West, Ukhrul, Thoubal, Bishnupur) of Manipur state. It has been observed that most parts of Manipur are vulnerable to seismic hazard for 500 and 2500 year return periods as compared to 100 year return period. Further, it has been found that at PGA, predicted S_a are found to be on the lower side as

compared to the value (0.36 g) recommended by IS: 1893. The highest level of hazard has been observed at Ukhrul, Senapati, Imphal east and Imphal west districts (located near to IBR) of Manipur state.

TH-994_06610404

Chapter 8

Conclusions and Suggestions for further research

8.1 Conclusions

In view of Manipur state's location in one of the most seismically active regions (i.e. Northeast region of India) of the world, and considering author's knowledge that no seismic hazard analysis of Manipur state (and its capital, Imphal city) has been reported, an attempt has been made in this present research to conduct a systematic study of seismic microzonation of Imphal city for estimating surface level ground motion using both deterministic and probabilistic approaches along with probabilistic seismic hazard assessment of Manipur state. Liquefaction hazard studies have also been reported in term of two indices *i.e.,* Liquefaction Potential Index and Liquefaction Severity Index. The results are expected to be useful for seismic hazard mitigation.

Based on the present research on *Seismic Microzonation of Imphal city and Probabilistic Seismic hazard assessment of Manipur State*, the following main conclusions are enumerated as follows.

1. Using a catalogue of past earthquakes and seismo-tectonic map, seven potential seismic zones/blocks *viz.*, Indo-Burmese ranges (IBR), Eastern Himalaya (EH), Mishmi thrust (MT), Shillong plateau (SP), Naga-Disang thrust (ND), Bengal basin (BB) and Assam valley (AV), that can affect the seismicity of Imphal city/Manipur state have been identified. Recurrence relationship of magnitude and frequency of occurrence has been established based on Gutenberg–Richter relation and seismic parameters, *a* and *b* have been computed considering the aforementioned seven seismic blocks. It has been seen that the seismic blocks EH, MT, IBR and SP control higher magnitude (> 7.5 M_w) earthquakes whilst BB, ND and AV control earthquakes of lower magnitudes. Deaggregation analysis showed that the entire faults of IBR, Fault no. 5 of EH, Fault no. 12 of MT and Fault no. 21 of SP (see Table 3.1) are the main contributing faults which control large earthquakes. As a remedy for the scarcity of strong motion data rock level acceleration time histories at Imphal city for 1988 Indo-Burmese (M_w 7.2) earthquakes, 1869 Cachar (M_w 7.5) earthquake in Kopilli fault, and a hypothetical M_w 8.1 event in Indo-Burmese subduction zone have been estimated deterministically using the methodology of finite-fault seismological model (Motazedian and Atkinson, 2005) with regional parameters *viz.,* stress drop, pulsing percentage, slip distribution, rupture velocity etc. as inputs.

2. Effect of local soils on seismic susceptibility of Imphal city with respect to synthetically generated ten samples for 1869 Cachar earthquake (M_w 7.5) in

Kopili faults and a hypothetical earthquake (M_w 8.1) in Indo-Burmese ranges, has been presented using nonlinear site response analysis (Idriss and Sun, 1992). The results are presented in the form of mean and standard deviation of surface level spectral acceleration at Peak Ground Acceleration (PGA) and natural periods of 0.3 sec and 1.0 sec. It has been observed that at important places around Kangla palace the amplification for PGA is around 2.0. Based on mean surface level spectral response analysis (for 5 % damping) it has been found that IS: 1893 overestimates S_a for scenario 1869 Cachar earthquake, whilst for M_w 8.1 in IBR for corresponding periods of 0.01 s – 0.1 s, IS: 1893 underestimates S_a at few locations in Imphal city. Further, effect of local soils has been modeled in terms of site coefficients (ratio of surface level response to the rock level response) using synthetically generated 700 earthquake time histories (based on various combinations of magnitude and distance of faults that can affect the Imphal city). Site coefficients developed in the present study have been computed at different periods of engineering purposes and these can be used for estimating surface level responses.

3. Probabilistic Seismic Hazard Analysis (PSHA) has been performed by incorporating site coefficients and ground motion induced by each of the twenty-seven major faults of potential seven seismic zones present around Imphal. The attenuation relations proposed by Boore and Atkinson (2008) for strike slip, thrust and reverses fault, and Atkinson and Boore (2003) for subduction zone have been used for computing PGA, for various uncertainties associated with location, magnitude, and local site conditions. Uniform Hazard Response Spectra (UHRS) (defined in terms of equal probability of exceedance for all frequencies of ground motion)

results are presented in the form of surface level PGA and response spectra for return periods of 500 and 2500 years as recommended by IBC (2006). It has been seen that predicted mean UHRS (for 500 return period) overestimates S_a recommended by IS: 1893 for longer period (> 1.0 s), whereas for periods greater than 0.2 s, IS: 1893 S_a values are underestimated for 2500 return period.

4. Liquefaction potential hazard studies using two indices 1) Liquefaction Potential Index (LPI) (Iwasaki *et. .al.*, 1982), and 2) Liquefaction Severity Index (LSI) (Sonmez and Gokceoglu, 2005) have been presented using Factor of Safety (FS) (= CRR (Cyclic Resistance Ratio) / CSR (Cyclic Stress Ratio) as input (Idriss and Boulanger, 2006). The results are presented in the form of liquefaction hazard contour map for Imphal city. It has been observed that for the two scenario earthquakes mentioned above Kangla Palace, RIMS and Sanamahi Temple area are under highest category (Very High) and Mantripukhri, Uripok and near Langol hill areas fall under the next level (High) of Liquefaction failure.

5. PSHA is extended for Manipur state by determining the seismic hazard at 0.05° x 0.05° (~ 5.5 km x 5.5 km) grid size along EW (94°45'E to 92°58'E) and NS (25°42'N to 23°50'N) directions at rock level. In addition, UHRS have been derived for return periods of 100, 500 and 2500 years for all nine districts (*viz.*, Senapati, Tamenglong, Churachandpur, Chandel, Imphal East, Imphal West, Ukhrul, Thoubal, Bishnupur) of Manipur state. It has been observed that most parts of Manipur are vulnerable for 500 and 2500 year return periods as compared to 100 year return period. Further, it has been found that at PGA, predicted S_a are found to be on the lower side as compared to the value (0.36 g) recommended by IS: 1893. The highest level

of hazard has been observed at Ukhrul, Senapati, Imphal east and Imphal west districts (located near to IBR) of Manipur state.

The present study is expected to help planners and engineers for site selection and identification of vulnerable areas, design of earthquake resistant structures (especially in construction of new structures and strengthening of the existing structures) and can further assist Manipur State administration in seismic hazard mitigation In addition, the systematic procedure followed in the present research for probabilistic seismic microzonation at surface level is anticipated for easy adaptation for any city.

8.2 Suggestions for further research

Although the work presented in this thesis give the impression of an extensive and comprehensive study on the *Seismic Microzonation of Imphal city and Probabilistic Seismic Hazard of Manipur state*. Many areas can be identified and suggested for future research which can improve the confidence level and reliability of the present results.

Several limitations in the present approach can be identified. In this thesis a 140 years (1866 - 2007) catalogue of past earthquakes has been considered to find out recurrence relation based on Gutenberg–Richter relation, to estimate *a* and *b* values. Although this earthquake catalogue satisfied the completeness criterion of Kijko and Selleveoll (1989a, 1989b), inclusion of more past earthquake data is likely to improve *a* and *b* values.

The present work adopts the attenuation relation model *viz.,* NGA attenuation for strike slip, reverse, transverse faults (Boore and Atkinson, 2008) and for subduction zone (Atkinson and Boore, 2003) to estimate the PGA for seismic hazard estimation. Even though these models are based on global strong motion

database, these models may be modified and this accuracy improved for NE region with the availability of more strong motion data are available.

It may be noted that strong motion data are very sparse for NE region and hence synthetic ground motion (earthquake time histories) simulated from stochastic seismological model have been used. If recorded strong motion data are available in future, it would help in validation and realistic simulation can be attempted

In the present work, shear wave velocities used in liquefaction and site coefficient studies have been empirically estimated using SPT-N values of 122 boreholes. If directly measured field shear wave velocities (e.g., using micro tremor, MASW technique etc.) at more refined grid points are used it will improve accuracy of liquefaction and site coefficients studies.

It is well reported that complex local geometries (e.g. basin, undulated topography, etc) can significantly affect the local site responses due to ground motion reflection. As Imphal city is located on alluvial valley surrounded by hills and with sparse hillocks, it is speculated that a three-dimensional model study is likely to give more realistic insights into the behaviour of soil response to obtain reliable surface accelerations.

It may be mentioned that in the present study for Manipur state, probabilistic seismic hazard analysis has been carried out at rock level due to unavailability of soil data at other districts apart from Imphal city. Hence, the study can be extended to estimate seismic microzonation at surface level for entire Manipur state by collecting soil data from all the districts. In estimating UHRS for Imphal city and Manipur state, only aleatory variability within a fixed bound of earthquake magnitude (e.g. 4 M_w – 8.1 M_w for IBR) has been considered in the probabilistic seismic hazard analysis. Uncertainties in maximum magnitude (8.1

M_w for IBR) have not been considered. Effect of adding of this uncertainty of maximum magnitude in the simulation would be interesting from hazard estimation point of view.

TH-994_06610404

References

1. Abrahamson, N. A., and Silva, W. J., (1997), Empirical response spectral attenuation relation for shallow crustal earthquake, *Seismological Research letters*, 68, 94-127.
2. Abrahamson, N. A., and Somerville, P.G., (1996), Effects of the hanging wall and foot wall on ground motions recorded during the Northridge earthquake, Burma., *Bulletin of Seismological. Society America*, 86, 93-99.
3. Acharyya, S. K., Mitra, N. D. and Nandy, D.R., (1986), Regional geology and tectonic setting of northeast India and adjoining region, *Geological Survey of India Memoirs*, 119, 61-72.
4. Adams, J., and Atkinson G., (2003), Development of seismic hazard maps for the 2003 National Building Code of Canada, *Canadian Journal of Civil Engineering*, 30, 255-271.
5. Agarwal, P., and Shrikhande, M., (2006), Earthquake resistant design of structures, PHI Learning Pvt. Ltd., New Delhi.
6. Algermissen, S. T., & Perkins, D. M., (1976), A probabilistic estimate of maximum acceleration in rock in the contiguous United States, *United State Geological Survey*, Open-file Report, 76-416.
7. Algermissen, S. T., Perkins, D. M., Thenhaus, P. C., Hanson, S. L., and Bender, B. L., (1982), Probabilistic estimates of maximum acceleration and velocity in rock in the contiguous United States, *United State Geological Survey*, Open file Report,82-1033.
8. Alvarez, L., Garcı, A. J., Vaccari, F., Panza, G. F., Gonza Lez, B., Reyes, C., Ferna´Ndez, B., Pico, R., Zapata, J. A., and Arango, E., (2004), Ground

motion zoning of Santiago de Cuba: An approach by SH waves modelling, *Pure and Applied Geophysics,* 161, 1041-1059.

9. Ambraseys, N. N, Simpson, K. A., and Bommer, J. J., (1996), Prediction of horizontal response spectra in Europe, *Earthquake Engineering and Structural Dynamics,* 25, 371-400.

10. Ambraseys, N., and Bilham, R., (2003), MSK Isoseismal intensities evaluated for the 1897 Great Assam Earthquake, *Bulletin of Seismological Society America,* 93, 655-673.

11. Anbazhagan P., and Sitharam, T. G., (2008), Seismic microzonation of Bangalore, India, *Journal Earth Science Systems,* 117, 833-852.

12. Anbazhagan P., Vinod, J. S. and Sitharam, T. G., (2009), Probabilistic seismic hazard Analysis for Bangalore, *Journal of Natural Hazards,* 48, 145-166.

13. Anderson, J., and Hough, S., (1984), A model for the shape of the Fourier amplitude spectrum of acceleration at high frequencies, *Bulletin of the Seismological Society of America,* 74, 1969-1993.

14. Ansal, A. M., (1994), Effects of geotechnical factors and behaviour of soil layers during earthquakes, state-of-the-art lecture, In *proceeding of 10th European Conference on Earthquake Engineering*, Vienna, Austria, 1, 467-476.

15. Ansal, A. M., (1999), Strong motions and site amplification, Theme Lecture, In *2nd international conference on earthquake geotechnical engineering*, Lisbon, Portugal, Balkema, Rotterdam, 3, 879-894.

16. Ansal, A. M., (2002), Seismic microzonation methodology, In *proceeding of 12th European Conference on Earthquake Engineering*, 830, London, UK.

17. Ansal, A. M., (2004), Recent advances in earthquake geotechnical engineering and microzonation, Kluwer Academic Publishers, New York.

18. Ansal, A., Springman, S., Studer, J., Demirba, E., Onalp, A., Erdik, M., Giardini, D., Sesetyan, K., Demircioglu, M., Akman, H., Fäh, D., Christen, A., Laue, J., Buchheister, J., Çetin, O., Siyahi, B., Fahjan, Y., Gulkan, P., Bakir, S., Lestuzzi, P., Elmas, M., Koksal, D., and Gokçe, O., (2003), Part 2 – Case studies, microzonation of pilot areas, Adapazarı, Gölcük, Ihsaniye

and Degimendere, *World Institute for Disaster Risk Management project on Microzonation for Earthquake Risk Mitigation*, Research Task Group Report.

19. Ansary, M. A., Yamazaki, F., and Katayama, T., (1995), Statistical analysis of peaks and directivity of earthquake ground motion, *Earthquake Engineering and Structural Dynamics*, 24, 1527-1539.

20. Armijo, R., Tapponnier, P., and Han, T., (1989), Late Cenozoic right-lateral strike-slip faulting in southern Tibet, *Journal of Geophysical Research*, 94, 2787-2838.

21. Athanasopoulus, G. A., Pelekis, P. C., and Leonidou, E. A., (1999), Effects of surface topography on seismic ground response in the Egion (Greece) 15 June 1995 Earthquake, *Soil Dynamics and Earthquake Engineering*, 18, 135-149.

22. Atkinson, G. M., (1997), Empirical ground motion relations for earthquakes in the Cascadia region, *Canadian Journal of Civil Engineering*, 24, 64-77.

23. Atkinson, G. M., and Boore, D. M., (1995), New ground motion relations for eastern north America, *Bulletin of the Seismological Society of America*, 85, 17-30.

24. Atkinson, G. M., and Boore, D. M., (1997), Some comparisons between recent ground motion relations, *Seismological Research Letters*, 68, 24-40.

25. Atkinson, G. M., and Boore, D. M., (2003), Empirical ground-motion relations for subduction-zone earthquakes and their application to Cascadia and other regions, *Bulletin of the Seismological Society of America,* 93, 1703-1729.

26. Banerji, R. D., (1923), Annual report, *Archaeological Society of India*, 80-81, New Delhi.

27. Bansal, B. K., and Vandana, C., (2007), Microzonation studies in India: DST initiatives, In *proceedings of Workshop on Microzonation*, Indian Institute of Science, Bangalore, 1-6.

TH-994_06610404

28. Bapat, A., Kulkarni, R. C., and Guha, S. K., (1983), Catalogue of earthquakes in India and neighbourhood from historical record up to 1979, *Indian Society of Earthquake Technology*, Roorkee, 211.

29. Baranowski, J., Armbruster, J., Seeber, L., and Molnar, P., (1984), Focal depths and fault plane solutions of earthquakes and active tectonics of the Himalaya, *Journal of Geophysical Research*, 89, 6918-6928.

30. Bard, P. Y., (1994), Effects of surface geology on ground motion: Recent results and remaining Issues, In *proceeding of 10th ECEE*, Vienna, Austria, 1, 305-323.

31. Bartlett, S. F., and Youd, T. L., (1995), Empirical prediction of liquefaction-induced lateral spread, *Journal of Geotechnical Engineering*, 121, 316-329.

32. Basu, S., and Nigam, N. C., (1978), On seismic zoning map of India, In *proceedings of VI symposium on earthquake engineering*, Roorkee, India, 83–90.

33. Bazzurro P. and Cornell, A. C., (2004), Ground-motion amplification in nonlinear soil sites with uncertain properties, *Bulletin of the Seismological Society of America*, 94, 2090–2109.

34. Bazzurro, P., and Cornell, A. C., (1999), Disaggregation of seismic hazard, *Bulletin of the Seismological Society of America*, 89, 501–520, 1999.

35. Bell, F. G., Cripps, J. C., Culshaw, M. G., and Ohara, M., (1987), Aspects of geology in planning. In: Planning and Engineering Geology, *Geological Society Engineering Geology, Special Publication*, 4, 1-38.

36. Bhatia, S. C., Kumar, R., and Gupta, H. K., (1999), A probabilistic seismic hazard map of India and adjoining regions (GSHAP), *Current Science*, 77, 447-450.

37. Bhattacharya, P. M., and Kayal, J. R., (2003), Mapping the b-value and its correlation with the fractal dimension in the northeast region of India, *Journal of Geological Society of India*, 62, 680-695.

38. Bilham, R. and England, P., (2001), Plateau pop-up in the great 1897 Assam earthquake, *Nature*, 410, 806-809.

TH-994_06610404

39. Boominathan, A., Dodagoudar, G. R., Suganthi A., and Uma Maheswar R., (2007), Seismic hazard assessment considering local site effects for microzonation studies of Chennai City, In *T.G. Sitharam and B.K. Bansal, Editors, A Workshop on Microzonation, Indian Institute of Science*, Interline Publishing, Bangalore , 94-104.

40. Boore D. M., and Joyner, W. B., (1997), Site amplification for generic soil sites, *Bulletin of the Seismological Society of America*, 87, 327-341.

41. Boore, D. M., (1983), Stochastic simulation of high-frequency ground motions based on seismological models of the radiated spectra, *Bulletin of the Seismological Society of America*, 73, 1865-1894.

42. Boore, D. M., and Atkinson, G. M., (1987), Stochastic prediction of ground motion in eastern North America, *Bulletin of the Seismological Society of America*, 4, 460-477.

43. Boore, D. M., and Atkinson, G. M., (2008), Ground-motion prediction equations for the average horizontal component of PGA, PGV, and 5%-damped PSA at spectral periods between 0.01 s and 10.0 s, *Earthquake Spectra*, 24, 99-138.

44. Boore, D. M., Joyner, W. B., and Fumal, T. E., (1997), Equations for estimating horizontal response spectra and peak acceleration from western north American earthquakes: A summary of recent work, *Seismological Research Letters*, 68, 128-153.

45. Boore, D. M., Stephens, C. D., and Joyner, W. B., (2002), Comments on baseline correction of digital strong-motion data: Examples from the 1999 Hector Mine, California, earthquake, *Bulletin of the Seismological Society of America*, 92, 1543-1560.

46. Borcherdt, R. D., (1970), Effects of local geology on ground motion near San Francisco Bay, *Bulletin of the Seismological Society of America*, 60, 29-61.

47. Brune, J. N., (1970), Tectonic stress and the spectra of seismic shear waves from earthquakes, *Journal of Geophysical Research*, 75, 4997-5009.

48. Brune, J. N., and King, C. Y., (1967), Excitation of mantle Rayleigh waves of period 100s as a function of magnitude, *Bulletin seismological Society of America*, 57, 1355-1365.

49. Brune, J. N., and Singh, D. D., (1986), Continent-like crustal thickness beneath the Bay of Bengal sediments, *Bulletin Seismological Society of America*, 76, 191-203.

50. Brunnschweiler, R. O., (1974), Indo-Burmese Ranges, *Geological Society London, Special Publication*, 4, 279-299.

51. Bullen, K. E., and Bolt, B. A., (1985), An introduction to the theory of seismology (4th edition), Cambridge University Press, U.K.

52. Campbell, K. W., (1981), Near-source attenuation of peak horizontal acceleration, *Bulletin of the Seismological Society of America*, 71, 2039-2070.

53. Campbell, K. W., (1989), The dependence of peak horizontal acceleration on magnitude, distance, and site effects for small-magnitude earthquakes in California and eastern North America, *Bulletin of the Seismological Society of America*, 79, 1311-1346.

54. Campbell, K. W., (1991), An empirical analysis of peak horizontal acceleration for the Loma Prieta, California, earthquake of 18 October, 1989, *Bulletin Seismological Society of America*, 81, 1838-1858.

55. Campbell, K. W., (1997), Empirical near-source attenuation relationships for horizontal and vertical components of peak ground acceleration, peak ground velocity and pseudo-absolute acceleration response spectra, *Seismological Research Letters*, 68, 154-179.

56. Campbell, K. W., (1998), Empirical analysis of peak horizontal acceleration, peak horizontal velocity, and Modified Mercalli Intensity, in The Loma Prieta, California, Earthquake of October 17, 1989, *Earth Structures and Engineering Characterization of Ground Motion, T. L. Holzer, Ed., U.S. Geological Survey*, Professional paper, 1552-D,47-68.

57. Campbell, K. W., (2003), Prediction of strong ground motion using the hybrid empirical method and its use in the development of ground-motion

(attenuation) relations in Eastern North America, *Bulletin of Seismological Society of America*, 93, 1012-1033.

58. Campbell, K. W., and Bozorgnia, Y., (1994), Near-source attenuation of peak horizontal acceleration from worldwide accelerograms recorded from 1957 to 1993, In *proceedings of the 5th U.S. National Conference on Earthquake Engineering*, 3, 283-292

59. Campbell, K. W., and Bozorgnia, Y., (2003), Updated near-source ground-motion (Attenuation) relations for the horizontal and vertical components of peak ground acceleration and acceleration response spectra, *Bulletin of the Seismological Society of America*, 93, 314-331.

60. Cascante, G., and Santamarina, J. C., (1996), Interparticle contact behavior and wave propagation, *Journal of Geotechnical and Geoenvironmental Engineering*, 122, 831-839.

61. Cetin, K. O., Der Kiureghian, A., and Seed, R. B., (2002), Probabilistic models for the initiation of seismic soil liquefaction, *Structural Safety*, 24, 67-82.

62. Cetin, K., O., Seed, B. R., Der Kiureghian, A., Tokumatsu K., Leslie, F. H. J., Robert, E. K., and Moss, R. E. S., (2004), Standard Penetration Test-Based probabilistic and deterministic assessment of seismic soil liquefaction potential, *Journal of Geotechnical and Geoenvironmental Engineering*, 130, 1314-1340.

63. Chandler, A. K., Lam, N. T. K., Tsang, H. H., (2006), Near-surface attenuation modeling based on rock shear-wave velocity profile, *Soil Dynamics and Earthquake Engineering*, 26, 1004-1014.

64. Chandra, U., (1978), Seismicity, earthquake mechanisms along the Himalayan mountain range and vicinity, *Physical Earth Planet International*, 16, 109-131.

65. Chandrasekaran, A. R., and Das, J. D., (1990), Strong motion arrays in India and characteristics of recent recorder events, *Bulletin of Indian Society of Earthquake Technology*, 27, 1-66.

66. Chandrasekaran, A. R., and Das, J. D., (1992), Strong motion arrays in India and analysis of data from Shillong array, *Current Science*, 62, 233-250.

67. Chandrasekaran, A. R., and Das, J. D., (1994), Analysis of strong motion accelerograms of N.E. India earthquake of January 10, 1990, *Report EQ.94-01, Department of Earthquake Engineering*, IIT Roorkee, India.

68. Chang Ta, (1963), The geology of China, U.S. Department of Commerce, Joint Publication Research Service, Washington DC., 548.

69. Chapman, M. C., (1995), A probabilistic approach to ground motion selection for engineering design, *Bulletin of the Seismological Society of America*, 85, 937-942.

70. Chaudhury, P. D., (1964), Archaeology in Assam, *Department of Archaeology*, Gauhati, India.

71. Chavez-Garcia, F. J., Sanchez, L. R., and Hatzfeld, D., (1996), Topographic site effects and HVSR. A comparison between observations and theory. *Bulletin of the Seismological Society of America*, 86, 1559-1573.

72. Chen, C. J., and Juang C. H., (2000), Calibration of SPT- and CPT-based liquefaction evaluation methods. In Mayne P. W., Hryciw R. (eds) Innovations and applications in geotechnical site characterization, *Geotechnical Special Publication, ASCE*, 97, 49-64.

73. Chen, W. P., and Molnar, P., (1990), Source parameters of earthquakes and intraplate deformation beneath the Shillong plateau and the northern Indo-Burmese ranges, *Journal of Geophysical Research*, 95, 527-552.

74. Chin-Hsiung, L., Jeng-Yaw, H., and Tzay-Chyn, S., (1998), Observed variation of earthquake motion across a Basin-Taipei City, *Earthquake Spectra*, 14, 115-134

75. City Development Plan, http//:manipur.nic.in.

76. Cooley, J. W., and Tukey, J. W., (1965), An algorithm for the machine calculation of complex fourier series, *Mathematics of Computation*, 19, 297-301.

TH-994_06610404

77. Coppersmith, K. J., (1991), Seismic source characterization for engineering seismic hazard analyses, In *Proceeding 4th international conference on seismic zonation*, Stanford University, 4, 3-60.

78. Cornell, C. A., (1968), Engineering seismic risk analysis, *Bulletin of the Seismological Society of America*, 58, 1583-1606.

79. Cornell, C. A., and Menz, H. A., (1975), Seismic risk analysis of Boston, *Journal of the Structural Division, ASCE*, 101, 2027-2043.

80. Cornell, C. A., and Van Marcke, E. H., (1969), The major influences on seismic risk: in Proceedings of the Third World Conference on Earthquake Engineering, Santiago, Chile, 1, 69-93.

81. Crouse, C. B., (1991a), Ground-motion attenuation equations for earthquakes on the Cascadia subduction zone, *Earthquake Spectra*, 7, 201-235.

82. Crouse, C. B., (1991b), Erratum: Ground-Motion Attenuation Equations for Earthquakes on the Cascadia Subduction Zone, Earthquake Spectra, 7, 506.

83. Crouse, C. B., Vyas, Y. K., and Schell B. A., (1988), Ground motion from subduction zone earthquakes, *Bulletin of the Seismological Society of America*, 78, 1-25.

84. Cummins, P., (2007), The potential for giant tsunamigenic earthquakes in the northern Bay of Bengal, *Nature*, 449, 75-78.

85. Curray, J. R., and Moore, D. G., (1974), Sedimentary and tectonic process in the Bengal deep-sea fan and geosyncline. In *The Geology of Continental Margins*, C. A. Burke and C. L. Drake (eds.), *Springer-Verlag*, New York, 617-628.

86. Curray, J. R., (1989), The Sunda Arc: A model for oblique plate convergence, *Journal of Sea Research*, 24, 131-140.

87. Curray, J. R., and Moore, D. G., (1971), Growth of the Bengal deep sea fan and denudation in the Himalayas, *Bulletin of the Seismological Society of America*, 82, 563-572.

88. Curray, J. R., Emmel, F. J., Moore, D. G., and Raitt, R. W., (1982), Structure tectonics and geological history of the northeastern Indian ocean, In *Nairn AEMc, Stehli F. G. (eds)*, Plenum, New York, 399-450.

89. Curray, J. R., Moore, D. G., Lawver, L. A., Emmel, F. J., Raitt, R. W., Henry, M. and Kieckhefer, R., (1979), Tectonics of the Andaman Sea and Burma, in Watkins, J. S., Montadert, L. and Dickenson, P. W., (eds.), Geological and geophysical investigations of continental margins, *American Association of Petroleum Geologists Memoir*, 29, 189-198.

90. CVDT (2008), http//:db.cosmos-eq.org.

91. Dahle, A., Bungum, H., and Kvamme, L. B., (1990), Attenuation models inferred from intraplate earthquake recordings, *Earthquake Engineering and Structural Dynamics*, 19, 1125-1141.

92. Dai, F. C., Liu, Y., and Wang, S., (1994), Urban geology: a case study of Tongchuan City, Shaanxi Province, China, *Engineering Geology*, 38, 165-175.

93. Das, B. M., (2006), Principals of Geotechnical Engineering, Cengage Learning.

94. Das, S., Gupta I. D., and Gupta V. K., (2006), A probabilistic seismic hazard analysis of northeast India, *Earthquake Spectra*, 22, 1-27.

95. Dasgupta, A. B., (1977), Geology of Assam–Arakan region, *Geologial, Mining and Metallurgical Society of India*, 49, 1-53.

96. DES, Directorate of Economics and Statistics (2008-09), Economic survey Manipur, Govt of Manipur.

97. Desikachar, S. V., (1974), A review of the tectonic and geological history of eastern India in terms of plate tectonics theory, *Journal of Geological Society of India*, 15, 137-149.

98. Ding, Z., Chen, Y. T., and Panza, G. F., (2004), Estimation of site effects In Beijing city, *Pure and Applied Geophysics*, 161, 1107-1123.

99. Dobry, R., Borcherdt, R. D., Crouse, C. B., Idriss, I. M., Joyner, W. B., Martin Power, G. R. M. S., Rinne, E. E., and Seed, R. B., (2000), New site

coefficients and site classification system used in recent building seismic code provisions, *Earthquake Spectra*, 16, 41-67.

100. DST (2008), Report on seismic microzonation of Guwahati region, http://www.amtron.inmicrozonation/.

101. DST, (2010) http://www.dst.gov.in/scientific-programme/ser-seismicity.htm, (accessed on July 2010)

102. Dutta, T. K., (1964), Seismicity of Assam—zones of tectonic activity, *Bulletin of National Geophysical Research Institute,* 2, 152.

103. Earthquake engineering handbook, (2003), edited, Wai-Fah, C., and Scawthorn, C., CRC Press.

104. Earthquake Engineering Research Institute (1989), The basics of seismic risk analysis, *Earthquake Spectra*, 5, 675-702.

105. El-Sayed, A., Korrat, I., and Hussein, H. M., (2004), Seismicity and seismic hazard in Alexandria (Egypt) and its surroundings, *Pure and Applied Geophysics*, 161, 1003-1019.

106. Evans, P., (1964), The tectonic framework of Assam, *Journal of Geological Society of India*, 5, 80-96.

107. Faccioli, E., (1991), Seismic amplification in the presence of geologic and topographic irregularities, *In proceeding of 2nd International Conference on Recent Advances in Geotechnical Earthquake Engineering and Soil Dynamics*, St. Louis.

108. Fah, D., Iodice, C., Suhadolc, P., and Panza, G. F., (1993), A new method for the realistic estimation of seismic groundmotion in megacities, The case of Rome, *Earthquake Spectra*, 9, 643-668.

109. Fah, D., Rüttener, E., Noack, T. and Kruspan, P., (1997), Microzonation of the City of Basel, *Journal of Seismology*, 1, 87-102.

110. Fah, D., Suhadolc, P., St. Müller and Panza, G. F., (1994), A hybrid method for the estimation of ground motion in sedimentary basin: Quantitative modeling for Mexico City, *Bulletin of the Seismological Society of America*, 84, 383-399.

TH-994_06610404

111. Field, E. H., and Jacob, K., (1995), A comparison and test of various site response estimation techniques, including three that are non reference-site dependent, *Bulletin of the Seismological Society of America*, 85, 1127-1143.

112. Fitech, T. J., (1970), Earthquake mechanisms in the Himalaya, Burmese and Andaman regions and continental tectonics in Cental Asia, *Journal. Geophysics Research*, 75, 2699-2709.

113. Flash earth, www.flashearth.com.

114. Frankel, A. D., Mueller, C. S., Barnhard, T. P., Leyendecker, E. V., Wesson, R. L., Harmsen, S. C., Klein, F. W., Perkins, D. M., Dickman, N. C., Hanson, S. L., and Hopper, M. G., (2000), *United State Geological Survey*, National seismic hazard maps, *Earthquake Spectra*, 16, 1-15.

115. Gansser, A., (1964), The Geology of the Himalayas, *Wiley Interscience*, London, 289.

116. Gansser, A., (1966), The Indian Ocean and the Himalayas: A geological interpretation, *Eclogae Geologicae Helvetiae*, 59, 831-848.

117. Gardner, J.K. and Knopoff, L. (1974), Is the sequence of earthquakes in Southern California, with aftershocks removed, Poissonian, *Bulletin of the Seismological Society of America*, 64, 1363–1367.

118. Gee, E. R., (1934), Dhubri earthquake of 3rd July 1930, *Geological Survey of India Memoirs*, 65, 106.

119. Golesorkhi, R., (1989), Factors influencing the computational determination of earthquake-induced shear stresses in sandy soils, *Ph.D. thesis, University of California, Berkeley*, 395.

120. Google earth, http://www.google.com.

121. Goswami, H. C., and Sarmah, S. K., (1982), Probabilistic earthquake expectancy in the northeast Indian region, *Bulletin of the Seismological Society of America*, 72, 999-1009.

122. GovindaRaju, L., Ramana, G. V., HanumanthaRao, C., and Sitharam, T. G., (2004), Site-specific ground response analysis, Current Sciences, 87, 1354-1362.

TH-994_06610404

123. GSHAP (1999), The Global Seismic Hazard Assessment Program (GSHAP) 1992-1999, *Annali Di Geofisica*, 42, 957-1229 (Summary volume edited by D. Giardini.

124. GSI (2000), Seismo-tectonic Atlas of India and its Environs, *Geological Survey of India*.

125. Guo, T., and Prakash, S., (1999), Liquefaction of silts and silt–clay mixtures, *Journal of Geotechnical and Geoenvironmental Engineering*, 125, 706-710.

126. Gutenberg, B., and Richter, C. F., (1944), Frequency of earthquakes in California, *Bulletin of the Seismological Society of America*, 34, 185-188.

127. Gutenberg, G., Richter, C. F., (1954), Seismicity of the Earth and its Associated Phenomena, *Princeton University Press*, Princeton, NJ, 310.

128. Gyi, L. T., (1973), Seismic zoning map of the union of Burma, *Bulletin International Institute of Seismology and Earthquake Engineering*, 9, 218 .

129. Hake, S. S., (1987), A review of engineering geological and geotechnical aspects of town and country planning with particular reference to minerals and the extractive processes. In *Culshaw, M. G., Bell, F. G., Cripps, J. C., O'Hara, M. (Eds.) Planning and Engineering Geology, Engineering Geology, Special Publication*, 4, 69-74.

130. Halchuck, S., Adams, J., and Anglin, F., (2007), Revised Deaggregation of Seismic Hazard for Selected Canadian Cities, In *proceedings of 9th Canadian Conference on Earthquake Engineering Ottawa,* Ontario, Canada, 1188.

131. Halchuck, S., and Adams, J., (2004), Deaggregation of seismic hazard for selected Canadian cities, In *proceedings of XIII World Conference on Earthquake Engineering, Vancouver*, Canada.

132. Hanks, T. C., and McGuire, R. K., (1981), The character of high frequency strong ground motion, *Bulletin of the Seismological Society of America*, 71, 2071-2095.

TH-994_06610404

133. Haokip, N., (2007), Basine Delineation Map of Manipur' Profile on State of Environment Report of Manipur, *Ministry of Environment and Forests*, Manipur, 4.

134. Harbi, A., Maouche, S., Ayadi, A., Benouar, D., Panza, G. F., And Benhallou, H. (2004), Seismicity and tectonic structures in the site of Algiers and its surroundings: A step towards microzonation, *Pure and Applied Geophysics*, 161, 949-967.

135. Harder, L. F. Jr., (1997), Application of the Becker Penetration Test for Evaluating the Liquefaction Potential of Gravelly Soils, In *procedings of NCEER Workshop on Evaluation of Liquefaction Resistance of Soils,* 22.

136. Harmsen, S., and Frankel, A., (2001), Geographic Deaggregation of Seismic Hazard in the United States, *Bulletin of the Seismological Society of America*, 91, 13-26.

137. Hartzell, S., Carver, D., and Williams, R. A., (2001), Site response, shallow shear-wave velocity and damage in Los Gatos, California, from the 1989 Loma Prieta Earthquake, *Bulletin of the Seismological Society of America*, 91, 468-478.

138. Herak, M., Lokmer, I., Vaccari, F., and Panza, G. F., (2004), Linear amplification of horizontal strong ground motion in Zagreb (Croatia) for a realistic range of scaled point sources, *Pure and Applied Geophysics*, 161, 1021-1040.

139. Hiller, K., and Elahi, M., (1984.), Structural development and hydrocarbon entrapment in the Surma Basin, Bangladesh. In *proceeding of 5th Offshore Southeast Asia Conference.*, Singapore, 364-387.

140. Holzer, T. L., Youd, T. L., and Hanks, T. C., (1989), Dynamics of liquefaction during the 1987 superstition hills California earthquake, *Science,* 244, 56-59.

141. Housner, G. W., (1947), Characteristics of strong motion earthquakes, *Bulletin of the Seismological Society of America*, 37, 19-31.

142. Housner, G. W., (1955), Properties of strong ground motion earthquakes, *Bulletin of the Seismological Society of America*, 45, 197-218.

143. Housner, G. W., (1989), Competing against time, Report to Governor Deukmejian of California, Governor's Board of Inquiry on the (1989) Loma Prieta Earthquake, George W. Housner, Chairman.

144. IBC (2006), International Building code, International code council.

145. Ibotombi, S., (1998), On the geology of Manipur, In *Proceedings of 9th Manipur science congress*, Imphal, 12-19.

146. Ibotombi, S., (2000), Structural and tectonic framework of Manipur, In *Manipur Science Congress*, Imphal.

147. Idriss I. M., (1985), Evaluating seismic risk in engineering practice, In *proceedings of the 11th InternationalConference on soil mechanics and foundation engineering*, San Francico, 1, 255-320.

148. Idriss I. M., (1999), An update to the Seed-Idriss simplified procedure for evaluating liquefaction potential, In *proceedings of TRB Workshop on New Approaches to Liquefaction*, Federal Highway Administration, 99-165.

149. Idriss, I. M., and Boulanger, R. W., (2004), Semi-empirical procedures for evaluating liquefaction potential during earthquakes, In *proceedings of 11th International Conference on Soil Dynamics and Earthquake Engineering, and 3rd International Conference on Earthquake Geotechnical Engineering*, D. Doolin *et. al.*, (eds.), Stallion Press, 32-56.

150. Idriss, I. M., and Boulanger, R. W., (2006), Semi-empirical procedures for evaluating liquefaction potential during earthquakes, *Soil Dynamics and Earthquake Engineering*, 26,115-130.

151. Idriss, I. M., and Sun, J. I., (1992), A Computer program for conducting equivalent linear seismic response analysis of horizontally layered soil deposits. *Users manual for SHAKE91.*

152. Idriss., I. M., and Seed, H. B., (1968), Seismic response of horizontal Soil layer, *Journal of the Soil Mechanics and Foundation Division*, ASCE, 94, 1003-1031.

153. Imai, T., and Tonouchi, K., (1982), Correlation of N-value with S-wave velocity and shear modulus, In *proceedings of 2nd European Symposium on Penetration Testing*, Amsterdam, 57-72.

154. Iman, R. L., and Conover, W. J., (1980), Small sample sensitivity analysis techniques for computer models, with an application to risk assessment. *Communications in Statistics*, 17, 1749-1842.

155. IS: 1893 (Part 1)-2002, Bureau of Indian Standard (BIS) (2002) revised its code of practice, Criteria for Earthquake Resistant Design of Structures.

156. Ishihara, K (1993), Rankine Lecture: 'Liquefaction and flow failure during earthquakes', Geotechnique, 43, 351-415.

157. Iwasaki, T., Tokida, K., Tatsuoka, F., Watanabe, S., Yasuda, S., and Sato, H., (1982), Microzonation for soil liquefaction potential using simplified method, In *proceedings of the 13th international conference on microzonation*, Seattle, USA, 3, 1319-1330.

158. Iyengar, R. N., Sharma D., and Siddiqui J. M., (1999), Earthquake history of India in medieval times, *Indian Journal of History of Sceience*, 34, 181-237.

159. Iyengar, R. N., (1999), Earthquakes in ancient India, *Current Science*, 77, 827-829.

160. Iyengar, R. N., and Ghosh, S., (2004), Microzonation of earthquake hazard in greater Delhi area, *Current Science*, 87, 1193-1202.

161. Iyengar, R. N., and Iyengar, K. T. S., (1969), A non-stationary random process model for earthquake accelerogram, *Bulletin of the Seismological Society of America*, 59, 1163-1188.

162. Iyengar, R. N., and Raghukanth, S. T. G., (2004), Attenuation of strong ground motion in Peninsular India, *Seismological Research Letters*, 75, 530-540.

163. Jain, S. K., Roshan, A. D., Arlekar, J. N., and Basu, P. C., (2000), Empirical attenuation relationships for the Himalayan earthquakes based on Indian strong motion data, In *proceedings of the 6th international conference of seismic zonation*, Palm Spring, CA, USA.

164. Jaiswal, K. and Ravi Sinha (2007). Probabilistic seismic-hazard estimation for peninsular India *Bulletin of the Seismological Society of America,*. 91(1B), 318-330.

165. Johnson, B. D., Powell, C. M. A., and Veevers, J. J., (1976), Spreading history of the eastern Indian Ocean and greater India's northward flight from Antarctica and Australia, *Geological Society of America Bulletin*, 87, 1560-1566.

166. Joyner, W. B., and Boore, D. M., (1981), Peak horizontal acceleration and velocity from strong motion records including records from the 1979 Imperial Valley, California, earthquake, *Bulletin of the Seismological Society of America*, 71, 2011-2038.

167. Juang, C. H., Yuan, H., Lee, D. H., and Lin, P. S., (2003), A simplified CPT-based method for evaluating liquefaction potential of soils, *Journal of Geotechnical and Geoenvironmental Engineering*, 129, 66-80.

168. Kailasam, L. N., (1979), Plateau uplift in Peninsular India, *Tectonophysics*, 61, 243-269.

169. Kamalian, M., Abdollah, S. B., Mkhah, A. R., Taghavi, A., and Rahmani, I., (2008), Considerations on seismic microzonation in areas with two-dimensional hills, *Journal Earth System and Sciences*, 117, 783-796.

170. Kanai, K., (1951), Relation between the nature of surface layer and the amplitude of earthquake motions, *Bulletin Tokyo Earthquake Research Institute*.

171. Kanai, K., (1957), Semi-empirical formula for seismic characteristics of the ground, *Bulletin of the Earthquake Research Institute*, 35, 308-325.

172. Kandpal, G. C., John, B., and Joshi, K. C., (2009), Geotechnical studies in relation to seismic microzonation of Union Territory of Chandigarh, *Journal of Indian Geophysical Union*, 13, 75-83.

173. Kawase, H., (1988), Time domain response of a semicircular crayon for Incident SV, P and Rayleigh waves calculated by discrete wave number

boundary element method, *Bulletin of the Seismological Society of America*, 78, 1415-1437.

174. Kayal, J. R., (1987), Microseismicity and source mechanism study: Shillong plateau, northeast India, *Bulletin of the Seismological Society of America,* 77, 184-194.

175. Kayal, J. R., (1989), Subduction structure at the India/Burma plate boundary: Seismic and gravity evidences. In *28th International Geology Congress*, USA, 2, 164-165.

176. Kayal, J. R., (1996), Earthquake source processes in northeast India-a review, *Himalayan Geology*, 17, 53-69.

177. Kayal, J. R., (1998), Seismicity of northeast India and surroundings Development over the past 100 years, *Journal of Geophysics*,19, 9-34.

178. Kayal, J. R., (2008), Microearthquake seismology and seismotectonics of South Asia, Capital Publishing Company, New Delhi.

179. Kayal, J. R., and De, R., (1991). Microseismicity and tectonics in northeast India, *Bulletin of the Seismological Society of America*, 81, 131-138.

180. Kayal, J. R., Arefiev, S. S., Barua, S.,Hazarika, D., Gogoi, N., Kumar, A., Chowdhury, S. N. and Kalita, S., (2006), Shillong plateau earthquakes in northeast India region: complex tectonic model, *Current Science*, 91, 109-114.

181. Khan, M. A. M., Ismail, M., and Ahmad, M., (1988), Geology and hydrocarbon prospects of the Surma Basin, Bangladesh. In *Proceedings of Offshore South East Asia (SEAPEX)*, 364-384.

182. Khattri, K. N., Rogers, A. M., Perkins, D. M., and Algermissen, S. T., (1984), A seismic hazard map of India and adjacent areas, *Tectonophysics*, 108, 93-134.

183. Khattri, K., and Wyss, M., (1978), Precursory variation of seismicity rate in Assam area, *India Geology*, 6, 685-688.

184. Kijko, A., and Sellevoll, M. A., (1989a), Estimation of seismic hazard parameters from Incomplete data files. Part I: Utilization of Extreme and

complete catalogues with different threshold magnitudes, *Bulletin of the Seismological Society of America*, 79, 645-654.

185. Kijko, A., and Sellevoll, M.A., (1989b), Estimation of seismic hazard parameters from Incomplete data files. Part II: Incorporation of magnitude heterogeneity, *Bulletin of the Seismological Society of America*. 79, 645-654.

186. Kilic, H., Ozener, P. T., Yildirm., Adatepe, S., and Demir, H., (2005), Seismic microzonation of Kucuhcehmece-Halkali region in Istanbul, *Underground space Use; Analysis of the Past and Lessons for the future*, Erdem & Solak (eds), 641-647.

187. Kiureghian, D, A., and Ang, A. H. S., (1977), A fault-rupture model for seismic risk analysis, *Bulletin of the Seismological Society of America*, 67, 1173-1194.

188. Koester, J. P., (1994), The influence of fines type and content on cyclic strength, *Ground failures under seismic conditions, Geotechnical special publication* 44, ASCE, Prakash, S. and Dakoulas, P. (eds), 17-33.

189. Kokusho, T., Motoyamaa, R. and Motoyamaa H.,(2007), Wave energy in surface layers for energy-based damage evaluation, *Soil Dynamics and Earthquake Engineering*, 27, 354-366.

190. Kramer, S. L., (2008), Geotechnical Earthquake Engineering, Pearson Education Ptd. Ltd, Reprinted 2003, Delhi, India.

191. Kvale, A., *(1955),* Seismic seiches in Norway and England during the Assam earthquake of August 15, 1950, *Bulletin of the Seismological Society of America,* 45, 93–113.

192. Lachet, C., Hatzfeld, D., Bard, P. Y., Theodulidis, N., Papaioannou, C., and Savvaidis, A., (1996), Site effects and microzonation in the city of Thessaloniki-comparison of different approaches, *Bulletin of the Seismological Society of America*, 86, 1692-1703.

193. Laiba, M. T., (1992), The geography of Manipur. Public Book Store, Imphal.

194. Le Dain, A. Y., Tapponnier, P., and Molnar, P., (1984), Active faulting and tectonics of Burma and surrounding regions, *Journal of Geophysical Research*, 89, 453-472.

195. Lee, D. H., Ku, C. S., and Yuan, H., (2003), A study of the liquefaction risk potential at Yuanlin, *Taiwan Engineering Geology*, 71, 97-117.

196. Lee, V. W., and Trifunac, M. D., (1987), Rocking strong earthquake accelerations. Soil Dynamics and Earthquake Engineering 6 , 75–89.

197. Legget, R. F., (1987), The value of geology in planning. *In Culshaw, M.G., Bell, F.G., Cripps, J.C., O'Hara, M. (Eds.) Planning and Engineering Geology, Geological Society Engineering Geology Special Publication*, 4, 53-58.

198. Lermo, J., and Chavez-Garcia, F. J., (1994), Are microtremors useful in site response evaluation, *Bulletin of the Seismological Society of America*, 84, 1350-1364.

199. Liao, S. S. C., Veneziano, D., and Whitman, R. V., (1988), Regression models for evaluating liquefaction probability, *Journal of Geotechnical Engineering*, 114, 389-409.

200. Luke, B., and Liu, Y., (2008), Site response zones and short-period earthquake ground motion projections for the Las Vegas Basin, *Journal of Earth System Science*, 117, 757-772.

201. Madabhushi, S. P. G., and Haigh, S. K., (2005), The Bhuj, India earthquake of 26th January 2001, *A Field Report By Earthquake Engineering Field Investigation Team*, London.

202. Mahajan, A. K., Siefko, S., Ranjan, R., Sporry, R., Ray, P. K. C., and Westen, C. J. V., (2007), Seismic microzonation of Dehradun City using geophysical and geotechnical characteristics in the upper 30 m of soil column, *Journal of Seismology*, 11, 355-370.

203. Mai, P. M., and Beroza, G. C., (2002), A spatial random field model to characterize complexity in earthquake slip, *Journal of Geophysical Research* 107, 1-21.

204. Mai, P. M., and Spudich, P., and Boatwright, J., (2005), Hypocenter locations in finite-source rupture models, *Bulletin of the Seismological Society of America*, 95, 965-980.

205. Maisnam, D., (2002), Political economy of underdevelopment: An enquiry about the Socio-Political conditions in the state of Manipur, *M.Phil dissertation*, JNU, New Delhi:

206. Manichandra, S., (2007), Personal communication, Manipur University.

207. Marcellini, A., Bard, P. Y., Iannaccone, G., Meneroud, J. P., Mouroux, P., Romeo, R., Silvestri, F., Duval, A., Martin, C., and Tento, A., (1995b), The Benevento seismic risk project: The microzonation, In *proceedings of the 5th international conference on seismic zonation*, Nice, France, 810-814.

208. Marcellini, A., Iannaccone, G., Romeo, R., Silvestri, F., Bard, P. Y., Improta, L., Meneroud, J. P., Mouroux, P., Mancuso, C., Rippa, F., Simonelli, A., Soddu, P., Tento, A., and Vinale, F., (1995a), Benevento seismic risk project: seismotectonic and geothecnical background, In *proceedings of the 5th international conference on seismic zonation,* Nice, France, 802-809.

209. Matsuoka, M., and Midorikawa, S., (1995), GIS-based integrated seismic hazard mapping for a large metropolitan area, In *proceedings of 5th international conference on seismic zonation*, 2, 1334-1341.

210. McGuire, R. K., (1995), Probabilistic seismic hazard and design earthquakes: closing the loop, *Bulletin of the Seismological Society of America,* 85, 1275-1284.

211. McGuire, R. K., (2004), Seismic Hazard and Risk Analysis, *Earthquake Engineering Research Institute*, Berkeley.

212. McGuire, R. K., and Shedlock, K. M., (1981), Statistical uncertainties in seismic hazard evaluations in the United States, *Bulletin of the Seismological Society of America*, 71, 1287-1308.

213. Merz, H. A., and Cornell, C. A., (1973), Seismic risk analysis based on a quadratic magnitude-frequency law, *Bulletin of the Seismological Society of America,* 63, 1999-2006.

214. Messele, H., (2004), Seismic microzonation for the city of Addis Ababa By using microtremors, In *proceeding of 13th World Conference On Earthquake Engineering Vancouver*, B. C., Canada, 2092.

215. Mitchell, A. H. G., (1981), Phanerozoic plate boundaries in mainland SE Asia, the Himalayas and Tibet, *Journal of Geological Society London*, 138, 109–122.

216. Mitchell, A. H. G., and McKerrow, W. S., (1975), Analogous evolution of the Burma orogen and the Scottish caledonides, *Geological Society of America Bulletin*, 86, 305-315.

217. Mithal, R. S., and Srivastava, L. S., (1959), Geotectonic position and earthquakes of Ganga-Brahmaputra region, In *H. L. Sally (Eds), Earthquake engineering seminar*, University of Roorkee, India.

218. Mitra. S., Priestley, K., Bhattacharyya, A. K. and Gaur, V. K., (2005), Crustal structure and earthquake focal depths beneath Northeastern India and Southern Tibet, *Geophysical Journal International*, 160, 227-248.

219. Mohanty, W. K., and Walling, M. Y., (2008), First order seismic microzonation of Haldia, Bengal Basin (India) using a GIS Platform, *Pure and Applied Geophysics*, 165, 1325-1350.

220. Mohanty, W. K., Walling, M. Y., Nath, S. K. and Pal, I., (2007), First order seismic microzonation of Delhi, India Using Geographic Information System (GIS), *Natural Hazards*, 40, 245-260.

221. Moldoveanu, C. L., Radulian, M., Marmureanu, G. H., and Panza, G. F., (2004), Microzonation of Bucharest: state of the art, *Pure and Applied Geophysics*, 161, 1125-1147.

222. Molnar, P., (1987), The distribution of intensity associated with the great 1897 Assam earthquake and bounds on the extent of the rupture zone, *Journal of Geological Society of India*, 30, 13-27

223. Molnar, P., and Pandey, M. R., (1989), Rupture zones of great earthquakes in the Himalaya region, In *proceedings of the Indian Academic Science (Earth Planet Science)*, 98, 61-70.

224. Molnar, P., Fitch, T. J., and Wu, F. T., (1973), Fault plane solutions of shallow earthquakes and contemporary tectonics in Asia, *Earth Planetary Science Letters*, 19, 101-112.

225. Montilla, J. A. P., Casado, C. L., and Romero, J. H., (2002), Deaggregation in Magnitude, Distance, and Azimuth in the South and West of the Iberian Peninsula, *Bulletin of the Seismological Society of America*, 92, 2177-2185.

226. Moss, R. E. S., Seed, R. B., Kayen, R. E., Stewart, J. P., and Der Kiureghian, A., (2006), Probabilistic seismic soil liquefaction triggering using the CPT, *Journal of Geotechnical and Geoenvironmental Engineering*, 132.

227. Motamed, R., Ghalandarzadeh, A. and Towhata, I., (2007), Seismic microzonation and damage assessment of Bam city, southeast of Iran, *Journal of Earthquake Engineering*, 11, 110-132.

228. Motazedian, D., and Atkinson, G. M., (2005), Stochastic finite-fault modeling based on a dynamic corner frequency, *Bulletin of the Seismological Society of America,* 95, 995-1010

229. Mukhopadhyay, M., (1984), Seismotectonics of transverse lineaments in the eastern Himalaya and its foredeep, *Tectonophysics*, 109, 227-240.

230. Murthy, M. V. N., Talukdar, S. C., Bhattacharya, A. C., and Chakrabarty, C., (1969), The Dauki fault of Assam, *Bulletin of Oil and Natural Gas Communication,* 6, 57-64.

231. Nakamura, Y., (1989), Earthquake Alarm System for Japan Railways, *Japanese Railway Engineering*, 28, 3-7.

232. Nandy, D. R. (1980), Tectonic patterns in Northeastern India, Indian Jourbal of Earth Sciences, 7, 103-107.

233. Nandy, D. R., (2001), Geodynamics of Northeastern India and the adjoining region, acb publications.

234. National Research council, (1988), Probabilistic Seismic Hazard Analysis, National Academy Press, Washington, D.C., 97.

TH-994_06610404

235. NCEER (1997), In *proceedings of the NCEER workshop on evaluation of liquefaction resistance of soils*, Edited by Youd, T. L., Idriss, I. M., Technical Report No. NCEER-97-0022.

236. NEDFI, North Eastern Development Finance Corporation Ltd., http://www.nedfi.com/.

237. Neelima, D. S, (2006), Seismic microzonation of Delhi Region, PhD thesis, IIT Delhi.

238. Newmark, N. M., and Rosenblueth, E., (1976), Fundamentals of earthquake engineering, Prentice Hall, N. J., Engelwood Cliffs.

239. Newmark, N. M., Blume, J. A., and Kapur, K. K., (1973), Seismic design spectra for nuclear power plant, *Journal of Power Division*, ASCE, 99, 287-303.

240. Ni, J. F., and Barazangi, M., (1984), Seismotectonics of the Himalayan collision zone: Geometry of the underthrusting India Plate beneath the Himalaya, *Journal of Geophysical Research*, 89, 1147-1163

241. Ni, J. F., Guzman-Speziale, M., Bevis, M., Holt, W. E., Wallace, T. C., Seager, W., (1989), Accretionary tectonics of Burma and three dimensional geometry of the Burma subduction zone, *Geology* 17, 68-71.

242. Ningthoukhongjam, K. S., (2005), *Cheitharol Kumpapa* (in Manipuri), Manipur Sahitya Parisad, Imphal.

243. Novikova, E. I., and Trifunac, M. D., (1994), Duration of strong ground motion in terms of earthquake magnitude, epicentral distance, site conditions and site geometry, *Earthquake Engineering and Structural Dynamics*, 23, 1023-1043.

244. Nunziata, C., (2004), Seismic ground motion in Napoli for the 1980 Irpinia earthquake, *Pure and Applied Geophysics*, 161, 1239-1264.

245. Oinam, A., (2007), Look east policy and Manipur, *The Sangai Express* (27 Dec 2003), Imphal.

246. Oldham, R. D., (1899), Report on the great earthquake of the 12th June 1897, *Geological Survey of India Memoirs*, 29, Reprinted, 1981, Geological Survey of India, Calcutta, 379 .

247. Oldham, T., (1882), The Cachar earthquake of 10th January, 1869, *Geological Survey of India Memoirs*, 19, 1-88.

248. Oldham, T., (1883), Catalogue of Indian earthquakes, *Geological Survey of India Memoirs*, 19,163-215.

249. Pal, I., Nath, S. K., Shukla, K., Pal, D. K., Raj, A., Thingbaijam K. K. S., and Bansal, B. K., (2008), Earthquake hazard zonation of Sikkim Himalaya using a GIS platform, *Natural Hazards* 45, 333-377.

250. Panza, G. F., (1985), Synthetic seismograms: the Rayleigh waves modal summation, *Journal of Geophysics*, 58, 125-145.

251. Panza, G. F., Paskaleva, I., and Nunziata, C., (2004), Seismic ground motion in large mega areas, Special Issue, *Pure and Applied Geophysics*, 161.

252. Parolai S, Richwalski, S.M. Milkereit, C., and Faeh, D., (2006), S-wave velocity profiles for earthquake engineering purposes for the Cologne area (Germany), *Bulletin of Earthquake Engineering*, 4, 65–94.

253. Parvez, I. A., Vaccari F., And Panza G. F. (2006), Influence of source distance on site effects in Delhi city, *Current Science*, 91, 827-835.

254. Parvez, I. A., Vaccari, F., and Panza, G. F., (2003), A deterministic seismic hazard map of India and adjacent areas, *Geophysical Journal International*, 155, 489-508.

255. Parvez, I. A., Vaccari, F., and Panza, G. F., (2004), Site-specific microzonation study in Delhi metropolitan city by 2-D modelling of SH and P-SV waves, *Pure and Applied Geophysics*, 161, 1165-1184.

256. Pearson, W. J., (Ed.), (1989), Seismological notes, July-August 1988, *Bulletin of Seismological Society of America*, 79, 925-932.

257. Poddar, M. C., (1950), Preliminary report of the Assam earthquake of 15th August 1950, *Geological Survey of India Bulletin*, 2, 1-40.

TH-994_06610404

258. Prakash, S., (1982), Problem of Deformation in Soil Structures, *Paper presented to the 19th Annual Meeting of Society of Engineering Science*, USA, October 27-29.

259. Prakash, S., and Guo, T., (1998), Liquefaction of Silts and Silt-clay Mixtures, *Geotechnical Earthquake Engineering and Soil Dynamics*, 1, 337-346.

260. Prakash, S., and Puri V. K., (2010), Recent advances in liquefaction of fine grained soils, In *5th International Conference on Recent Advances in Geotechnical Earthquake Engineering and Soil Dynamics*, San Diego(California).

261. PTI (2010), Press Trust of India, Rail link from Manipur to Vietnam on cards, April 9.

262. Puri, V. K., Das, B. M., Prakashm, S., (1996), Liquefaction of silty soils *International Journal of Offshore and Polar Engineering*, 6,

263. RaghuKanth, S. T. G., (2008), Modeling and synthesis of strong ground motion, *Journal Of Earth System Science*, 117, 683-705.

264. RaghuKanth, S. T. G., (2010), Estimation of Seismicity parameters for India, Seismological Research letters, 8, 207-217.

265. Raghukanth, S. T. G., and Dash, S. K., (2010), Deterministic seismic scenarios for North East India, *Journal of Seismology*, 14, 143-167.

266. RaghuKanth, S. T. G., and Iyengar, R. N., (2006), Seismic hazard estimation for Mumbai city, *Current Science*, 91, 1486-1494.

267. RaghuKanth, S. T. G., and Somala, S. N., (2009), Modeling of strong motion data in Northeastern India: Q, Stress Drop and Site Amplification, *Bulletin of the Seismological Society of America*, 99, 705-725.

268. RaghuKanth, S. T. G., Sreelatha, S., and Dash, S. K., (2008), Ground motion estimation at Guwahati city for a M_w 8.1 earthquake in the Shillong plateau. *Tectonophysics*, 448, 98-114.

269. Rajendran, C. P., Rajendran, K., Durah, B. P., Baruah, S., and Earnest, A., (2004), Interpreting the style of faulting and paleoseismicity associated

TH-994_06610404

with the 1897 Shillong, northeast India earthquake: Implications for regional tectonism, *Tectonics*, 23, TC4009, 12.

270. Rao, A., (1983), Geology and hydrocarbon potential of a part of Assam-Arakan basin and its adjacent region. In: Petroliferous basins of India, B.P. Radhakrishna (eds.), *Petroleum Asia Journal*, 127-158.

271. Rao, M. B. R., (1953), A compilation of papers on the Assam earthquake of August 15, 1950, *The Central Board of Geophysics*, Government of India.

272. Rau, J. L., (1994), Urban and environmental issues in East and Southeast asian coastal lowlands, *Engineering Geology*, 37, 25-29.

273. Reiter, L., (1990), Earthquake Hazard Analysis-Issues and Insights, Columbia University Press, New York, 254.

274. Robertson, P. K., and Campanella, R. G., (1985), Liquefaction of sands using the CPT, *Journal of Geotechnical Engineering Division, ASCE*, 111, 384-403.

275. Roy, D., (2008), Coupled use of cone tip resistance and small strain shear modulus to assess liquefaction potential, Journal of Geotechnical and Geoenvironmental Engineering, 134, 519-530.

276. Sadigh, K., Chang, C. Y., Abrahamson, N. A., Chiou, S. J., and Power, M. S., (1993), Specification of long period ground motions: Updated attenuation relationships for rock site conditions and adjustment factors for near-fault effects, In *proceedings of AtC-17-1 seminar on seismic isolation, passive energy dissipation, and active control*, San Francisco, California, 59-70.

277. Sadigh, K., Chang, C. Y., Egan, J., Makdisi, F., and Youngs, R., (1997), Attenuation relationships for shallow crustal earthquakes based on california strong motion data, *Seismological Research Letters*, 68, 180-189.

278. Safak, E., (1997), Model and methods to characterize site amplification from a pair of records, *Earthquake Spectra*, 13, 97-129.

279. Saragoni, G. R., and Hart, G. C., (1974), Simulation of artificial earthquakes, *Earthquake Engineering and Structural Dynamics*, 2, 249-267.

280. Sarangthem, B. S., (2005), In Meetei Ningthourol (in Manipuri), Imphal.

281. Satyabala, S. P., (2003), Oblique plate convergence in the Indo-Burma Myanmar subduction region, *Pure and Applied Geophysics*, 160, 1611-1650.

282. Scordilis, E. M. (2006), Empirical global relations converting Ms and mb to moment magnitude, Journal of Seismology, 10, 225-236.

283. Seeber, L., and Armbruster, J. G., (1981). Great detachment earthquakes along the Himalayan arc and long-term forecasting, In *Earthquake Prediction – An International Review, Manrice Ewing Ser., American Geophysical Union*, 4, 259-277.

284. Seed, H. B., and Idriss, I. M., (1970), Soil moduli and damping factors for dynamic response analyses, *Earthquake Engineering Research Center*, University of California, Berkeley, California, EERC-70/10.

285. Seed, H. B., and Idriss, I. M., (1971), Simplified procedure for evaluating soil liquefaction potential, *Journal of the Soil Mechanics and Foundation Division*, ASCE, 97, 1249-1274.

286. Seed, H. B., and Idriss, I. M., (1982), Ground motion and soil liquefaction during earthquakes, Monograph, *Earthquake Engineering Research Institute*, Oakland, Ca.

287. Seed, H. B., and Lee, K. L., (1967), Undrained strength characteristics of sands, *Journal of Soil Mechanics and Foundation*, 93, 333-360.

288. Seed, H. B., and Schnabel, P. B., (1972), Soil and geological effects on site response during earthquakes, In *proceedings of first international conference on microzonation for safer construction – Research and Application*, Seattle, USA, 1, 61-74.

289. Seed, H. B., Tokimatsu, K., Harder, L. F., and Chung, R. M., (1985), Influence of SPT Procedures in soil liquefaction resistance evaluations, *Journal of Geotechnical Engineering*, ASCE, 111, 1425-1445.

290. Seed, R. B., Centin, K. O., Moss, R. E. S., Kammerer, A. M., Wu, J., Pestana, J. M., Reimer, M. F., Sancio, R. B., Bray, J. D., Kayen, R. E., and Faris, A., (2003), Recent advances in soil liquefaction engineering, A

TH-994_06610404

unified and consistent framework, *Earthquake Engineering Research center*, University of California, Berkeley, EERC 2003-06.

291. Shanker, D., And Sharma, M. L., (1997), Estimation of seismic hazard parameters for the North East India and its vicinity, In *proceedings of workshop on earthquake disaster preparedness*, Roorkee, 49-57.

292. Sharafi, H., Baziar, M. H., and Haeri, S. M., (2009), Seismic Microzonation of the Urban Area Using Microtremor Measurement (Case study: Kermanshah City), *Electronic Journal of Geotechnical Engineering*, 14, 1-10.

293. Sharma, M. L., (1998), Attenuation relationship for estimation of peak ground acceleration using data from strong motion arrays in India, *Bulletin of the Seismological Society of America*, 88, 1063-1069.

294. Shinozuka, M., and Deodatis, G., (1996), Simulation of multi_dimensional Gaussian stochastic fields by spectral representation, *Applied Mechanics Reviews*, ASME, 49, 29-53.

295. Shrikhande, M., and Gupta, V. K., (2001), On the characterization of the phase spectrum for strong motion synthesis, *Journal of Earthquake Engineering*, 5, 465-482.

296. Singh, J. P., (1985), Earthquake ground motions: implications for designing structures and reconciling structural damage, *Earthquake Spectra*, 1, 239-270.

297. Singh, R. K. H., (2004), Tectonic significance of minor structures of the rocks of Imphal Valley, PhD thesis, Manipur University, India.

298. Singh, S. K., Ordaz, M., Dattatrayam, R. S., And Gupta, H. K. (1999), A Spectral analysis of the 21 May 1997, Jabalpur, India, Earthquake (Mw = 5.8) and estimation of ground motion from future earthquakes in the Indian Shield region, *Bulletin of the Seismological Society of America*, 89, 1620–1630.

299. Sitharam, T. G., and Anbazhagan, P., (2007), Seismic Hazard Analysis for the Bangalore Region, *Natural Hazards*, 40, 261-278.

300. Sitharam, T.G., Anbazhagan, P., (2008), Seismic Microzonation: Principles, Practices and Experiments, *EJGE Special Volume,* Bouquet 08, online, p. 61. <http://www.ejge.com/Bouquet08/Preface.htm>.

301. Sladen, J. A., D'Hollander, R. D., and Krahn, J., (1985), Back analysis of the Nerlerk berm liquefaction slides, *Canadian Geotechnical Journal,* 22, 579-588.

302. Slavov, S., Paskaleva, I., Kouteva, M., Vaccari, F., and Panza, G., (2004), Deterministic earthquake scenarios for the city of Sofia, *Pure and Applied Geophysics*, 161, 1221-1237.

303. Sonmez, H., (2003), Modification to the liquefaction potential index and liquefaction susceptibility mapping for a liquefaction-prone area (Inegol-Turkey), *Environmental Geology*, 44, 862-871.

304. Sonmez, H., and Gokceoglu, C., (2005), A liquefaction severity index suggested for engineering practice, *Environmental Geology*, 48, 81-91.

305. Spudich, P., Joyner, W. B., Lindh, A. G., Boore, D. M., Margaris, B. M., and Fletcher, J. B., (1999), SEA99: A Revised Ground Motion Prediction Relation for Use in Extensional Tectonic Regimes, *Bulletin of Seismological Society of America*, 89, 1156-1170.

306. Stepp, J. C., (1972), Analysis of completeness of the earthquake sample in the Puget Sound area and its effect on statistical estimates of earthquake hazard, In *proceedings of the first microzonation conference*, 897-909, Seattle, WA.

307. Stepp, J. C., Silva, W. J., McGuire, R. K., and Sewell, R. T., (1993), Determination of earthquake design loads for a high level nuclear waste repository facility, In *proceeding 4th Department of Energy natural Phenomena of Hazard Mitigation Conference, Atlanta*, 651-657, 1993.

308. Sunder, S., and Connor, J., (1982), A new procedure for processing strong-motion earthquake signals, *Bulletin of Seismological Society of America*, 72, 643-661.

309. Sunder, S., and Schumacker, B., (1982), Earthquake motions using a new data processing scheme, *Journal of Engineering Mechanics*, ASCE, 108, 1313-1329.

310. Tajimi, H., (1960), A statistical method of determining the maximum response of a building structure during an earthquake, In *proceeding of 2nd world conference of earthquake engineering*, Japan, 781-797.

311. Talukdar, S. N., (1982), Geology and hydrocarbon prospects of east coast basins of India and their relationship to evolution of the Bay of Bengal, *Offshore South East Asia, Conference*, Singapore, 1-8.

312. Tandon, A. N., (1954), Study of Assam earthquake of August 1950 and its aftershocks, *Indian Journal of Meteorology and Geophysics*, 5, 95–137.

313. Tandon, A. N., (1955), Direction of faulting in the great Assam earthquake of 15 August 1950, *Indian Journal of Meteorology and Geophysics*, 6, 61-64.

314. Tandon, A. N., (1956), Zone in India liable to earthquake damage, *Indian Journal of Meteorology and Geophysics*, 10, 137-146.

315. Tandon, A. N., and Srivastava, H. N., (1975), Focal mechanisms of some recent Himalayan earthquakes and regional plate tectonics, *Bulletin of Seismological Society of America*, 65, 963-969.

316. Tapponnier, P., Peltzer, G., Le Dain, A. Y., Armijo, R., and Cobbold, P., (1982), Propagating extrusion tectonics in Asia: New insights from simple experiments with plasticine, *Geology*, 10, 611-616.

317. TC4-ISSMGE (1999), Manual for zonation on seismic geotechnical hazard, ,Revised edition, Technical committee for earthquake geotechnical engineering (TC4) of the International Society of Sol Mechanics and Geotechnical Engineering, 209.

318. Thenhaus, P. C., and Campbell, K. W., (2003), Seismic hazard analysis: In Earthquake Engineering Handbook, edited by W. F. Chen and C. Scawthorn, 1 – 50: CRC Press, Boca Raton.

319. Todorovska, M. I., Gupta, I. D., Gupta, V. K., Lee, V. W., and Trifunac, M. D., (1995), SelectedTopics in Probabilistic Seismic Hazard Analysis, *Report*

no. CE95-08, Department of Civil Engineering, University of Southern California, Los Angeles, CA.

320. Topal, T., Doyuran, V., Karahanoglu, N., Toprak, V., Suzen, M. L,. and Yesilnacar, E., (2003), Microzonation for earthquake hazards: Yenisehir settlement, Bursa, Turkey, *Engineering Geology*, 70, 93–108.

321. Toro, G. R., Abrahamson, N. A., and Schneider, J. F., (1997), Model of strong ground motions from earthquakes in Central and Eastern North America: best estimates and uncertainties, *Seismological Research Letters*, 68, 41–57.

322. Trifunac, M. D., (1972), A note on correction of strong-motion accelerograms for instrument response, *Bulletin of Seismology Society of America*, 62, 401–409.

323. Trifunac, M. D., (1990), Seismic microzonation mapping via uniform risk spectra, *Soil dynamics and earthquake engineering*, 9, 34-43.

324. Tuladhar, R., Cuong, N. N. H., And Yamazaki, F., (2004), Seismic Microzonation Of Hanoi, Vietnam Using Microtremor Observations, In *proceeding of 13th world conference earthquake engineerin*g, Vancouver, B. C., Canada,2539.

325. Tuladhar, R., Yamazaki, F., Warnitchai, P., and Saita, J., (2004), Seismic microzonation of the Greater Bangkok area using microtremor observations, *Earthquake Engineering and Structural Dynamics*, 33, 211–225.

326. Turnbull, M. L., (2000), Seismic Microzonation of Bundaberg, Queensland, In *proceedings of the Australian Earthquake Engineering Society Annual Conference*, Hobart.

327. Uhrhammer, R. (1986). Characteristics of northern and southern California seismicity, Earthq. Notes, 57, 21.

328. USGS website (http://neic.usgs.gov/).

329. Valdiya, K. S., (1976), Himalayan transverse faults and their parallelism with subsurface structures of north Indian plains, *Tectonophysics*, 32, 352-386.

330. Van Roy, J. L., and Stiff, J. S., (2001), Guidelines for urban engineering geological investigations in South Africa, *Bulletin of Engineering and Geological Environment*, 59, 285– 295.

331. Verma, R. K., Mukhopadhyay, M., and Ahluwalia, M. S., (1976), Earthquake mechanisms and tectonic features of northern Burma, *Tectonophysics*, 32, 387-399.

332. Vipin K.S., Anbazhagan P, Sitharam T.G. (2009), Estimation of peak ground acceleration and spectral acceleration for South India with local site effects: probabilistic approach. *Nat Hazards*, 9, 865–878

333. Virieux, J., (1984), SH-wave propagation in heterogeneous media: velocity stress finite difference method, *Geophysics*, 49, 1933–1957.

334. Virieux, J., (1986), P-SV wave propagation in heterogeneous media: velocity–stress finite difference method, *Geophysics*, 51, 889-901.

335. Vucetic, M., and Dobry, R., (1991), Effect of soil plasticity on cyclic response, *Journal of the Geotechnical Engineering*, 117, 89-107.

336. Wang, K., Chen, Q. F., Sun, S., and Wang, A., (2006), Predicting the 1975 Haicheng earthquake, *Bulletin of the Seismological Society of America*, 96, 757–795.

337. Wong, I., Silva, W., Bott, J., Wright, D., Thomas, P., Gregor, N., Li, S., Mabey, M., Sojourner, A., and Wang, Y., (2000), Earthquake scenario ground shaking map for the portland, oregon, metropolitan area, portland hills fault M 6.8 earthquake, peak horizontal acceleration (g) at the ground surface, *Oregon Department of Geology and Mineral Industries Interpretative Map Series*, IMS-15, scale 1: 62,500.

338. Wong, I., Silva, W., Olig, S., Thomas, P., Wright, D., Ashland, F., Gregor, N., Pechmann, J., Dober, M., Christenson, G., Gerth, R., (2002), Earthquake Scenario and Probabilistic Ground Shaking Maps for the Salt Lake City, Utah, Metropolitan Area, *Utah Geological Survey Miscellaneous Publication*, MP-02- 05, 50.

339. Youd, T. L., and Noble, S. K. (1997), Liquefaction Criteria Based on Statistical and Probabilistic Analyses, In *proceedings of the NCEER Workshop on Evaluation of Liquefaction Resistance of Soils*, 201-205.

340. Youd, T. L., Idriss I. M., Andrus, R. D., Arango, I., Castro, G., Christian, J. T., Dobry, R., Finn, W. D. L., Harder, L. F., Hynes, M .E., Ishihara, K., Koester, J. P., Liao, S. S. C., Marcuson, W. F., Martin, G. R., Mitchell, J. K., Moriwaki, Y., Power, M. S., Robertson, P. K., Seed, R. B., Stokoe, K. H., (2001), Liquefaction resistance of soils: Summary report from the 1996 NCEER and 1998 NCEER/NSF workshops on evaluation of liquefaction resistance of soils, *Journal of Geotechnical and Geoenvironmental Engineering*, 817–833.

341. Youngs, R. R., Chiou S.J., Silva, W.J., and Humphrey, J. R., (1997), Strong ground motion attenuation relationships for subduction zone earthquakes, *Seismological Research letters*, 68, 58-73.

342. Youngs, R. R., Day, S. M., and Stevens, J. L., (1988), Near field ground motions on rock for large subduction earthquake, In proceedings of earthquake engineering and soil dynamics II: recent advances in ground motion evaluation, *Geotechnical Special Publication* 20, ASCE, New York, 445-462.

343. Zerva, A., (1988), Seismic source mechanisms and ground motion models, *Probabilistic Engineering Mechanics*, 3, 64-74.

TH-994_06610404

Appendix-A

Some Terminologies used in Earthquake Engineering and Engineering Seismology

Relevant glossary of specialized terms taken from Earthquake Engineering handbook edited by Wai-Fah Chen and Charles Scawthorn (2003), Geotechnical Earthquake Engineering by Steven L. Kramer (2008), Recent Advances in Earthquake Geotechnical Engineering and Microzonation edited by Atilla Ansal (2004), Microearthquake Seismology and Seismotectonics of South Asia by J. R. Kayal (2008) and Geodynamics of Northeastern India and the Adjoining Region by D. R. Nandy (2001) used in the present study are briefly defined below.

Sr. no.	Terminology	Definition
1.	Acceleration time history	A paired data set or series of acceleration values versus time.
2.	Accelerogram	A record showing acceleration as a function of time.
3.	Accelerometer	An instrument for measuring acceleration as a function of time.
4.	Aleatory	Uncertainty in the data used in analysis; generally accounts for randomness associated with the prediction of a parameter from a specific model,

		assuming that the model is correct. Specification of the standard deviation of a mean ground-motion attenuation relationship is a representation of aleatory variability.
5.	Aleatory variability	Uncertainty due to randomness in the phenomena, as differentiated from epistemic uncertainty.
6.	Alluvium	Alluvium is sediment that has been carried by and deposited from running water.
7.	Amplification	Increase in ground motion due to the presence of soil deposits, usually expressed in terms of the ratio of ground surface to bedrock motion.
8.	Amplitude (wave)	The maximum height of a wave crest or depth of a trough.
9.	Anelastic attenuation	The diminution of ground motion with distance from the source due to material damping and scattering of waves from inhomogeneities in the crust.
10.	Archaean	Of or relating to the oldest known rocks, those of the Precambrian Eon, that are predominantly igneous in composition
11.	Argillaceous	a sedimentary rock formed from clay deposits
12.	Arias intensity	A ground motion parameter derived from an accelerogram and proportional to the integral over time of the acceleration squared.
13.	Aseismic	This term describes a fault on which no earthquakes have been observed.
14.	Asperities (fault)	Roughness on the fault surface subject to slip.
15.	Attenuation	Decrease in amplitude and change in frequency content of the seismic waves with distance, because of geometric spreading, energy absorption, and scattering.
16.	Attenuation relation	An equation or tabulation used to estimate a strong-motion parameter from one or more

		seismological parameters; also known as a ground motion relation.
17.	Basement rock	The more resistant, generally crystalline rock that lies beneath layers or irregular deposits of younger relatively deformed sedimentary rock.
18.	Benioff zone	A narrow zone, defined by earthquake foci
19.	Body waves	Vibrational waves transmitted through the body of the Earth; are of two types.
20.	Bracketed duration	Time between the first and last exceedance of a given threshold acceleration during a seismic event.
21.	Characteristic earthquake	Surface-rupturing earthquakes occurring on a known tectonic structure, within a relatively narrow range of magnitudes at an increased frequency over that which would be estimated from the Gutenberg–Richter relationship.
22.	Completeness	Homogeneity of the seismicity record.
23.	Control motion	Amplitude and frequency characteristics of the input motion.
24.	Corner frequency	The frequency above which earthquake radiation spectra vary with ω^{-3}, below corner frequency the spectra are proportional to seismic moment.
25.	Creatceous	Interval of geologic time from 145.5 to 65.5 million years ago.
26.	Critical damping	The value of damping such that free vibration of a structure will cease after one cycle ($C_{crit}=2m\omega$). Damping represents the force or energy lost in the process of material deformation (damping coefficient, c = force per velocity).
27.	Critical reflection	The incidence angle below which the ground-motion ray is completely reflected off a layer of higher wave velocity.
28.	Crust	The Earth's outermost layer.
29.	Cyclic resistance	Cyclic stress ratio above which liquefaction is

	ratio (CRR)	triggered.
30.	Cyclic strength	Shear stress during cyclic loading at which the resulting deformations are considered excessive.
31.	Cyclic stress ratio (CSR)	Ratio of earthquake-induced equivalent shear stress amplitude to effective overburden stress.
32.	Damage	Permanent cracking, yielding, or buckling of a structural element or structural assemblage.
33.	Damping	Energy dissipation that occurs in a dynamically deforming structure, either as a result of frictional forces, viscous behavior, or structural yielding. Increased damping tends to reduce the amount that a structure responds to ground shaking.
34.	Damping curve	Relationship between viscous damping coefficient and shear strain for nonlinear soils.
35.	Denudational hills	They are low relief hills mostly covered with vegetation.
36.	Design basis earthquake (DBE)	The maximum earthquake employed for the design or analysis of a dam, usually specified in terms of acceleration time histories or response spectrum at the site or both. It may be defined in terms of magnitude and epicentral distance from the dam site.
37.	Dip	The angle between a plane, such as a fault, and the Earth's surface.
38.	Dip-slip	Motion at right angles to the strike, up- or down-slip.
39.	Epicenter	The projection on the surface of the Earth directly above the hypocenter.
40.	Epistemic uncertainty	Uncertainty due to lack of knowledge (e.g., omission of a key parameter due to not recognizing its importance in a phenomenon, uncertainty in a parameter or model).
41.	Equivalent damping ratio	Ratio between the dissipated and stored energies within a hysteretic loop at a given shear strain.

42.	Equivalent-linear analysis	In an equivalent-linear analysis, in which the properties (damping coefficient and shear modulus) are iteratively adjusted in a series of successive linear elastic analyses to become compatible with the average computed shear strains within the elements of the numerical model. The average strain is taken as a fixed percentage of the peak strain in each element. Iterations are stopped when convergence is achieved for the estimated properties, based on the computed average strains.
43.	Excess pore pressure	Corresponds to an increase of internal pore water pressure within a saturated soil medium as a result of a reduction in skeleton volume caused by earthquake shaking.
44.	Fault	A fracture or fracture zone along which displacement has occurred parallel to the fracture.
45.	Fault plane	The plane that coincides with the rupture surface of a fault.
46.	Faulting mechanism	The type or style of faulting defined by the direction of slip on the fault rupture plane; usually referred to by such terms as strike slip, reverse, thrust, normal, or oblique.
47.	Flow failures	Soil failure due to liquefaction involving large lateral displacements that occur when the static shear stress along a potential failure plane is larger than the shear strength of the liquefied soil.
48.	Fluvial	Fluvial is used in geography and Earth science to refer to the processes associated with rivers and streams and the deposits and landforms created by them.
49.	Fluvio-lacustrine	Of or pertaining to sedimentation partly in lake water and partly in streams, or to deposits laid down under alternating or overlapping lacustrine

		and fluviatile conditions
50.	Flysch	Flysch is a sequence of sedimentary rocks that is deposited in a deep marine facies in the foreland basin of a developing orogen.
51.	Focal mechanism	Refers to the direction of slip in an earthquake, and the orientation of the fault on which it occurs.
52.	Fourier amplitude spectrum	The relative amplitude at different component frequencies that are derived from a time history by Fourier analysis.
53.	Fourier transform	The mathematical operation that converts a time function into a function of frequency, and vice versa.
54.	Free-field	The regions of the ground surface that are not influenced by man-made structures. Also designates a medium containing no structure (free-field profile) and where boundary effects do not significantly influence the response of the medium to earthquake motion.
55.	Free-field ground motion	Motion that would essentially exist in the soil at the level of the foundation in the absence of the structure and any excavation.
56.	Gaussian noise spectrum	The spectrum of a time history whose sample values are generated by random selection from a normal or Gaussian statistical population that has a specified mean and standard deviation.
57.	Genesis	A banded or foliated metamorphic rock
58.	Geometric attenuation	The diminution of ground motion with distance from the source as the area of the wave front expands.
59.	Geosynclines	Linear trough of subsidence of the Earth's crust, in which vast amounts of sediment accumulate.
60.	Ground motion	The vibration of the ground in the time or frequency domain measured by a seismometer that records acceleration, velocity, or

		displacement, or an estimate of this vibration or a ground-motion parameter that characterizes this vibration.
61.	Ground shaking	A random, rapid cyclic motion of the ground produced by an earthquake.
62.	Half space	A mathematical model bounded only by one plane surface.
63.	Hypocenter	The location of initial radiation of seismic waves (i.e., the first location of dynamic rupture).
64.	Hysteresis	A form of energy dissipation that is related to inelastic deformation of a structure.
65.	Intensity	A metric of the effect, or the strength, of an earthquake hazard at a specific location, commonly measured on qualitative scales such as MMI, MSK, and JMA.
66.	Lateral spreading	Small to moderate lateral displacements associated with liquefaction that occur due to seismic shaking when the static shear stress is less than the shear strength of the liquefied soil.
67.	Lineaments	A lineament is a linear feature in a landscape which is an expression of an underlying geological structure such as a fault.
68.	Liquefaction	A process resulting in a soil's loss of shear strength, due to a transient excess of pore water pressure.
69.	Local site conditions	A qualitative or quantitative description of the material properties of the soil and sedimentary rock layers above basement rock.
70.	Magnitude	A unique measure of an individual earthquake's release of strain energy, measured on a variety of scales, of which the moment magnitude M_W (derived from seismic moment) is preferred.
71.	Magnitude scaling factors	Factors to be applied to the cyclic resistance ratio obtained from the standard penetration test, cone

		penetration test, and shear wave velocity liquefaction charts for earthquakes of magnitude other than 7.5.
72.	Magnitude – frequency relation	The probability of occurrence of a selected magnitude.
73.	Maximum credible earthquake (MCE)	(Also Maximum considered earthquake) The largest earthquake considered in an analysis that appears possible along a recognized fault or within a geographically defined tectonic province. Little regard is given to its probability of occurrence. Usually the largest reasonably conceivable event. MCE sometimes also used to denote maximum credible earthquake, although this term is not favored now.
74.	Meizoseismal	The area of strong shaking and damage.
75.	Mode shape	A deformed shape, in which a structure can oscillate freely, when displaced.
76.	Modulus reduction curve	Relationship expressing the rate at which the maximum shear modulus of soil decreases with shear strain due to nonlinear effects.
77.	Moment magnitude (M_W)	The moment magnitude M_W of an earthquake is proportional to the logarithm of the seismic moment. This is a measure of the energy released and is related to the physical characteristics of the causative fault rupture.
78.	Natural frequency	The reciprocal of natural period.
79.	Natural period	The period of an oscillator or structure during free (i.e., unforced) vibration.
80.	Near-field	Within one source dimension of the epicenter, where source dimension refers to the length or width of faulting, whichever is less.
81.	Normal fault	A fault that exhibits dip-slip motion, where the two sides are in tension and move away from each other.

82.	Oligocene	The Oligocene epoch is part of the Tertiary Period in the Cenozoic Era, and lasted from about 33.7 to 23.8 million years ago (mya).
83.	Ophiolite	Generally considered to be fragments of oceanic rocks.
84.	Paleoseismicity	Prehistoric earthquakes, since there is no human record, these earthquakes are identified (*i.e.*, location, magnitude, etc.) via geologic trenching and other evidence.
85.	Peak ground acceleration (PGA)	The maximum amplitude of recorded acceleration (also termed the ZPA, or zero period acceleration).
86.	Period	The amount of time it takes a structure that has been displaced in a particular natural mode and then released to undergo one complete cycle of motion.
87.	Period (wave)	The time interval between successive crests in a sinusoidal wave train; the period is the inverse of the frequency of a cyclic event.
88.	Phase	The angle of lag or lead (or the displacement) of a harmonic wave with respect to a reference.
89.	Piedmont plain	Piedmont Plains are those plains which are found on the foot of mountains or hills. Piedmont Plains are formed by the deposition of materials.
90.	Power spectrum	A graph of power spectral density versus frequency.
91.	Pseudostatic approach	Stability analysis procedure in which inertial forces caused by earthquake shaking are approximated by equivalent static forces that are a function of peak ground motion acceleration and soil weight.
92.	Quality factor	An index of the dissipative nature of the earth's transmission path on propagating seismic waves.
93.	Radiation pattern	A geometric description of the amplitude of

		ground motion and the sense of initial motion at the source which for shear waves has a low-order symmetry that can be used to infer the faulting mechanism.
94.	Rake angle	The angle between the direction of slip on the fault rupture plane and the fault strike.
95.	Rayleigh wave	Seismic surface wave with ground motion only in a vertical plane containing the direction of propagation of the waves.
96.	Response spectrum	A plot of maximum acceleration, velocity, or displacement for a single-degree of- freedom oscillator as a function of system period, for a given input motion and system damping (typically 5%).
97.	Return period	The reciprocal of the annual probability of occurrence i.e., earthquake probabilities of occurrence are commonly stated in terms of a return period, which misleads some people since they infer the earthquake, occurs on a regular cycle equal to the return period.
98.	Reverse fault	A fault that exhibits dip-slip motion, where the two sides are in compression and move away towards each other.
99.	Rupture front	The instantaneous boundary between the slipping and locked parts of a fault during an earthquake.
100.	Rupture velocity	The velocity at which the fault ruptures propagates along the fault length.
101.	S wave (shear wave)	Body wave in which the particle motion is at right angles to the direction of wave propagation.
102.	Sand boils	Ejection of solids (i.e., sand, silt) carried to the surface by water, due to liquefaction.
103.	Seismic gap	A portion of a fault or seismogenic zone that can be deduced to be likely to rupture in the near

		term, based on patterns of seismicity and geological evidence.
104.	Seismic hazard	The likelihood or probability of experiencing a specified intensity of any damaging phenomenon, at a specific site, or over a region.
105.	Seismic moment	The moment generated by the forces generated on an earthquake fault during slip.
106.	Seismic risk	The product of the hazard and the vulnerability (i.e., the expected damage or loss, or the full probability distribution).
107.	Seismic waves	Waves originating from an earthquake event and traveling through geologic media, including compressional p-waves, shear S-waves, surface Love waves, and long-period Rayleigh waves.
108.	Seismogenic	That part of the Earth's crust that is capable of generating ground motion at periods of engineering interest, usually 10 sec or less.
109.	Seismological parameter	A parameter used to characterize a seismological property of the earthquake source, the propagation medium, or the response of the materials beneath the site.
110.	Seismotectonic model	An analytical model combining models of earthquake sources, occurrence, and attenuation
111.	Shear-wave velocity	The speed at which shear waves travel through a material; shear waves are waves whose amplitude is perpendicular to the direction of propagation and are the most potentially damaging to man-made structures.
112.	Slip model	A kinematic model that describes the amount, distribution, and timing of slip associated with an earthquake.
113.	Slip rate	The rate of movement of the two sides of a fault slipping relative to one another, as determined from geodetic measurements, from offset man-

		made structures, or from offset geologic features whose age can be estimated.
114.	Source	The released forces that generate seismic waves, also called the earthquake source.
115.	Source function	The ground motion generated at the fault during rupture.
116.	Spectral acceleration	The maximum response acceleration that a structure of given period will experience when subjected to a specific ground motion.
117.	Spectral displacement	The maximum response displacement that a structure of given period will experience when subjected to a specific ground motion.
118.	Spectral velocity	The maximum response velocity that a structure of given period will experience when subjected to a specific ground motion.
119.	Spectrum amplification factor	The ratio of a response spectral parameter to the ground motion parameter (where parameter indicates acceleration, velocity, or displacement).
120.	Stochastic	Adjective denoting processes having random characteristics.
121.	Stress drop	The amount of stress released at the rupture front during an earthquake.
122.	Strike	The orientation of a fault on the Earth's surface, usually measured clockwise from north.
123.	Strike-slip fault	A fault in which movement is principally horizontal.
124.	Strong ground motion	Ground motion having the potential to cause measurable damage to a structure's architectural or structural components; usually associated with a PGA of 0.05 *g* or greater.
125.	Strong motion	Ground motion of sufficient amplitude and duration to be potentially damaging to man-made structures.
126.	Strong-motion	A parameter characterizing the amplitude of

	parameter	strong ground motion in the time domain (time-domain parameter) or the frequency domain (frequency-domain parameter).
127.	Subduction	Refers to the plunging of a tectonic plate (e.g., the Indian plate) beneath another (e.g., the Burmese plate) down into the mantle, due to convergent motion.
128.	Surface faulting	Displacement that reaches the Earth's surface during slip along a fault.
129.	Surface waves	Vibrational waves transmitted within the surficial layer of the Earth; are of two types, horizontally oscillating Love waves, analogous to S body waves, and vertically oscillating Rayleigh Waves.
130.	Suture zone	The area where two continental plates have joined together through continental collision.
131.	Syntaxis	A convergence of mountain ranges, or geological folds, towards a single point.
132.	Synthetic acceleration time history	An acceleration time history that is not recorded during an actual earthquake but is developed, using analytical and theoretical methods, to be representative of an acceleration time history that could be recorded during an earthquake.
133.	Tectonic	Relating to, causing, or resulting from structural deformation of the Earth's crust.
134.	Tectonic environment	The type of tectonic deformation that occurs in a region, usually described by such terms as active, stable, compressional, extensional, or subduction.
135.	Theory of elastic rebound	Concept that the Earth's crust is deformed by plate movements, thus storing strain energy, until energy is released by fault rupture, resulting in an earthquake.
136.	Thrust fault	A fault along which relative movement of the overhanging side of the fault occurs upward (reverse displacement), and primarily due to a

		compressive tectonic stress regime.
137.	Time history	A data set, usually composed of one vertical and two orthogonal horizontal components, describing a strong-motion parameter (such as ground acceleration) as a function of time.
138.	Trans-Alpide belt	A zone of major global seismicity, extending from the Mediterranean through the Middle East, the Himalayas, and the Indonesian archipelago, resulting from the collision of several major tectonic plates.
139.	Transform or strike-slip fault	A fault where relative fault motion occurs in the horizontal plane, parallel to the strike of the fault.
140.	Uniform hazard spectra (UHS)	Ground response spectra generated so as to have the same probability of exceedance for all structural frequencies of interest.
141.	Viscous	A form of energy dissipation that is proportional to velocity.
142.	Vulnerability	The expected damage given a specified value of a hazard parameter.
143.	Wave length	Distance between two consecutive wave fronts.
144.	White noise	Random energy containing all frequency components in equal proportions.

TH-994_06610404

Appendix B

Soil Investigation data for 122 boreholes located in Imphal city

This appendix presents the soil investigation data collected from various construction sites in Imphal city.

Site	Depth (m)		N - Value	Description of Strata
	From	To		
1	2	2.45	6	Firm brownish to bluish grey silty clay
wl. 0.83m	5	5.45	5	Firm grey silty clay with high silt content and trace of sand
	8	8.45	8	
	11	11.45	10	Stiff grey/bluish grey silty clay with varying percentage of sand
	14	14.45	12	
	17	17.45	22	Very stiff bluish grey silty clay
	20	20.45	25	
2	3	3.45	9	Firm brownish grey silty clay with kankar
wl. 0.38m	6	6.45	6	Firm grey silty clay with high silt content and traces of sand
	9	9.45	5	
	12	12.45	4	Firm to stiff grey silty clay with varying percentage of sand
	15	15.45	9	
	18	18.45	29	Very stiff bluish silty clay
	21	21.45	20	
	24	24.45	24	
3	1.5	1.95	14	Stiff brownish silty clay
0.51m	4.5	4.95	5	Soft grey silty clay with high silt content and traces of sand

TH-994_06610404

	7.5	7.95	3	
	10.5	10.95	11	Stiff grey silty clay with trace of sand
	13.5	13.95	15	Stiff grey silty clay with trace of sand
4	3.5	3.95	2	Firm grey silty clay
wl.	6.5	6.95	3	Soft grey silty clay with high silt content and traces of sand
0.20m	9.5	9.95	3	
	12.5	12.95	11	Stiff grey silty clay with trace of sand
	15.5	15.95	29	Very stiff grey silty clay with traces of silt
	18.5	18.95	18	
5	1.5	1.95	11	Stiff brownish grey silty clay
wl.	4.5	4.95	3	Very soft bluish silty clay with high silt content
0.82m	7.5	7.95	1	
	10.5	10.95	8	Stiff grey silty clay with trace of sand
	13.5	13.95	10	
6	3	3.45	8	Stiff brownish grey silty clay
wl.	6	6.45	6	Firm grey silty clay with trace of sand
0.55m	9	9.45	6	
	12	12.45	7	
	15	15.45	20	Stiff bluish silty clay
	18	18.45	7	
7	1.5	1.95	8	Firm brownish to bluish grey silty clay
wl.	4.5	4.95	4	Firm grey silty clay with high silt content
0.76m	7.5	7.95	8	
	10.5	10.95	6	Firm grey silty clay with trace of sand
	13.5	13.95	7	
8	1.5	1.95	4	Brick bat
wl.	4.5	4.95	6	Firm brownish grey clay
0.5m	7.5	7.95	11	
	10.5	10.95	9	Stiff grey silty clay with traces of sand
	13.5	13.95	10	
	16.5	16.95	22	Very stiff grey silty clay
	19.5	19.95	11	
9	3	3.45	6	Firm brownish grey silty clay
wl.	6	6.45	6	Grey silty clay with silt and sand content
0.6m	9	9.45	4	Firm grey silty clay with varying percentage of sand
	12	12.45	7	
	15	15.45	14	Stiff to very stiff grey silty clay
	18	18.45	18	

TH-994_06610404

10	1.5	1.95	7	Firm brownish grey silty clay
wl.	4.5	4.95	4	Firm grey silty clay with silt and sand
0.76m	7.5	7.95	6	content
	10.5	10.95	8	Stiff grey silty clay with varying percentage of sand
	13.5	13.95	14	
11	1.5	1.95	4	Soft brownish grey silty clay
wl.	4.5	4.95	1	
1.3m	7.5	7.95	1	Very soft grey silty clay with high silt content
	10.5	10.95	0	
	13.5	13.95	6	Firm bluish grey silty clay with sand
	17.5	17.95	13	Stiff grey silty clay with traces of sand
	20.5	20.95	15	
12	3	3.45	5	Firm grey silty clay
wl.	6	6.45	10	Stiff bluish grey silty clay, silt traces sand
0.75m	9	9.45	13	
	12	12.45	12	Stiff bluish grey silty clay with varying percentage of sand
	15	15.45	24	
	18	18.45	20	Very stiff grey silty clay with trace of decomposed wood
	22	22.45	22	
	26	26.45	29	
	30	30.45	39	Very stiff bluish grey silty clay with high silt content
	34	34.45	20	
	38	38.45	28	
13	1.5	1.95	10	Stiff brown grey silty clay
wl.	4.5	4.95	4	Soft bluish grey silty clay with high silt content and traces
1.0m	7.5	7.95	3	of sand
	10.5	10.95	5	
	13.5	13.95	23	Very stiff grey silty clay with sand
	16.5	16.95	20	Very stiff bluish grey silty clay
	19.5	19.95	18	
	22.5	22.95	43	
	25.5	25.95	18	
	28.5	28.95	26	
	31.5	31.95	33	
	34.5	34.95	39	Hard bluish grey silty clay with high silt content
	37.5	37.95	57	
14	3	3.45	6	Firm brown grey silty clay
wl.	6	6.45	6	Firm to stiff grey silty clay with high silt content and traces
1.2m	9	9.45	12	of sand

TH-994_06610404

	12	12.45	4	Firm grey silty clay with varying sand
	15	15.45	22	Very stiff to hard bluish grey silty clay
	18	18.45	39	
15	3	3.6	1	Very soft grey silty clay
wl.	5	5.6	4	Soft bluish grey silty clay with high silt content and traces of sand
1.2m	7.5	8.1	4	
	10.5	11.1	8	Stiff grey silty clay with varying percentage of sand
	12	12.6	13	
	15	15.6	38	Hard grey silty clay with brown spot
	16.5	17.1	42	
	18	18.6	39	
	20	20.6	40	
16	3	3.45	8	Firm brown silty clay with yellow spot
wl.	6	6.45	4	Firm grey silty clay, silt content, traces sand
1.75m	9	9.45	7	
	12	12.45	25	Very stiff grey silty clay with varying percentage of sand
	15	15.45	28	
17	1.5	1.95	13	Firm brownish grey silty clay with rusty brown spot
wl.	4.5	4.95	7	
0.9m	7.5	7.95	13	Stiff grey silty clay with high silt content and traces of sand
	9.5	9.95	11	
	12.5	12.95	8	
	14	14.45	15	Stiff grey to bluish grey silty clay with varying percentage of sand
	15	15.45	21	
18	1.5	1.95	9	Stiff brownish grey silty clay with rusty brown spots
wl.	4.5	4.95	12	
0.94m	7.5	7.95	11	
	10.5	10.95	10	Stiff grey silty clay, high silt content, sand
	13.5	13.95	32	Very stiff bluish grey silty clay with varying percentage of sand
	16.5	16.95	29	
	20.5	20.95	38	
19	3	3.45	9	Stiff brownish grey silty clay with rusty brown spots
wl.	6	6.45	12	
1.94m	9	9.45	11	Stiff grey silty clay, high silt, traces of sand
	12	12.45	24	Very stiff to hard grey silty clay
	15	15.45	38	
20	3	3.45	4	Firm brownish grey silty clay
0.4m	6	6.45	10	Stiff grey silty clay with high silt content and traces of sand

TH-994_06610404

	9	9.45	8	
	12	12.45	13	Stiff grey silty clay with varying percentage of sand
	15	15.45	13	
21	1.5	1.95	13	Stiff brownish to bluish grey silty clay with rusty brown spots
wl.	4.5	4.95	2	Soft to firm bluish grey silty clay with high silt content/sandy silty clay
1.65m	7.5	7.95	7	
	9.5	9.95	8	
	12.0	12.45	24	Medium dense grey silty sand
	13.5	13.95	26	
	16.5	16.95	25	Very stiff bluish grey silty clay wit occasional traces of kankars
	19.5	19.95	22	
	22.5	22.95	25	
	25.5	25.95	13	Stiff blackish grey silty clay with high percentage of decomposed wood/organic matter m peaty soil matter ,
	28.5	28.95	20	
	31.5	31.95	23	Very stiff bluish grey/grey silty clay with traces of kankars
	34.5	34.95	110	very dense yellow grey silty sand with mica
22	3.0	3.45	11	Stiff brownish to bluish grey silty clay with rusty brown spots
wl.	6.0	6.45	7	Soft to firm bluish grey to grey silty clay with high silt content silty clay with sand
1.65m	8.0	8.45	8	
	10.5	10.95	19	Medium dense grey silty sand
	12.5	12.95	23	
	14.0	14.45	24	
	15.5	15.95	23	Very stiff bluish grey silty clay with occasional traces of kankars
	17.0	17.45	22	
	20.0	20.45	24	
	21.5	21.95	23	
	24.5	24.95	10	Stiff blackish grey silty clay with high % of decomposed wood
	27.5	27.95	22	Very stiff bluish grey silt clay with traces of kankars
	30.5	30.95	23	
	33.5	33.95	29	
	35.0	35.45	115	Dense to very dense yellowish grey silty sand with mica
23	4.0	4.45	4	Stiff brownish to bluish grey silty clay with rusty brown spots
wl.	7.0	7.45	6	Soft to firm bluish grey to grey silty clay with high silt content silty clay with sand
1.6m	10.0	10.45	7	
	13.0	13.45	23	Medium dense grey silty sand
	14.5	14.95	28	

TH-994_06610404

	16.0	16.45	25	
	19.0	19.45	22	Very stiff bluish grey silty clay with occasional traces of kankars
	22.0	22.45	31	
	25.0	25.45	11	Stiff blackish grey silty clay with high % of decomposed wood/organic matter
	28.0	28.45	24	Very stiff bluish grey silt clay with traces of Kankars
	31.0	31.45	28	
	34.5	34.95	35	Dense to very dense yellowish grey silty sand with mica
	36.0	36.45	118	
24	2.0	2.45	8	Stiff brownish to bluish grey silty clay with rusty brown spots
wl.	5.0	5.45	4	Soft to firm bluish grey to grey silty clay with high silt content silty content
1.7m	8.0	8.45	8	
	11.0	11.45	8	Medium dense grey silty sand
	13.0	13.45	20	
	14.5	14.95	26	
	16.0	16.45	23	
	19.0	19.45	19	Very stiff bluish grey silty clay with occasional traces of kankars
	20.5	20.95	21	
	24.0	24.45	11	Stiff blackish grey silty clay with high % of decomposed wood/organic matter
	27.5	27.95	23	Very stiff bluish grey silt clay with traces of kankars
	30.5	30.95	22	
	34.5	34.95	34	
	36.0	36.45	136	Dense to very dense yellowish grey silty sand with mica
25	3.0	3.45	8	Stiff brownish grey silty clay with rusty brown/blue spot: kankars and gravel
wl.	6.0	6.45	7	Firm bluish grey/grey silty clay (high silt content) with occasional traces of sand
1.75m	8.0	8.45	8	
	10.0	10.45	15	Grey /bluish grey silty sand/sandy silt with little clay as binder
	11.5	11.95	16	
	13.0	13.45	20	
	14.0	14.45	22	
	16.0	16.45	28	
	19.0	19.45	20	Very stiff bluish grey silty clay
	22.0	22.45	22	Stiff grey/blackish grey silty clay with varying percentage of decomposed wood
	25.0	25.45	12	Very stiff grey/bluish grey silty clay with occasional traces of kankars
	28.0	28.45	15	
	29.5	29.95	26	
	34.0	34.45	112	Dense grey silty sand with traces of mica

TH-994_06610404

26	1.5	1.95	9	Stiff brownish bluish grey silty clay with rusty
wl.	4.5	4.95	6	brown/yellow spots; kankars and gravel
2.0m	7.5	7.95	7	Firm to stiff bluish grey silty clay
	9.5	9.95	12	(high silt content) with occasional traces of sand
	11.0	11.45	14	Grey /bluish grey silty sandy clay/silty clayey sand
	12.5	12.95	18	
	14.0	14.45	23	
	15.5	15.95	26	
	17.0	17.45	20	Very stiff bluish grey silty clay
	20.0	20.45	23	
	21.5	21.95	20	Stiff grey/blackish grey silty clay with varying percentage of decomposed wood
	24.5	24.95	10	
	27.5	27.95	20	Very stiff grey/bluish grey silty clay with occasional traces of kankars
	30.5	30.95	24	
	33.5	33.95	31	
	35.0	35.45	117	Dense grey silty sand with traces of mica
27	3.5	3.95	6	Firm brownish/bluish grey silty clay with rusty brown spot; trace of gravels
wl.	6.5	6.95	7	Bluish grey/grey silty sandy clay/silty clayey sand
1.7m	9.5	9.95	13	
	12.5	12.95	15	Grey/bluish grey silty sand/sandy silty with little clay as binder
	15.5	15.95	21	Very stiff bluish grey/grey silty clay with occasional brown spots
	17.0	17.45	25	
	18.5	18.95	26	
	21.5	21.95	22	Stiff blackish grey silty clay with varying % of decomposed wood
	24.5	24.95	19	
	27.5	27.95	23	Very stiff to hard bluish grey/grey silty clay with traces of kankars
	30.0	30.45	32	Very stiff to hard bluish grey /grey silty clay with traces of kankars
	32.0	32.45	35	
	35.0	35.45	32	
	38.0	38.45	31	
	40.0	40.45	34	
28	2.0	2.45	5	Firm brownish /bluish grey silty clay with rusty brown spot: gravels observed at top
wl.	5.0	5.45	6	
1.75m	8.0	8.45	10	Bluish grey silty sandy clay/silty clayey sand
	9.5	9.95	12	
	11.0	11.45	14	
	14.0	14.45	18	Very stiff bluish grey/grey silty clay with occasional brown spots
	16.0	16.45	22	

TH-994_06610404

	18.5	18.95	23	
	20.0	20.45	25	
	21.5	21.95	18	Stiff blackish grey/grey silty clay with varying % of decomposed wood
	24.5	24.95	20	
	26.0	26.45	21	
	29.5	29.95	26	Very stiff to hard bluish grey/grey silty clay with traces of kankars
	32.5	32.95	33	
	35.5	35.95	33	
	38.5	38.95	34	
	40.0	40.45	35	
29	2.5	2.95	9	Firm/stiff brownish/bluish grey silty clay with rusty brown spots: kankars/gravels at top
wl.	5.5	5.95	6	
2.0m	8.5	8.95	10	Grey silty sandy clay/silty clayey sand
	11.0	11.45	14	
	12.5	12.95	15	
	14.5	14.95	15	
	17.5	17.95	20	Very stiff bluish grey silty clay with occasional brown spots and kankars
	19.0	19.45	23	
	21.0	21.45	24	Stiff blackish grey/grey silty clay with varying percentage of decomposed wood
	24.5	24.95	19	
	27.5	27.95	25	Very stiff to hard bluish grey/grey silty clay with traces of kankars; traces of sand observed
	29.0	29.45	29	
	32.0	32.45	31	
	35.0	35.45	31	
	36.5	36.95	32	
	38.0	38.45	34	
30	3.5	3.95	7	Firm brownish /bluish grey silty clay with rusty brown spots: kankars/nodules
wl.	6.5	6.95	9	Grey silty sandy clay /silty clayey sand
1.7m	8.0	8.45	10	
	11.0	11.45	13	
	12.5	12.95	13	
	14.0	14.45	22	
	15.5	15.95	24	
	18.5	18.95	21	Very stiff bluish grey silty clay with occasional brown spots and kankars
	20.0	20.45	22	
	21.5	21.95	24	
	24.5	24.95	15	Stiff blackish grey /grey silty clay with varying percentage of decomposed wood
	26.0	26.45	25	
	29.0	29.45	26	Very stiff bluish grey silty clay with traces of kankars; occasional percentage of semi-decomposed wood
	33.5	33.95	27	

TH-994_06610404

31	4.0	4.45	7	Firm bluish grey silty clay
wl.	8.0	8.45	8	Stiff bluish grey silty clay (high silt content)/clayey silt
0.78m				
32	4.0	4.45	7	Firm bluish grey silty clay with traces of kankar
wl. 0.29m	8.0	8.45	13	Stiff bluish grey /grey silty clay (high silt content)/clayey silt
33	2.5	2.95	5	Firm bluish grey silty clay with traces of kankar
wl.	4.5	4.95	4	Firm to stiff brownish grey/grey silty clay (high silt content)
1.2m	6.0	6.45	5	
	9.0	9.45	8	
34	1.5	1.95	10	Firm to stiff yellowish /brownish grey silty clay with rusty brown patches
wl.	4.5	4.95	7	Stiff grey sandy silty clay High sand content noticed
1.0m	7.5	7.95	8	
	10.0	10.45	9	
35	3.0	3.6	5	Medium stiff brownish grey silty clay with traces of gravels at top
wl.	6.0	6.6	5	Medium stiff grey /bluish grey sandy silty clay with varying percentage of sand; high percentage of sand
0.8m	9.0	9.6	9	
	11.0	11.6	6	
	12.5	13.1	5	
	14.0	14.6	7	
	16.5	17.1	21	Stiff to very sandy silty clay/clayey sandy silt
	18.0	18.6	20	
	21.0	21.6	13	
	24.0	24.6	16	Stiff grey/dark grey silty clay with traces of sand and kankars
	27.0	27.6	15	
	30.0	30.6	18	Very stiff dark grey sandy silty clay/clayey sandy silt
	33.0	33.6	26	
	36.0	36.6	26	
	39.0	39.6	21	
36	3.0	3.6	8	Firm brownish grey silty clay with traces of gravels at top
wl.	6.0	6.1	6	Firm to stiff bluish grey silty clay (high silt content) with occasional traces of sand
0.8m	9.0	9.6	7	
	10.5	11.1	6	
	12.0	12.6	8	
	15.0	15.6	9	Grey /bluish grey silty sandy clay/silty clayey sand
	18.0	18.6	23	

TH-994_06610404

	19.5	20.1	11	Stiff to very stiff grey/bluish grey silty clay with traces of sand and l presence kankars
	21.0	21.6	12	
	23.5	24.1	12	Stiff blackish grey silty clay with varying percentage of decomposed wood
	26.5	27.1	17	
	29.5	30.1	18	
	32.5	33.1	20	Very stiff grey/bluish grey silty clay with occasional traces of kankars
	35.5	36.1	20	
	38.5	39.1	22	
	40.0	40.6	26	
37	1.5	1.65	4	Fill up soil brownish grey in colour
wl.	3.0	3.15	6	Clay grey in colour
0.9m	4.5	4.65	4	Clay black in colour
	6.0	6.15	4	Clay grey in colour
	7.5	7.65	3	
	9.0	9.15	4	
	10.5	10.65	8	Soil black in colour
	12.0	12.15	6	Clay grey in colour
	13.5	13.65	6	Clay grey in colour
	15.0	15.15	5	
	16.5	16.65	6	
	18.0	\18.15	6	Clay black in colour
	19.5	19.65	7	
38	1.5	2.0	2	Fill up soil upto 1.5 m depth
wl.	3.0	3.5	4	Clay grey to black in colour
1.1m	4.5	5.0	5	
	6.0	6.5	4	
	7.5	8.0	5	
	9.0	9.5	8	
	10.5	11.0	7	
	12.0	12.5	8	
	13.5	14.0	6	
	15.0	15.0	5	
	16.5	17.0	7	
	18.0	18.5	8	
	19.5	20.0	8	
39	1.5	2.0	2	Clay grey in colour
wl.	3.0	3.5	3	
1.2m	4.5	5.0	1	
	6.0	6.5	5	
	7.5	8.0	4	
	9.0	9.5	4	Clay soil black in colour

TH-994_06610404

	10.5	11.0	4	
	12.0	12.5	7	Clay grey in colour
	13.5	14.0	4	
	15.0	15.0	5	
	16.5	17.0	6	
	18.0	18.5	6	
	19.5	20.0	7	
40	1.5	2.0	2	Clay grey in colour
wl.	3.0	3.5	1	Clay grey in colour
0.9m	4.5	5.0	3	
	6.0	6.5	4	
	7.5	8.0	4	
	9.0	9.5	5	Clay black in colour
	10.5	11.0	3	
	12.0	12.5	5	Clay grey in colour
	13.5	14.0	7	
	15.0	15.0	8	
	16.5	17.0	7	
	18.0	18.5	6	
	19.5	20.0	8	
41	2.0	2.6	11	Med. Stiff, deep grey, silty clay with organic matters
wl.	3.4	4.0	6	
0.6m	5.5	6.1	11	
	8.0	8.6	9	
	11	11.6	13	Stiff light/deep grey, silty clay with lime patches and decay vegetation
	13	13.6	20	
	15.5	16.1	8	Med. Stiff to stiff, deep grey, clayey silt with lime patches, decay wood
	18	18.6	10	
	20.6	21.2	32	
	25	25.6	31	Very stiff, deep grey silty clay
	29.7	30.3	39	
42	1.5	2.1	10	Medium stiff deep grey silty clay with organic matters and decay vegetation
wl.	4.0	4.6	6	
0.6m	6.6	7.2	7	
	9.1	9.7	10	Stiff light grey silty clay with lime patched and decay wood/organic matter
	12.2	12.8	25	
	15.0	15.6	15	Very stiff, deep grey clayey silt with lime patched and micro trace of mica
	17.5	18.1	17	
	20.0	20.6	30	
	24.0	24.6	28	Very stiff, deep grey silty clay with lime
	28.0	28.6	31	

TH-994_06610404

	30.0	30.6	31	
43	1.6	2.1	8	Medium stiff, deep grey, silty clay with traces of organic matter
wl.	3.0	3.6	3	
0.75m	6.0	6.6	8	
	8.5	9.1	15	
	11.5	12.1	12	Stiff, deep grey, silty clay with lime patches and decay vegetation
	14.5	15.1	24	
	17.0	17.6	34	Very stiff deep grey clayey silt to silty clay with lime and decay wood, traces of sand
	20.0	20.6	29	
	23.0	23.6	31	
	26.5	27.1	45	Very stiff light grey silty clay
	29.5	30.1	46	
44	0.7	1.3	6	Medium stiff to stiff deep grey silty clay with traces of organic matter
wl.	2.5	3.1	8	
0.75m	7.0	7.6	6	
	11.0	11.6	11	Stiff deep grey silty clay with light grey patches and decay vegetation
	13.6	14.1	16	
	17.0	17.6	26	Very stiff deep grey clayey silt with patches of lime
	22.0	22.6	29	
	24.0	24.6	31	Very stiff light grey silty clay with traces of kankars
	28.0	28.6	32	
	29.4	30.0	38	
45	3	3.45	4	Grayish yellow firm silty clay
wl.	6	6.45	4	Grayish black soft silty clay
1.0m	9	9.45	4	Geryish black firm silty clay with occasional traces of decomposed wood
	12	12.45	4	
	15	15,45	9	
	18	18.45	12	Blackish to bluish grey firm clay with decomposed wood
	21	21.45	9	
	24	24.45	16	Grayish blue stiff silty clay
	27	27.45	11	
	30	30.45	17	
46	1	1.45	4	Greyish yellow to bluish grey firm silty clay
wl.	4	4.45	4	
0.7m	7	7.45	4	Greyish black soft silty clay with wood
	10	10.45	7	Greyish black firm silty clay with decomposed wood
	13	13.45	5	
	16	16.45	5	
	19	19.45	9	Bluish to blackish firm silty clay
	22	22.45	17	Grayish blue stiff silty clay

TH-994_06610404

	25	25.45	17	
	28	28.45	19	
	31	31.45	13	
	35	35.45	17	
47	1.5	2.0	3	Filled up soil mixed with bricks and boulder, gravel etc up to 0.9 m, clay, grey
wl.	3.0	3.5	3	Clay grey in black colour
0.5m	4.5	5.0	3	Clay grey in colour
	6.0	6.5	3	
	7.5	8.0	3	
	9.0	9.5	4	
	10.5	11.0	4	Clay grey to black in colour
	12.0	12.5	5	Clay grey in colour
	13.5	14.0	6	Clay mixed with silt and sand black in colour
	15.0		6	Pit Soil black in colour
	16.5	17	6	Clay grey to ash in Colour
	18.0	18.5	8	
	19.5	20.0	8	
	21.0	21.5	9	
	22.5	23.0	9	
	24.0	24.5	11	
48	1.5	2.0	3	Filled up soil mixed with bricks and boulder, gravel etc up to 0.8 m,
wl.	3.0	3.5	3	clay mixed with silt grey to ash in colour
0.52m	4.5	5.0	2	Clay grey to ash in colour
	6.0	6.5	3	
	7.5	8.0	4	
	9.0	9.5	4	
	10.5	11.0	4	Clay black in colour
	12.0	12.5	4	
	13.5	14.0	6	Clay grey to ash in colour
	15.0		5	Pit soil black in colour
	16.5	17.0	6	Clay grey to ash in colour
	18.0	18.5	6	
	19.5	20.0	7	
	21.0	21.5	7	
	22.5	23.0	8	Clay grey in colour
	24.0	24.5	10	
49	1.5	2.0	2	Filled up soil mixed with bricks and boulder, gravel etc up to 0.8 m, clay mixed with silt grey to ash in colour

TH-994_06610404

wl. 0.75m	3.0	3.5	3	Clay grey to black in colour
	4.5	5.0	2	Clay grey to ash in colour
	6.0	6.5	3	
	7.5	8.0	2	
	9.0	9.5	5	
	10.5	11.0	4	Clay black to ash in colour
	12.0	12.5	6	
	13.5	14.0	5	
	15.0	15.5	5	
	16.5	17.0	6	Clay grey to ash in colur
	18.0	18.5	8	
	19.5	20.0	7	
	21.0	21.5	6	
	22.5	23.0	7	Silty Sand brown in colour
	24.0	24.5	8	Clay grey to ash in colour
50	1.5	2.0	2	Filled up soil mixed with bricks and boulder, gravel etc up to 1.2 m
wl. 0.53m	3.0	3.5	3	clay mixed with silt grey to ash in colour
	4.5	5.0	3	Clay grey to ash in colour
	6.0	6.5	3	
	7.5	8.0	4	
	9.0	9.5	4	
	10.5	11.0	5	Clay black in colour
	12.0	12.5	4	
	13.5	14.0	6	
	15.0	15.5	5	
	16.5	17.0	6	Clay grey to ash in colour
	18.0	18.5	7	Silty Sand brown in colour
	19.5	20.0	7	
	21.0	21.5	8	
	22.5	23.0	9	
	24.0	24.5	9	Clay grey to ash in colour
51	1.5	2.0	3	Filled up soil mixed with bricks and boulder, gravel etc up to 1.0 m
wl. 0.79m	3.0	3.5	2	clay mixed with silt grey to ash in colour
	4.5	5.0	2	
	6.0	6.5	3	Clay grey to ash in colour
	7.5	8.0	4	
	9.0	9.5	4	Clay black in colour
	10.5	11.0	4	Clay black to ash in colour
	12.0	12.5	5	
	13.5	14.0	5	Clay grey to ash in colour
	15.0	15.5	4	Clay mixed with pit soil

TH-994_06610404

	16.5	17.0	6	Clay grey in colur
	18.0	18.5	6	Clay grey to ash in colour
	19.5	20.0	7	Clay black in colour
	21.0	21.5	8	Clay grey to ash in colour
	22.5	23.0	8	
	24.0	24.5	8	
52	1.5	2.0	3	Filled up soil mixed with bricks and gravel etc up to 0.8 m
wl. 0.65m	3.0	3.5	2	Clay grey in colour
	4.5	5.0	3	
	6.0	6.5	4	
	7.5	8.0	4	
	9.0	9.5	4	Clay grey to black in colour
	10.5	11.0	3	Clay black in colour
	12.0	12.5	4	
	13.5	14.0	5	Clay grey to ash in colour
	15.0	15.5	4	Pit soil black in colour
	16.5	17.0	5	
	18.0	18.5	6	
	19.5	20.0	7	Clay grey to ash in colour
	21.0	21.5	8	
	22.5	23.0	8	
	24.0	24.5	9	
53	1.05		9	Hard hilly soil
wl. 0.5m	2		12	Hard soil, very hard and dry in nature
	3.1		15	Hard soil, very hard and dry in nature
	4.0		20	Hard dense soil, hard and dry in nature
54	2.2		2	Medium stiff clay light grey in colour
wl. 1.5m	3.15		4	Peat and other organic swamp
	4.1		6	Soft clay, grey in colour
	5.15		6	Peat and other organic swamp
	6.1		6	Soft clay, grey in colour
55	2.1		2	Medium stiff clay, light grey in colour
wl. 1.5m	3.15		4	Peat and other organic swamp mix with clay
	4.2		5	Soft clay, grey in colour
	5.2		7	Peat and other organic swamp
	6.1		5	Soft clay, dark grey in colour
56	2		2	Medium stiff clay, black in colour
wl. 0.5m	3.2		4	Soft clay, grey in colour
	4.1		6	

TH-994_06610404

	5.2		5	Peat and other organic swamp
	6.1		9	Silty sand mix with clay binders
57	2.2		2	Medium stiff clay, black in colour
wl.	3.1		4	Soft clay, grey in colour
1.0m	4.15		6	
	5.2		5	Peat and other organic swamp
	6.15		9	Silty sand mix with clay binders
58	1.5		4	Soft clay, brownish in colour
wl.	2.1		6	Sandy clay, brownish in colour
0.2m	3.35		6	
	4.0		5	Soft clay, grey in colour
	5.25		5	Stiff clay, light grey in colour
59	1.2		4	Medium Stiff grayish clay
wl.	2.15		6	Medium Stiff grayish clay
1.2m	3.15		7	Medium Stiff grayish clay mixed with peat and organic
	4.1		5	swamp soil
	5.3		5	Medium Stiff grayish clay. Soft in nature
60	1.2		5	Medium Stiff clay, grey in colour
wl.	2.1		6	Very stiff in nature
0.55m	3.15		6	
	4.05		8	
	5.2		6	Very stiff clay, light grey in colour
	6.1		7	
	7.15		9	Stiff clay, grey in colour
61	3.1		6	Medium stiff clay, grey in colour
wl.	4.2		5	
0.5m	5.2		6	Mix with peat and other organic swamp
62	1.5		5	Medium stiff clay, grey in colour
wl.	2.1		6	Medium stiff clay, light grey in colour
0.35m	3.3		5	
	4.15		5	Loose soft soil, organic swamp
	5.1		6	Soft clay, grey in colour, silt in traces
63	1.2		5	Medium stiff clay, light grey in colour
wl.	2.15		6	Medium stiff clay, dark grey in colour
0.5m	3.2		8	Stiff clay, grey in colour
	4.1		9	Medium stiff clay, grey in colour, soft in nature
	5.2		12	

TH-994_06610404

64	2.4		5	Soft silty sand, mix with clay
wl.	3.2		6	
1.05m	4.1		7	Low to medium consistency, Greyey colour
	5.2		8	Soft silty clay, grey in colour
	6.15		10	Silty clay, grey in colour
65	1.2		8	Hard soil, brownish colour
wl.	2.25		10	Hard dense soil mix with shale
1.55m	3.1		15	
66	1.25		5	Medium stiff clay, light grey in colour
wl.	2.2		6	Medium stiff clay, grey in colour
2.25m	3		8	Soft silty clay, grey in colour
	4.1		8	
67	1.05		5	Medium stiff clay, light grey in colour
wl.	2.15		7	Stiff clay, grey in colour
0.5m	3.1		8	
	4.05		11	Medium stiff clay, trace of silt, grey in colour
	5.1		13	
68	1.5		5	Medium stiff clay, light grey in colour
wl.	2.4		6	Medium stiff clay, brown in colour
0.5m	3.45		7	Medium stiff clay, grey in colour
	4.0		8	
	4.75		9	Soft clay, dark grey in colour
	5.9		11	
69	1.25		4	Medium stiff clay,dark grey colour
wl.	2.2		5	Medium stiff clay, grey colour, organic
0.53m	3		6	Medium stiff clay, black in colour, soft nature
	4.2		7	
	5.15		10	Medium stiff clay, dark grey in colour, soft
70	1.2		4	Medium stiff clay, dark grey colour
wl.	2.15		5	Medium stiff clay, dark grey colour, organic
0.5m	3.1		6	Medium stiff clay, black colour
	4.15		6	Medium stiff clay, dark grey colour, silt trace
	5.2		9	
71	1.15		4	Medium stiff clay, brownish colour
wl.	2.05		5	Medium stiff clay, dark grey colour, organic
0.53m	3.15		6	stiff clay, grey colour

TH-994_06610404

	4.25		9	Medium stiff clay, dark grey in colour, silt trace, soft in nature
	5.1		10	
72	1.05		4	Medium stiff clay, brownish in colour
wl.	2.2		6	Very clay, dark grey in colour, organic
0.3m	3.1		7	Medium stiff clay, grey colour, soft nature
	4.05		9	
	5.0		11	stiff clay, black in colour, silt trace
73	1.1		4	Medium stiff clay, light grey colour
wl.	2.15		5	Medium stiff clay, grey colour, organic
0.54m	3.2		6	Medium stiff clay, black in colour, soft nature
	4.15		8	
	5.05		9	Medium stiff clay, dark grey color, silt trace
74	1.2		4	stiff clay, brownish in colour
wl.	2.05		6	stiff clay, grey colour
0.52m	3.15		6	Medium stiff clay, dark grey colour
	4.15		8	
	5.2		10	Medium stiff clay, dark grey, soft nature
75	1.15		4	Medium stiff clay, grey colour
wl.	2.1		5	
0.60m	3.05		7	stiff clay, grey colour, soft nature
	4.2		8	Medium stiff clay, grey in colour, silt trace
	5.1		10	
76	1.1		4	Medium stiff clay, light grey colour
wl.	2.15		5	Medium stiff clay, grey colour
0.65m	3.1		6	Medium stiff clay, grey colour, soft nature
	4.15		8	Medium stiff clay, black in colour
	5.2		9	Medium stiff clay, black in colour, silt trace
77	1.2		4	Medium stiff clay. Brownish colour
wl.	2.2		5	Stiff clay, dark grey in colour
0.62m	3.15		6	Stiff clay, grey in colour and soft nature
	4.2		7	
	5.15		8	Medium stiff clay, grey in colour, silt mixes
78	1.2		4	Sandy soil, drak grey in colour, silt traces
wl.	2.2		6	Medium stiff clay, light grey in colour
0.35m	3.0		6	Very stiff clay, light grey in colour
	4.2		7	Silty clay, grey in colour

TH-994_06610404

	5.35		8	Very stiff silty clay, grey in colour
79	1.15		4	Sandy soil, drak grey in colour, silt traces
wl.	2.25		5	Medium stiff clay, grey in colour
0.33m	3.1		6	
	4.15		8	Sand silty clay,black in colour
	5.2		8	soft stiff silty clay, dark grey in colour
80	1.1		4	Sandy soil, drak grey in colour, silt traces
wl.	2.3		6	Medium stiff clay, grey in colour
0.34m	3.2		7	Sandy clay, silt traces,dark grey in colour
	4.25		8	Silty clay, grey in colour
	5.3		8	silty clay, dark grey in colour
81	2.38		4	Medium stiff clay, brownish in clour
wl.	3.2		6	Medium stiff clay, light grey in colour
0.5m	4.05		8	Silty sand mix with clay, grey in colour
	5.15		11	Silty sand mix with clay, soft in nature
82	2.35		4	Medium stiff clay, brownish in clour
wl.	3.4		8	Medium stiff clay, grey in colour
0.52m	4.25		8	Silty sand mix with clay, light grey in colour
	5.05		11	Silty sand mix with clay, soft in nature
83	2.25		4	Medium stiff clay, brownish in clour
wl.	3.3		6	Very stiff clay, grey in colour
0.55m	4.25		8	Silty sand mix with clay, dark grey in colour
	5.2		8	Silty sand mix with clay, soft in nature
84	2.25		4	Medium Stiff clay, grey in colour
wl.	3.3		6	
0.55m	4.25		8	Medium Stiff clay, dark grey in colour
	5.2		10	Silty sand, mix with clay, grey in colour
85	1.05		18	Hard soil, medium stiff, brown in colour
wl.	2.02		28	Stiff clay, mix with dust, brownish in colour
2.5m	3.15		30	Hard Shale, very stiff
86	1.1		20	Hard soil, medium stiff, brown in colour
wl.	2.5		26	Hard dense soil, brownish in colour
2.0m	3.0		30	Hard Shale, very stiff
87	2.3		4	Medium stiff clay, black in colour
1.5m	3.2		5	Medium stiff clay, silt in traces, light in colour

TH-994_06610404

	4.2		4	Medium stiff clay, grey in colour, poorly graded
	5.2		5	Medium stiff clay, soft in nature, grey in colour.
	6.1		7	
88	2.2		4	Medium stiff clay, black in colour
wl.	3.15		5	Medium stiff clay, dark grey in colour, poorly graded
1.4m	4.1		5	
	5.15		6	Medium stiff clay, grey in colour, traces of silt
	6.0		7	
89	2.3		3	Soft clay, silt traces, black
wl.	2.6		3	Soft sandy clay, light grey
2.25m	3.2		4	Soft sandy clay, light grey, poorly graded
	3.6		5	Medium stiff clay, grey
	4.1		5	Silty clay, mix with sand, grey
	4.55		6	
	5.2		7	Silty sand with clay binders, dark grey
	5.6		7	Sandy clay, grey, traces of silt
90	1.2		4	Medium stiff clay, brownish
wl.	2.05		5	Medium stiff clay, black
1.0m	3.15		3	Soft silty clay, grey
	4.2		8	Silty sand, grey
	5.2		9	Medium stiff clay, sand silt in mixes
91	1.45		4	Soft clay, grey
wl.	2.2		6	Soft silty clay, grey
0.12m	3.1		7	
	4.25		8	Soft silty clay, grey
	5.15		8	Soft silty clay, light grey in colour
92	1.25		4	Soft clay, mix with sand, dark grey
wl.	2.3		5	Medium stiff clay, poorly graded, grey
0.73m	3.05		8	Stiff clay, grey in colour
	4.3		9	Medium stiff clay, light grey
	5.2		9	Medium stiff clay, soft nature, dark grey
93	1.5		4	Sandy soil, light grey
wl.	2.1		5	Medium stiff clay, sand silt mixes, grey
0.72m	3.2		8	Medium stiff clay, dark grey
	4.2		9	
	5.35		10	Stiff clay, dark grey
94	1.3		4	Soft clay, poorly graded, dark grey

TH-994_06610404

wl. 0.75m	2.15		6	Sand silt clay, grey
	3.1		8	Sandy clay, dark grey
	4.25		9	Medium stiff clay, grey
	5.1		9	Medium stiff clay, dark grey, soft in nature
95	1.2		4	Soft clay, poorly graded
wl. 0.75m	2.4		5	Sand silt clay, grey
	3.25		7	Sandy clay, dark grey
	4.3		8	Medium stiff clay, grey
	5.25		9	Medium stiff clay, dark grey, soft in nature
96	1.3		5	Medium stiff clay, light grey
wl. 0.7m	2.65		5	Medium stiff clay, sand silt in mixes, brown
	3.25		7	Sandy soil, soft nature, grey
	4.3		8	Clayey silt, grey
	5.25		9	Soft clay, dark grey, silt traces
97	1.2		5	Medium stiff clay, light grey
wl. 0.8m	2.5		5	Medium stiff clay, sand silt mixes, brown
	3.25		6	Sandy soil, soft nature
	4.4		8	Sandy loam, silt traces, grey
	5.7		11	Clayey silt, dark grey
98	1.25		5	Stiff clay, grey
wl. 0.75m	2.3		6	Medium stiff clay, grey
	3.2		8	Medium stiff clay, dark grey, soft nature
	4.25		9	
	5.2		10	Clayey silt, steel grey
99	1.2		5	Medium stiff clay, grey
wl. 0.65m	2.25		6	
	3.3		6	Silty clay, grey, soft nature
	4.25		8	
	5.15		10	Clayey silt, dark grey
100	1.25		4	Fill up portion with clay binders
wl. 0.80m	2.5		8	Medium stiff clay
	2.75		9	Clay, light grey, with silt
101	1.0	1.45	4	Grayish yellow to bluish grey firm silty clay
wl. 0.85m	4.0	4.45	4	
	7.0	7.45	4	Grayish black soft silty clay with occasional traces of decomposed wood
	10.0	10.45	7	Blackish to bluish gray firm silty clay with varying

TH-994_06610404

	13.0	13.45	5	percentage of decomposed wood
	16.0	16.45	5	
	19.0	19.45	9	Bluish to blackish grey firm silty clay with varying percentage of decomposed wood
	22.0	22.45	17	Grayish blue stiff silty clay
	25.0	25.45	17	
	28.0	28.45	19	
	31.0	31.45	13	
	35.0	35.45	17	
102	3.00	3.45	4	Grayish yellow to Bluish grey firm silty clay
wl.	6.00	6.45	4	Grayish black soft silty clay with occasional traces of
0.85m	9.00	9.45	4	decomposed wood
	12.0	12.45	4	Blackish to bluish gray firm silty clay with varying percentage of decomposed wood
	15.0	15.45	9	
	18.0	18.45	12	
	21.0	21.45	9	Grayish blue /bluish grey stiff silty clay
	24.0	24.45	16	
	27.0	27.45	11	
	30.0	30.45	17	
103	1.2		5	Medium stiff clay, grey
wl.	2.1		6	Medium stiff clay, silt in traces, dark grey
0.5m	3.15		7	Silty clay, grey, soft nature
	4.2		9	Clay, dark grey, silt in traces
	5.1		10	Clay, still grey, soft nature
104	1.5		7	Soft clay, dark grey
wl.	2.25		10	Sandy soil silt trace
0.4m	3.2		6	Stiff clay, light grey
	3.75		8	Medium stiff clay, grey
	5.3		11	Soft clay, silt traces, dark grey
105	1.45		4	Medium stiff clay, silt in traces, grey
wl.	2.35		5	Sandy clay, silt in traces with clay binders,
0.5m	3.35		7	Grey
	4.1		7	Sand silt clay, grey, soft nature
	5.0		8	
	5.9		9	Silty sand mix with clay, dark grey
106	1.5		4	Soft clay, medium stiff, silt sand mixes, grey
wl.	2.4		4	Sand silt clay, light grey
0.5m	3.45		7	Medium stiff clay, silt sand in mixes, grey
	4.0		7	

TH-994_06610404

	4.75		8	Soft clay, dark grey
	5.9		9	Silty sand mixes with clay, dark grey
107	1.8		6	Stiff clay, brown
wl.	2.75		9	Stiff clay, yellow
0.5m	3.3		9	Medium stiff clay, grey
	4.6		9	Clay, dark grey, soft nature
	5.55		10	Soft clay, poorly graded
108	1.75		6	Medium stiff clay, light grey
wl.	2.8		8	Stiff clay, brown
0.5m	3.7		9	Medium stiff clay, grey
	4.5		9	Soft clay, dark grey
	5.45		10	Soft clay, poorly graded, dark grey
109	1.5		6	Medium stiff clay, light grey
wl.	2.25		7	Clay, grey, silt in traces
0.5m	3.5		8	Soft clay grey
	4.0		9	
	4.75		10	Soft silty clay, grey
110	2.2		7	Sandy clay, grey, soft nature
wl.	2.8		4	Medium stiff clay, grey
0.3m	3.25		4	Soft silty clay, grey
	5.35		7	Silty sand mix with clay binders, grey
111	2.0		5	Sandy clay, grey
wl.	2.75		6	
0.2m	3.45		9	Medium stiff clay, grey
	5.35		10	Silty sand mix with clay binders, grey
112	1.6		4	Medium stiff clay, light grey
wl.	2.25		5	Medium stiff clay, grey
0.5m	3.05		7	Medium stiff clay, brown
	3.5		7	Soft silty clay, grey
	4.1		8	Silty clay, grey
	4.5		8	
	5.0		10	
	5.55		12	Clayey silt, loamy clay
	6.25		13	
113	3.0		6	soft silty clay, light grey
wl.	3.6		6	Soft clay, decayed organic matters, grey
0.5m	4.1		6	Soft clay sandy silt in mix

TH-994_06610404

	4.75		7	Medium stiff clay, grey
	5.3		9	Soft clay, grey
	5.8		9	Medium stiff clay, soft in nature
114	2.35		5	Silty sand mix with clay binders,yellow
wl.	3.6		6	Soft silty clay, grey in colour
0.5m	4.25		6	Soft clay, sand silt mix
	4.7		8	Medium stiff clay, grey
	5.4		9	Sandy soil silt trace
	5.85		9	Stiff clay, dark grey
115	1.5		8	Medium stiff clay, light grey
wl.	2.5		8	Clayey silt
0.85m	3.0		9	Clayey silt
	3.5		9	Very soft clay, grey
	4.0		8	Sandy clay, silt in traces
	4.5		8	Sandy clay silt in traces
	5.0		8	Soft clay, grey
116	2.75		4	Medium stiff clay, brown
wl.	3.5		5	Soft silty clay, grey, silt in traces
0.5m	4.5		7	Medium stiff clay, grey, silt in traces
	5.5		13	Medium stiff clay, dark grey, soft nature
117	1.0		5	Clay, poorly graded, light grey
wl.	2.0		6	Clayey silt, grey, soft nature
0.5m	3.0		8	Medium stiff clay, light grey, silt in traces
	4.0		8	Sand silt, clay binders, grey, soft nature
	5.0		9	Very soft silt sand mix, with clay binders
118	1.0		5	Clay, poorly graded, grey
wl.	2.0		6	Stiff clay
0.5m	3.0		7	Sand silt with clay binders, grey, soft nature
	4.0		8	Soft clay, sand silt mixture, grey
	5.0		8	Very soft clay, sand and silt mix
119	1.0		6	Medium stiff clay
wl.	2.0		6	Clayey silt, grey, soft nature
0.5m	3.0		8	Silty sand with clay, grey, soft nature
	4.0		8	Soft clay, sand silt mix
	5.0		9	Clayey silt with fine sand, soft nature
	6.0		9	Very soft clay, silt sand mix
120	1.0		6	Stiff clay
0.5m	2.0		5	Clayey silt, light grey

TH-994_06610404

	3.0		6	Soft silty sand, with clay binders, grey
	4.0		5	
	5.0		9	Very soft clay, sand and silt mix
121	9		7	Clay deposits
wl.	12		8	clay loam, grey
0.4m	15		7	Clay, soft in nature
122	1.25		4	Silty sand mix with clay binder, brown
wl.	2.0		5	Soft silty clay, grey
0.5m	3.1		6	
	4.05		7	Silty sand, soft nature
	5.1		8	Sandy loam

TH-994_06610404

Appendix C

Site coefficients developed in Chapter 4 for 122 boreholes are shown below:

Site 1				**Site 2**			
period	**a_1**	**a_2**	**δ**	**period**	**a_1**	**a_2**	**δ**
PGA	0.1094	0.4330	0.1882	PGA	-0.1322	0.4671	0.1886
0.030	0.0571	0.4385	0.1909	0.030	-0.0847	0.4641	0.1901
0.040	0.1103	0.4330	0.1882	0.040	-0.1324	0.4672	0.1886
0.100	-0.0896	0.4330	0.1597	0.100	-0.3040	0.4502	0.1659
0.200	0.0207	0.3826	0.1355	0.200	-0.1410	0.4233	0.1438
0.300	-0.1358	0.7007	0.1980	0.300	-0.2177	0.4821	0.1462
0.400	0.0123	0.7776	0.2354	0.400	-0.3093	0.8035	0.1976
1.000	0.1741	0.1456	0.0600	1.000	0.3243	0.2556	0.1029
2.000	-0.0332	0.1063	0.0727	2.000	0.0193	0.1321	0.1154
3.000	-0.1734	0.1450	0.0973	3.000	-0.2597	0.1771	0.1461
Site 3				**Site 4**			
period	**a_1**	**a_2**	**δ**	**period**	**a_1**	**a_2**	**δ**
PGA	0.0565	0.4385	0.2029	PGA	-0.0475	0.5413	0.2231
0.030	0.0364	0.4426	0.2050	0.030	-0.0199	0.5378	0.2251
0.040	0.0567	0.4385	0.2029	0.040	-0.0471	0.5413	0.2231
0.100	-0.1658	0.4333	0.1691	0.100	-0.2325	0.5847	0.1952
0.200	-0.1492	0.4618	0.1634	0.200	-0.0387	0.4967	0.1598
0.300	-0.2208	0.9096	0.2802	0.300	-0.2255	0.7380	0.1971
0.400	0.1255	0.6453	0.2366	0.400	-0.2083	0.9878	0.2699
1.000	0.1524	0.1038	0.0479	1.000	0.2546	0.1864	0.0806
2.000	-0.0200	0.0927	0.0522	2.000	-0.0123	0.1168	0.0983
3.000	-0.1053	0.1153	0.0699	3.000	-0.2217	0.1631	0.1317

Site 5				**Site 6**			
period	**a_1**	**a_2**	**δ**	**period**	**a_1**	**a_2**	**δ**
PGA	-0.2479	0.5191	0.2204	PGA	0.0195	0.4379	0.1877
0.030	-0.2353	0.5196	0.2235	0.030	0.0387	0.4372	0.1893
0.040	-0.2477	0.5192	0.2204	0.040	0.0200	0.4379	0.1876
0.100	-0.2472	0.4502	0.1937	0.100	-0.0840	0.3837	0.1549
0.200	-0.2977	0.3834	0.1930	0.200	-0.0407	0.3333	0.1424
0.300	-0.5578	0.7182	0.1990	0.300	-0.1584	0.6078	0.1718
0.400	-0.4482	1.0371	0.2799	0.400	-0.1087	0.8528	0.2436
1.000	0.3163	0.1942	0.1074	1.000	0.1893	0.1728	0.0686
2.000	-0.0096	0.1351	0.1299	2.000	-0.0365	0.1114	0.0848
3.000	-0.3011	0.1944	0.1699	3.000	-0.2176	0.1593	0.1173
Site 7				**Site 8**			
period	**a_1**	**a_2**	**δ**	**period**	**a_1**	**a_2**	**δ**
PGA	0.0775	0.4148	0.1998	PGA	0.0879	0.4244	0.1824
0.030	0.0460	0.4196	0.2009	0.030	0.0440	0.4302	0.1829
0.040	0.0782	0.4148	0.1998	0.040	0.0888	0.4243	0.1824
0.100	-0.1145	0.4715	0.1926	0.100	-0.0550	0.4341	0.1567
0.200	-0.1464	0.4793	0.1780	0.200	-0.0053	0.3445	0.1312
0.300	-0.1225	0.8447	0.2776	0.300	-0.1365	0.6331	0.1775
0.400	0.2232	0.5264	0.1979	0.400	-0.0244	0.7850	0.2311
1.000	0.1121	0.0924	0.0384	1.000	0.1645	0.1568	0.0619
2.000	-0.0258	0.0895	0.0415	2.000	-0.0427	0.1080	0.0757
3.000	-0.0853	0.0997	0.0598	3.000	-0.1905	0.1496	0.1032
Site 9				**Site 10**			
period	**a_1**	**a_2**	**δ**	**period**	**a_1**	**a_2**	**δ**
PGA	-0.0808	0.4642	0.1939	PGA	0.1268	0.4322	0.2096
0.030	-0.0427	0.4622	0.1942	0.030	0.1203	0.4335	0.2106
0.040	-0.0803	0.4642	0.1939	0.040	0.1278	0.4321	0.2095
0.100	-0.1567	0.4229	0.1611	0.100	-0.1173	0.4948	0.2010
0.200	-0.0848	0.3661	0.1437	0.200	-0.0793	0.4979	0.1821
0.300	-0.2281	0.6740	0.1883	0.300	-0.1007	0.8643	0.2803
0.400	-0.1658	0.8860	0.2499	0.400	0.2390	0.5496	0.2033
1.000	0.2486	0.1607	0.0704	1.000	0.1235	0.0960	0.0409
2.000	-0.0150	0.1140	0.0884	2.000	-0.0237	0.0911	0.0441
3.000	-0.2070	0.1610	0.1174	3.000	-0.0889	0.1042	0.0630

Site 11				**Site 12**			
period	**a_1**	**a_2**	**δ**	**period**	**a_1**	**a_2**	**δ**
PGA	-0.5101	0.6320	0.2211	PGA	-0.1940	0.4384	0.1464
0.030	-0.4853	0.6322	0.2240	0.030	-0.1398	0.4327	0.1484
0.040	-0.5100	0.6320	0.2211	0.040	-0.2025	0.4393	0.1464
0.100	-0.6412	0.5623	0.2212	0.100	-0.3108	0.4306	0.1307
0.200	-0.4691	0.7004	0.1643	0.200	-0.3276	0.5779	0.1342
0.300	-0.2263	0.4961	0.1974	0.300	-0.0428	0.3422	0.1239
0.400	-0.4462	0.6571	0.1824	0.400	-0.1490	0.4407	0.1243
1.000	0.2421	0.5783	0.2386	1.000	0.3080	0.3801	0.1143
2.000	0.1004	0.2335	0.2002	2.000	0.0607	0.1618	0.1180
3.000	-0.3913	0.2379	0.2223	3.000	-0.2362	0.1652	0.1347
Site 13				**Site 14**			
period	**a_1**	**a_2**	**δ**	**period**	**a_1**	**a_2**	**δ**
PGA	-0.1390	0.5291	0.1797	PGA	-0.1059	0.4375	0.1845
0.030	-0.0923	0.5266	0.1806	0.030	-0.0430	0.4303	0.1863
0.040	-0.1386	0.5290	0.1797	0.040	-0.1200	0.4391	0.1844
0.100	-0.2945	0.4835	0.1547	0.100	-0.2679	0.4960	0.1745
0.200	-0.3845	0.5488	0.1447	0.200	-0.1474	0.3238	0.1429
0.300	-0.0853	0.6415	0.1430	0.300	-0.3194	0.7141	0.2019
0.400	-0.0672	0.6480	0.1474	0.400	-0.1500	0.8176	0.2494
1.000	0.3965	0.3728	0.1226	1.000	0.2043	0.1419	0.0628
2.000	0.0824	0.1663	0.1316	2.000	-0.0321	0.1121	0.0806
3.000	-0.2384	0.1732	0.1493	3.000	-0.1951	0.1544	0.1085
Site 15				**Site 16**			
period	**a_1**	**a_2**	**δ**	**period**	**a_1**	**a_2**	**δ**
PGA	0.2234	0.5827	0.2577	PGA	0.1163	0.4301	0.2111
0.030	0.1868	0.5864	0.2577	0.030	0.0736	0.4376	0.2115
0.040	0.2246	0.5826	0.2577	0.040	0.1175	0.4300	0.2111
0.100	-0.1223	0.6755	0.2394	0.100	-0.0971	0.4460	0.1851
0.200	0.0779	0.6506	0.2094	0.200	-0.1157	0.5416	0.2020
0.300	-0.0869	0.9298	0.2652	0.300	-0.0371	0.8360	0.2841
0.400	0.0804	0.8945	0.2771	0.400	0.2761	0.4958	0.1897
1.000	0.2165	0.1505	0.0691	1.000	0.0978	0.0908	0.0353
2.000	-0.0092	0.1064	0.0773	2.000	-0.0271	0.0860	0.0378
3.000	-0.1702	0.1431	0.1038	3.000	-0.0873	0.0955	0.0579

Site 17				**Site 18**			
period	**a_1**	**a_2**	**δ**	**period**	**a_1**	**a_2**	**δ**
PGA	0.0622	0.3809	0.1785	PGA	0.1359	0.3712	0.1738
0.030	0.0582	0.3826	0.1787	0.030	0.1193	0.3730	0.1750
0.040	0.0625	0.3809	0.1785	0.040	0.1370	0.3711	0.1738
0.100	-0.1812	0.4890	0.1927	0.100	-0.0654	0.3743	0.1495
0.200	-0.1568	0.3941	0.1438	0.200	-0.0509	0.4063	0.1423
0.300	-0.1657	0.7818	0.2440	0.300	-0.0641	0.7223	0.2287
0.400	0.1258	0.5678	0.2035	0.400	0.1860	0.5423	0.1841
1.000	0.1229	0.0994	0.0415	1.000	0.1046	0.1038	0.0391
2.000	-0.0345	0.0973	0.0481	2.000	-0.0372	0.0956	0.0469
3.000	-0.1091	0.1100	0.0675	3.000	-0.1002	0.1074	0.0673
Site 19				**Site 20**			
period	**a_1**	**a_2**	**δ**	**period**	**a_1**	**a_2**	**δ**
PGA	0.1955	0.3474	0.1854	PGA	0.1061	0.4088	0.1949
0.030	0.1700	0.3501	0.1862	0.030	0.1101	0.4085	0.1941
0.040	0.1966	0.3473	0.1854	0.040	0.1067	0.4088	0.1949
0.100	0.0389	0.3619	0.1647	0.100	-0.1363	0.5154	0.2028
0.200	-0.0986	0.5858	0.2327	0.200	-0.1065	0.4458	0.1588
0.300	0.1545	0.5808	0.2185	0.300	-0.1342	0.8144	0.2574
0.400	0.2659	0.3212	0.1243	0.400	0.1777	0.5706	0.2025
1.000	0.0549	0.0677	0.0217	1.000	0.1227	0.1010	0.0419
2.000	-0.0128	0.0735	0.0270	2.000	-0.0318	0.0957	0.0477
3.000	0.0246	0.0790	0.0754	3.000	-0.1022	0.1096	0.0678
Site 21				**Site 22**			
period	**a_1**	**a_2**	**δ**	**period**	**a_1**	**a_2**	**δ**
PGA	-0.2347	0.5235	0.1728	PGA	-0.2694	0.5766	0.1827
0.030	-0.2027	0.5209	0.1743	0.030	-0.2011	0.5672	0.1844
0.040	-0.2346	0.5235	0.1728	0.040	-0.2689	0.5766	0.1827
0.100	-0.4022	0.4951	0.1494	0.100	-0.5498	0.6304	0.1676
0.200	-0.4441	0.7288	0.1866	0.200	-0.4567	0.8515	0.2147
0.300	-0.0137	0.4735	0.1304	0.300	-0.0050	0.4783	0.1331
0.400	-0.1304	0.5650	0.1376	0.400	-0.1276	0.5468	0.1343
1.000	0.3765	0.3663	0.1295	1.000	0.3626	0.3935	0.1421
2.000	0.1769	0.1538	0.1299	2.000	0.2419	0.1571	0.1356
3.000	-0.1593	0.1681	0.1472	3.000	-0.1308	0.1697	0.1511

Site 23				**Site 24**			
period	**a_1**	**a_2**	**δ**	**period**	**a_1**	**a_2**	**δ**
PGA	-0.2503	0.5037	0.1665	PGA	-0.2623	0.4902	0.1636
0.030	-0.2193	0.5014	0.1676	0.030	-0.2364	0.4893	0.1646
0.040	-0.2500	0.5037	0.1665	0.040	-0.2620	0.4901	0.1635
0.100	-0.5137	0.5162	0.1466	0.100	-0.5667	0.4980	0.1452
0.200	-0.5524	0.6759	0.1618	0.200	-0.5317	0.6483	0.1514
0.300	-0.0439	0.4608	0.1243	0.300	-0.0663	0.4341	0.1254
0.400	-0.1634	0.5475	0.1322	0.400	-0.1829	0.5115	0.1293
1.000	0.3533	0.3822	0.1360	1.000	0.3293	0.4117	0.1411
2.000	0.2110	0.1555	0.1326	2.000	0.2153	0.1634	0.1354
3.000	-0.1430	0.1692	0.1491	3.000	-0.1544	0.1724	0.1508
Site 25				**Site 26**			
period	**a_1**	**a_2**	**δ**	**period**	**a_1**	**a_2**	**δ**
PGA	-0.2240	0.4482	0.1589	PGA	-0.2689	0.4712	0.1624
0.030	-0.1973	0.4466	0.1605	0.030	-0.2568	0.4711	0.1636
0.040	-0.2241	0.4482	0.1589	0.040	-0.2689	0.4713	0.1624
0.100	-0.4283	0.4266	0.1461	0.100	-0.5069	0.4616	0.1462
0.200	-0.5480	0.6633	0.1617	0.200	-0.6919	0.7013	0.1651
0.300	-0.0597	0.3430	0.1397	0.300	-0.0510	0.3676	0.1376
0.400	-0.2102	0.5270	0.1371	0.400	-0.2128	0.5021	0.1320
1.000	0.3712	0.3455	0.1404	1.000	0.3386	0.3949	0.1434
2.000	0.2587	0.1398	0.1301	2.000	0.2308	0.1568	0.1349
3.000	-0.1134	0.1715	0.1485	3.000	-0.1448	0.1721	0.1510
Site 27				**Site 28**			
period	**a_1**	**a_2**	**δ**	**period**	**a_1**	**a_2**	**δ**
PGA	-0.1535	0.4863	0.1618	PGA	-0.2203	0.4891	0.1596
0.030	-0.0774	0.4805	0.1626	0.030	-0.1630	0.4841	0.1610
0.040	-0.1529	0.4863	0.1618	0.040	-0.2201	0.4891	0.1596
0.100	-0.5366	0.4892	0.1466	0.100	-0.5491	0.5021	0.1410
0.200	-0.5149	0.6160	0.1371	0.200	-0.5876	0.6351	0.1399
0.300	0.0316	0.4570	0.1403	0.300	0.0460	0.4379	0.1341
0.400	-0.0501	0.4864	0.1373	0.400	-0.0408	0.4733	0.1311
1.000	0.4377	0.4160	0.1435	1.000	0.4259	0.4153	0.1361
2.000	0.3106	0.1643	0.1399	2.000	0.2498	0.1677	0.1363
3.000	-0.0848	0.1663	0.1521	3.000	-0.1257	0.1665	0.1492

Site 29				**Site 30**			
period	**a_1**	**a_2**	**δ**	**period**	**a_1**	**a_2**	**δ**
PGA	-0.2717	0.4859	0.1659	PGA	-0.2267	0.4746	0.1687
0.030	-0.2453	0.4853	0.1669	0.030	-0.1619	0.4686	0.1715
0.040	-0.2717	0.4859	0.1659	0.040	-0.2264	0.4746	0.1687
0.100	-0.6496	0.4838	0.1550	0.100	-0.4551	0.4632	0.1538
0.200	-0.6659	0.6020	0.1425	0.200	-0.6723	0.6653	0.1624
0.300	-0.0463	0.4482	0.1384	0.300	0.0188	0.3885	0.1460
0.400	-0.1021	0.5035	0.1333	0.400	-0.1150	0.5309	0.1371
1.000	0.3419	0.4320	0.1598	1.000	0.3970	0.3775	0.1596
2.000	0.3185	0.1651	0.1458	2.000	0.3252	0.1488	0.1426
3.000	-0.1018	0.1745	0.1599	3.000	-0.0920	0.1738	0.1587
Site 31				**Site 32**			
period	**a_1**	**a_2**	**δ**	**period**	**a_1**	**a_2**	**δ**
PGA	-0.0302	0.3700	0.2003	PGA	0.0796	0.3359	0.1894
0.030	0.0093	0.3655	0.2003	0.030	0.1224	0.3268	0.1883
0.040	-0.0297	0.3699	0.2003	0.040	0.0798	0.3358	0.1894
0.100	-0.0840	0.3305	0.1611	0.100	-0.0531	0.3595	0.1795
0.200	-0.3197	0.7681	0.3264	0.200	0.1867	0.5813	0.2884
0.300	0.4064	0.3575	0.2089	0.300	0.2897	0.2629	0.1591
0.400	0.2304	0.2381	0.1935	0.400	0.2487	0.1511	0.1267
1.000	0.2346	0.0334	0.0504	1.000	0.1305	0.0364	0.0501
2.000	0.0349	0.0744	0.0366	2.000	-0.0128	0.0815	0.0196
3.000	-0.0207	0.0853	0.0289	3.000	0.0130	0.0646	0.0325
Site 33				**Site 34**			
period	**a_1**	**a_2**	**δ**	**period**	**a_1**	**a_2**	**δ**
PGA	-0.3688	0.4701	0.2059	PGA	-0.1672	0.3929	0.1975
0.030	-0.3762	0.4718	0.2057	0.030	-0.1366	0.3881	0.1979
0.040	-0.3690	0.4701	0.2059	0.040	-0.1673	0.3929	0.1975
0.100	-0.6072	0.4690	0.1855	0.100	-0.0785	0.3336	0.1614
0.200	-0.4561	0.3917	0.1701	0.200	-0.6125	0.7006	0.2764
0.300	-0.9393	0.8017	0.2261	0.300	0.1611	0.5757	0.2569
0.400	-0.3601	0.8607	0.2699	0.400	0.3219	0.3313	0.1928
1.000	0.3645	0.1716	0.1277	1.000	0.2527	0.0469	0.0445
2.000	0.0762	0.1407	0.1392	2.000	0.0434	0.0752	0.0370
3.000	-0.2927	0.2160	0.1675	3.000	-0.0390	0.0901	0.0397

Site 35				**Site 36**			
period	**a_1**	**a_2**	**δ**	**period**	**a_1**	**a_2**	**δ**
PGA	-0.3667	0.4985	0.1519	PGA	-0.5714	0.4851	0.1498
0.030	-0.3677	0.5009	0.1522	0.030	-0.5579	0.4863	0.1501
0.040	-0.3668	0.4985	0.1519	0.040	-0.5715	0.4852	0.1498
0.100	-0.6753	0.4723	0.1507	0.100	-0.8697	0.4581	0.1555
0.200	-0.4645	0.4685	0.1345	0.200	-0.5310	0.4622	0.1282
0.300	-0.3021	0.5836	0.1169	0.300	-0.4141	0.5727	0.1154
0.400	-0.1884	0.4593	0.1268	0.400	-0.3084	0.4232	0.1298
1.000	0.1258	0.6061	0.1725	1.000	-0.0558	0.6763	0.1804
2.000	0.2996	0.2160	0.1518	2.000	0.3532	0.2322	0.1546
3.000	-0.1438	0.1888	0.1636	3.000	-0.0951	0.1950	0.1681
Site 37				**Site 38**			
period	**a_1**	**a_2**	**δ**	**period**	**a_1**	**a_2**	**δ**
PGA	-0.2122	0.4681	0.1813	PGA	-0.1846	0.4675	0.1832
0.030	-0.2087	0.4703	0.1824	0.030	-0.1360	0.4629	0.1847
0.040	-0.2122	0.4682	0.1813	0.040	-0.1846	0.4675	0.1832
0.100	-0.4122	0.4406	0.1668	0.100	-0.3508	0.4757	0.1601
0.200	-0.2090	0.4597	0.1413	0.200	-0.0235	0.3900	0.1420
0.300	-0.2259	0.3973	0.1548	0.300	-0.2504	0.4343	0.1448
0.400	-0.3921	0.7026	0.1732	0.400	-0.3855	0.7647	0.1902
1.000	0.3577	0.3161	0.1294	1.000	0.3391	0.2631	0.1085
2.000	0.0677	0.1472	0.1284	2.000	0.0448	0.1325	0.1158
3.000	-0.2534	0.1809	0.1526	3.000	-0.2529	0.1797	0.1441
Site 39				**Site 40**			
period	**a_1**	**a_2**	**δ**	**period**	**a_1**	**a_2**	**δ**
PGA	-0.2379	0.5325	0.1894	PGA	-0.1773	0.5473	0.1980
0.030	-0.1977	0.5319	0.1904	0.030	-0.1336	0.5441	0.1989
0.040	-0.2376	0.5325	0.1894	0.040	-0.1937	0.5490	0.1981
0.100	-0.4500	0.4795	0.1729	0.100	-0.3634	0.5124	0.1771
0.200	-0.4143	0.6885	0.1618	0.200	-0.1968	0.6545	0.1610
0.300	-0.0709	0.4398	0.1560	0.300	-0.1039	0.4778	0.1509
0.400	-0.2998	0.6993	0.1707	0.400	-0.2952	0.7687	0.1868
1.000	0.3757	0.3581	0.1456	1.000	0.3857	0.3178	0.1307
2.000	0.0869	0.1605	0.1400	2.000	0.0649	0.1508	0.1330
3.000	-0.2574	0.1878	0.1637	3.000	-0.2584	0.1818	0.1575

Site 41				**Site 42**			
period	**a_1**	**a_2**	**δ**	**period**	**a_1**	**a_2**	**δ**
PGA	-0.1092	0.4338	0.1636	PGA	-0.0122	0.4374	0.1654
0.030	-0.1022	0.4332	0.1653	0.030	-0.0155	0.4380	0.1663
0.040	-0.1091	0.4338	0.1636	0.040	-0.0118	0.4374	0.1654
0.100	-0.2987	0.4174	0.1471	0.100	-0.2307	0.4230	0.1455
0.200	-0.1208	0.4403	0.1234	0.200	-0.1191	0.5486	0.1395
0.300	-0.1349	0.3933	0.1314	0.300	-0.0520	0.4275	0.1260
0.400	-0.2428	0.6665	0.1628	0.400	-0.1572	0.6714	0.1686
1.000	0.3247	0.2610	0.0968	1.000	0.3053	0.2404	0.0890
2.000	0.0352	0.1288	0.1077	2.000	0.0241	0.1221	0.1002
3.000	-0.2308	0.1673	0.1344	3.000	-0.2262	0.1668	0.1272
Site 43				**Site 44**			
period	**a_1**	**a_2**	**δ**	**period**	**a_1**	**a_2**	**δ**
PGA	0.1298	0.4934	0.1998	PGA	-0.0282	0.4517	0.1734
0.030	0.1208	0.4928	0.2015	0.030	-0.0041	0.4492	0.1754
0.040	0.1308	0.4933	0.1998	0.040	-0.0275	0.4516	0.1734
0.100	-0.1465	0.5576	0.1854	0.100	-0.2356	0.4507	0.1533
0.200	-0.1007	0.6501	0.1822	0.200	-0.1647	0.5768	0.1485
0.300	-0.0055	0.6435	0.1748	0.300	-0.0342	0.4779	0.1312
0.400	-0.0171	0.8210	0.2226	0.400	-0.1152	0.7162	0.1822
1.000	0.2457	0.1893	0.0745	1.000	0.3012	0.2316	0.0863
2.000	-0.0054	0.1094	0.0875	2.000	0.0192	0.1203	0.0995
3.000	-0.1992	0.1553	0.1172	3.000	-0.2220	0.1643	0.1278
Site 45				**Site 46**			
period	**a_1**	**a_2**	**δ**	**period**	**a_1**	**a_2**	**δ**
PGA	-0.2995	0.5296	0.1736	PGA	-0.3204	0.5203	0.1633
0.030	-0.2804	0.5299	0.1751	0.030	-0.2949	0.5201	0.1639
0.040	-0.2992	0.5296	0.1736	0.040	-0.3202	0.5203	0.1633
0.100	-0.6120	0.5107	0.1639	0.100	-0.5172	0.4749	0.1606
0.200	-0.5034	0.5182	0.1520	0.200	-0.3402	0.4549	0.1488
0.300	-0.0876	0.5082	0.1380	0.300	-0.2067	0.5669	0.1214
0.400	-0.1487	0.5177	0.1426	0.400	-0.1383	0.4809	0.1373
1.000	0.3074	0.5313	0.1697	1.000	0.2292	0.6149	0.1745
2.000	0.1581	0.2075	0.1553	2.000	0.1681	0.2314	0.1570
3.000	-0.2479	0.1928	0.1699	3.000	-0.2596	0.2009	0.1714

Site 47				**Site 48**			
period	**a_1**	**a_2**	**δ**	**period**	**a_1**	**a_2**	**δ**
PGA	-0.2747	0.5265	0.1811	PGA	-0.2931	0.5211	0.1785
0.030	-0.2473	0.5258	0.1824	0.030	-0.2696	0.5215	0.1790
0.040	-0.2747	0.5265	0.1811	0.040	-0.2930	0.5211	0.1785
0.100	-0.4732	0.4795	0.1694	0.100	-0.5227	0.4818	0.1671
0.200	-0.5779	0.6215	0.1559	0.200	-0.5054	0.6348	0.1560
0.300	-0.0512	0.4328	0.1560	0.300	-0.0338	0.3977	0.1604
0.400	-0.2187	0.5552	0.1490	0.400	-0.2320	0.5187	0.1486
1.000	0.3314	0.4735	0.1698	1.000	0.3002	0.4936	0.1738
2.000	0.1429	0.1894	0.1520	2.000	0.1489	0.1948	0.1524
3.000	-0.2479	0.1913	0.1696	3.000	-0.2455	0.1894	0.1684
Site 49				**Site 50**			
period	**a_1**	**a_2**	**δ**	**period**	**a_1**	**a_2**	**δ**
PGA	-0.2808	0.5044	0.1773	PGA	-0.2850	0.5110	0.1767
0.030	-0.2454	0.5028	0.1798	0.030	-0.2650	0.5112	0.1772
0.040	-0.2805	0.5044	0.1772	0.040	-0.2850	0.5110	0.1767
0.100	-0.4652	0.4465	0.1703	0.100	-0.4859	0.4742	0.1632
0.200	-0.6670	0.6410	0.1561	0.200	-0.5282	0.6383	0.1543
0.300	-0.0409	0.3975	0.1585	0.300	-0.0431	0.3861	0.1596
0.400	-0.2271	0.5409	0.1476	0.400	-0.2446	0.5236	0.1475
1.000	0.3323	0.4504	0.1615	1.000	0.3098	0.4721	0.1671
2.000	0.1307	0.1829	0.1467	2.000	0.1414	0.1877	0.1486
3.000	-0.2434	0.1876	0.1647	3.000	-0.2450	0.1881	0.1654
Site 51				**Site 52**			
period	**a_1**	**a_2**	**δ**	**period**	**a_1**	**a_2**	**δ**
PGA	-0.3066	0.5320	0.1800	PGA	-0.3706	0.4003	0.1750
0.030	-0.2810	0.5316	0.1812	0.030	-0.3801	0.4062	0.1739
0.040	-0.3066	0.5320	0.1800	0.040	-0.3708	0.4003	0.1750
0.100	-0.5497	0.4998	0.1663	0.100	-0.2586	0.3355	0.2185
0.200	-0.4940	0.6379	0.1551	0.200	-0.5238	0.3572	0.2143
0.300	-0.0240	0.4143	0.1587	0.300	-0.2765	0.3417	0.1599
0.400	-0.2172	0.5163	0.1486	0.400	-0.2329	0.3202	0.1730
1.000	0.2909	0.5107	0.1784	1.000	-0.0761	0.7722	0.2070
2.000	0.1569	0.1993	0.1550	2.000	0.3122	0.2628	0.1617
3.000	-0.2508	0.1912	0.1702	3.000	-0.1548	0.2145	0.1768

Site 53				**Site 54**			
period	**a_1**	**a_2**	**δ**	**period**	**a_1**	**a_2**	**δ**
PGA	-0.4759	0.8248	0.2707	PGA	-0.6214	0.8457	0.2413
0.030	-0.4790	0.8280	0.2735	0.030	-0.6085	0.8443	0.2445
0.040	-0.4757	0.8248	0.2707	0.040	-0.6214	0.8457	0.2413
0.100	-0.6072	0.7729	0.2328	0.100	-0.7762	0.8418	0.2169
0.200	-0.3542	0.8558	0.2180	0.200	-0.5251	1.0734	0.2230
0.300	-0.2575	0.6872	0.2181	0.300	-0.1726	0.5353	0.2451
0.400	-0.5529	1.1250	0.2441	0.400	-0.5657	0.7052	0.2154
1.000	0.4229	0.4022	0.1805	1.000	0.2428	0.7752	0.2836
2.000	-0.0062	0.1928	0.1779	2.000	0.0304	0.2938	0.2302
3.000	-0.3698	0.2106	0.2063	3.000	-0.5132	0.2700	0.2490
Site 55				**Site 56**			
period	**a_1**	**a_2**	**δ**	**period**	**a_1**	**a_2**	**δ**
PGA	-0.4834	0.8763	0.2560	PGA	-0.7707	0.8721	0.2416
0.030	-0.4934	0.8795	0.2589	0.030	-0.7732	0.8737	0.2446
0.040	-0.4832	0.8763	0.2560	0.040	-0.7708	0.8722	0.2416
0.100	-0.5052	0.8143	0.2269	0.100	-0.9357	0.8494	0.2186
0.200	-0.4587	0.9053	0.1922	0.200	-0.8175	1.0068	0.1951
0.300	-0.0943	0.6973	0.2251	0.300	-0.0716	0.6604	0.2187
0.400	-0.2404	0.7574	0.2086	0.400	-0.2799	0.6777	0.2086
1.000	0.4054	0.7229	0.2526	1.000	0.1771	0.8600	0.3100
2.000	0.0184	0.2867	0.2217	2.000	0.1319	0.3106	0.2401
3.000	-0.4781	0.2602	0.2405	3.000	-0.4577	0.2802	0.2574
Site 57				**Site 58**			
period	**a_1**	**a_2**	**δ**	**period**	**a_1**	**a_2**	**δ**
PGA	-0.7126	0.8045	0.2431	PGA	-1.2526	0.7437	0.2309
0.030	-0.7136	0.8056	0.2472	0.030	-1.2460	0.7471	0.2319
0.040	-0.7148	0.8047	0.2426	0.040	-1.2527	0.7437	0.2309
0.100	-0.9325	0.7829	0.2249	0.100	-1.4503	0.6658	0.2457
0.200	-1.1538	0.9970	0.2145	0.200	-1.0535	0.5911	0.2412
0.300	-0.2454	0.5628	0.2318	0.300	-0.5166	0.6271	0.2107
0.400	-0.4670	0.6820	0.2143	0.400	-0.5701	0.5335	0.2381
1.000	0.2156	0.7853	0.3109	1.000	-0.5343	1.3020	0.3396
2.000	0.0967	0.2917	0.2369	2.000	0.2448	0.4289	0.2562
3.000	-0.4681	0.2709	0.2546	3.000	-0.3456	0.3232	0.2611

Site 59				**Site 60**			
period	**a_1**	**a_2**	**δ**	**period**	**a_1**	**a_2**	**δ**
PGA	-0.7402	0.8195	0.2465	PGA	-0.6528	0.8375	0.2556
0.030	-0.7506	0.8225	0.2499	0.030	-0.6382	0.8390	0.2594
0.040	-0.7403	0.8195	0.2465	0.040	-0.6527	0.8375	0.2556
0.100	-0.8546	0.7646	0.2337	0.100	-0.7038	0.7694	0.2398
0.200	-1.1657	0.9289	0.2126	0.200	-1.0349	0.7934	0.2189
0.300	-0.2586	0.6196	0.2191	0.300	-0.1518	0.6962	0.2306
0.400	-0.4598	0.7558	0.2139	0.400	-0.3907	0.7864	0.2053
1.000	0.2861	0.7071	0.2743	1.000	0.3508	0.7377	0.2872
2.000	0.0566	0.2769	0.2275	2.000	0.0765	0.2881	0.2337
3.000	-0.4781	0.2627	0.2474	3.000	-0.4697	0.2668	0.2513
Site 61				**Site 62**			
period	**a_1**	**a_2**	**δ**	**period**	**a_1**	**a_2**	**δ**
PGA	-0.8517	0.7854	0.2363	PGA	-0.7262	0.7939	0.2393
0.030	-0.8430	0.7866	0.2384	0.030	-0.7159	0.7934	0.2426
0.040	-0.8518	0.7854	0.2363	0.040	-0.7262	0.7939	0.2393
0.100	-1.0488	0.7899	0.2155	0.100	-0.8160	0.7621	0.2198
0.200	-1.2866	0.8824	0.2003	0.200	-1.0652	1.0136	0.2132
0.300	-0.3154	0.5443	0.2309	0.300	-0.3264	0.5312	0.2420
0.400	-0.6833	0.6599	0.2135	0.400	-0.7321	0.7168	0.2081
1.000	0.0938	0.8753	0.3219	1.000	0.2234	0.7688	0.2979
2.000	0.1142	0.3106	0.2381	2.000	0.0832	0.2875	0.2303
3.000	-0.4785	0.2813	0.2545	3.000	-0.4650	0.2667	0.2480
Site 63				**Site 64**			
period	**a_1**	**a_2**	**δ**	**period**	**a_1**	**a_2**	**δ**
PGA	-0.5136	0.8369	0.2516	PGA	-0.7120	0.8099	0.2520
0.030	-0.5200	0.8392	0.2554	0.030	-0.7181	0.8116	0.2571
0.040	-0.5134	0.8369	0.2517	0.040	-0.7120	0.8099	0.2520
0.100	-0.6402	0.7960	0.2238	0.100	-0.7753	0.7553	0.2336
0.200	-0.5126	0.9854	0.2111	0.200	-1.1811	1.0321	0.2162
0.300	-0.1852	0.6067	0.2269	0.300	-0.2871	0.5736	0.2382
0.400	-0.4486	0.8931	0.2087	0.400	-0.6101	0.7895	0.2123
1.000	0.4617	0.5297	0.2166	1.000	0.2967	0.6611	0.2587
2.000	0.0229	0.2336	0.1999	2.000	-0.0085	0.2688	0.2224
3.000	-0.3935	0.2303	0.2238	3.000	-0.4929	0.2598	0.2459

Site 65				**Site 66**			
period	**a_1**	**a_2**	**δ**	**period**	**a_1**	**a_2**	**δ**
PGA	-0.5778	0.9103	0.2755	PGA	-0.3868	0.9065	0.2822
0.030	-0.5988	0.9151	0.2786	0.030	-0.3667	0.9067	0.2851
0.040	-0.5778	0.9103	0.2755	0.040	-0.3865	0.9065	0.2822
0.100	-0.6518	0.7990	0.2508	0.100	-0.4117	0.8170	0.2442
0.200	-0.7212	1.1104	0.2302	0.200	-0.7301	1.1274	0.2360
0.300	-0.1381	0.7478	0.2200	0.300	-0.1379	0.7842	0.2204
0.400	-0.3391	0.9453	0.2242	0.400	-0.3264	1.0839	0.2265
1.000	0.4302	0.5695	0.2324	1.000	0.4776	0.4651	0.2000
2.000	0.0060	0.2512	0.2176	2.000	-0.0039	0.2195	0.1920
3.000	-0.4504	0.2481	0.2424	3.000	-0.3745	0.2207	0.2155
Site 67				**Site 68**			
period	**a_1**	**a_2**	**δ**	**period**	**a_1**	**a_2**	**δ**
PGA	-0.4927	0.8316	0.2534	PGA	-0.5260	0.9234	0.2818
0.030	-0.4827	0.8338	0.2575	0.030	-0.5076	0.9254	0.2848
0.040	-0.4926	0.8316	0.2534	0.040	-0.5259	0.9234	0.2817
0.100	-0.5165	0.7322	0.2363	0.100	-0.5619	0.7898	0.2610
0.200	-0.6988	1.0150	0.2113	0.200	-0.7823	0.9152	0.2139
0.300	-0.1379	0.6099	0.2327	0.300	-0.2261	0.8772	0.2409
0.400	-0.3654	0.8110	0.2091	0.400	-0.2718	0.9593	0.2154
1.000	0.4202	0.6067	0.2295	1.000	0.4531	0.6077	0.2342
2.000	0.0030	0.2561	0.2093	2.000	-0.0181	0.2670	0.2254
3.000	-0.4443	0.2447	0.2321	3.000	-0.4733	0.2549	0.2503
Site 69				**Site 70**			
period	**a_1**	**a_2**	**δ**	**period**	**a_1**	**a_2**	**δ**
PGA	-1.0292	0.7468	0.2317	PGA	-0.7438	0.7958	0.2382
0.030	-1.0150	0.7492	0.2336	0.030	-0.7477	0.7965	0.2404
0.040	-1.0293	0.7469	0.2317	0.040	-0.7434	0.7958	0.2377
0.100	-1.3128	0.6941	0.2341	0.100	-0.8689	0.7490	0.2176
0.200	-1.3154	0.7815	0.1988	0.200	-0.3462	0.8860	0.1971
0.300	-0.2825	0.5057	0.2384	0.300	-0.3654	0.4953	0.2554
0.400	-0.7168	0.5735	0.2284	0.400	-0.9204	0.7424	0.2052
1.000	-0.1678	1.0594	0.3507	1.000	0.1934	0.7235	0.2814
2.000	0.1838	0.3528	0.2432	2.000	0.0605	0.2746	0.2214
3.000	-0.4298	0.2982	0.2564	3.000	-0.4714	0.2602	0.2409

Site 71				**Site 72**			
period	**a_1**	**a_2**	**δ**	**period**	**a_1**	**a_2**	**δ**
PGA	-0.8971	0.8805	0.2761	PGA	-0.6496	0.8541	0.2493
0.030	-0.8904	0.8868	0.2769	0.030	-0.6492	0.8555	0.2524
0.040	-0.8971	0.8805	0.2761	0.040	-0.6494	0.8541	0.2493
0.100	-1.1562	0.7706	0.2886	0.100	-0.8059	0.8432	0.2234
0.200	-1.1082	0.6829	0.3217	0.200	-0.9161	1.0272	0.2138
0.300	-1.6618	1.1012	0.2019	0.300	-0.1848	0.6370	0.2225
0.400	-0.4254	0.9228	0.2463	0.400	-0.3755	0.7794	0.2086
1.000	0.0871	1.0442	0.3528	1.000	0.3675	0.6834	0.2643
2.000	0.1952	0.3730	0.2712	2.000	0.0714	0.2724	0.2235
3.000	-0.4830	0.3227	0.2894	3.000	-0.4433	0.2570	0.2434
Site 73				**Site 74**			
period	**a_1**	**a_2**	**δ**	**period**	**a_1**	**a_2**	**δ**
PGA	-0.9997	0.8148	0.2610	PGA	-0.6371	0.8718	0.2550
0.030	-0.9869	0.8193	0.2612	0.030	-0.6256	0.8737	0.2589
0.040	-0.9999	0.8149	0.2610	0.040	-0.6372	0.8718	0.2550
0.100	-1.2838	0.7347	0.2647	0.100	-0.7273	0.7639	0.2415
0.200	-1.1727	0.6172	0.3344	0.200	-0.8140	1.0019	0.2065
0.300	-1.6292	1.0140	0.1899	0.300	-0.1107	0.6892	0.2188
0.400	-0.3688	0.7822	0.2121	0.400	-0.3147	0.8062	0.2098
1.000	-0.0934	1.0628	0.3580	1.000	0.3766	0.6766	0.2578
2.000	0.1597	0.3688	0.2573	2.000	0.0653	0.2724	0.2248
3.000	-0.4830	0.3137	0.2724	3.000	-0.4399	0.2577	0.2460
Site 75				**Site 76**			
period	**a_1**	**a_2**	**δ**	**period**	**a_1**	**a_2**	**δ**
PGA	-0.7296	0.8281	0.2491	PGA	-0.3461	0.8917	0.2874
0.030	-0.7311	0.8322	0.2530	0.030	-0.2809	0.8858	0.2906
0.040	-0.7295	0.8281	0.2491	0.040	-0.3456	0.8916	0.2873
0.100	-0.8411	0.7242	0.2428	0.100	-0.4383	0.8412	0.2394
0.200	-0.9934	0.8643	0.1982	0.200	-0.4050	1.0542	0.2387
0.300	-0.1555	0.6724	0.2199	0.300	-0.1553	0.7675	0.2194
0.400	-0.3475	0.7272	0.2051	0.400	-0.4184	1.1967	0.2518
1.000	0.2733	0.7868	0.2987	1.000	0.4615	0.3987	0.1773
2.000	0.1094	0.2950	0.2358	2.000	0.0073	0.1932	0.1754
3.000	-0.4564	0.2716	0.2535				

Site 77				**Site 78**			
period	**a_1**	**a_2**	**δ**	**period**	**a_1**	**a_2**	**δ**
PGA	-1.1535	0.7355	0.2441	PGA	-0.6144	0.8640	0.2573
0.030	-1.1658	0.7401	0.2461	0.030	-0.6250	0.8652	0.2604
0.040	-1.1538	0.7355	0.2441	0.040	-0.6144	0.8640	0.2573
0.100	-1.5671	0.7044	0.2459	0.100	-0.6964	0.8077	0.2288
0.200	-1.2019	0.5668	0.3434	0.200	-0.3563	0.9770	0.2074
0.300	-1.2118	0.8151	0.1837	0.300	-0.2070	0.5846	0.2402
0.400	-0.4818	0.6013	0.2232	0.400	-0.5937	0.8872	0.2112
1.000	-0.3992	1.2226	0.3715	1.000	0.3879	0.5679	0.2313
2.000	0.1949	0.4055	0.2580	2.000	0.0056	0.2454	0.2117
3.000	-0.4140	0.3187	0.2646	3.000	-0.4436	0.2456	0.2371
Site 79				**Site 80**			
period	**a_1**	**a_2**	**δ**	**period**	**a_1**	**a_2**	**δ**
PGA	-0.5858	0.9113	0.2657	PGA	-0.5864	0.8271	0.2449
0.030	-0.5545	0.9102	0.2703	0.030	-0.5826	0.8288	0.2486
0.040	-0.5610	0.9088	0.2658	0.040	-0.5865	0.8271	0.2449
0.100	-0.7369	0.8688	0.2317	0.100	-0.7066	0.7792	0.2228
0.200	-0.8399	0.9565	0.2181	0.200	-0.8148	1.0384	0.2260
0.300	-0.1755	0.8010	0.2235	0.300	-0.1908	0.5941	0.2272
0.400	-0.3197	0.9361	0.2086	0.400	-0.4565	0.8271	0.2084
1.000	0.4594	0.6036	0.2409	1.000	0.4156	0.5876	0.2343
2.000	0.0430	0.2593	0.2212	2.000	0.0492	0.2461	0.2065
3.000	-0.4293	0.2498	0.2447	3.000	-0.4085	0.2400	0.2287
Site 81				**Site 82**			
period	**a_1**	**a_2**	**δ**	**period**	**a_1**	**a_2**	**δ**
PGA	-1.9971	0.7333	0.2315	PGA	-0.6680	0.8455	0.2474
0.030	-1.9936	0.7350	0.2330	0.030	-0.6773	0.8482	0.2498
0.040	-1.9972	0.7333	0.2315	0.040	-0.6680	0.8455	0.2474
0.100	-1.9536	0.6886	0.2201	0.100	-0.8499	0.8166	0.2245
0.200	-2.1663	0.7082	0.2036	0.200	-0.6837	0.9372	0.2033
0.300	-0.9462	0.5114	0.2207	0.300	-0.1594	0.6178	0.2250
0.400	-1.5921	0.5908	0.2482	0.400	-0.3258	0.7018	0.2149
1.000	-0.5573	1.1564	0.3254	1.000	0.2530	0.7931	0.3018
2.000	0.1778	0.3728	0.2167	2.000	0.1059	0.2950	0.2378
3.000	-0.3630	0.2904	0.2265	3.000	-0.4624	0.2713	0.2551

Site 83				**Site 84**			
period	**a_1**	**a_2**	**δ**	**period**	**a_1**	**a_2**	**δ**
PGA	-0.4825	0.9134	0.2718	PGA	-0.6462	0.8091	0.2489
0.030	-0.4762	0.9154	0.2753	0.030	-0.6566	0.8129	0.2521
0.040	-0.4823	0.9134	0.2718	0.040	-0.6461	0.8091	0.2489
0.100	-0.5324	0.8158	0.2380	0.100	-0.8258	0.7427	0.2348
0.200	-0.7457	1.0247	0.2284	0.200	-0.9209	1.0376	0.2234
0.300	-0.1416	0.8056	0.2218	0.300	-0.2532	0.5782	0.2314
0.400	-0.2950	1.0026	0.2198	0.400	-0.4997	0.8181	0.2098
1.000	0.5168	0.5325	0.2183	1.000	0.3673	0.5933	0.2416
2.000	0.0381	0.2390	0.2059	2.000	0.0334	0.2488	0.2139
3.000	-0.3856	0.2335	0.2291	3.000	-0.4310	0.2464	0.2380
Site 85				**Site 86**			
period	**a_1**	**a_2**	**δ**	**period**	**a_1**	**a_2**	**δ**
PGA	-0.7211	0.8425	0.2659	PGA	-1.1385	0.7093	0.2234
0.030	-0.7374	0.8491	0.2696	0.030	-1.1235	0.7112	0.2236
0.040	-0.7211	0.8425	0.2659	0.040	-1.1387	0.7093	0.2234
0.100	-0.9181	0.7547	0.2570	0.100	-1.3251	0.6670	0.2189
0.200	-1.2398	0.7891	0.2389	0.200	-1.1382	0.7044	0.1972
0.300	-0.3142	0.7683	0.2246	0.300	-0.3170	0.4413	0.2418
0.400	-0.4916	0.9000	0.2041	0.400	-0.9284	0.5329	0.2501
1.000	0.3830	0.6459	0.2529	1.000	-0.3948	1.1869	0.3437
2.000	0.0492	0.2668	0.2239	2.000	0.2119	0.3842	0.2439
3.000	-0.4432	0.2568	0.2465	3.000	-0.3728	0.3038	0.2520
Site 87				**Site 88**			
period	**a_1**	**a_2**	**δ**	**period**	**a_1**	**a_2**	**δ**
PGA	-0.8577	0.8878	0.2759	PGA	-0.5090	0.8879	0.2638
0.030	-0.8817	0.8933	0.2791	0.030	-0.5026	0.8901	0.2672
0.040	-0.8578	0.8878	0.2759	0.040	-0.5090	0.8879	0.2638
0.100	-1.0951	0.8334	0.2655	0.100	-0.4781	0.7687	0.2471
0.200	-1.1278	0.6846	0.3228	0.200	-0.7140	0.8494	0.2094
0.300	-1.2841	1.0609	0.2132	0.300	-0.1410	0.7834	0.2313
0.400	-0.3729	0.8965	0.2298	0.400	-0.2375	0.8533	0.2101
1.000	0.2113	0.8990	0.3290	1.000	0.4494	0.6560	0.2390
2.000	0.1033	0.3378	0.2619	2.000	0.0045	0.2758	0.2230
3.000	-0.5241	0.3017	0.2806	3.000	-0.4731	0.2552	0.2441

Site 89				**Site 90**			
period	**a_1**	**a_2**	**δ**	**period**	**a_1**	**a_2**	**δ**
PGA	-4.7182	0.8298	0.2373	PGA	-0.4334	0.8823	0.2718
0.030	-4.7044	0.8268	0.2374	0.030	-0.4234	0.8833	0.2747
0.040	-4.7185	0.8299	0.2373	0.040	-0.4332	0.8824	0.2718
0.100	-4.9717	0.9497	0.2234	0.100	-0.6144	0.8507	0.2378
0.200	-4.5851	0.8908	0.2282	0.200	-0.7493	1.1045	0.2427
0.300	-1.1449	0.4526	0.1820	0.300	-0.1409	0.7387	0.2250
0.400	-2.5209	0.5853	0.2667	0.400	-0.3034	1.0255	0.2249
1.000	-2.3029	1.2189	0.3405	1.000	0.5254	0.4687	0.2097
2.000	0.1225	0.5227	0.2480	2.000	0.0387	0.2206	0.1981
3.000	0.2902	0.3025	0.2153	3.000	-0.3562	0.2257	0.2232
Site 91				**Site 92**			
period	**a_1**	**a_2**	**δ**	**period**	**a_1**	**a_2**	**δ**
PGA	-1.1150	0.7572	0.2225	PGA	-0.4787	0.8946	0.2714
0.030	-1.1132	0.7587	0.2245	0.030	-0.4746	0.8965	0.2746
0.040	-1.1151	0.7572	0.2225	0.040	-0.4786	0.8947	0.2714
0.100	-1.3951	0.7246	0.2148	0.100	-0.5482	0.8175	0.2343
0.200	-1.1629	0.7439	0.1925	0.200	-0.8080	1.1078	0.2356
0.300	-0.2462	0.4977	0.2333	0.300	-0.1450	0.7480	0.2203
0.400	-0.8076	0.5593	0.2333	0.400	-0.3360	1.0097	0.2218
1.000	-0.2802	1.1392	0.3456	1.000	0.5082	0.4962	0.2106
2.000	0.1951	0.3716	0.2437	2.000	0.0246	0.2274	0.1975
3.000	-0.4108	0.3036	0.2548	3.000	-0.3692	0.2242	0.2207
Site 93				**Site 94**			
period	**a_1**	**a_2**	**δ**	**period**	**a_1**	**a_2**	**δ**
PGA	-0.9591	0.7665	0.2353	PGA	-1.7293	0.7254	0.2282
0.030	-0.9624	0.7687	0.2370	0.030	-1.6359	0.7197	0.2298
0.040	-0.9592	0.7665	0.2353	0.040	-1.7295	0.7254	0.2281
0.100	-1.0649	0.7142	0.2259	0.100	-1.4419	0.6226	0.2360
0.200	-1.5591	0.8896	0.1963	0.200	-1.9917	0.8153	0.1941
0.300	-0.3445	0.5195	0.2275	0.300	-1.1726	0.5214	0.2446
0.400	-0.9094	0.6831	0.2096	0.400	-1.4126	0.5921	0.2345
1.000	0.0385	0.8607	0.3056	1.000	-0.3064	1.0235	0.3241
2.000	0.1054	0.3024	0.2288	2.000	0.1455	0.3375	0.2146
3.000	-0.4681	0.2762	0.2462	3.000	-0.4020	0.2802	0.2282

Site 95				**Site 96**			
period	**a_1**	**a_2**	**δ**	**period**	**a_1**	**a_2**	**δ**
PGA	-2.7002	0.6415	0.2349	PGA	-1.7099	0.7001	0.2397
0.030	-2.8759	0.6564	0.2398	0.030	-1.7258	0.7050	0.2402
0.040	-2.7002	0.6415	0.2349	0.040	-1.7101	0.7001	0.2397
0.100	-3.1321	0.6270	0.2543	0.100	-1.8471	0.6608	0.2296
0.200	-1.4559	0.4939	0.2082	0.200	-1.7475	0.5878	0.2692
0.300	-1.1537	0.6144	0.1561	0.300	-0.6571	0.5804	0.1976
0.400	-1.1804	0.4680	0.3038	0.400	-1.1426	0.5271	0.2591
1.000	-3.3610	1.3902	0.2095	1.000	-0.9438	1.3644	0.3259
2.000	-0.0216	0.6769	0.2243	2.000	0.1804	0.4769	0.2584
3.000	0.0145	0.3866	0.2134	3.000	-0.3174	0.3343	0.2519
Site 97				**Site 98**			
period	**a_1**	**a_2**	**δ**	**period**	**a_1**	**a_2**	**δ**
PGA	-1.1387	0.7592	0.2381	PGA	-1.5692	0.7213	0.2296
0.030	-1.1357	0.7645	0.2391	0.030	-1.5623	0.7235	0.2315
0.040	-1.1388	0.7592	0.2381	0.040	-1.5692	0.7213	0.2296
0.100	-1.2850	0.6685	0.2449	0.100	-1.6511	0.6602	0.2330
0.200	-1.1805	0.6427	0.2407	0.200	-1.9995	0.6918	0.2219
0.300	-0.4612	0.6985	0.2049	0.300	-0.6953	0.5207	0.2158
0.400	-0.5470	0.6085	0.2134	0.400	-1.3363	0.5947	0.2372
1.000	-0.2342	1.1026	0.3534	1.000	-0.4396	1.1215	0.3257
2.000	0.1825	0.3685	0.2469	2.000	0.1737	0.3625	0.2229
3.000	-0.4396	0.3074	0.2602	3.000	-0.3997	0.2940	0.2350
Site 99				**Site 100**			
period	**a_1**	**a_2**	**δ**	**period**	**a_1**	**a_2**	**δ**
PGA	-1.8357	0.7263	0.2219	PGA	-0.7274	0.8109	0.2374
0.030	-1.8494	0.7285	0.2252	0.030	-0.7266	0.8138	0.2402
0.040	-1.8358	0.7263	0.2219	0.040	-0.7274	0.8109	0.2374
0.100	-2.0807	0.7064	0.2098	0.100	-0.8636	0.7394	0.2266
0.200	-2.1392	0.6317	0.2528	0.200	-0.7689	0.8295	0.1978
0.300	-0.6423	0.5417	0.1945	0.300	-0.1166	0.6224	0.2205
0.400	-1.3233	0.5465	0.2485	0.400	-0.3506	0.6393	0.2125
1.000	-0.9384	1.3470	0.3078	1.000	0.1411	0.8958	0.3372
2.000	0.2250	0.4417	0.2315	2.000	0.1448	0.3190	0.2413
3.000	-0.2860	0.3154	0.2353	3.000	-0.4536	0.2815	0.2572

Site 101				**Site 102**			
period	**a_1**	**a_2**	**δ**	**period**	**a_1**	**a_2**	**δ**
PGA	-0.8485	0.7925	0.2440	PGA	-0.6981	0.8707	0.2673
0.030	-0.8313	0.7963	0.2453	0.030	-0.7239	0.8764	0.2710
0.040	-0.8486	0.7925	0.2440	0.040	-0.6981	0.8707	0.2673
0.100	-1.0040	0.7239	0.2383	0.100	-0.9375	0.8558	0.2389
0.200	-1.2664	0.7099	0.2433	0.200	-1.3392	0.8953	0.2276
0.300	-0.3061	0.6940	0.2218	0.300	-0.3506	0.7864	0.2220
0.400	-0.4578	0.6899	0.2063	0.400	-0.4295	0.9470	0.2154
1.000	0.1319	0.8997	0.3251	1.000	0.4270	0.5781	0.2325
2.000	0.1432	0.3220	0.2434	2.000	0.0150	0.2530	0.2170
3.000	-0.4609	0.2844	0.2599	3.000	-0.4446	0.2487	0.2412
Site 103				**Site 104**			
period	**a_1**	**a_2**	**δ**	**period**	**a_1**	**a_2**	**δ**
PGA	-0.6398	0.7988	0.2368	PGA	-0.7993	0.9311	0.2747
0.030	-0.6234	0.7978	0.2395	0.030	-0.8444	0.9412	0.2787
0.040	-0.6398	0.7988	0.2368	0.040	-0.7994	0.9311	0.2747
0.100	-0.8068	0.7449	0.2202	0.100	-1.0658	0.8314	0.2685
0.200	-0.6875	0.9937	0.2055	0.200	-1.0471	0.7858	0.2588
0.300	-0.3050	0.5170	0.2458	0.300	-0.7743	1.0785	0.2397
0.400	-0.6936	0.7223	0.2068	0.400	-0.3965	0.9765	0.2118
1.000	0.2739	0.7316	0.2886	1.000	0.3413	0.7585	0.2799
2.000	0.0899	0.2772	0.2242	2.000	0.0742	0.3025	0.2429
3.000	-0.4447	0.2590	0.2419	3.000	-0.4818	0.2763	0.2625
Site 105				**Site 106**			
period	**a_1**	**a_2**	**δ**	**period**	**a_1**	**a_2**	**δ**
PGA	-3.5203	0.8087	0.2295	PGA	-0.8607	0.8034	0.2266
0.030	-3.4954	0.8065	0.2302	0.030	-0.8938	0.8083	0.2289
0.040	-3.5204	0.8087	0.2295	0.040	-0.8609	0.8035	0.2266
0.100	-3.8068	0.8072	0.2089	0.100	-0.9850	0.7258	0.2195
0.200	-2.0713	0.8395	0.2215	0.200	-0.9546	1.0308	0.2085
0.300	-0.4415	0.5085	0.2043	0.300	-0.1300	0.5087	0.2240
0.400	-1.0804	0.4743	0.2323	0.400	-0.4367	0.5863	0.2187
1.000	-2.9064	1.3584	0.3133	1.000	0.0093	0.9114	0.3037
2.000	-0.1179	0.6448	0.2999	2.000	0.1496	0.3152	0.2249
3.000	0.3147	0.3660	0.2587	3.000	-0.4273	0.2767	0.2421

Site 107				**Site 108**			
period	**a_1**	**a_2**	**δ**	**period**	**a_1**	**a_2**	**δ**
PGA	-0.8513	0.8582	0.2536	PGA	-0.7794	0.9040	0.2638
0.030	-0.8927	0.8669	0.2571	0.030	-0.7496	0.9064	0.2673
0.040	-0.8515	0.8583	0.2536	0.040	-0.7794	0.9040	0.2638
0.100	-1.0587	0.7536	0.2528	0.100	-1.0318	0.8150	0.2584
0.200	-1.2370	0.8769	0.2037	0.200	-0.8737	0.6888	0.2913
0.300	-0.3065	0.7512	0.2079	0.300	-1.2586	1.1183	0.1989
0.400	-0.4644	0.8243	0.2026	0.400	-0.3712	0.9281	0.2201
1.000	0.2872	0.7274	0.2713	1.000	0.2614	0.9174	0.3186
2.000	0.0733	0.2838	0.2266	2.000	0.1671	0.3399	0.2574
3.000	-0.4579	0.2617	0.2457	3.000	-0.4654	0.2979	0.2757
Site 109				**Site 110**			
period	**a_1**	**a_2**	**δ**	**period**	**a_1**	**a_2**	**δ**
PGA	-0.6054	0.8615	0.2601	PGA	-0.7158	0.8231	0.2518
0.030	-0.5913	0.8632	0.2647	0.030	-0.7287	0.8259	0.2558
0.040	-0.6052	0.8615	0.2601	0.040	-0.7158	0.8231	0.2518
0.100	-0.7841	0.8171	0.2343	0.100	-0.8398	0.7869	0.2298
0.200	-1.0546	0.9015	0.2184	0.200	-1.2787	1.0232	0.2203
0.300	-0.2300	0.7411	0.2175	0.300	-0.2386	0.6186	0.2247
0.400	-0.3632	0.8862	0.2049	0.400	-0.3914	0.7764	0.2144
1.000	0.4545	0.6099	0.2384	1.000	0.3378	0.6533	0.2650
2.000	0.0577	0.2574	0.2176	2.000	0.0583	0.2644	0.2250
3.000	-0.4189	0.2493	0.2407	3.000	-0.4427	0.2581	0.2483
Site 111				**Site 112**			
period	**a_1**	**a_2**	**δ**	**period**	**a_1**	**a_2**	**δ**
PGA	-0.2374	0.8969	0.2969	PGA	-0.5734	0.8208	0.2516
0.030	-0.2308	0.8974	0.3007	0.030	-0.5767	0.8212	0.2547
0.040	-0.2367	0.8969	0.2969	0.040	-0.5734	0.8209	0.2516
0.100	-0.4140	0.8625	0.2477	0.100	-0.6029	0.7990	0.2219
0.200	-0.3677	1.0507	0.2493	0.200	-0.3259	0.8713	0.2014
0.300	-0.1167	0.8105	0.2289	0.300	-0.2756	0.5711	0.2417
0.400	-0.3282	1.2589	0.2671	0.400	-0.6435	0.8980	0.2079
1.000	0.4969	0.3702	0.1723	1.000	0.3889	0.5316	0.2205
2.000	0.0356	0.1858	0.1737	2.000	-0.0246	0.2360	0.2044
3.000	-0.3160	0.2034	0.2002	3.000	-0.4414	0.2367	0.2314

Site 113				**Site 114**			
period	**a_1**	**a_2**	**δ**	**period**	**a_1**	**a_2**	**δ**
PGA	-2.2710	0.7286	0.2289	PGA	-1.2044	0.7630	0.2311
0.030	-2.3013	0.7338	0.2294	0.030	-1.2114	0.7642	0.2333
0.040	-2.2710	0.7286	0.2289	0.040	-1.2044	0.7630	0.2311
0.100	-2.3334	0.6737	0.2316	0.100	-1.3052	0.7331	0.2152
0.200	-2.3388	0.6231	0.2623	0.200	-0.9699	0.8631	0.1978
0.300	-0.8952	0.6122	0.1778	0.300	-0.3237	0.4531	0.2491
0.400	-1.6326	0.5813	0.2340	0.400	-0.9868	0.5477	0.2559
1.000	-0.9448	1.2842	0.3220	1.000	-0.4370	1.2175	0.3706
2.000	0.1852	0.4225	0.2158	2.000	0.1908	0.3989	0.2548
3.000	-0.2934	0.3011	0.2219	3.000	-0.4026	0.3119	0.2586
Site 115				**Site 116**			
period	**a_1**	**a_2**	**δ**	**period**	**a_1**	**a_2**	**δ**
PGA	-0.8017	0.7670	0.2304	PGA	-0.4171	0.9109	0.2834
0.030	-0.8446	0.7748	0.2340	0.030	-0.3961	0.9090	0.2868
0.040	-0.8017	0.7670	0.2304	0.040	-0.4168	0.9109	0.2834
0.100	-0.9647	0.6786	0.2344	0.100	-0.5295	0.9009	0.2402
0.200	-0.6039	0.8298	0.1763	0.200	-0.5601	1.1124	0.2463
0.300	-0.1430	0.4874	0.2333	0.300	-0.1754	0.7758	0.2153
0.400	-0.7024	0.5836	0.2342	0.400	-0.3984	1.1521	0.2423
1.000	-0.1126	1.0311	0.3093	1.000	0.4768	0.4265	0.1868
2.000	0.0650	0.3496	0.2300	2.000	0.0121	0.2029	0.1832
3.000	-0.5087	0.2939	0.2480	3.000	-0.3552	0.2143	0.2081
Site 117				**Site 118**			
period	**a_1**	**a_2**	**δ**	**period**	**a_1**	**a_2**	**δ**
PGA	-0.5161	0.8765	0.2636	PGA	-3.1643	0.6827	0.2381
0.030	-0.5164	0.8784	0.2671	0.030	-3.1067	0.6823	0.2326
0.040	-0.5160	0.8766	0.2636	0.040	-3.1647	0.6827	0.2381
0.100	-0.6132	0.8091	0.2343	0.100	-2.9861	0.5928	0.2666
0.200	-0.7414	1.0454	0.2296	0.200	-2.7511	0.5918	0.2631
0.300	-0.1416	0.6984	0.2209	0.300	-0.9023	0.4613	0.1843
0.400	-0.3166	0.9204	0.2163	0.400	-2.5137	0.5740	0.3606
1.000	0.4709	0.5501	0.2254	1.000	-2.7649	1.4531	0.2570
2.000	0.0283	0.2436	0.2116	2.000	0.1189	0.5565	0.2135
3.000	-0.4135	0.2398	0.2361	3.000	-0.0834	0.3341	0.2060

Site 119				**Site 120**			
period	**a_1**	**a_2**	**δ**	**period**	**a_1**	**a_2**	**δ**
PGA	-0.9084	0.8425	0.2565	PGA	-0.8381	0.7648	0.2383
0.030	-0.8996	0.8457	0.2586	0.030	-0.8808	0.7698	0.2421
0.040	-0.9085	0.8425	0.2565	0.040	-0.8382	0.7648	0.2383
0.100	-1.2967	0.8183	0.2429	0.100	-1.0978	0.7493	0.2239
0.200	-1.3192	0.6979	0.2892	0.200	-1.3891	0.9895	0.2096
0.300	-0.7616	0.8878	0.2250	0.300	-0.3016	0.5012	0.2390
0.400	-0.4520	0.7790	0.2112	0.400	-0.7946	0.6983	0.2095
1.000	0.1176	0.9415	0.3318	1.000	0.1148	0.7833	0.2971
2.000	0.1407	0.3392	0.2520	2.000	0.0791	0.2875	0.2262
3.000	-0.4814	0.2975	0.2695	3.000	-0.4724	0.2680	0.2435
Site 121				**Site 122**			
period	**a_1**	**a_2**	**δ**	**period**	**a_1**	**a_2**	**δ**
PGA	-0.4185	0.9054	0.2731	PGA	-0.2347	0.8669	0.2743
0.030	-0.4120	0.9070	0.2766	0.030	-0.1537	0.8613	0.2763
0.040	-0.4183	0.9054	0.2731	0.040	-0.2340	0.8668	0.2743
0.100	-0.4399	0.8212	0.2379	0.100	-0.3459	0.7749	0.2379
0.200	-0.4780	1.0167	0.2226	0.200	-0.4041	1.0944	0.2321
0.300	-0.1282	0.7596	0.2171	0.300	-0.0563	0.6699	0.2281
0.400	-0.3124	0.9810	0.2189	0.400	-0.2503	0.9546	0.2158
1.000	0.4584	0.5344	0.2126	1.000	0.3967	0.5056	0.1966
2.000	-0.0269	0.2424	0.2045	2.000	-0.0686	0.2333	0.1931
3.000	-0.4293	0.2354	0.2292	3.000	-0.4442	0.2257	0.2166